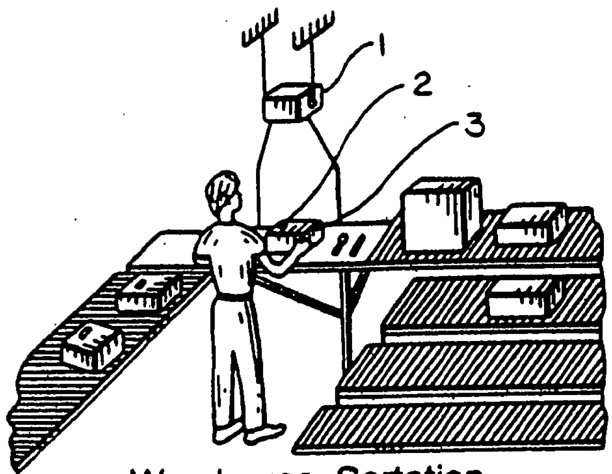

Warehouse Sortation

FIG. 1A

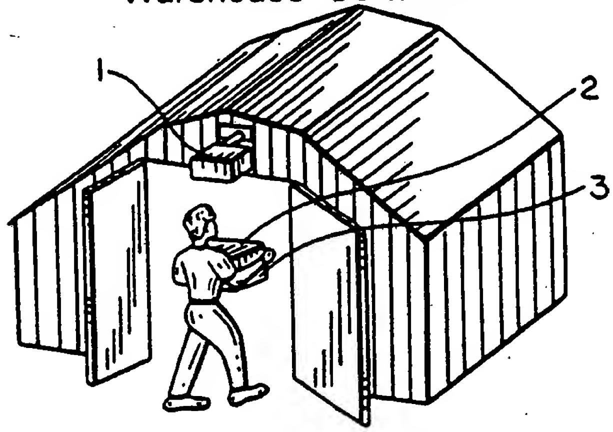

Container Loading

FIG. 1B

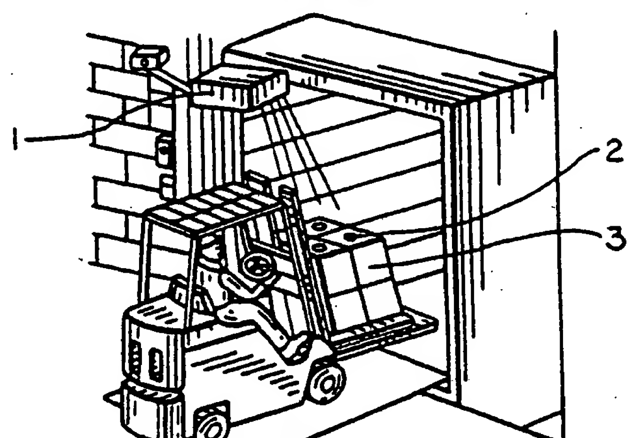

FIG. 1C

Bulk Package Loading

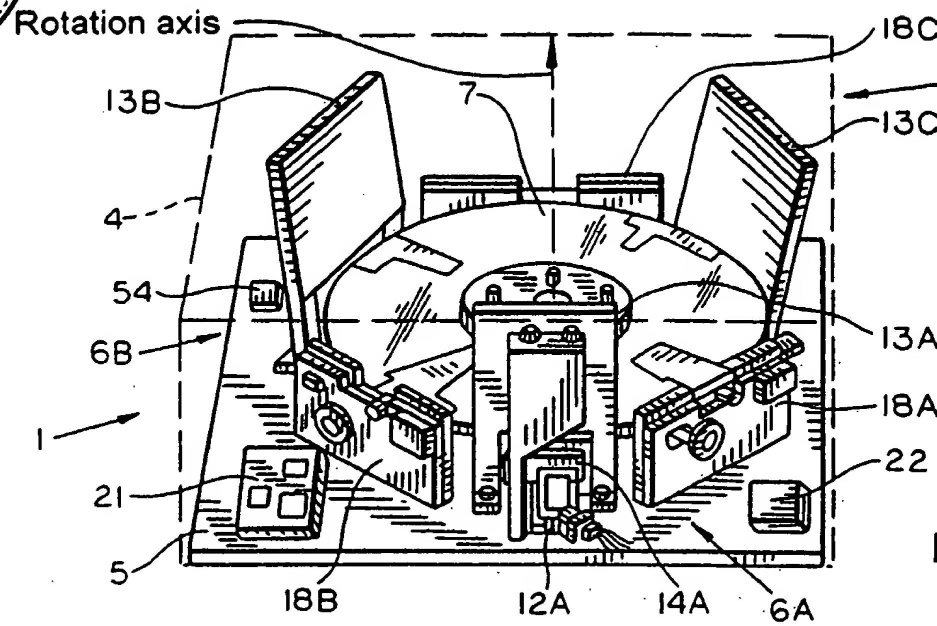
Rotation axis
18C
6C
13B
7
13C
4
54
13A
6B
18A
1
22
21
5
18B
12A
14A
6A

FIG. 2A

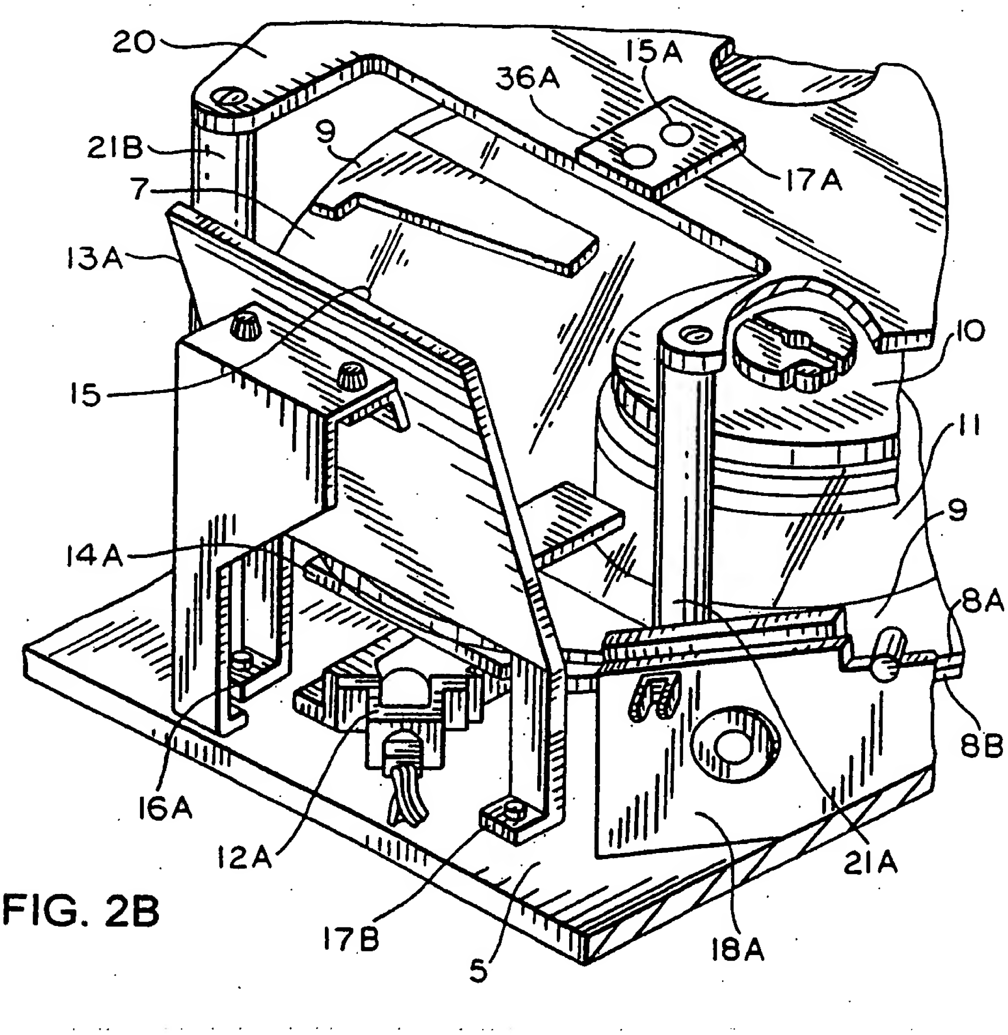
20
15A
36A
21B
9
17A
7
13A
10
15
11
9
14A
8A
8B
16A
12A
21A
17B
5
18A

FIG. 2B

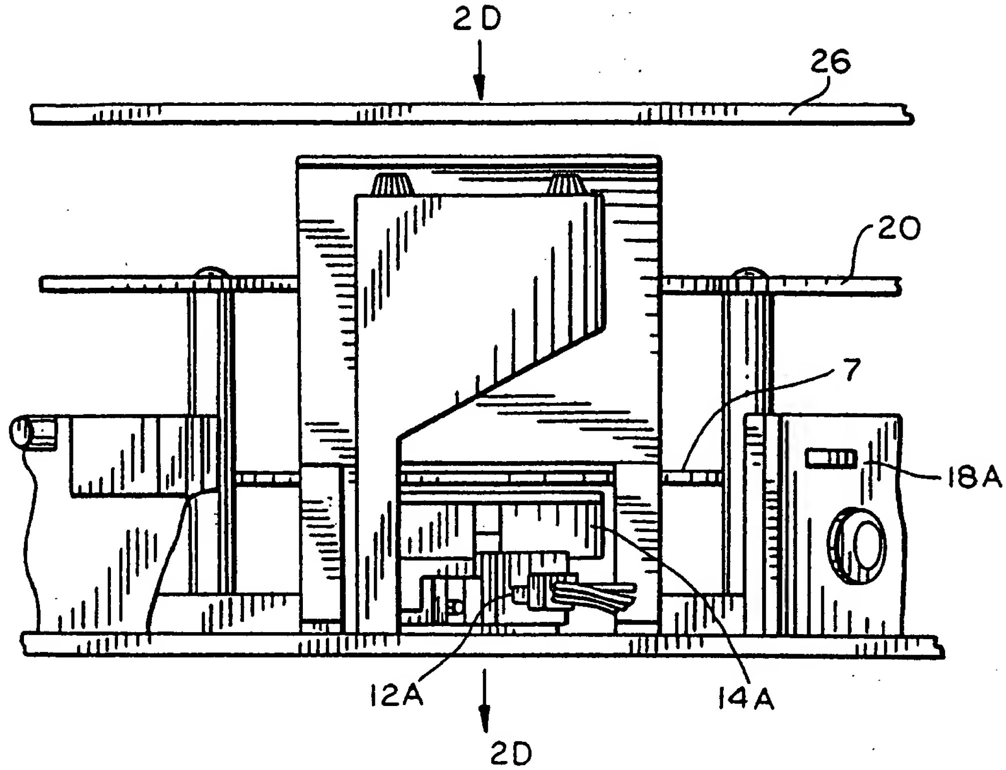

FIG. 2C

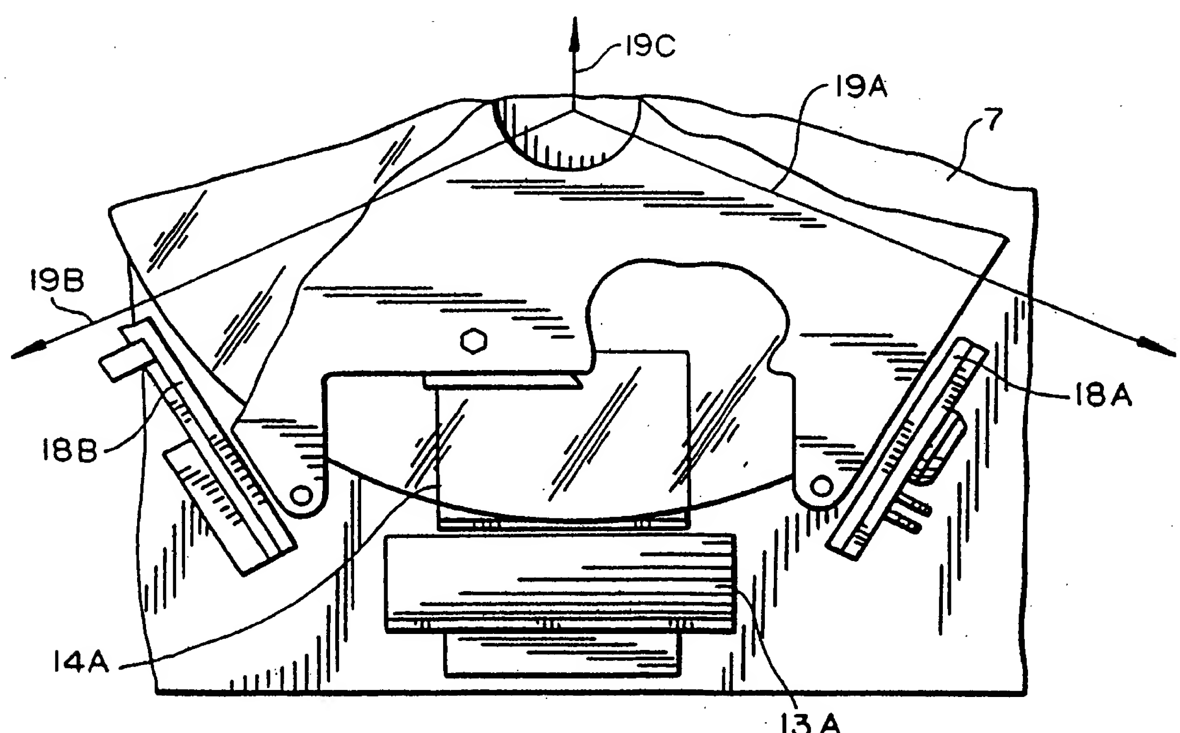

FIG. 2D

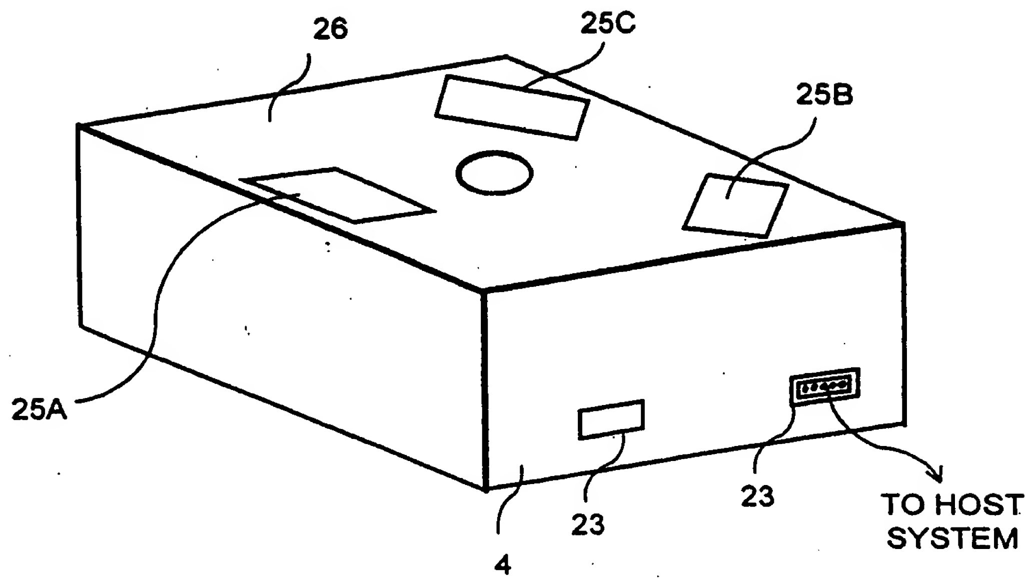

FIG. 2E

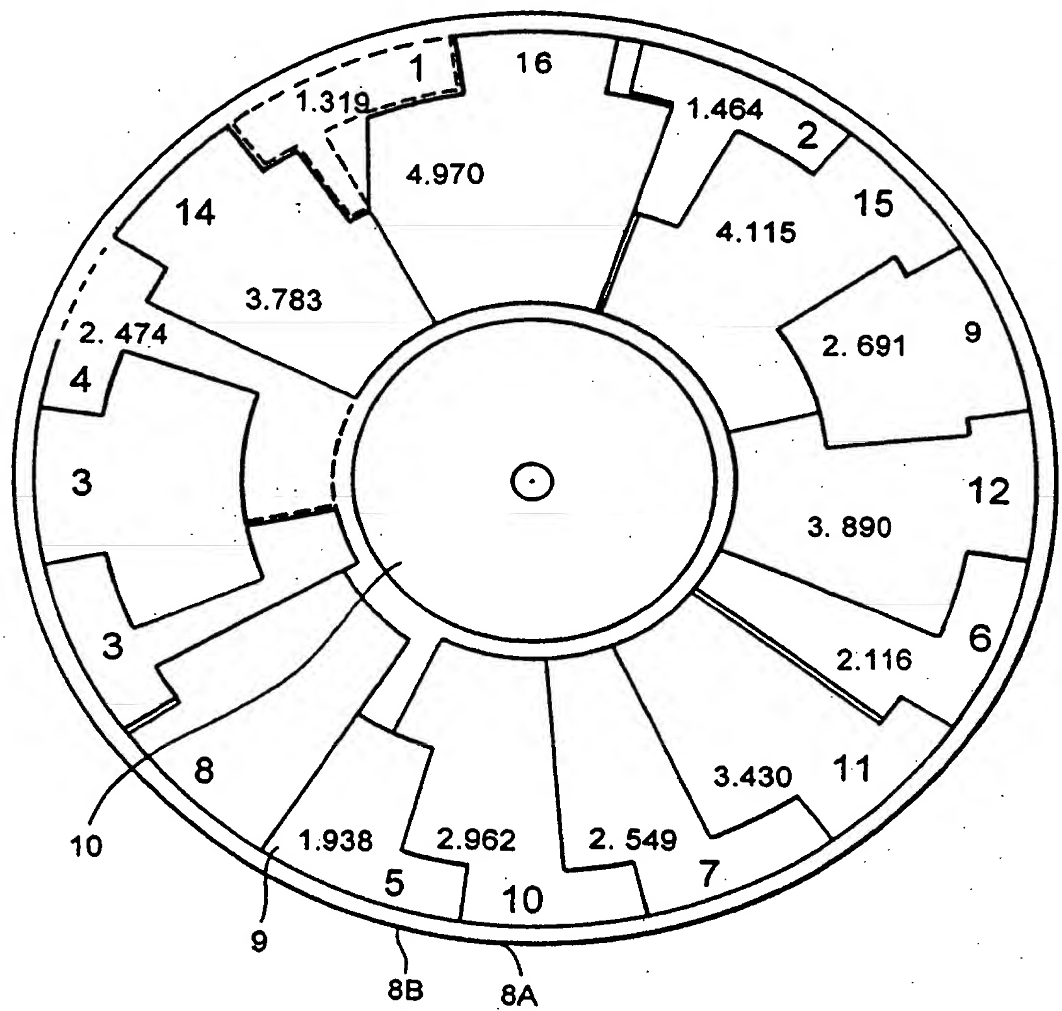
1
16
1.319
1.464
2
4.970
14
15
4.115
3.783
2. 474
2. 691
9
4
3
12
3. 890
3
6
2.116
8
3.430
11
10
1.938
2.962
2. 549
7
5
10
9
8B
8A

FIG. 3

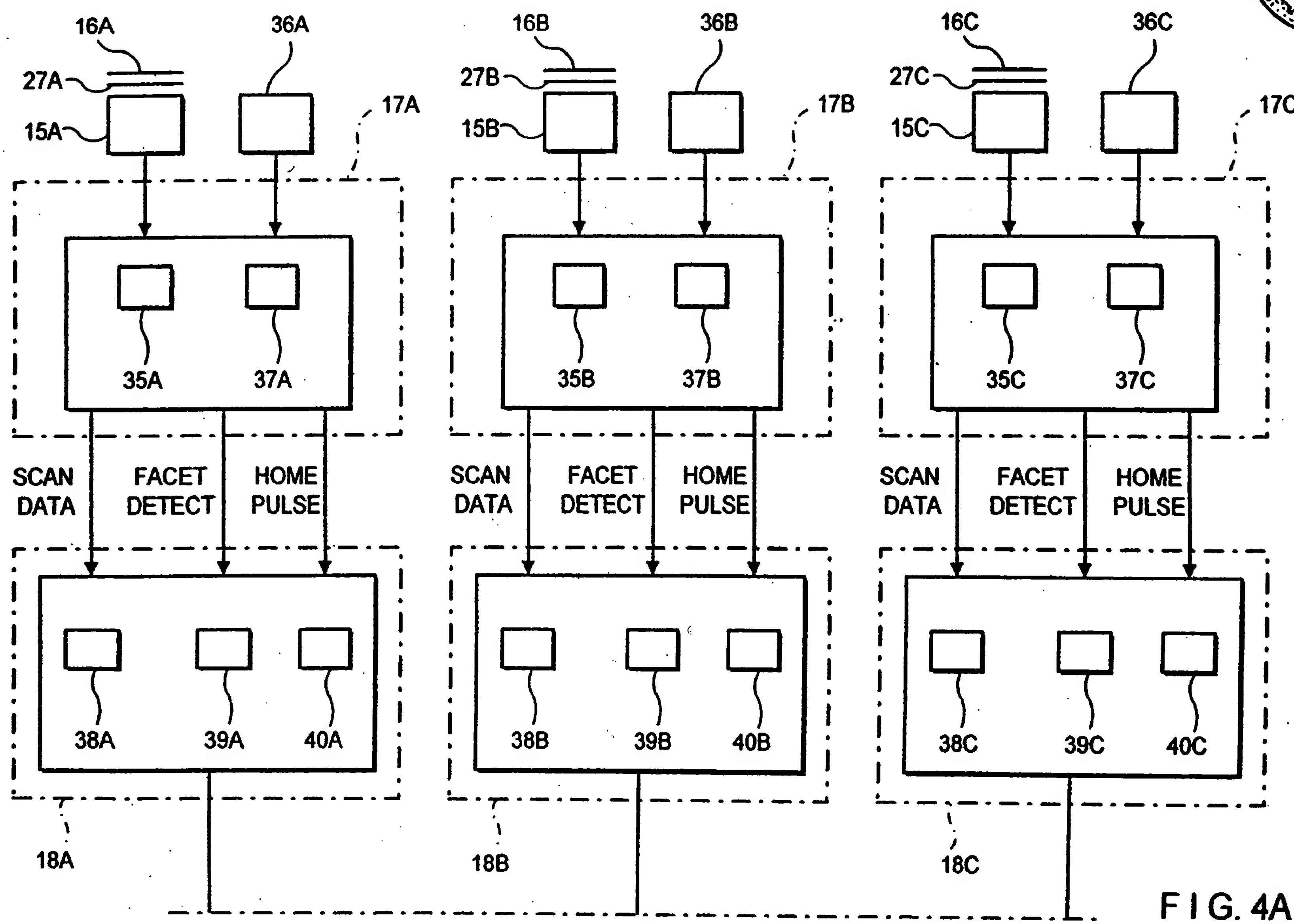
16A
27A
15A
36A
17A
35A
37A
SCAN DATA
FACET DETECT
HOME PULSE
38A
39A
40A
18A
16B
27B
15B
36B
17B
35B
37B
SCAN DATA
FACET DETECT
HOME PULSE
38B
39B
40B
18B
16C
27C
15C
36C
17C
35C
37C
SCAN DATA
FACET DETECT
HOME PULSE
38C
39C
40C
18C
FIG. 4A

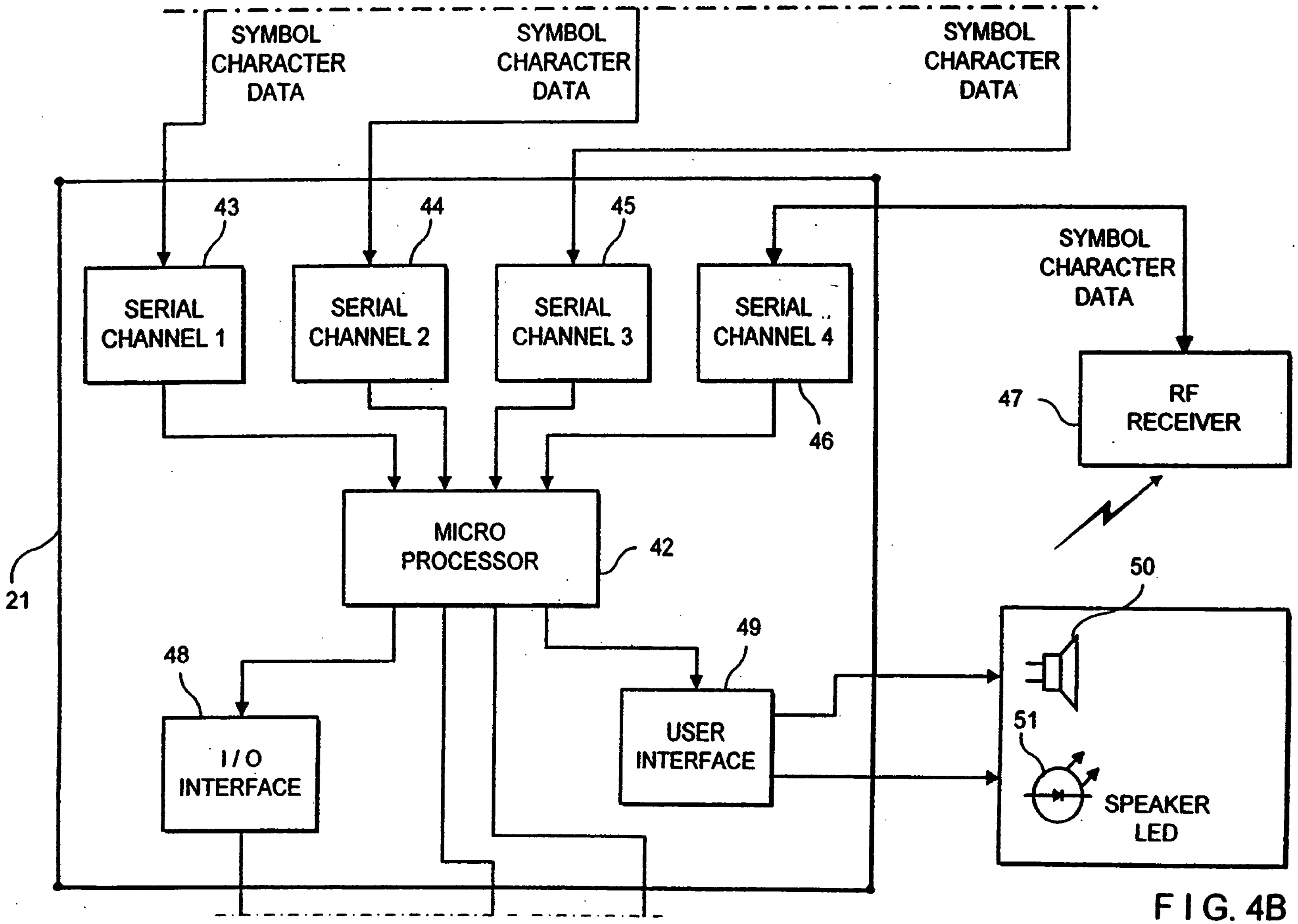
SYMBOL CHARACTER DATA
SYMBOL CHARACTER DATA
SYMBOL CHARACTER DATA
SYMBOL CHARACTER DATA
43
44
45
SERIAL CHANNEL 1
SERIAL CHANNEL 2
SERIAL CHANNEL 3
SERIAL CHANNEL 4
46
47
RF RECEIVER
MICRO PROCESSOR
42
21
50
48
49
51
I / O INTERFACE
USER INTERFACE
SPEAKER
LED

F I G. 4B

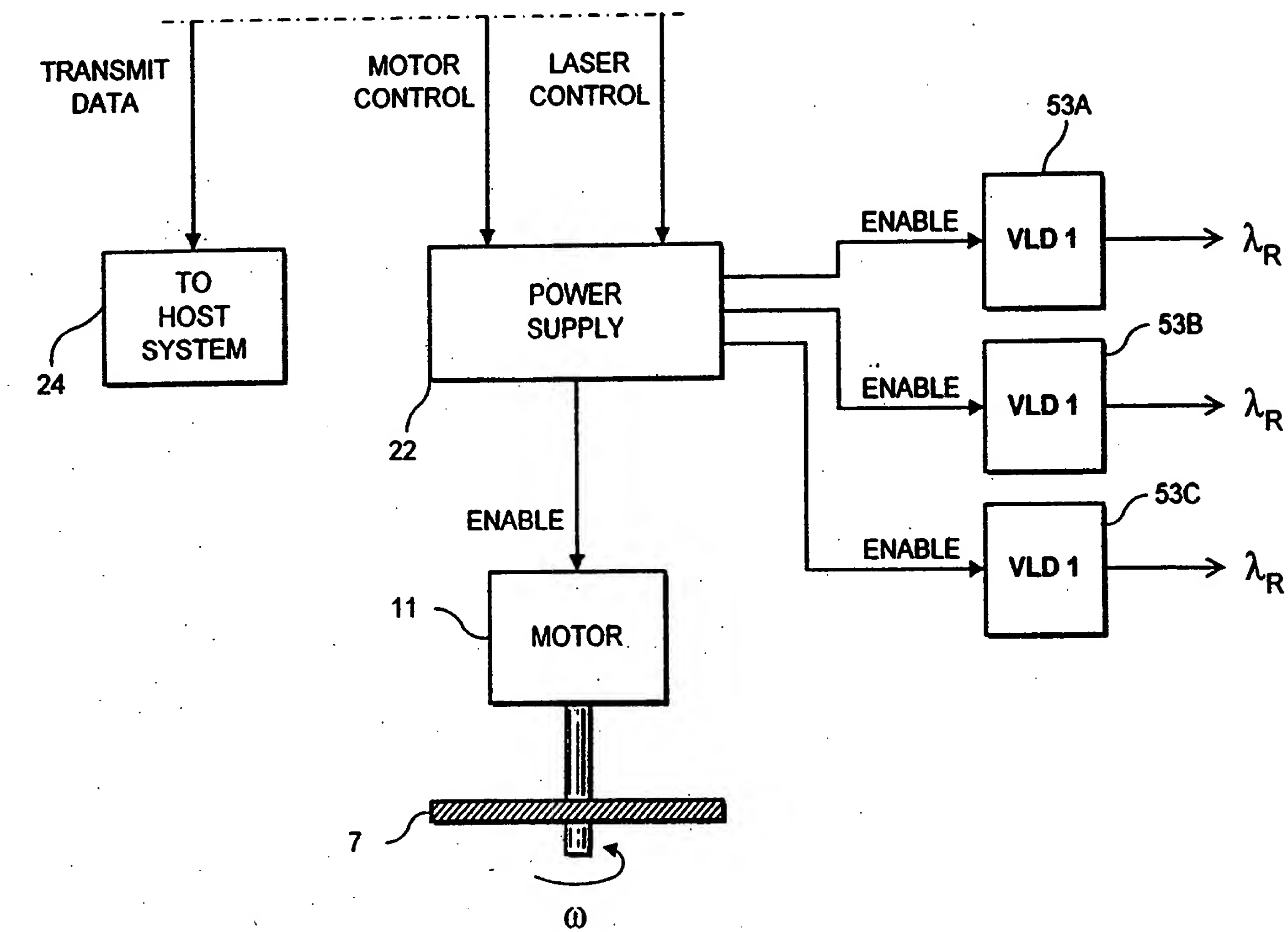
TRANSMIT DATA
MOTOR CONTROL
LASER CONTROL
TO HOST SYSTEM
24
POWER SUPPLY
22
ENABLE
MOTOR
11
7
ω
53A
VLD 1
ENABLE
λR
53B
VLD 1
ENABLE
λR
53C
VLD 1
ENABLE
λR

F I G. 4C

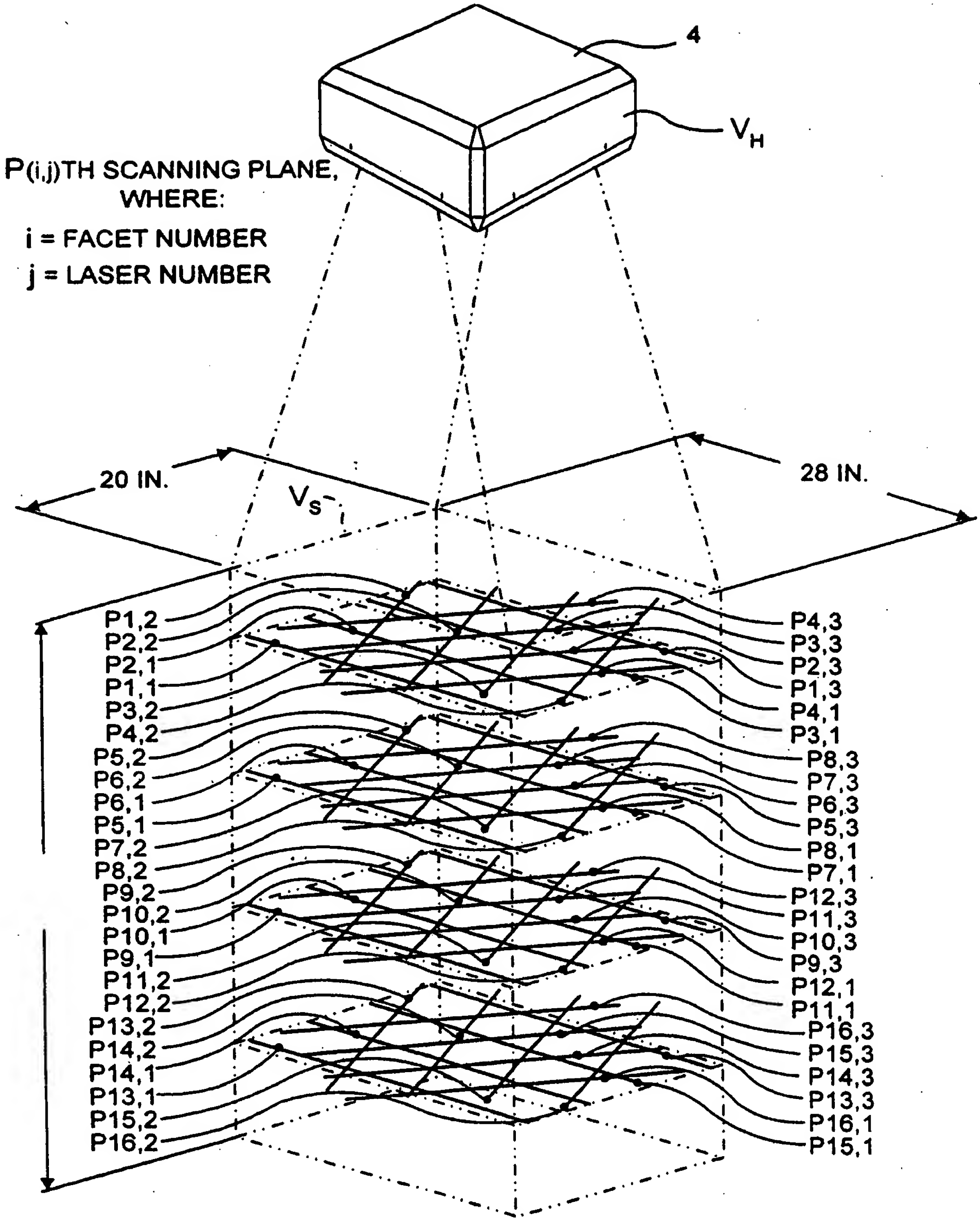
4
V_H
P(i,j)TH SCANNING PLANE, WHERE:
i = FACET NUMBER
j = LASER NUMBER
20 IN.
28 IN.
V_S
P1,2
P2,2
P2,1
P1,1
P3,2
P4,2
P5,2
P6,2
P6,1
P5,1
P7,2
P8,2
P9,2
P10,2
P10,1
P9,1
P11,2
P12,2
P13,2
P14,2
P14,1
P13,1
P15,2
P16,2
P4,3
P3,3
P2,3
P1,3
P4,1
P3,1
P8,3
P7,3
P6,3
P5,3
P8,1
P7,1
P12,3
P11,3
P10,3
P9,3
P12,1
P11,1
P16,3
P15,3
P14,3
P13,3
P16,1
P15,1

FIG. 5

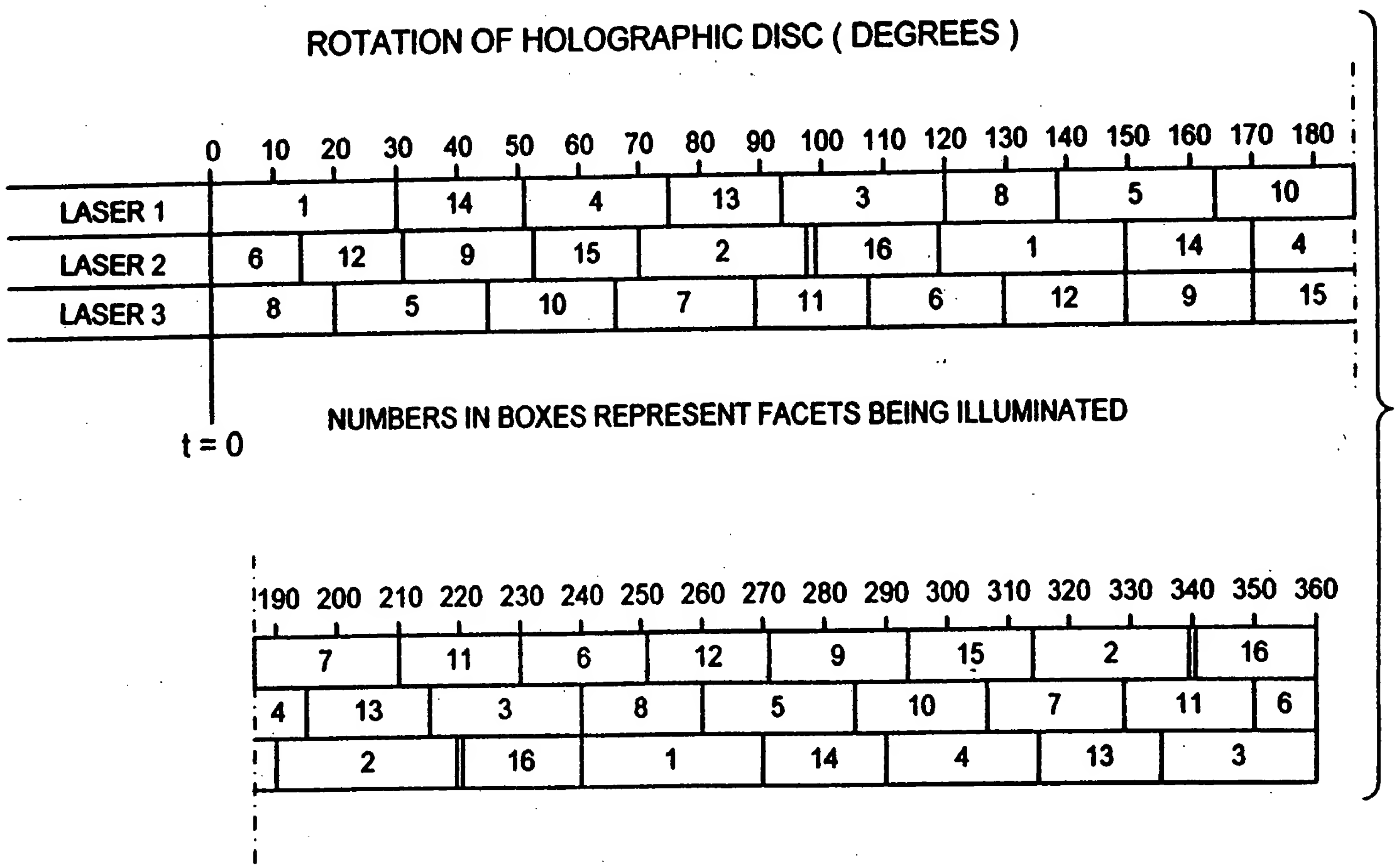
ROTATION OF HOLOGRAPHIC DISC (DEGREES)
0 10 20 30 40 50 60 70 80 90 100 110 120 130 140 150 160 170 180
LASER 1
1 14 4 13 3 8 5 10
LASER 2
6 12 9 15 2 16 1 14 4
LASER 3
8 5 10 7 11 6 12 9 15
t = 0
NUMBERS IN BOXES REPRESENT FACETS BEING ILLUMINATED
190 200 210 220 230 240 250 260 270 280 290 300 310 320 330 340 350 360
7 11 6 12 9 15 2 16
4 13 3 8 5 10 7 11 6
2 16 1 14 4 13 3

F I G. 5A

ADJACENT FOCAL REGIONS OF THE HOLOGRAPHIC DISC

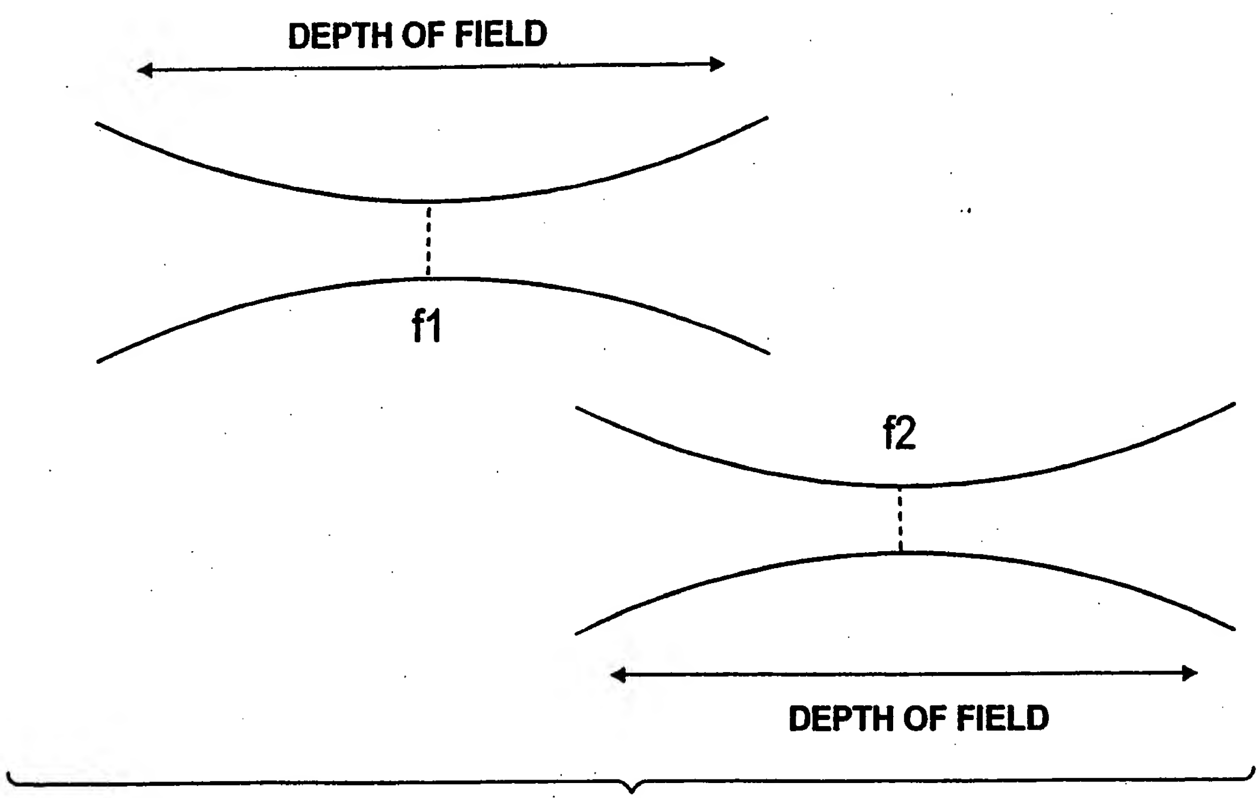

F I G. 6A

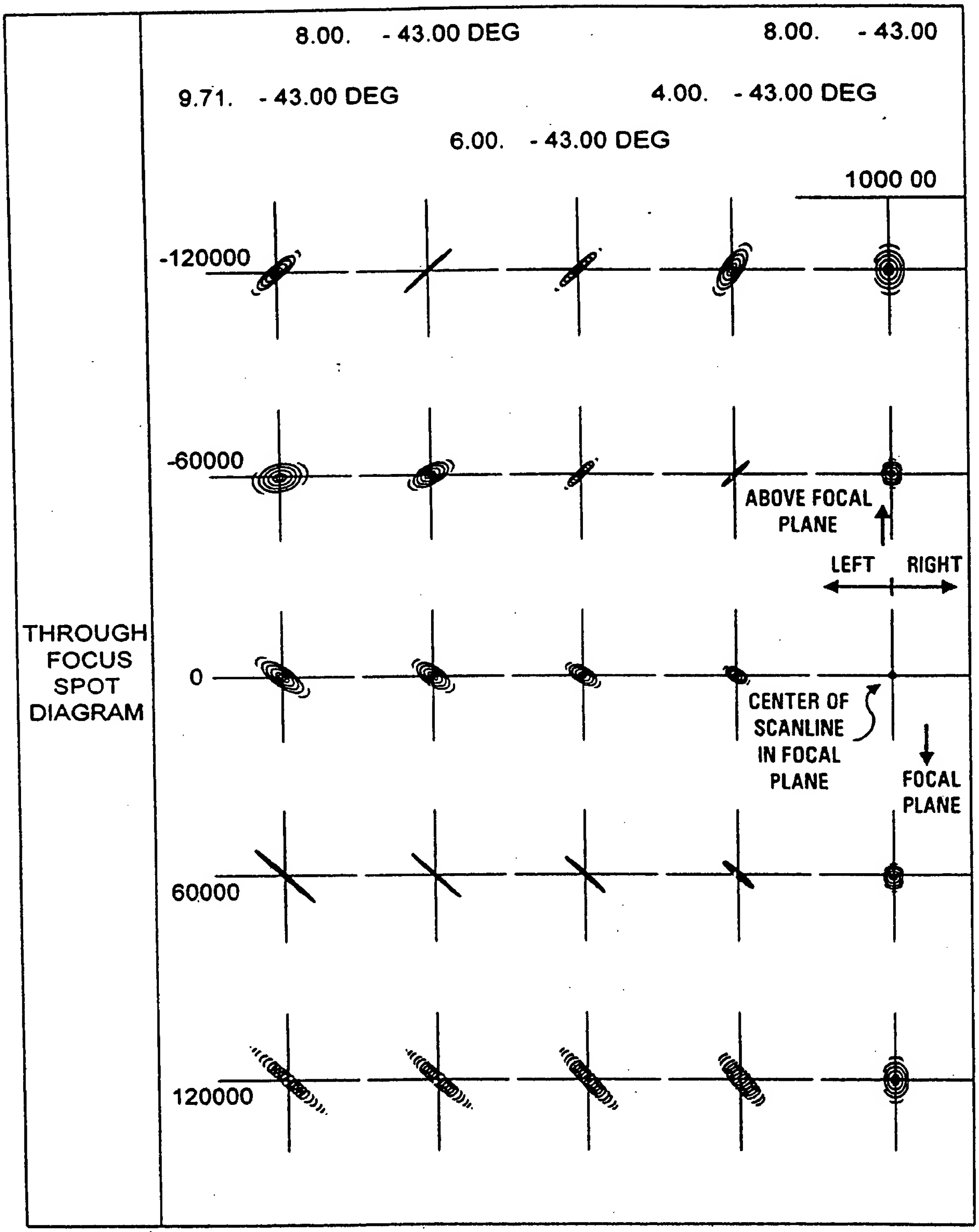
8.00. - 43.00 DEG
8.00. - 43.00
9.71. - 43.00 DEG
4.00. - 43.00 DEG
6.00. - 43.00 DEG
1000 00
-120000
-60000
ABOVE FOCAL PLANE
LEFT
RIGHT
THROUGH FOCUS SPOT DIAGRAM
0
CENTER OF SCANLINE IN FOCAL PLANE
FOCAL PLANE
60000
120000

F I G. 6B

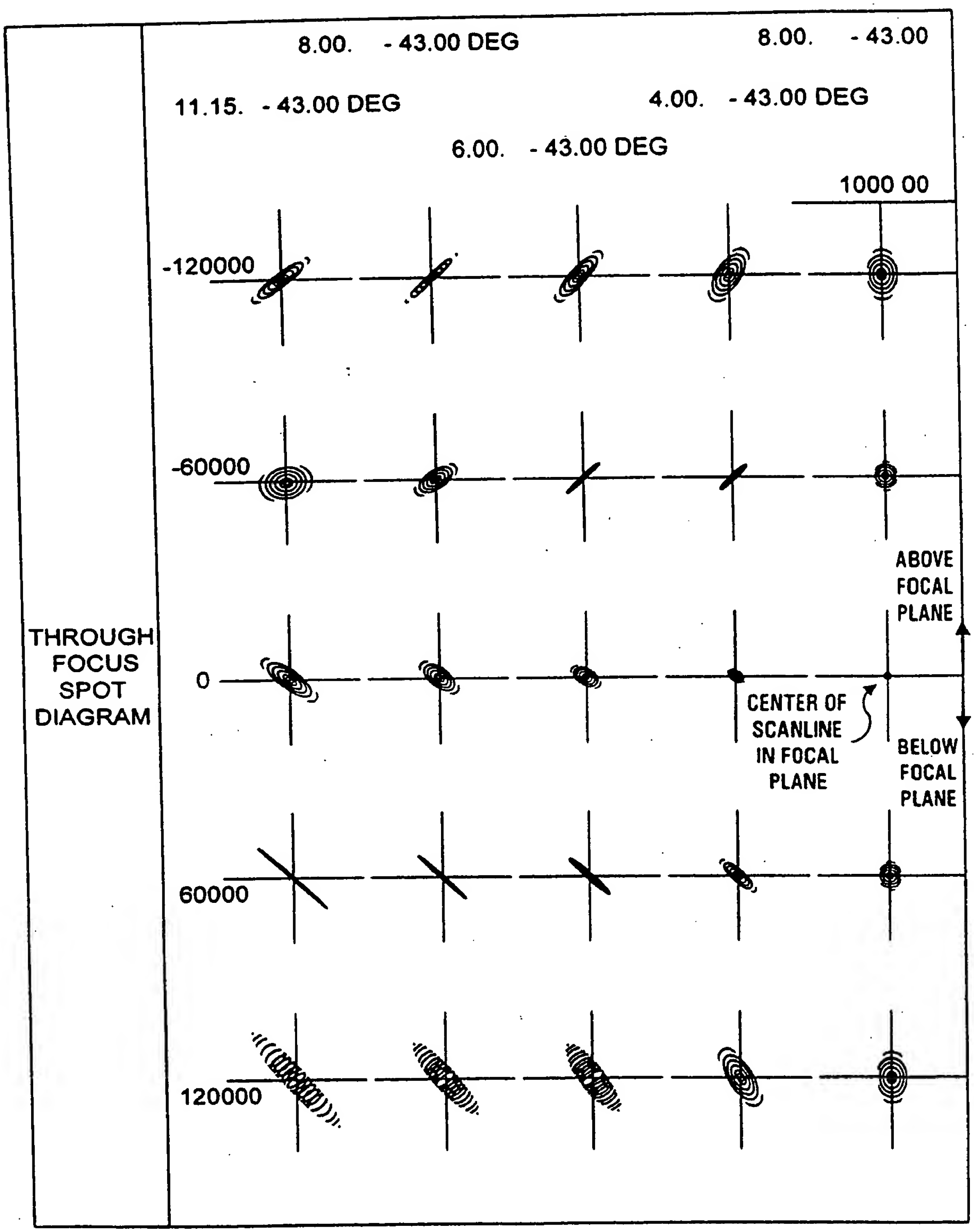
8.00. - 43.00 DEG
8.00. - 43.00
11.15. - 43.00 DEG
4.00. - 43.00 DEG
6.00. - 43.00 DEG
1000 00
THROUGH FOCUS SPOT DIAGRAM
-120000
-60000
0
60000
120000
ABOVE FOCAL PLANE
CENTER OF SCANLINE IN FOCAL PLANE
BELOW FOCAL PLANE

FIG. 6C

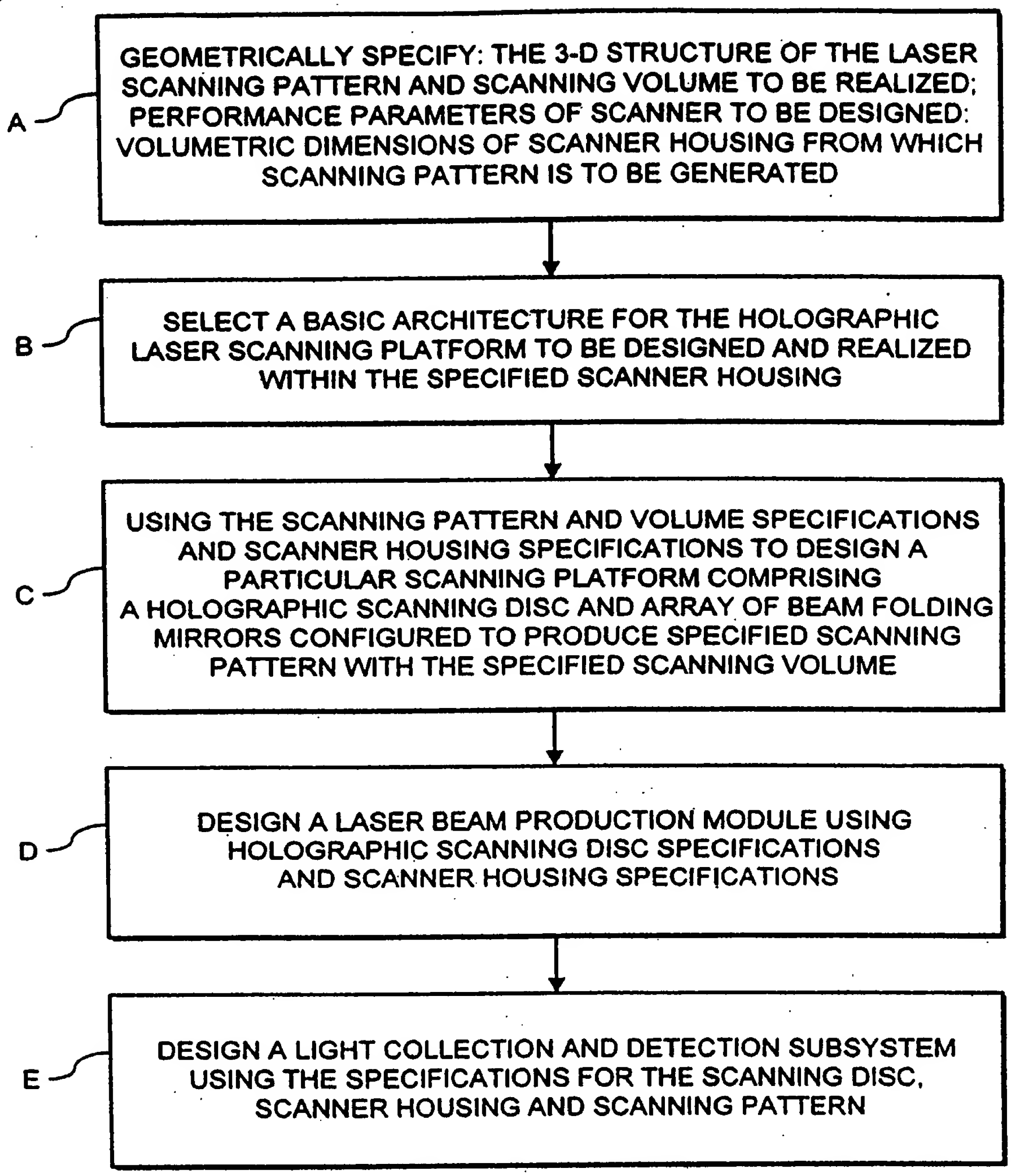
GEOMETRICALLY SPECIFY: THE 3-D STRUCTURE OF THE LASER SCANNING PATTERN AND SCANNING VOLUME TO BE REALIZED; PERFORMANCE PARAMETERS OF SCANNER TO BE DESIGNED: VOLUMETRIC DIMENSIONS OF SCANNER HOUSING FROM WHICH SCANNING PATTERN IS TO BE GENERATED
A
SELECT A BASIC ARCHITECTURE FOR THE HOLOGRAPHIC LASER SCANNING PLATFORM TO BE DESIGNED AND REALIZED WITHIN THE SPECIFIED SCANNER HOUSING
B
USING THE SCANNING PATTERN AND VOLUME SPECIFICATIONS AND SCANNER HOUSING SPECIFICATIONS TO DESIGN A PARTICULAR SCANNING PLATFORM COMPRISING A HOLOGRAPHIC SCANNING DISC AND ARRAY OF BEAM FOLDING MIRRORS CONFIGURED TO PRODUCE SPECIFIED SCANNING PATTERN WITH THE SPECIFIED SCANNING VOLUME
C
DESIGN A LASER BEAM PRODUCTION MODULE USING HOLOGRAPHIC SCANNING DISC SPECIFICATIONS AND SCANNER HOUSING SPECIFICATIONS
D
DESIGN A LIGHT COLLECTION AND DETECTION SUBSYSTEM USING THE SPECIFICATIONS FOR THE SCANNING DISC, SCANNER HOUSING AND SCANNING PATTERN
E

FIG. 7

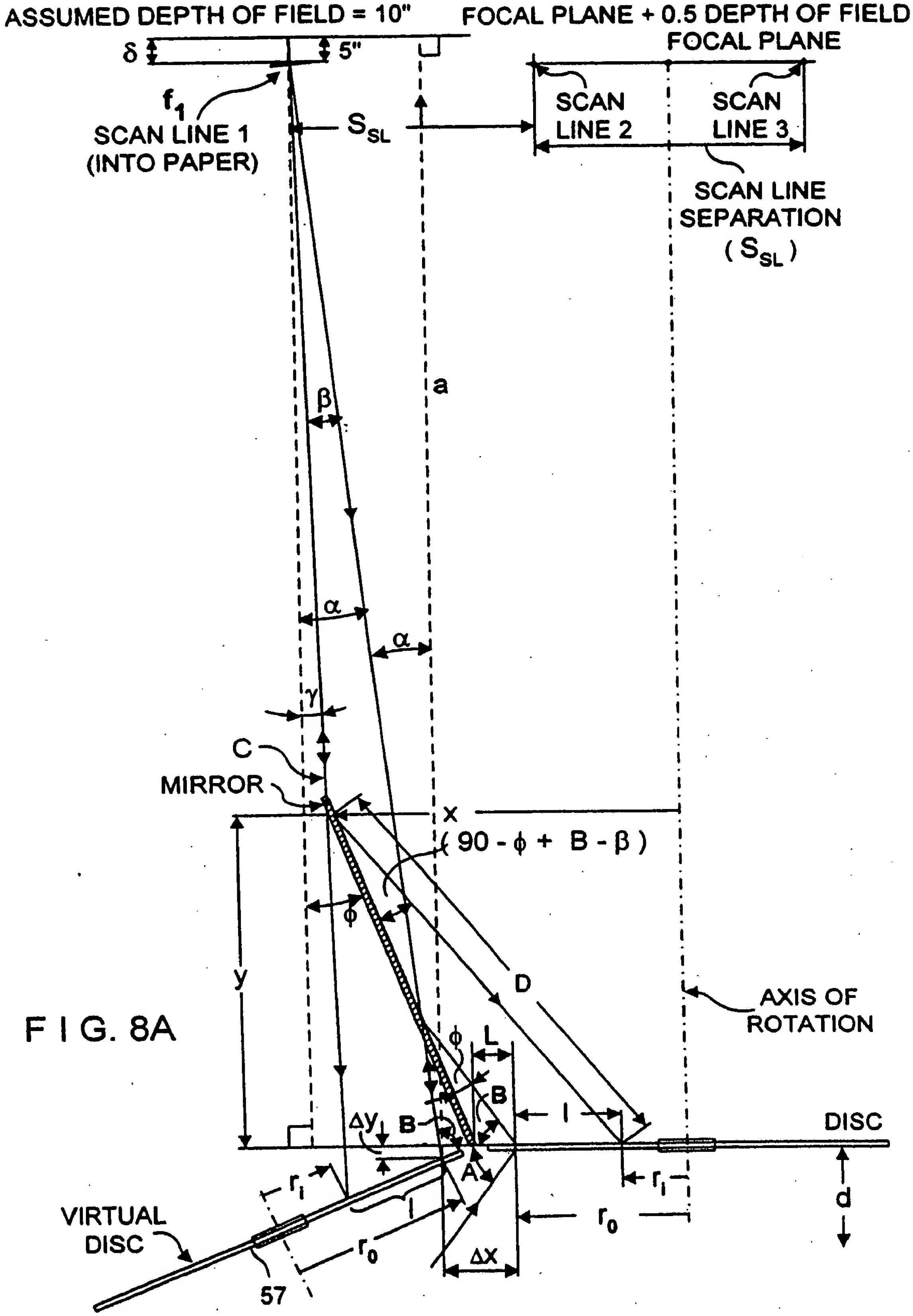
ASSUMED DEPTH OF FIELD = 10"
FOCAL PLANE + 0.5 DEPTH OF FIELD
FOCAL PLANE
δ
5"
f_1
SCAN LINE 1 (INTO PAPER)
S_{SL}
SCAN LINE 2
SCAN LINE 3
SCAN LINE SEPARATION (S_{SL})
a
β
α
α
γ
C
MIRROR
x
(90 - φ + B - β)
φ
y
D
AXIS OF ROTATION
φ
L
B
B
l
DISC
Δy
A
r_i
r_i
l
d
VIRTUAL DISC
r_0
r_0
ΔX
57

F I G. 8A

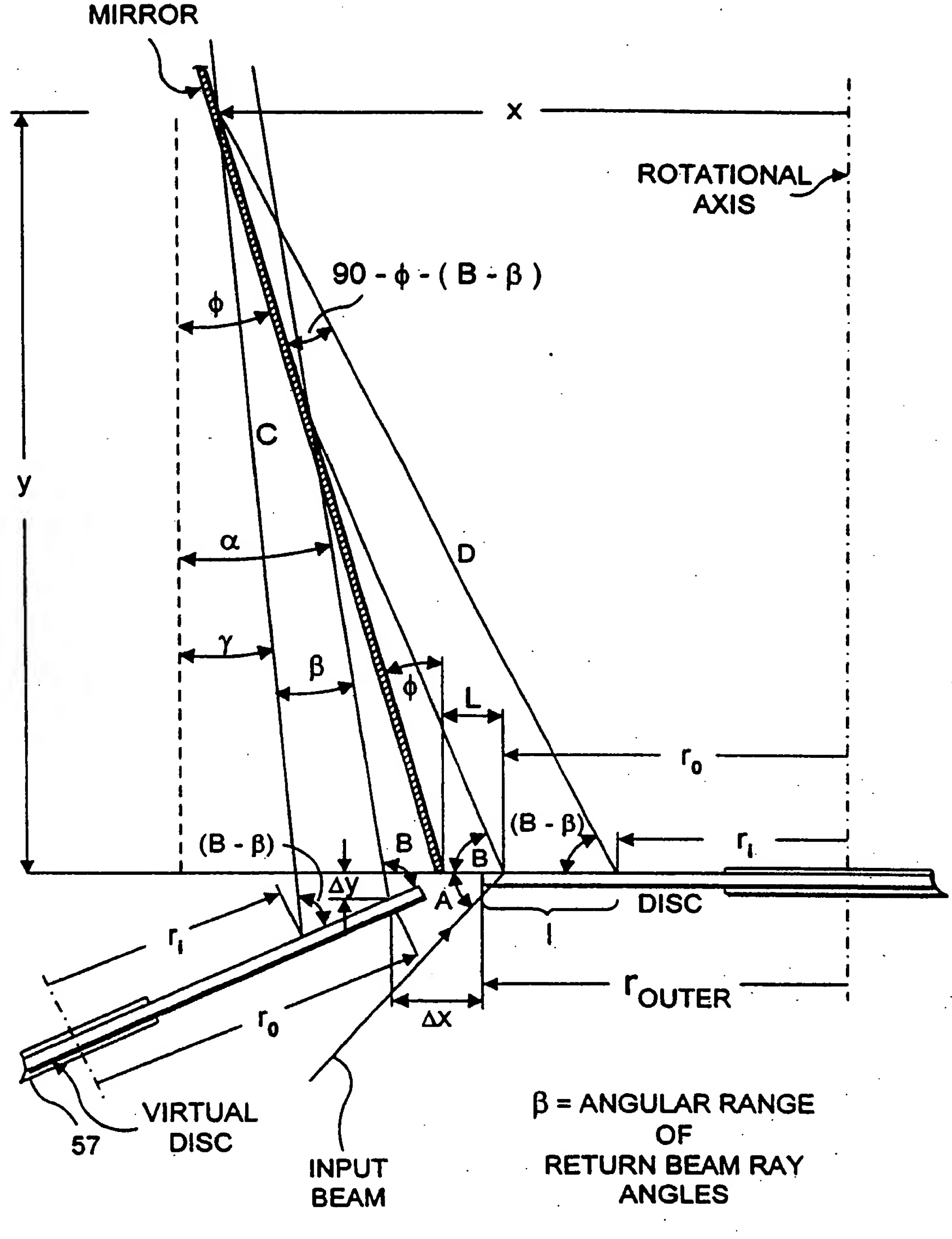
MIRROR
x
ROTATIONAL AXIS
90 - ϕ - (B - β)
ϕ
C
y
α
D
γ
β
ϕ
L
r0
(B - β)
(B - β)
B
B
ri
Δy
A
DISC
l
ri
rOUTER
r0
ΔX
VIRTUAL DISC
57
INPUT BEAM
β = ANGULAR RANGE OF RETURN BEAM RAY ANGLES

FIG. 8A1

(1) THE RADIUS TO BEAM-INCIDENT-POINT ON THE HOLOGRAPHIC SCANNING DISC, ASSIGNED THE SYMBOLIC NOTATION "r_0"

(2) SCANLINE SEPARATION BETWEEN ADJACENT SCANLINES AT THE FOCAL PLANE OF THE (i, J)-TH SCANLINE, ASSIGNED THE SYMBOLIC NOTATION "S_{SL}"

(3) THE SCANLINE LENGTH (MEASURED INTO THE PAPER) FOR THE (i, J)-TH SCANLINE, ASSIGNED THE SYMBOLIC NOTATION "L_{SL}"

(4) THE DISTANCE MEASURED FROM THE SCANNING DISC TO THE FOCAL PLANE OF THE (i, J)-TH SCANLINE, ASSIGNED THE SYMBOLIC NOTATION "a_i"

(5) THE DISTANCE FROM RADIUS TO BEAM-INCIDENT-POINT r_0 TO BEAM FOLDING MIRROR, ASSIGNED THE SYMBOLIC NOTATION "L"

(6) THE TILT ANGLE OF THE J-TH BEAM FOLDING MIRROR ASSOCIATED WITH GENERATION OF THE (i, J)-TH SCANLINE, ASSIGNED THE SYMBOLIC NOTATION "ϕ_j"

(7) THE TILT ANGLE OF THE VIRTUAL SCANNING DISC, ASSIGNED THE SYMBOLIC NOTATION "2ϕ"

(8) THE LATERAL SHIFT OF THE BEAM INCIDENT POINT ON THE VIRTUAL SCANNING DISC, ASSIGNED THE SYMBOLIC NOTATION "ΔX"

(9) THE VERTICAL SHIFT OF THE BEAM INCIDENT POINT ON THE VIRTUAL SCANNING DISC, ASSIGNED THE SYMBOLIC NOTATION "ΔY"

(10) THE DISTANCE FROM THE ROTATION AXIS TO THE BEAM INCIDENT POINT ON THE VIRTUAL SCANNING DISC, ASSIGNED THE SYMBOLIC NOTATION "$r_0+\Delta X$"

(11) THE DISTANCE FROM THE BEAM INCIDENT POINT ON THE VIRTUAL SCANNING DISC TO THE FOCAL PLANE WITHIN WHICH THE (i, j)-TH SCANLINE RESIDES, ASSIGNED THE SYMBOLIC NOTATION "f_i"

(12) THE DIAMETER OF THE CROSS-SECTION OF THE LASER BEAM SCANNING STATION, ASSIGNED THE SYMBOLIC NOTATION "d_{BEAM}"

(13) THE ANGULAR GAP BETWEEN ADJACENT HOLOGRAPHIC SCANNING FACETS, ASSIGNED THE SYMBOLIC NOTATION "d_{GAP}"

(14) THE OUTER RADIUS OF THE AVAILABLE LIGHT COLLECTION REGION ON THE HOLOGRAPHIC SCANNING DISC, ASSIGNED THE SYMBOLIC NOTATION "r_{OUTER}"

F I G. 8B1

(15) THE INNER RADIUS OF THE AVAILABLE LIGHT COLLECTION REGION ON THE HOLOGRAPHIC SCANNING FACET, ASSIGNED THE SYMBOLIC NOTATION "r_{INNER}"

(16) ONE-HALF OF THE DEPTH OF FIELD OF THE (i, J)-TH SCANLINE, ASSIGNED THE SYMBOLIC NOTATION "δ"

(17) THE DISTANCE FROM THE MAXIMUM READ DISTANCE (f_i + 5") TO THE INNER RADIUS r_i OF THE SCANNING FACET, ASSIGNED THE SYMBOLIC NOTATION "C"

(18) THE OUTER RAY ANGLE MEASURED RELATIVE TO THE NORMAL TO THE i-TH HOLOGRAPHIC FACET, ASSIGNED THE SYMBOLIC NOTATION "α"

(19) THE INNER RAY ANGLE MEASURED RELATIVE TO THE NORMAL TO THE i-TH HOLOGRAPHIC FACET, ASSIGNED THE SYMBOLIC NOTATION "γ"

(20) THE LIGHT COLLECTION ANGLE MEASURED FROM THE FOCAL POINT OF THE i-TH FACET TO THE LIGHT COLLECTION AREA OF THE SCANNING FACET, ASSIGNED THE SYMBOLIC NOTATION "β"

(21) THE INTERSECTION OF THE BEAM FOLDING MIRROR AND LINE C, ASSIGNED THE SYMBOLIC NOTATION "X"

(21A) THE INTERSECTION OF THE BEAM FOLDING MIRROR AND LINE C, ASSIGNED THE SYMBOLIC NOTATION "Y"

(22) THE DISTANCE MEASURED FROM THE INNER RADIUS TO THE POINT OF MIRROR INTERSECTION, ASSIGNED THE SYMBOLIC NOTATION "D"

(23) THE DISTANCE MEASURED FROM THE BASE OF THE SCANNER HOUSING TO THE TOP OF THE j -TH BEAM FOLDING MIRROR , ASSIGNED THE SYMBOLIC NOTATION "h"

(24) THE DISTANCE MEASURED FROM THE SCANNING DISC TO THE BASE OF THE HOLOGRAPHIC SCANNER, ASSIGNED THE SYMBOLIC NOTATION "d"

(25) THE FOCAL LENGHT OF THE i-TH HOLOGRAPHIC SCANNING FACET FROM THE SCANNING FACET TO THE CORRESPONDING FOCAL PLANE WITHIN THE SCANNING VOLUME, ASSIGNED THE SYMBOLIC NOTATION "f_i"

(26) INCIDENT BEAM ANGLE, ASSIGNED THE SYMBOLIC NOTATION "A_i"

F I G. 8B2

(27) DIFFRACTED BEAM ANGLE, ASSIGNED THE SYMBOLIC NOTATION "B_i"

(28) THE ANGLE OF THE J-TH LASER BEAM MEASURED FROM THE VERTICAL, ASSIGNED THE SYMBOLIC NOTATION "α"

(29) THE SCAN ANGLE OF THE LASER BEAM , ASSIGNED THE SYMBOLIC NOTATION "θ_{SI}"

(30) THE SCAN MULTIPLICATION FACTOR FOR THE i-TH HOLOGRAPHIC FACET, ASSIGNED THE SYMBOLIC NOTATION "M_i"

(31) THE FACET ROTATION ANGLE FOR THE i-TH HOLOGRAPHIC FACET, ASSIGNED THE SYMBOLIC NOTATION "θ_{ROTi}"

(32) ADJUSTED FACET ROTATION ANGLE ACCOUNTING FOR DEADTIME, ASSIGNED THE SYMBOLIC NOTATION "θ'_{ROTi}"

(33) THE LIGHT COLLECTION EFFICIENCY FACTOR FOR THE i-TH HOLOGRAPHIC FACET, NORMALIZED RELATIVE TO THE 16TH FACET, ASSIGNED THE SYMBOLIC NOTATION "ξ_i"

(34) THE MAXIMUM LIGHT COLLECTION AREA FOR THE i-TH HOLOGRAPHIC FACET, ASSIGNED THE SYMBOLIC NOTATION "$Area_i$"

(35) THE BEAM SPEED AT THE CENTER OF THE (i, j)-TH SCANLINE, ASSIGNED THE SYMBOLIC NOTATION "V_{CENTER}"

(36) THE ANGLE OF SKEW OF THE DIFFRACTED LASER BEAM AT THE CENTER OF THE i-TH HOLOGRAPHIC FACET, ASSIGNED THE SYMBOLIC NOTATION "ϕ_{SKEW}"

(37) THE MAXIMUM BEAM SPEED OF ALL LASER BEAMS PRODUCED BY THE HOLOGRAPHIC SCANNING DISC, ASSIGNED THE SYMBOLIC NOTATION "V_{MAX}"

(38) THE MINIMUM BEAM SPEED OF ALL LASER BEAMS PRODUCED BY THE HOLOGRAPHIC SCANNING DISC, ASSIGNED THE SYMBOLIC NOTATION "V_{MIN}"

(39) THE RATIO OF THE MAXIMUM BEAM SPEED TO THE MINIMUM BEAM SPEED, ASSIGNED THE SYMBOLIC NOTATION " V_{MAX} / V_{MIN}"

(40) THE DEVIATION OF THE LIGHT RAYS REFLECTED OFF THE PARABOLIC LIGHT REFLECTING MIRROR BENEATH THE SCANNING DISC, FROM THE BRAGG ANGLE FOR THE FACET, ASSIGNED THE SYMBOLIC NOTATION "δ_e"

F I G. 8B3

PARAMETER EQUATION USED IN THE SPREADSHEET DESIGN OF THE SCANNER

(1) $\Delta x \quad := L\,(1 + \cos(2\phi))$

(2) $\Delta y \quad := L \sin(2\phi)$

(3) $\Delta y \quad := r_0 + \Delta x$

(4) $C \quad := \sqrt{(f+\delta)^2 + l^2 + 2\,(f+\delta)\,l\cos(B)}$

LAW OF COSINES, WHERE : $l = r_{outer} - r_{inner}$

$\beta = \alpha - \gamma = B + 2\phi - 90 - \gamma$

(5) $\alpha \quad := B - 90 + 2\phi$

(6) $r \quad := \alpha - \cos\left[\dfrac{(f+\delta)^2 + C^2 - l^2}{2\,(f+\delta)\,C}\right]$

(7) $\beta \quad := \alpha - \gamma$

(8) $X \quad := D\cos(B-\beta) + r_i$

(9) $Y \quad := D\sin(B-\beta)$

(10) $D \quad := \dfrac{\left[r_0 + L - r_i\right]\sin(90+\phi)}{\sin(90 - B + \beta - \phi)}$ (LAW OF SINES)

(11) $h \quad := Y + d$

F I G. 8C1

$$(12)\quad f_i := \sqrt{a_i^2 + \left[m\,S_{SL} - \left[r_0 + \Delta x\right]\right]^2}$$

m IS A FACTOR THAT VARIES FROM SCAN LINE TO SCAN LINE AND IS DETERMINED BY SCAN LINE SEPARATION AND DISTANCE FROM THE ROTATIONAL AXIS OF THE DISC.

$$(13)\quad B_i := \operatorname{atan}\left[\left[\frac{m\,S_{SL} - \left[r_0 + \Delta x\right]}{a_i}\right]\right] + 90 - 2\phi$$

$$(14)\quad \theta_{si} := 2\operatorname{atan}\left[\left[\frac{\frac{1}{2}\ \mathrm{ScanLineLength}}{f_i}\right]\right]$$

$$(15)\quad M_i := \frac{r_0}{f_i} + \cos(\lambda_i) + \cos(B_i)$$

$$(16)\quad \theta_{roti} := \frac{\theta_{si}}{M_i}$$

$$(17)\quad \theta'_{roti} := \theta_{roti} + \underbrace{\frac{d_{beam}}{r_0} + \frac{d_{gap}}{r_0}}_{\Theta_{dead}}$$

$$(18)\quad \xi_i := \left[\frac{f_i}{f_{16}}\right]^2 \frac{\sin\left[B_{16}\right]}{\sin(B_i)}\ H_i$$

$$(19)\quad \mathrm{Area}_i := \pi\left[r_{outer}^2 + r_{inner}^2\right]\frac{\xi_i}{\sum_{i=1}^{16}\left[\xi_i\right]} \qquad i = 1,2,\ldots 16$$

F I G. 8C2

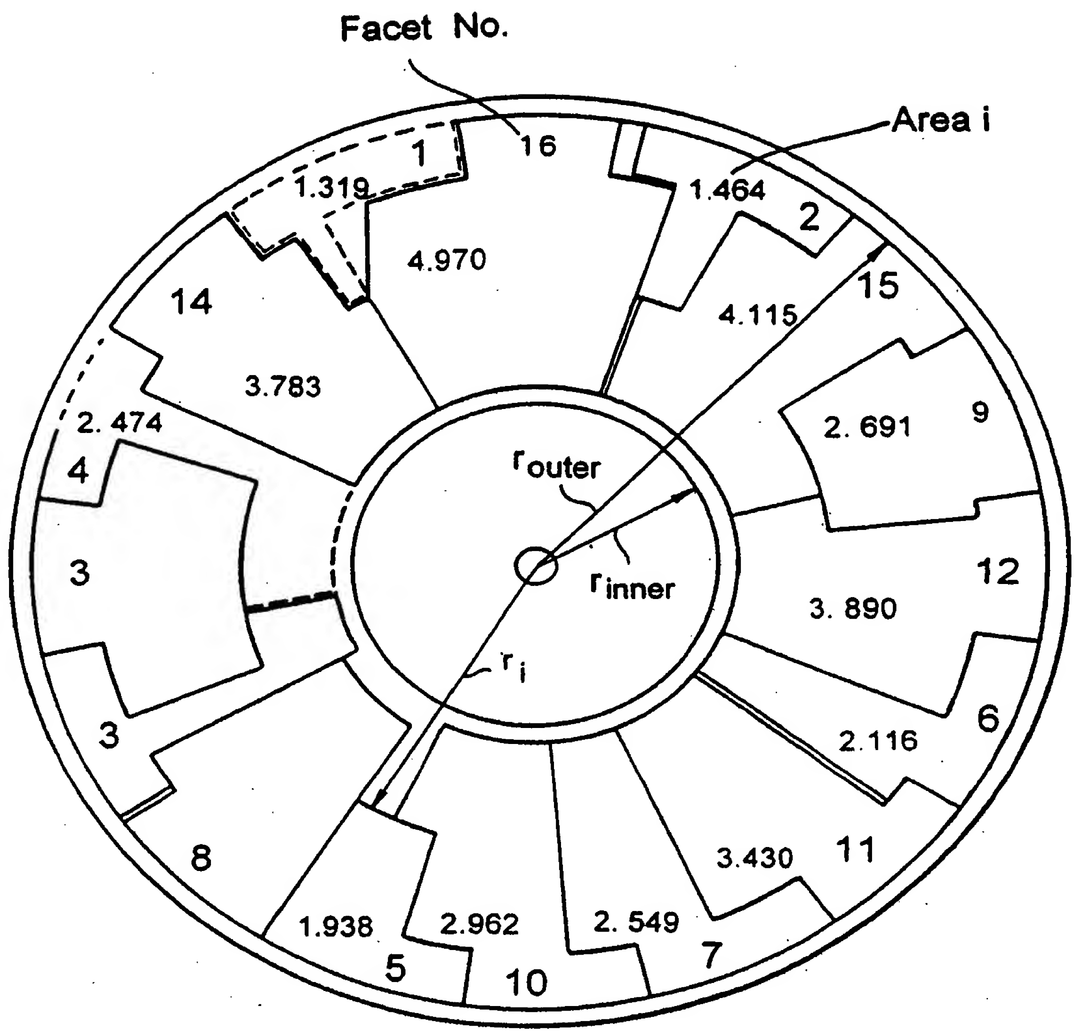
Facet No.
Area i
16
1
1.319
1.464
2
4.970
14
15
4.115
3.783
2. 474
2. 691
9
4
r_{outer}
r_{inner}
3
12
3. 890
r_i
3
6
2.116
8
3.430
11
1.938
2.962
2. 549
7
5
10

FIG. 9

GEOMETRICAL OPTICS MODEL FOR HOLOGRAPHIC (TOTAL OUT AND BACK) LIGHT DIFFRACTION EFFICIENCY CALCULATIONS

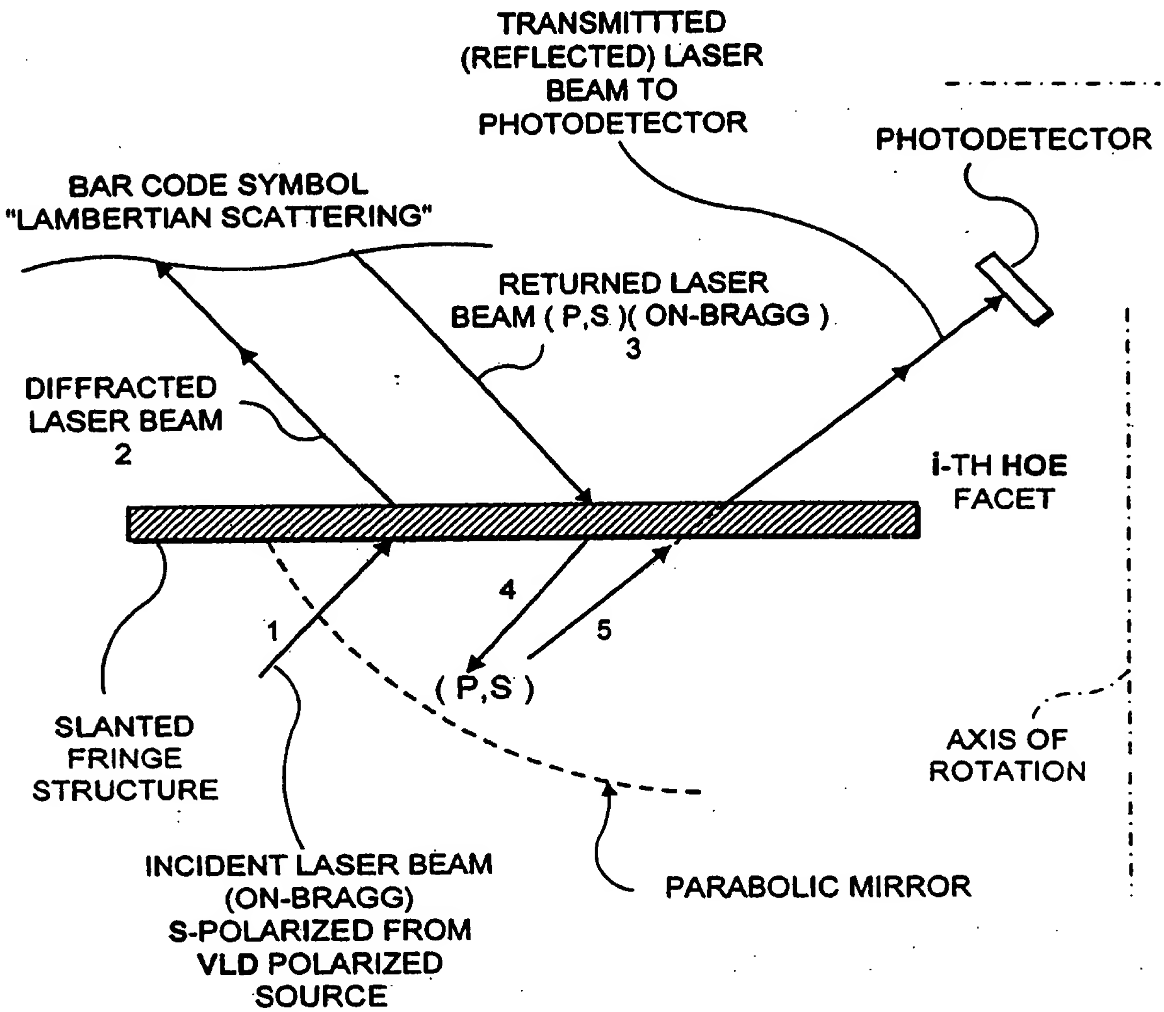

F I G. 10A1

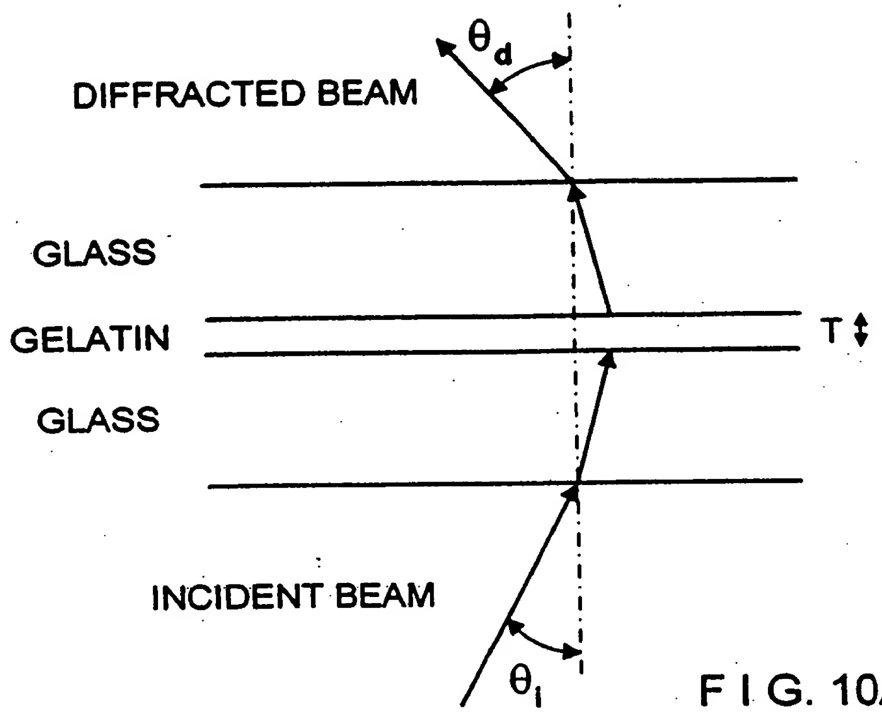

FIG. 10A2

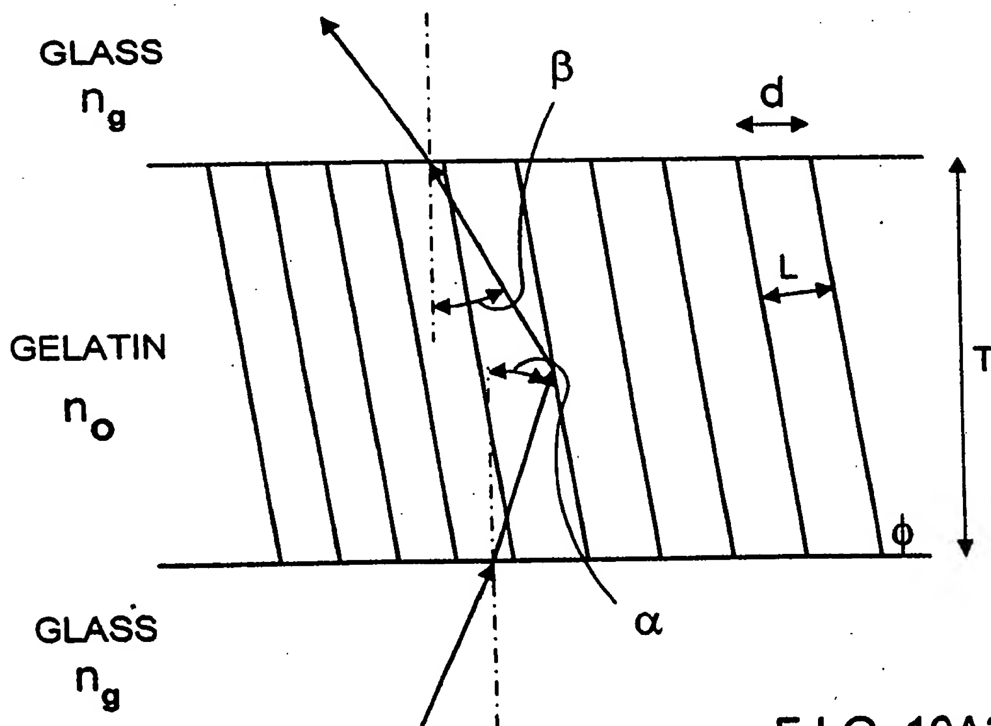

FIG. 10A3

SCANNING DISC ANALYSIS INCLUDING FRESNEL LOSSES AND ESTIMATED INTERNAL LOSSES OF 10% .THE 10% LOSS INCLUDES ABOUT 8% SCATTERING AND ABSORPTION AND ABOUT 2% FRESNEL LOSSES AT THE DCG/GLASS INTERFACES

S AND P POLARIZATION DIFFRACTION EFFICIENCIES FOR THE MOST GENERAL CASE

S AND P DIFFRACTION EFFICIENCIES AT THE BRAGG ANGLE AS A FUNCTION OF **n1**, THE **delta-n** OF THE HOLOGRAPHIC MEDIUM. SLANTED FRINGES AND EXTERNAL ANGLES ARE INCLUDED. THIS IS A GENERALIZATION OF THE MORE COMMON CASE OF ZERO SLANT. **Delta-n (n1)** IS IN STEPS OF 0.001 **microns**.

DEFINITIONS:

θ_i = ANGLE OF INCIDENCE (EXTERNAL) ($\theta_i = 90^o - A_i$)
α = ANGLE OF INCIDENCE (INTERNAL)
θ_d = ANGLE OF DIFFRACTION (EXTERNAL) ($\theta_d = 90^o - B_i$)
β = ANGLE OF DIFFRACTION (INTERNAL)
δ = DEVIATION FROM THE BRAGG ANGLE
ϕ = TILT OF BRAGG PLANES
= $\pi/2$ FOR NO TILT
L = SEPARATION OF THE BRAGG PLANES
T = THICKNESS OF HOE MEDIUM
d = EXTERNAL FRINGE SPACING
ng = REFRACTIVE INDEX OF THE GLASS SUBSTRATE
n0 = AVERAGE REFRACTIVE INDEX OF THE HOE MEDIUM
Δn1 = delta-n OF HOE FRINGE STRUCTURE
λ_a = WAVELENGTH IN AIR
$\delta\lambda$ = DEVIATION FROM λ_a (BRAGG λ)

FIG. 10B

FIXED, OR ESTABLISHED PARAMETERS:

$n0, \Delta n1, \theta_i, \theta_d, \delta, \delta\lambda, \lambda_a, T.$

$n_0 := 1.4$ $n_g := 1.515$ $deg = \frac{\pi}{180}$

$\Delta n_1 := 0, .001, \ldots, .2$

$\theta_i := 43\ deg$

$\theta_d := 26.6\ deg$

$\delta := 0\ deg$

$\delta_\lambda := 0$

$T := 2.2$

$\lambda_a := .670$

F I G. 10B1

(1) $\alpha := \mathrm{asin}\left[\frac{\sin[\theta_i]}{n_0}\right]$

(2) $\beta := \mathrm{asin}\left[\frac{\sin[\theta_d]}{n_0}\right]$

(3) $\phi := \frac{\pi}{2} - \frac{\beta - \alpha}{2}$

(4) $d := \frac{\lambda_a}{\sin[\theta_i] + \sin[\theta_d]}$

GRATING EQUATION

(5) $L := d \sin(\phi)$

(6) $C_R := \cos(\alpha)$

(7) $C_S := \cos(\alpha) - \frac{\lambda_a}{n_0 L}\cos(\phi)$

(8) $N[n_1] := \pi n_1 \frac{T}{\lambda_a \sqrt{C_R C_S}}$

(9) $\Gamma := 2\pi\delta \frac{\sin(\phi - \alpha)}{L} - \delta_\lambda \frac{\pi}{n_0 L^2}$

(10) $S[n_1] := \Gamma \frac{T}{2 C_S}$

F I G. 10C1

DIFFRACTION EFFICIENCIES: E_s AND E_p (INCLUDING FRESNEL REFLECTION LOSSES AND ESTIMATED INTERNAL LOSSES OF 10%)
ASSUMING n - glass = 1.5155 AND ANGLES AS GIVEN BELOW:

$\theta_i = 43$ deg $\qquad \theta_d = 26.6$ deg

(11) $$E_S[n_1] := \frac{\left[\sin\left[\sqrt{N[n_1]^2 + S[n_1]^2}\right]\right]^2}{1 + \dfrac{S[n_1]^2}{N[n_1]^2}} \cdot t_S(1 - .1)$$

(12) $$E_P[n_1] :=$$

$$= \frac{\left[\sin\left[\sqrt{[N[n_1]\ \cos(2(\alpha - \phi))]^2 + S[n_1]^2}\right]\right]^2}{1 + \dfrac{S[n_1]^2}{[N[n_1]\ \cos(2(\alpha - \phi))]^2}} \cdot t_P(1 - .1)$$

POLARIZED INCIDENT BEAM

RETURN BEAM

(13) $$T_S[n_1] := E_S[n_1] \cdot \frac{E_S[n_1] + E_P[n_1]}{2}$$

(T.s IS THE TOTAL OUT-AND-BACK DIFFRACTION EFFICIENCY FOR AN S-POLARIZED OUTGOING BEAM INCIDENT ON THE DISC . INCLUDES FRESNEL REFLECTION LOSSES AND INTERNAL LOSSES OF 10%)

(14) $$H_i(\Delta n) := \frac{T_{S16}(\Delta n)}{T_{S1}(\Delta n)}$$

F I G. 10C2

PARAMETERS FOR CALCULATING THE FRESNEL REFLECTION LOSSES AND TRANSMISSION

(15) $\theta_{r.1} := \operatorname{asin}\left[\dfrac{\sin[\theta_i]}{n_g}\right]$

(16) $\theta_{r.2} := \operatorname{asin}\left[\dfrac{\sin[\theta_d]}{n_g}\right]$

(17) $R_{S.1} := \left[\dfrac{\sin[\theta_i - \theta_{r.1}]}{\sin[\theta_i + \theta_{r.1}]}\right]^2$ S-POLARIZATION REFLECTION AT FIRST (ENTRY) SURFACE OF DISC

(18) $R_{S.2} := \left[\dfrac{\sin[\theta_d - \theta_{r.2}]}{\sin[\theta_d + \theta_{r.2}]}\right]^2$ S-POLARIZATION REFLECTION AT SECOND (EXIT) SURFACE OF DISC

(19) $R_{P.1} := \left[\dfrac{\tan[\theta_i - \theta_{r.1}]}{\tan[\theta_i + \theta_{r.1}]}\right]^2$ P-POLARIZATION REFLECTION AT FIRST (ENTRY) SURFACE OF DISC

(20) $R_{P.2} := \left[\dfrac{\tan[\theta_d - \theta_{r.2}]}{\tan[\theta_d + \theta_{r.2}]}\right]^2$ P-POLARIZATION REFLECTION AT SECOND (EXIT) SURFACE OF DISC

BOTH SURFACES

(21) $t_s := [1 - R_{S.1}] \cdot [1 - R_{S.2}]$ S-POLARIZED FRESNEL TRANSMISSION

(22) $t_p := [1 - R_{P.1}] \cdot [1 - R_{P.2}]$ P-POLARIZED FRESNEL TRANSMISSION

FIG. 10D

FACET No. 1

DIFFRACTION EFFICIENCIES: E_s, E_p, T_s - INCLUDING FRESNEL REFLECTION LOSSES AND ESTIMATED INTERNAL LOSSES OF 10%. (ASSUMING n GLASS = 1.515 AND ANGLES ARE AS GIVEN BELOW)

$\theta_i = 43$ deg $\quad \theta_d = 26.6$ deg $\quad n_0 = 1.4$

$T = 2.2$ microns $\quad \lambda_a = 0.67$

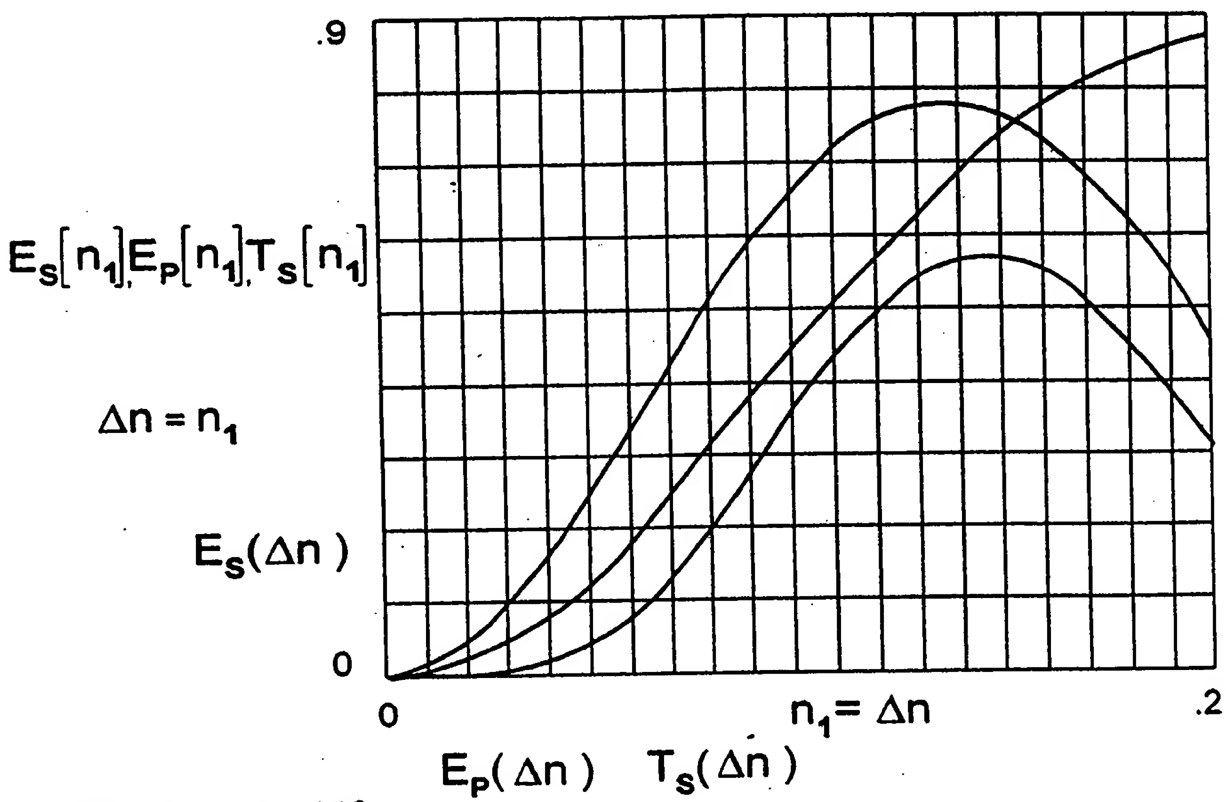

FOR: $n_1 := .146$

$E_s[n_1] = 0.769 \quad E_p[n_1] = 0.694 \quad T_s[n_1] = 0.562$

$H_1 := \dfrac{0.474}{T_s[n_1]} \quad H_1 = 0.843$

H.1 IS THE OUT-AND-BACK DIFFRACTION EFFICIENCY OF FACET 1 RELATIVE TO THE OUT-AND-BACK DIFFRACTION EFFICIENCY OF FACET 16

F I G. 10E1

DIFFRACTION EFFICIENCIES: E_S, E_P, T_S - INCLUDING FRESNEL REFLECTION LOSSES AND ESTIMATED INTERNAL LOSSES OF 10%. (ASSUMING n GLASS = 1.515 AND ANGLES ARE AS GIVEN BELOW)

$\theta_i = 43$ deg $\qquad \theta_d = 41.8$ deg $\qquad n_0 = 1.4$

$T = 2.2$ microns $\qquad \lambda_a = 0.67$

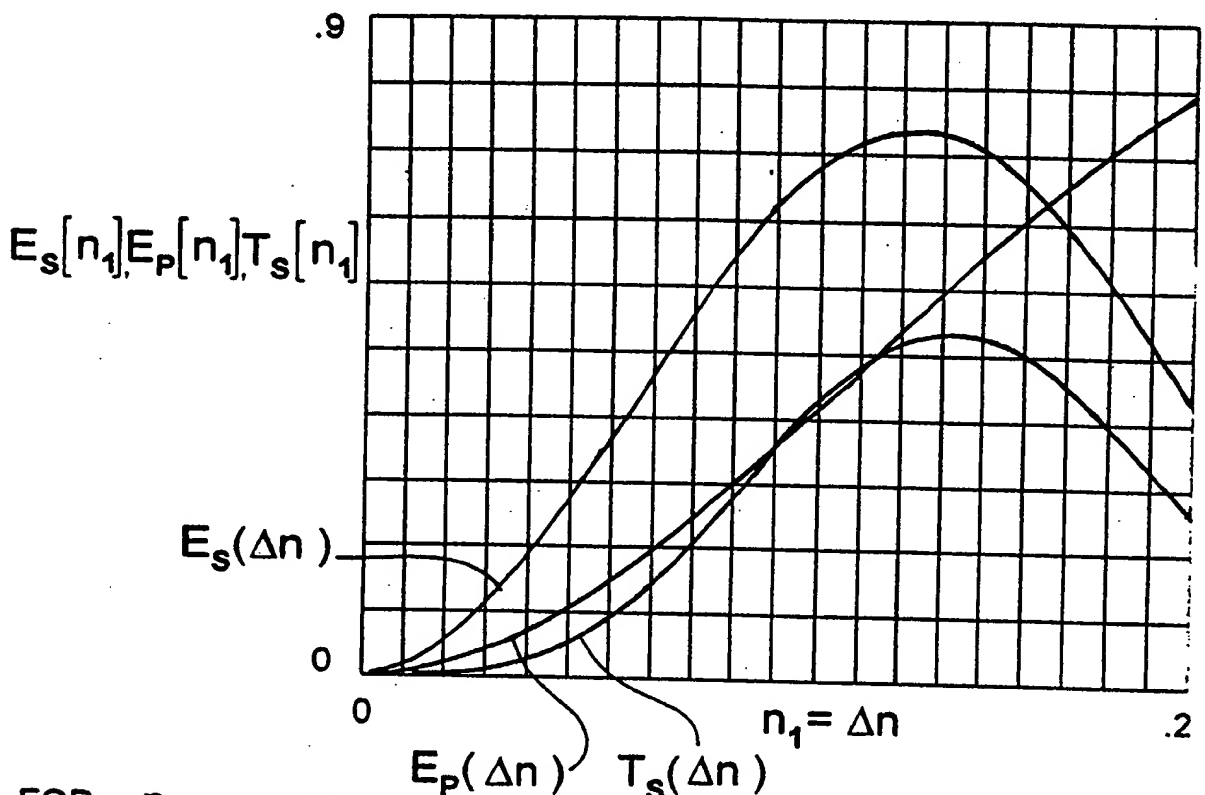

FOR: $n_1 := .145$

$E_S[n_1] = 0.736 \qquad E_P[n_1] = 0.552 \qquad T_S[n_1] = 0.474$

$H_{16} := \dfrac{0.474}{T_S[n_1]} \qquad H_{16} = 1$

H.16 IS THE OUT-AND-BACK DIFFRACTION EFFICIENCY OF FACET 16 RELATIVE TO THE OUT-AND-BACK DIFFRACTION EFFICIENCY OF FACET 1

FIG. 10E2

GEOMETRICAL OPTICS MODEL FOR HOLOGRAPHIC (TOTAL OUT AND BACK) LIGHT DIFFRACTION EFFICIENCY CALCULATIONS

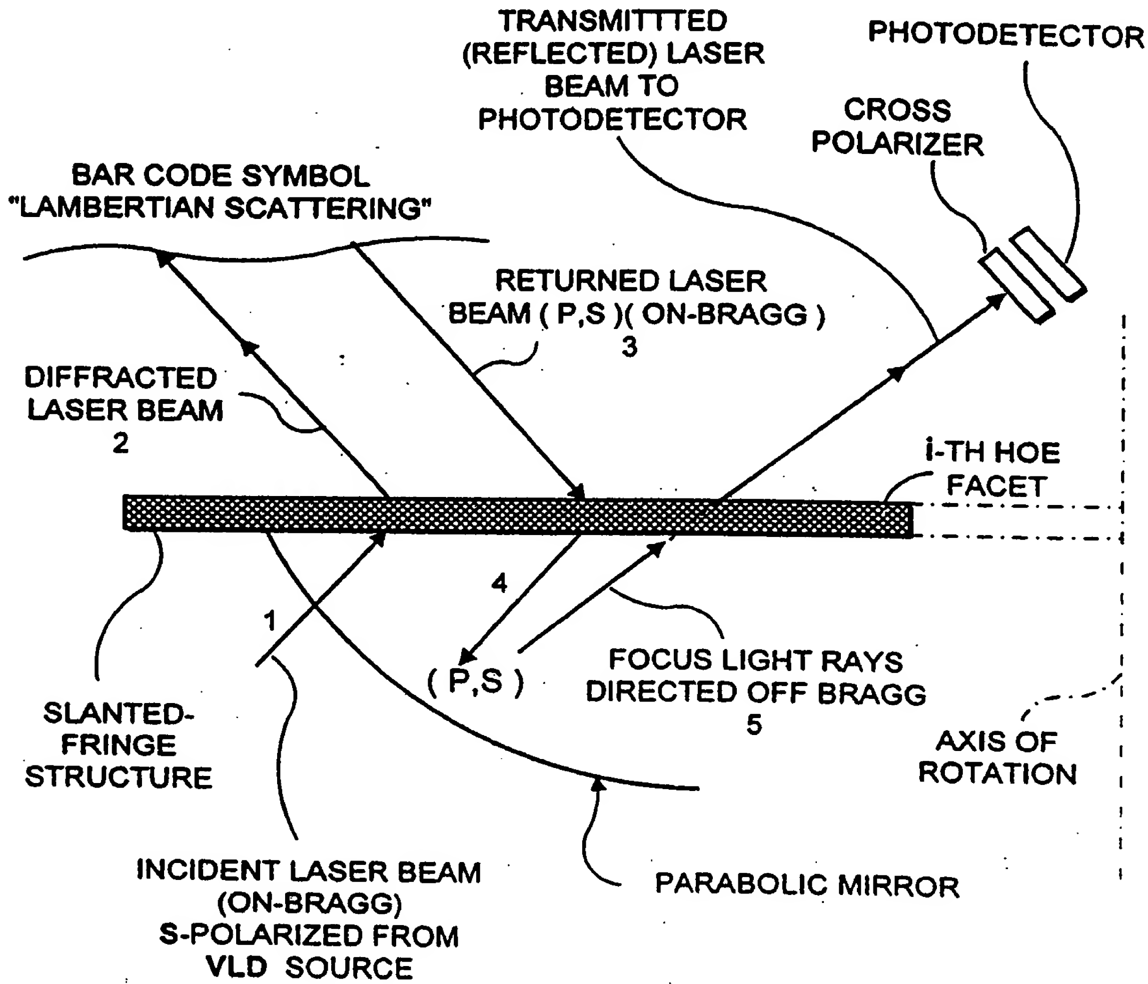

F I G. 10F

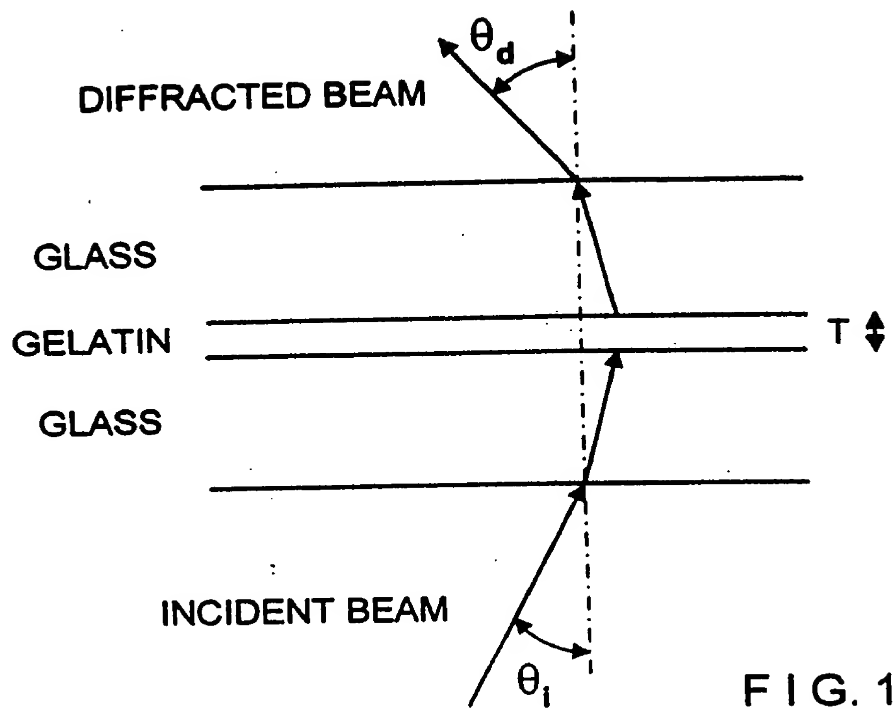

FIG. 10F1

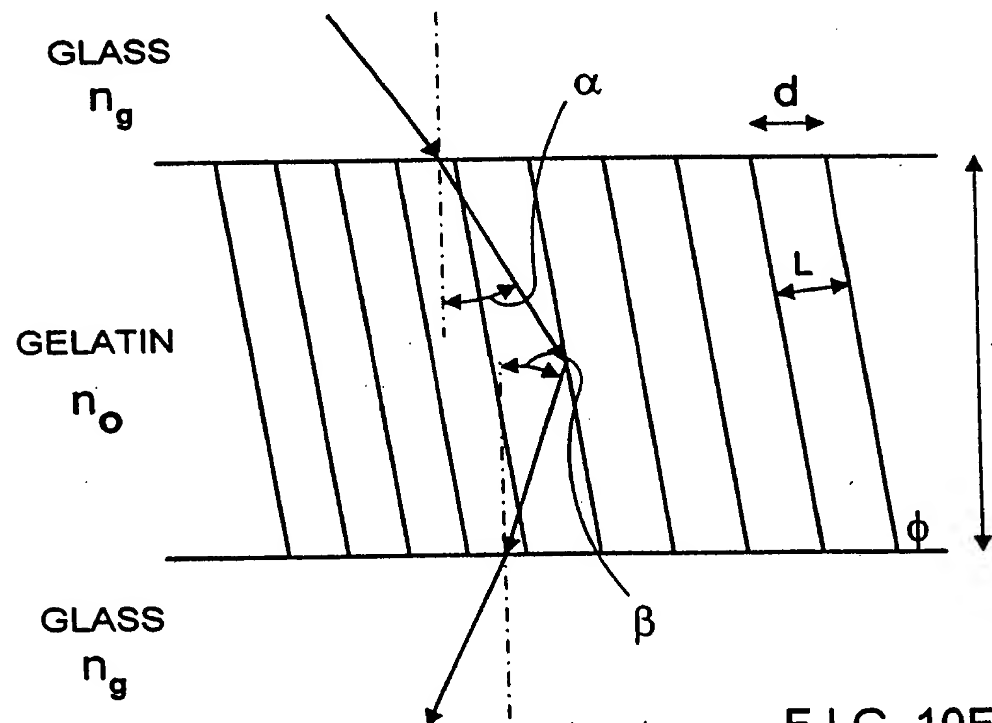

FIG. 10F2

SCANNING DISC ANALYSIS INCLUDING FRESNEL LOSSES AND ESTIMATED INTERNAL LOSSES OF 10% .THE 10% LOSS INCLUDES ABOUT 8% SCATTERING AND ABSORPTION AND ABOUT 2% FRESNEL LOSSES AT THE DCG/GLASS INTERFACES

S AND P POLARIZATION DIFFRACTION EFFICIENCIES FOR MOST GENERAL CASE

S AND P DIFFRACTION EFFICIENCIES AT THE BRAGG ANGLE AS A FUNCTION OF **nl** AND **delta-n** OF THE HOLOGRAPHIC MEDIUM. SLANTED FRINGES AND EXTERNAL ANGLES ARE INCLUDED. THIS IS A GENERALIZATION OF THE MORE COMMON CASE OF ZERO SLANT. **Delta-n (nl)** IS IN STEPS OF 0.001 **microns**.

DEFINITIONS:

θ_i = ANGLE OF INCIDENCE (EXTERNAL) ($\theta_i = 90^\circ - A_i$)

α = ANGLE OF INCIDENCE (INTERNAL)

θ_d = ANGLE OF DIFFRACTION (EXTERNAL) ($\theta_d = 90^\circ - B_i$)

β = ANGLE OF DIFFRACTION (INTERNAL)

δ = DEVIATION FROM THE BRAGG ANGLE

ϕ = TILT OF BRAGG PLANES

= $\pi/2$ FOR NO TILT

L = SEPARATION OF THE BRAGG PLANES

T = THICKNESS OF HOE MEDIUM

d = EXTERNAL FRINGE SPACING

ng = REFRACTIVE INDEX OF THE GLASS SUBSTRATE

n0 = AVERAGE REFRACTIVE INDEX OF THE HOE MEDIUM

n1 = delta-n OF HOE FRINGE STRUCTURE

λ_a = WAVELENGTH IN AIR

$\delta\lambda$ = DEVIATION FROM λ_a (BRAGG λ)

FIG. 10G

FIXED, OR ESTABLISHED PARAMETERS: n0, Δn1, θ_i, δ, $\delta\lambda$, λ_a, T.

$n_0 := 1.4$ $n_g := 1.515$ $deg = \frac{\pi}{180}$

$\Delta n_1 := 0, .001, \ldots 2$

$\theta_i := 43\ deg$

$\theta_d := 26.6\ deg$

$\delta := 0\ deg$

$\delta_\lambda := 0$

$T := 2.2$

$\lambda_a := .670$

F I G. 10G1

$$(1)\quad \alpha := \operatorname{asin}\left[\frac{\sin[\theta_i]}{n_0}\right]$$

$$(2)\quad \beta := \operatorname{asin}\left[\frac{\sin[\theta_d]}{n_0}\right]$$

INTERNAL ANGLES DECIVED FROM SNELL'S LAW AT INTERFACIAL SURFACES

$$(3)\quad \phi := \frac{\pi}{2} - \frac{\beta - \alpha}{2}$$

$$(4)\quad d := \frac{\lambda_a}{\sin[\theta_i] + \sin[\theta_d]}$$

$$(5)\quad L := d \sin(\phi)$$

GRATING EQUATION

$$(6)\quad C_R := \cos(\alpha)$$

$$(7)\quad C_S := \cos(\alpha) - \frac{\lambda_a}{n_0 L}\cos(\phi)$$

$$(8)\quad N[n_1] := \pi n_1 \frac{T}{\lambda_a \sqrt{C_R C_S}}$$

$$(9)\quad \Gamma := 2\pi\delta \frac{\sin(\phi - \alpha)}{L} - \delta_\lambda \frac{\pi}{n_0 L^2}$$

$$(10)\quad S[n_1] := \Gamma \frac{T}{2 C_S}$$

FROM "WAVE COUPLING THEORY"

FIG. 10H1

DIFFRACTION EFFICIENCIES: E_s AND E_p INCLUDING FRESNEL REFLECTION LOSSES AND ESTIMATED INTERNAL LOSSES OF 10%
(ASSUMING n - glass = 1.515 AND ANGLES AS GIVEN BELOW)

θ_i = 43 deg $\qquad\qquad$ θ_d = 26.6 deg

(11) $$E_S[n_1] := \frac{\left[\sin\left[\sqrt{N[n_1]^2 + S[n_1]^2}\right]\right]^2}{1 + \dfrac{S[n_1]^2}{N[n_1]^2}} t_S(1 - .1)$$

(12) $$E_P[n_1] :=$$

$$= \frac{\left[\sin\left[\sqrt{[N[n_1] \cos(2(\alpha - \phi))]^2 + S[n_1]^2}\right]\right]^2}{1 + \dfrac{S[n_1]^2}{[N[n_1] \cos(2(\alpha - \phi))]^2}} t_P(1 - .1)$$

(13) $$E_t[n_1] := E_S[n_1] \cdot [E_P[n_1]]$$

(E.t IS THE TOTAL OUT-AND-BACK DIFFRACTION EFFICIENCY, ASSUMING THAT A CROSSED POLARIZER IS USED ON THE DETECTOR. IN THIS CASE, THE TOTAL EFFICIENCY IS JUST THE PRODUCT OF THE OUTGOING EFFICIENCY FOR THE INCIDENT P (OR S) POLARIZATION AND THE RETURN EFFICIENCY FOR THE ORTHOGONAL S (OR P) POLARIZATION. INCLUDES FRESNEL - REFLECTION LOSSES AND ESTIMATED INTERNAL LOSSES OF 10%)

$$\Delta n = n_1$$

(14) $$H_I(\Delta n) := \frac{E_{t1}(\Delta n)}{E_{t16}(\Delta n)}$$

FIG. 10H2

PARAMETERS FOR CALCULATING THE FRESNEL REFLECTION LOSSES AND TRANSMISSION

$$\theta_{r.1} := \operatorname{asin}\left[\frac{\sin[\theta_i]}{n_g}\right]$$

$$\theta_{r.2} := \operatorname{asin}\left[\frac{\sin[\theta_d]}{n_g}\right]$$

$$R_{s.1} := \left[\frac{\sin[\theta_i - \theta_{r.1}]}{\sin[\theta_i + \theta_{r.1}]}\right]^2$$

S-POLARIZATION REFLECTION AT FIRST (ENTRY) SURFACE OF DISC

$$R_{s.2} := \left[\frac{\sin[\theta_d - \theta_{r.2}]}{\sin[\theta_d + \theta_{r.2}]}\right]^2$$

S-POLARIZATION REFLECTION AT SECOND (EXIT) SURFACE OF DISC

$$R_{P.1} := \left[\frac{\tan[\theta_i - \theta_{r.1}]}{\tan[\theta_i + \theta_{r.1}]}\right]^2$$

P-POLARIZATION REFLECTION AT FIRST (ENTRY) SURFACE OF DISC

$$R_{P.2} := \left[\frac{\tan[\theta_d - \theta_{r.2}]}{\tan[\theta_d + \theta_{r.2}]}\right]^2$$

P-POLARIZATION REFLECTION AT SECOND (EXIT) SURFACE OF DISC

BOTH SURFACES

$$t_s := [1 - R_{s.1}] \cdot [1 - R_{s.2}]$$

S-POLARIZED FRESNEL TRANSMISSION

$$t_p := [1 - R_{P.1}] \cdot [1 - R_{P.2}]$$

P-POLARIZED FRESNEL TRANSMISSION

FIG. 10H3

DIFFRACTION EFFICIENCIES: E_S, E_P, E_t - INCLUDING FRESNEL REFLECTION LOSSES AND ESTIMATED INTERNAL LOSSES OF 10%. (ASSUMING n GLASS = 1.515 AND ANGLES ARE AS GIVEN BELOW)

$\theta_i = 43$ deg $\quad n_0 = 1.4 \quad \theta_d = 26.6$ deg

$T = 2.2$ microns $\quad \lambda_a = 0.67$

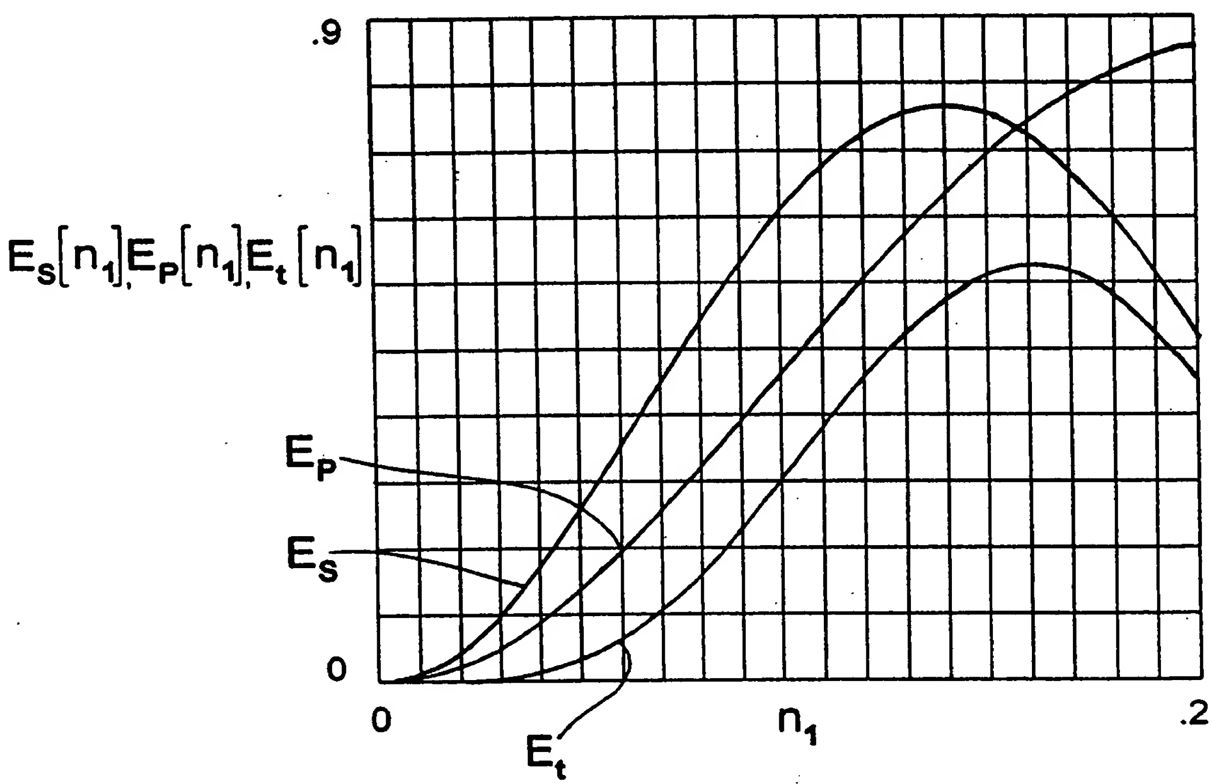

FOR: $n_1 := .16$

$E_S[n_1] = 0.72915 \qquad E_P[n_1] = 0.76037 \qquad E_t[n_1] = 0.55442$

$$H_1 := \frac{0.42745}{E_t[n_1]} \qquad H_1 := 0.77098$$

H.1 IS THE OUT-AND-BACK DIFFRACTION EFFICIENCY OF FACET 1 RELATIVE TO THE OUT-AND-BACK DIFFRACTION EFFICIENCY OF FACET 16

F I G. 10I1

FACET No. 16

DIFFRACTION EFFICIENCIES: E_s, E_p, E_t - INCLUDING FRESNEL REFLECTION LOSSES AND ESTIMATED INTERNAL LOSSES OF 10%. (ASSUMING n GLASS = 1.515 AND ANGLES ARE AS GIVEN BELOW)

$\theta_i = 43$ deg $\quad \theta_d = 41.8$ deg $\quad n_0 = 1.4$

$T = 2.2$ microns $\quad \lambda_a = 0.67$

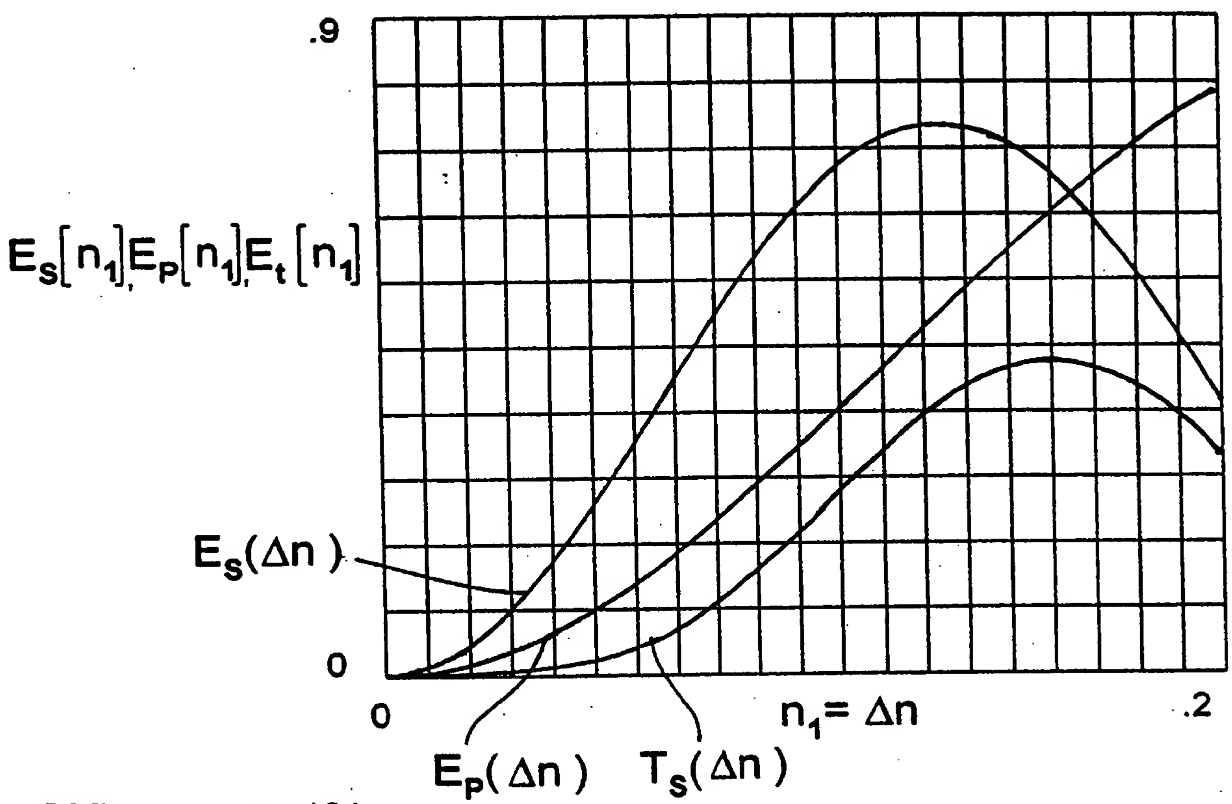

FOR: $n_1 := .161$

$E_s[n_1] = 0.67386 \quad E_P[n_1] = 0.63433 \quad E_t[n_1] = 0.42745$

$$H_{16} := \frac{E_t[n_1]}{0.42745} \qquad H_{16} = 1$$

H.16 IS THE OUT-AND-BACK DIFFRACTION EFFICIENCY OF FACET 16 RELATIVE TO THE OUT-AND-BACK DIFFRACTION EFFICIENCY OF FACET 16

F I G. 10I2

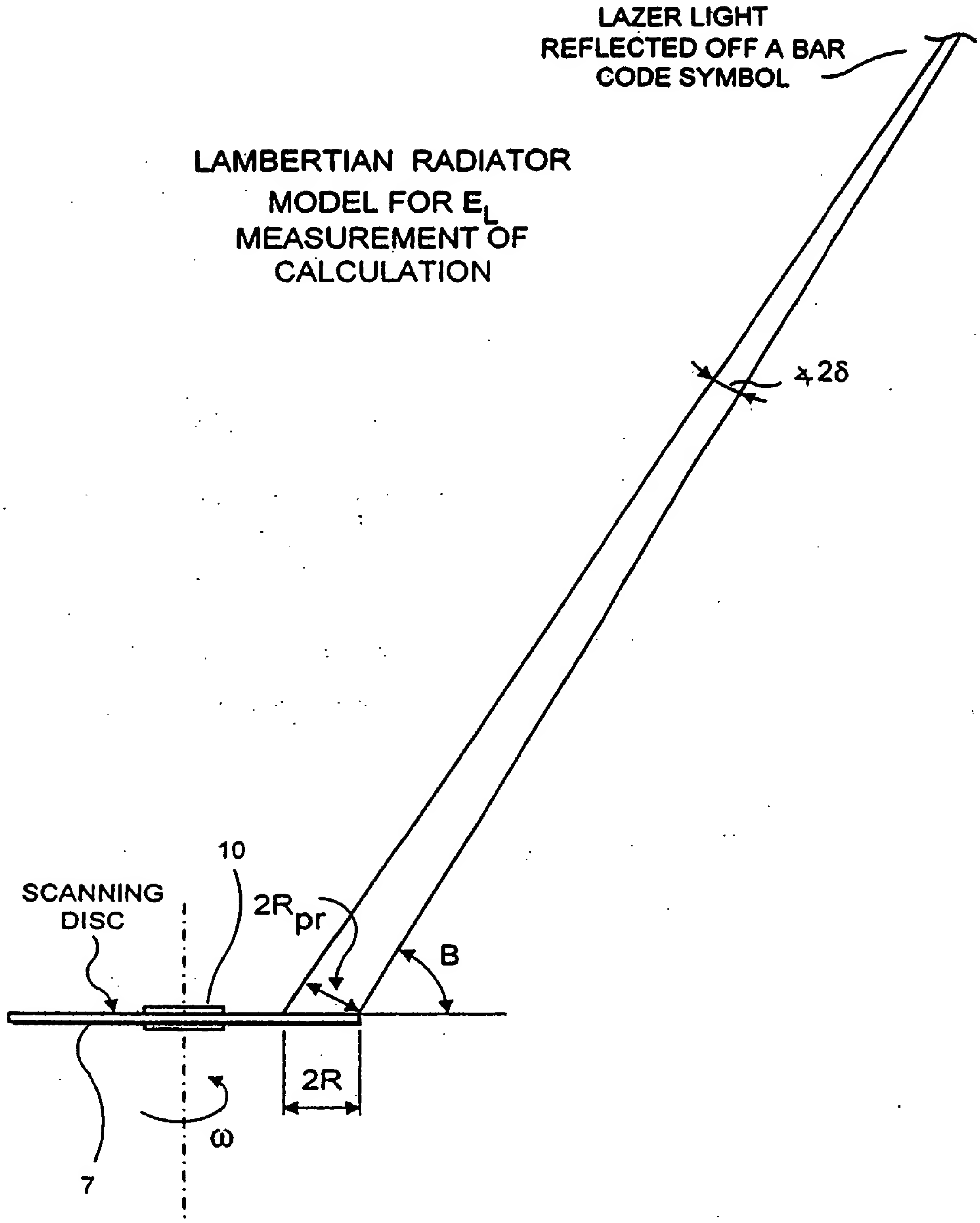
LAZER LIGHT
REFLECTED OFF A BAR
CODE SYMBOL
LAMBERTIAN RADIATOR
MODEL FOR E_L
MEASUREMENT OF
CALCULATION
∡2δ
10
SCANNING
DISC
$2R_{pr}$
B
2R
ω
7

F I G. 10J

FACET LIGHT COLLECTION EFFICIENCY

Z = DISTANCE FROM SCAN POINT ON LABEL (MAX = FOCAL) LENGTH PLUS 5 INCHES)

A = AREA OF CORRESPONDING FACET

R = RADIUS OF EFFECTIVE CIRCULAR APERTURE

R.pr = RADIUS OF PROJECTED EFFECTIVE CIRCULAR APERTURE

B = ANGLE BETWEEN OUTGOING BEAM AND THE DISC SURFACE

δ = HALF-ANGLE SUBTENDED BY EFFECTIVE PROJECTED CIRCULAR APERTURE

E.L = LAMBERTIAN LIGHT COLLECTION EFFICIENCY

FIG. 10K

$$R_{pr} := \sqrt{\frac{A \sin B}{\pi}} \qquad \delta := \operatorname{atan}\left[\frac{R_{pr}}{Z}\right]$$

$$E_L := (\sin(\delta))^2$$

FIG. 10L1

FOR FACET 16 :

$Z := 70$ inches

$A := 4.7$ square inches

$B := 48.2$ deg

$\mathrm{deg} = \frac{\pi}{180}$

$E_L := 0.00022756$

FIG. 10L

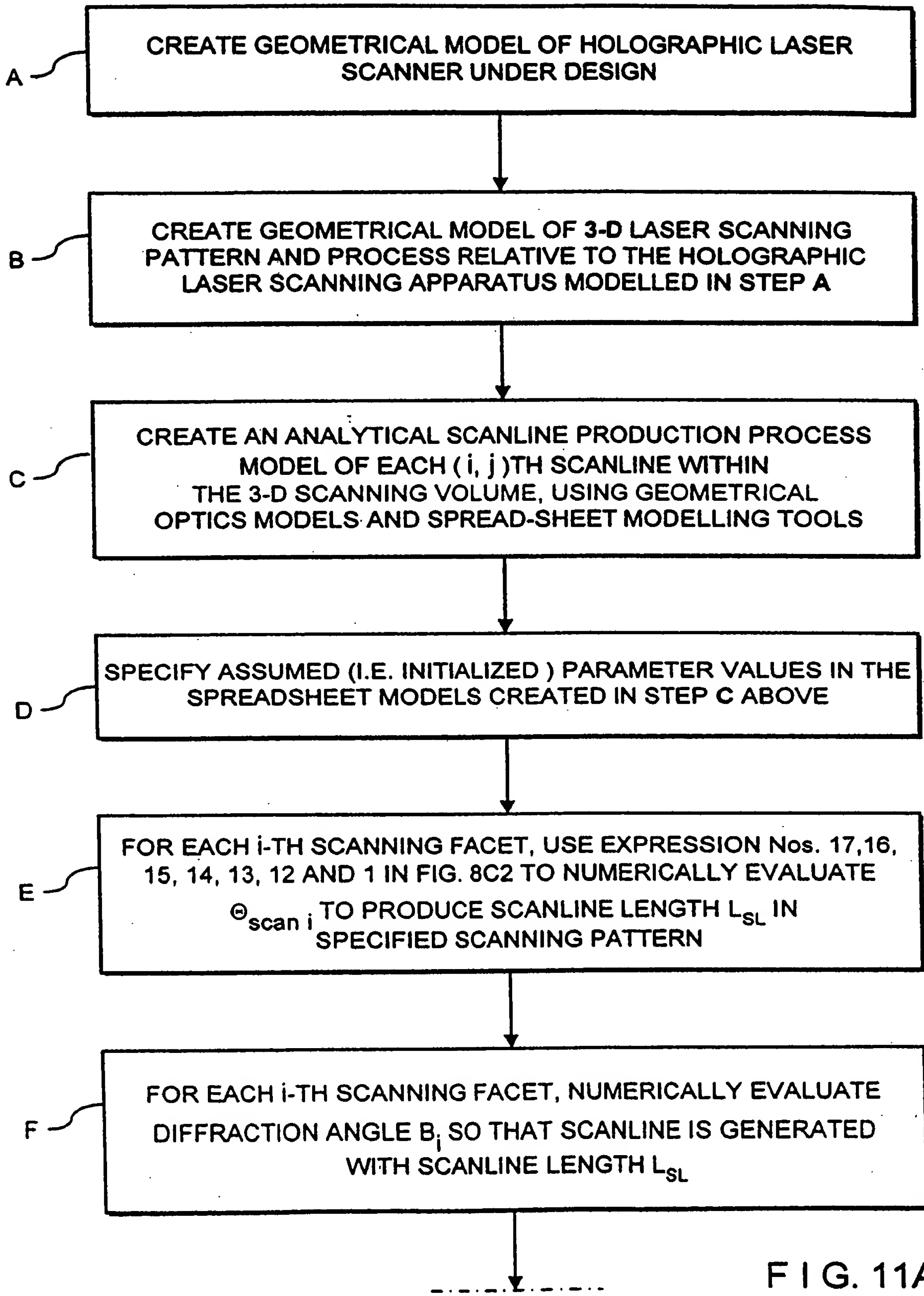
A
CREATE GEOMETRICAL MODEL OF HOLOGRAPHIC LASER SCANNER UNDER DESIGN
B
CREATE GEOMETRICAL MODEL OF 3-D LASER SCANNING PATTERN AND PROCESS RELATIVE TO THE HOLOGRAPHIC LASER SCANNING APPARATUS MODELLED IN STEP A
C
CREATE AN ANALYTICAL SCANLINE PRODUCTION PROCESS MODEL OF EACH (i, j)TH SCANLINE WITHIN THE 3-D SCANNING VOLUME, USING GEOMETRICAL OPTICS MODELS AND SPREAD-SHEET MODELLING TOOLS
D
SPECIFY ASSUMED (I.E. INITIALIZED) PARAMETER VALUES IN THE SPREADSHEET MODELS CREATED IN STEP C ABOVE
E
FOR EACH i-TH SCANNING FACET, USE EXPRESSION Nos. 17,16, 15, 14, 13, 12 AND 1 IN FIG. 8C2 TO NUMERICALLY EVALUATE $\Theta_{scan\ i}$ TO PRODUCE SCANLINE LENGTH L_{SL} IN SPECIFIED SCANNING PATTERN
F
FOR EACH i-TH SCANNING FACET, NUMERICALLY EVALUATE DIFFRACTION ANGLE B_i SO THAT SCANLINE IS GENERATED WITH SCANLINE LENGTH L_{SL}

FIG. 11A

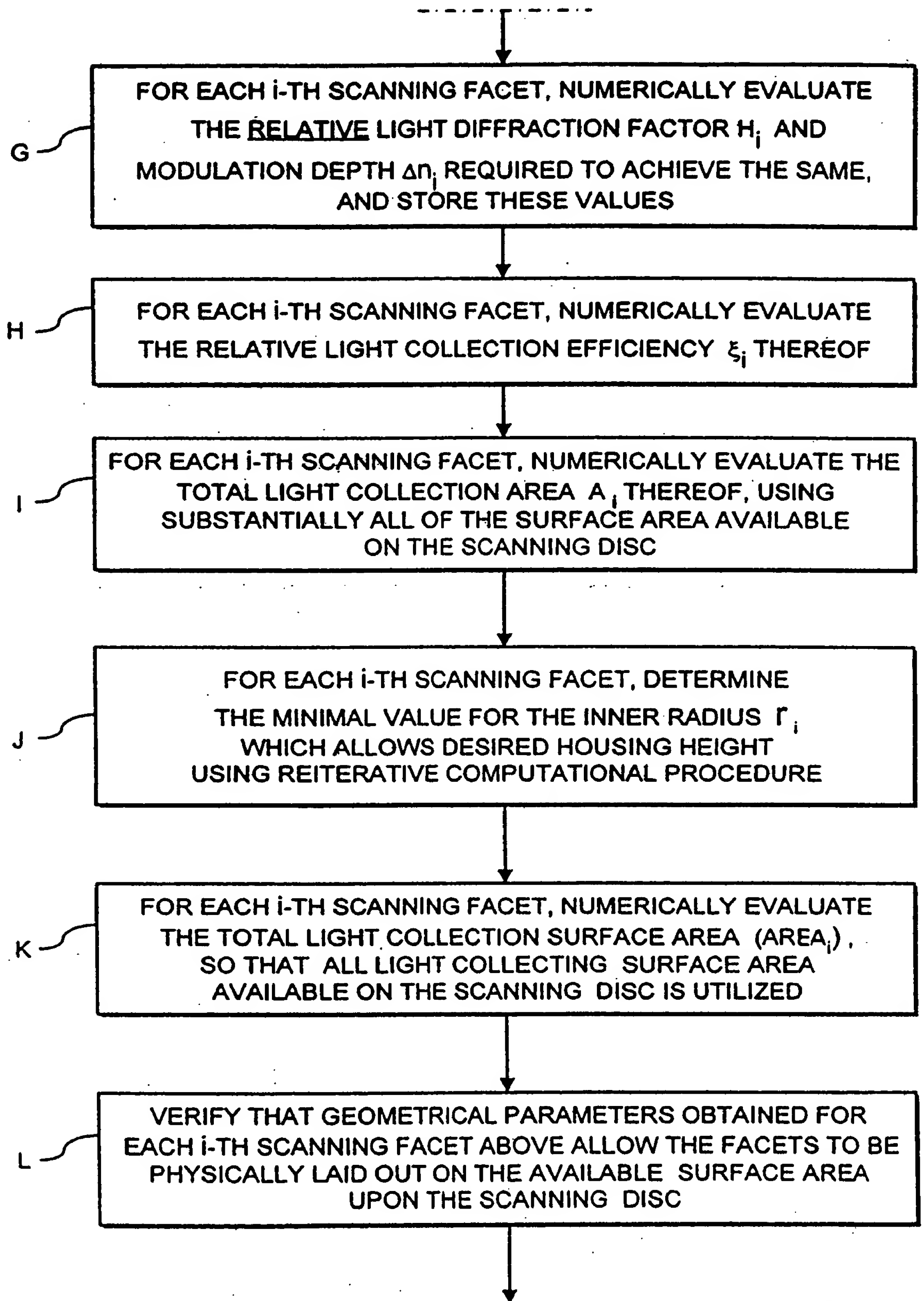
G
FOR EACH i-TH SCANNING FACET, NUMERICALLY EVALUATE THE RELATIVE LIGHT DIFFRACTION FACTOR H_i AND MODULATION DEPTH Δn_i REQUIRED TO ACHIEVE THE SAME, AND STORE THESE VALUES
H
FOR EACH i-TH SCANNING FACET, NUMERICALLY EVALUATE THE RELATIVE LIGHT COLLECTION EFFICIENCY ξ_i THEREOF
I
FOR EACH i-TH SCANNING FACET, NUMERICALLY EVALUATE THE TOTAL LIGHT COLLECTION AREA A_i THEREOF, USING SUBSTANTIALLY ALL OF THE SURFACE AREA AVAILABLE ON THE SCANNING DISC
J
FOR EACH i-TH SCANNING FACET, DETERMINE THE MINIMAL VALUE FOR THE INNER RADIUS r_i WHICH ALLOWS DESIRED HOUSING HEIGHT USING REITERATIVE COMPUTATIONAL PROCEDURE
K
FOR EACH i-TH SCANNING FACET, NUMERICALLY EVALUATE THE TOTAL LIGHT COLLECTION SURFACE AREA ($AREA_i$), SO THAT ALL LIGHT COLLECTING SURFACE AREA AVAILABLE ON THE SCANNING DISC IS UTILIZED
L
VERIFY THAT GEOMETRICAL PARAMETERS OBTAINED FOR EACH i-TH SCANNING FACET ABOVE ALLOW THE FACETS TO BE PHYSICALLY LAID OUT ON THE AVAILABLE SURFACE AREA UPON THE SCANNING DISC

FIG. 11B

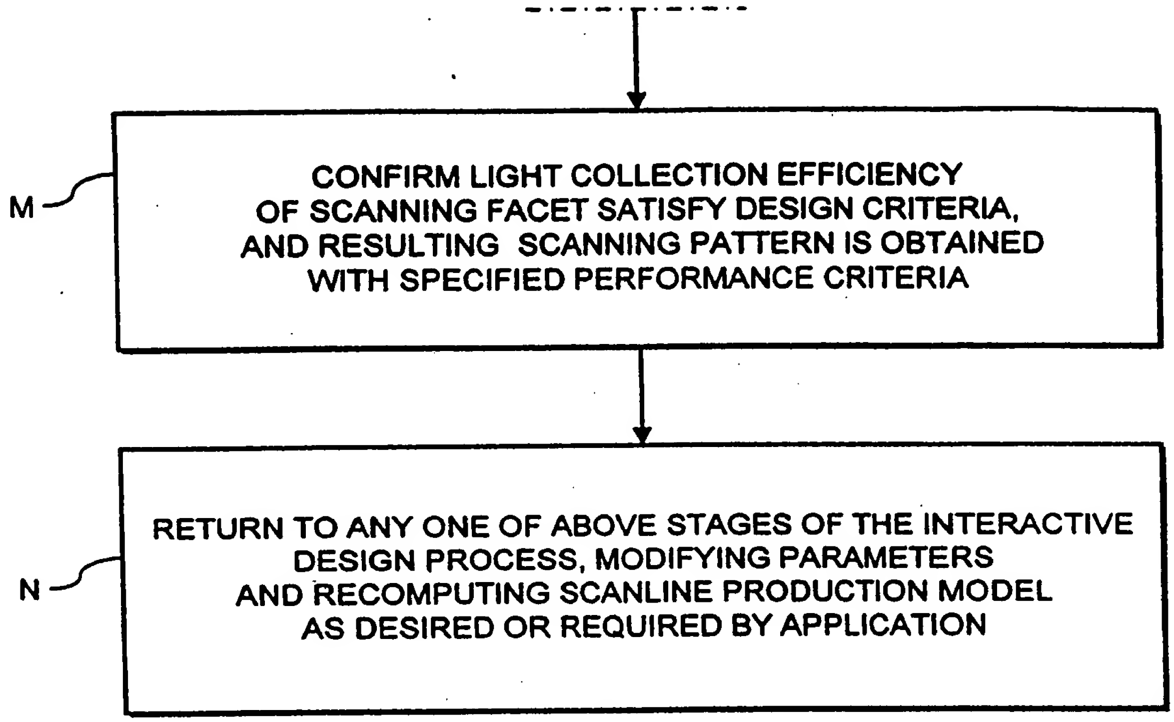
CONFIRM LIGHT COLLECTION EFFICIENCY OF SCANNING FACET SATISFY DESIGN CRITERIA, AND RESULTING SCANNING PATTERN IS OBTAINED WITH SPECIFIED PERFORMANCE CRITERIA
M
RETURN TO ANY ONE OF ABOVE STAGES OF THE INTERACTIVE DESIGN PROCESS, MODIFYING PARAMETERS AND RECOMPUTING SCANLINE PRODUCTION MODEL AS DESIRED OR REQUIRED BY APPLICATION
N

FIG. 11C

DIFFRACTION EFFICIENCIES: E_s AND E_p INCLUDING FRESNEL REFLECTION LOSSES AND ESTIMATED INTERNAL LOSSES OF 8%
(ASSUMING n - glass = 1.515 AND ANGLES AS GIVEN BELOW)

θ_i = 43 deg θ_d = 47.5 deg n_0 = 1.4

T = 2.2 microns λ_a = 0.67

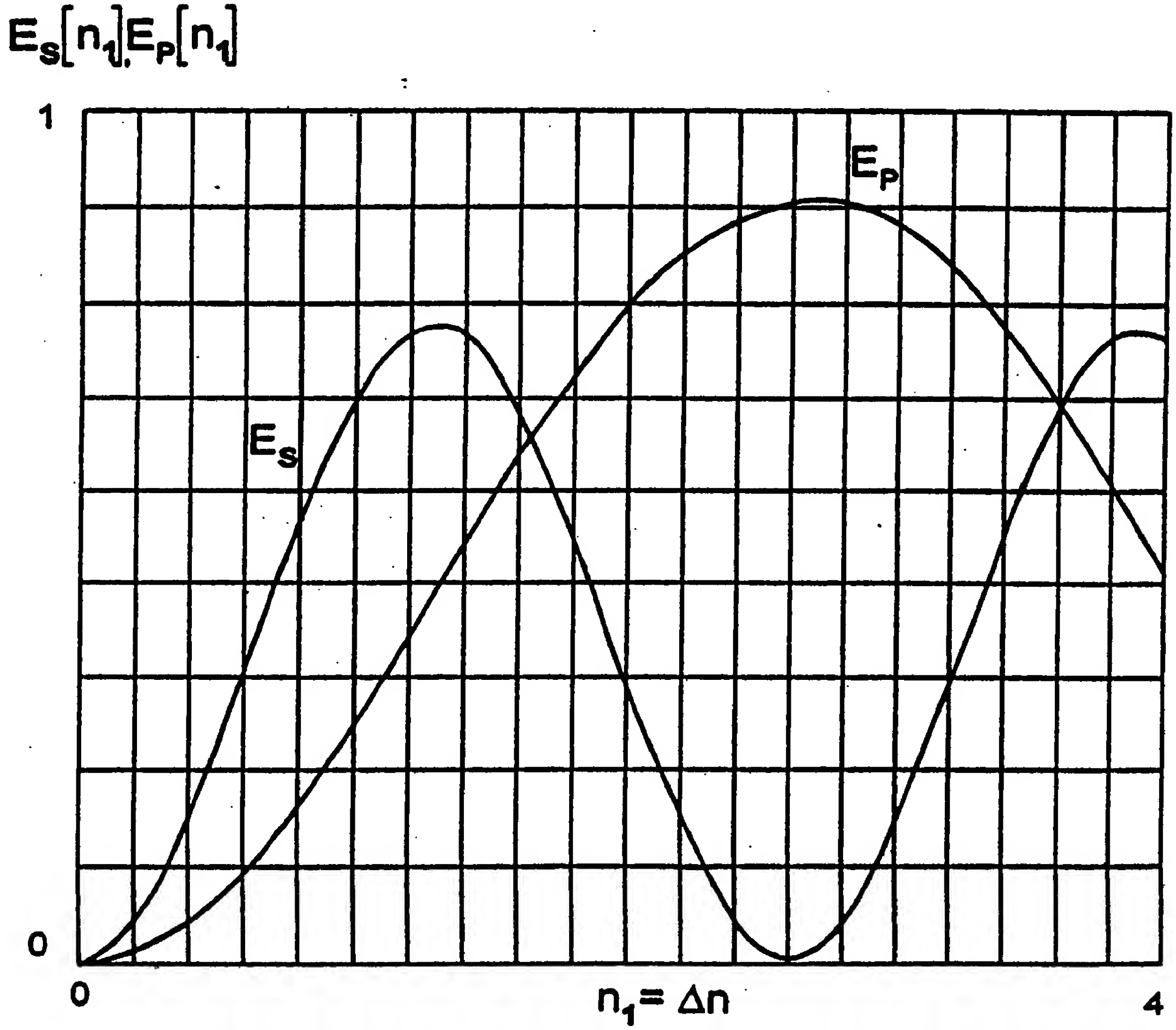

FIG. 12

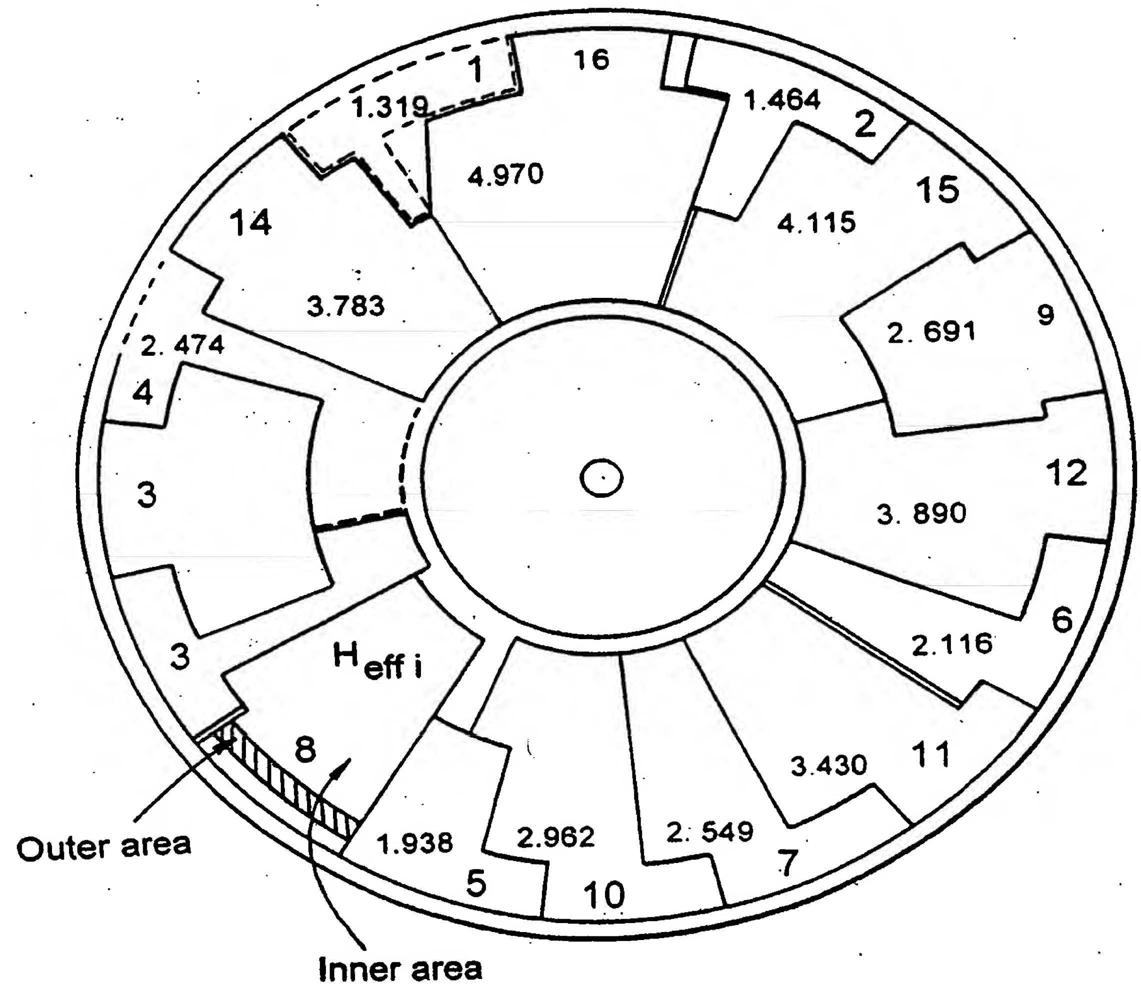
1
16
1.319
1.464
2
4.970
15
14
4.115
3.783
9
2. 474
2. 691
4
12
3
3. 890
6
2.116
3
$H_{eff\ i}$
11
8
3.430
1.938
2.962
2. 549
7
5
10
Outer area
Inner area

FIG. 12A

A — CREATE GEOMETRICAL MODEL OF HOLOGRAPHIC LASER SCANNER UNDER DESIGN

B — CREATE GEOMETRICAL MODEL OF **3-D** LASER SCANNING PATTERN AND PROCESS RELATIVE TO THE HOLOGRAPHIC LASER SCANNING APPARATUS MODELLED IN STEP **A**

C — CREATE AN ANALYTICAL SCANLINE PRODUCTION PROCESS MODEL OF EACH (i, j)TH SCANLINE WITHIN THE 3-D SCANNING VOLUME, USING GEOMETRICAL OPTICS MODELS AND SPREAD-SHEET MODELLING TOOLS

D — SPECIFY ASSUMED (I.E. INITIALIZED) PARAMETER VALUES IN THE SPREADSHEET MODELS CREATED IN STEP **C** ABOVE

E — FOR EACH i-TH SCANNING FACET, USE EXPRESSION NOs. 17,16, 15, 14, 13, 12 AND 1 IN FIG. 8C2 TO NUMERICALLY EVALUATE $\Theta_{scan\ i}$ TO PRODUCE SCANLINE LENGTH L_{SL} IN SPECIFIED SCANNING PATTERN

F — FOR EACH i-TH SCANNING FACET, NUMERICALLY EVALUATE DIFFRACTION ANGLE B_i SO THAT SCANLINE IS GENERATED WITH SCANLINE LENGTH L_{SL}

FIG. 12B1

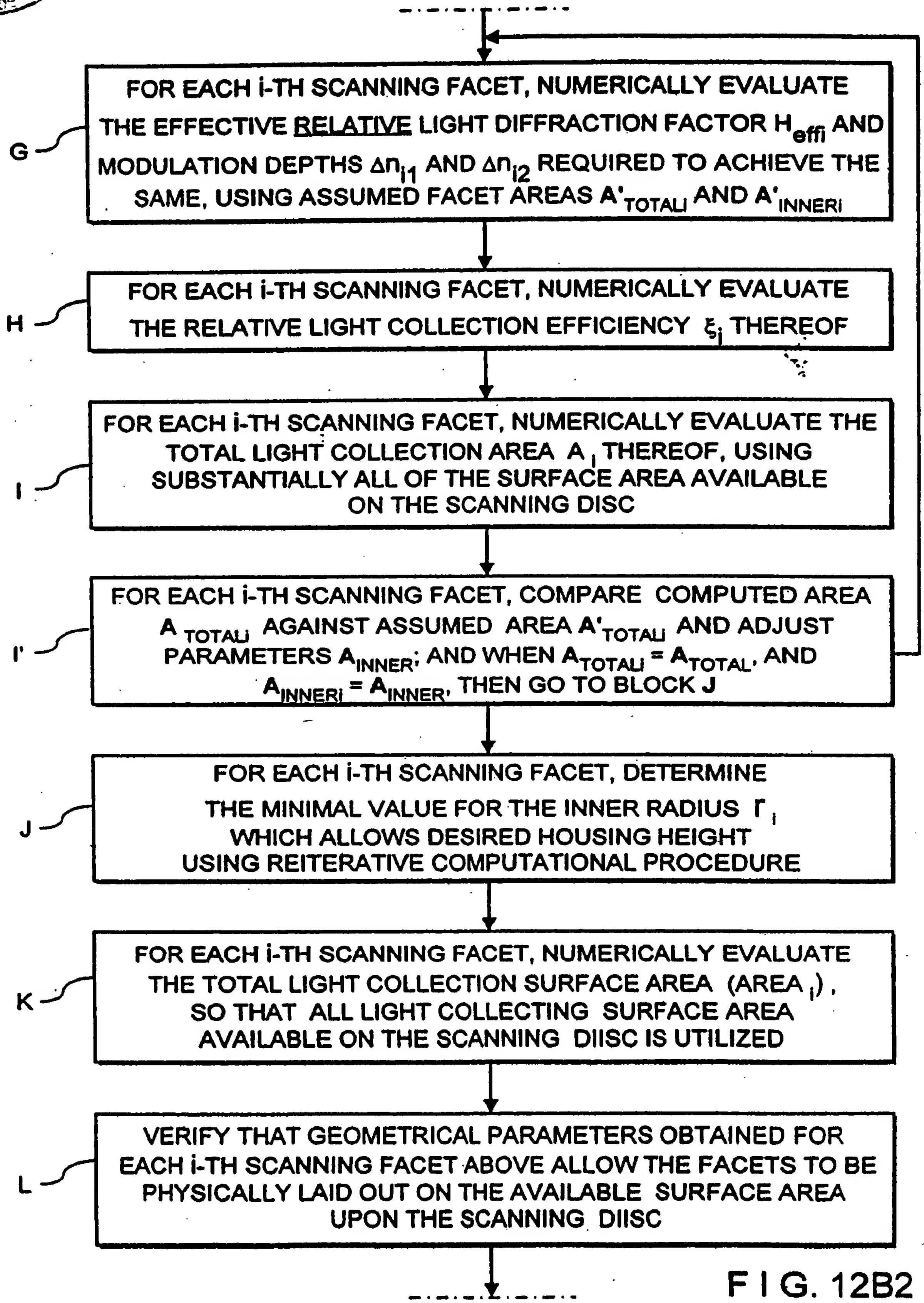
G
FOR EACH i-TH SCANNING FACET, NUMERICALLY EVALUATE THE EFFECTIVE RELATIVE LIGHT DIFFRACTION FACTOR H_{effi} AND MODULATION DEPTHS Δn_{i1} AND Δn_{i2} REQUIRED TO ACHIEVE THE SAME, USING ASSUMED FACET AREAS A'_{TOTALi} AND A'_{INNERi}
H
FOR EACH i-TH SCANNING FACET, NUMERICALLY EVALUATE THE RELATIVE LIGHT COLLECTION EFFICIENCY ξ_i THEREOF
I
FOR EACH i-TH SCANNING FACET, NUMERICALLY EVALUATE THE TOTAL LIGHT COLLECTION AREA A_i THEREOF, USING SUBSTANTIALLY ALL OF THE SURFACE AREA AVAILABLE ON THE SCANNING DISC
I'
FOR EACH i-TH SCANNING FACET, COMPARE COMPUTED AREA A_{TOTALi} AGAINST ASSUMED AREA A'_{TOTALi} AND ADJUST PARAMETERS A_{INNERi} AND WHEN $A_{TOTALi} = A_{TOTAL}$, AND $A_{INNERi} = A_{INNER}$, THEN GO TO BLOCK J
J
FOR EACH i-TH SCANNING FACET, DETERMINE THE MINIMAL VALUE FOR THE INNER RADIUS r_i WHICH ALLOWS DESIRED HOUSING HEIGHT USING REITERATIVE COMPUTATIONAL PROCEDURE
K
FOR EACH i-TH SCANNING FACET, NUMERICALLY EVALUATE THE TOTAL LIGHT COLLECTION SURFACE AREA (AREA $_i$), SO THAT ALL LIGHT COLLECTING SURFACE AREA AVAILABLE ON THE SCANNING DIISC IS UTILIZED
L
VERIFY THAT GEOMETRICAL PARAMETERS OBTAINED FOR EACH i-TH SCANNING FACET ABOVE ALLOW THE FACETS TO BE PHYSICALLY LAID OUT ON THE AVAILABLE SURFACE AREA UPON THE SCANNING DIISC

FIG. 12B2

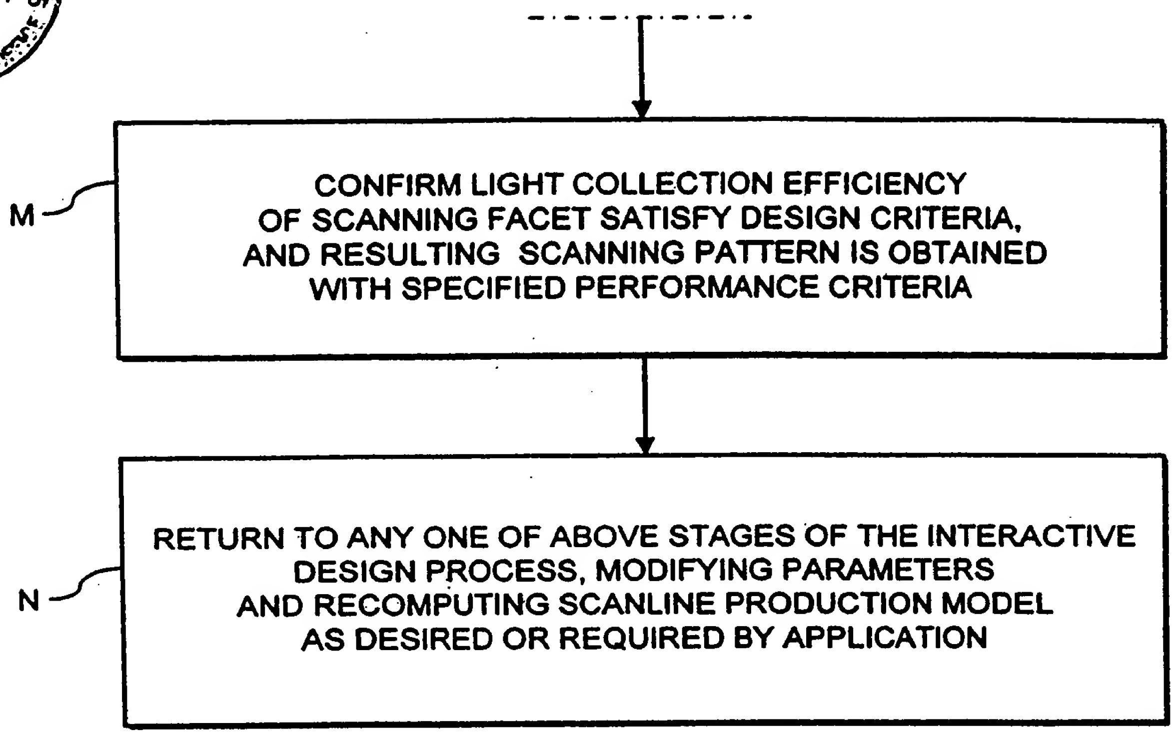
M
CONFIRM LIGHT COLLECTION EFFICIENCY OF SCANNING FACET SATISFY DESIGN CRITERIA, AND RESULTING SCANNING PATTERN IS OBTAINED WITH SPECIFIED PERFORMANCE CRITERIA
N
RETURN TO ANY ONE OF ABOVE STAGES OF THE INTERACTIVE DESIGN PROCESS, MODIFYING PARAMETERS AND RECOMPUTING SCANLINE PRODUCTION MODEL AS DESIRED OR REQUIRED BY APPLICATION

FIG. 12B3

$$H_1 := \frac{\dfrac{E_{S.o.16}}{A_{T.16}}\left[E_{P.o.16}A_{o.16} + E_{P.i.16}A_{i.16}\right]}{\dfrac{E_{S.o.1}}{A_{T.1}}\left[E_{P.o.1}A_{o.1} + E_{P.i.1}A_{i.1}\right]}$$

WHERE :

E.S.o.16 = S-POLARIZATION EFFICIENCY OF THE OUTER SEGMENT OF FACET 16

E.S.o.1 = S-POLARIZATION EFFICIENCY OF THE OUTER SEGMENT OF FACET 1

E.P.o.16 = P-POLARIZATION EFFICIENCY OF THE OUTER SEGMENT OF FACET 16

E.P.o.1 = P-POLARIZATION EFFICIENCY OF THE OUTER SEGMENT OF FACET 1

E.P.i.16 = P-POLARIZATION EFFICIENCY OF THE INNER SEGMENT OF FACET 16

E.P.i.1 = P-POLARIZATION EFFICIENCY OF THE INNER SEGMENT OF FACET 1

A.T.16 = TOTAL AREA OF FACET 16

A.T.1 = TOTAL AREA OF FACET 1

A.o.16 = OUTER AREA OF FACET 16

A.o.1 = OUTER AREA OF FACET 1

A.i.16 = OUTER AREA OF FACET 16

A.i.1 = OUTER AREA OF FACET 1

FIG. 12C

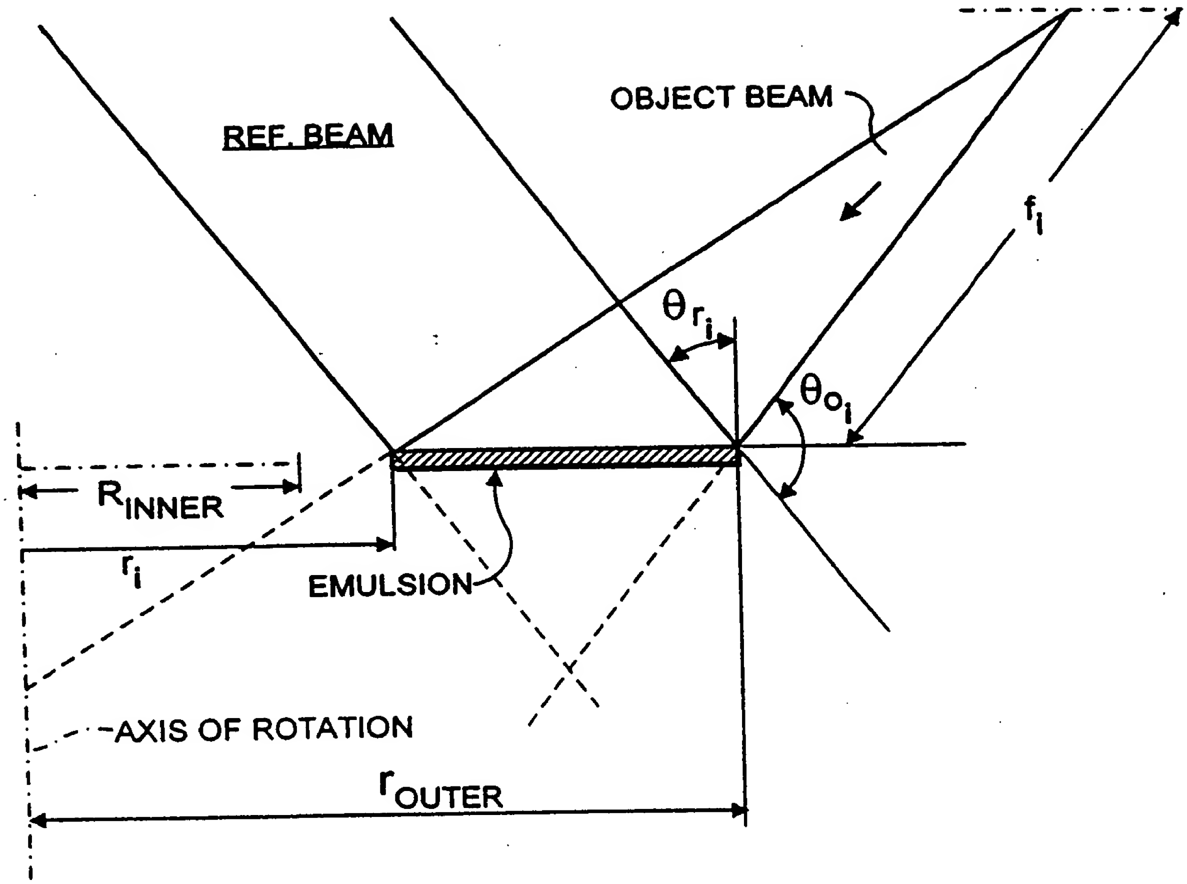
OBJECT BEAM
REF. BEAM
f_i
θ_{r_i}
θ_{o_i}
R_{INNER}
r_i
EMULSION
AXIS OF ROTATION
r_{OUTER}

FIG. 13

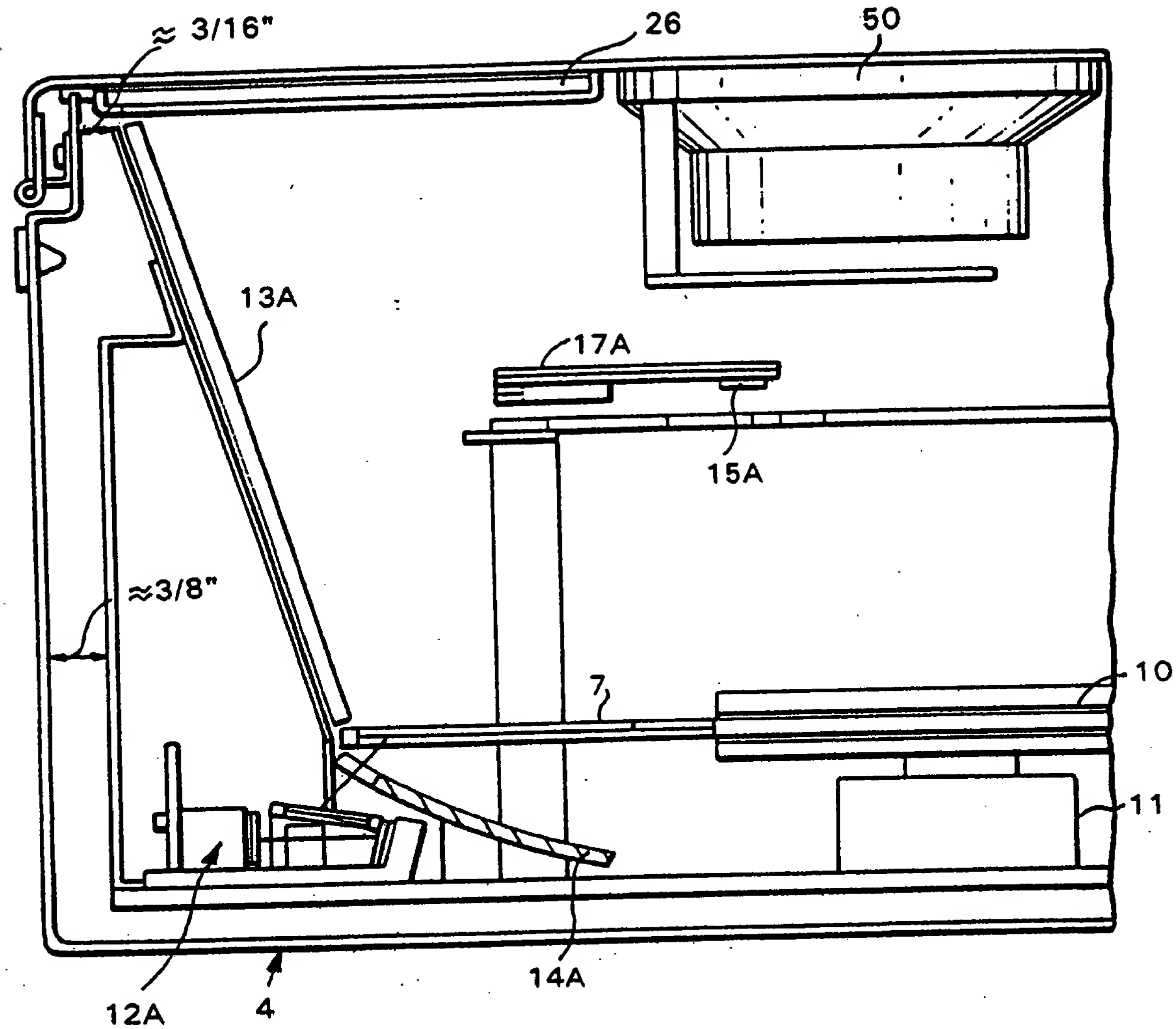

FIG. 14

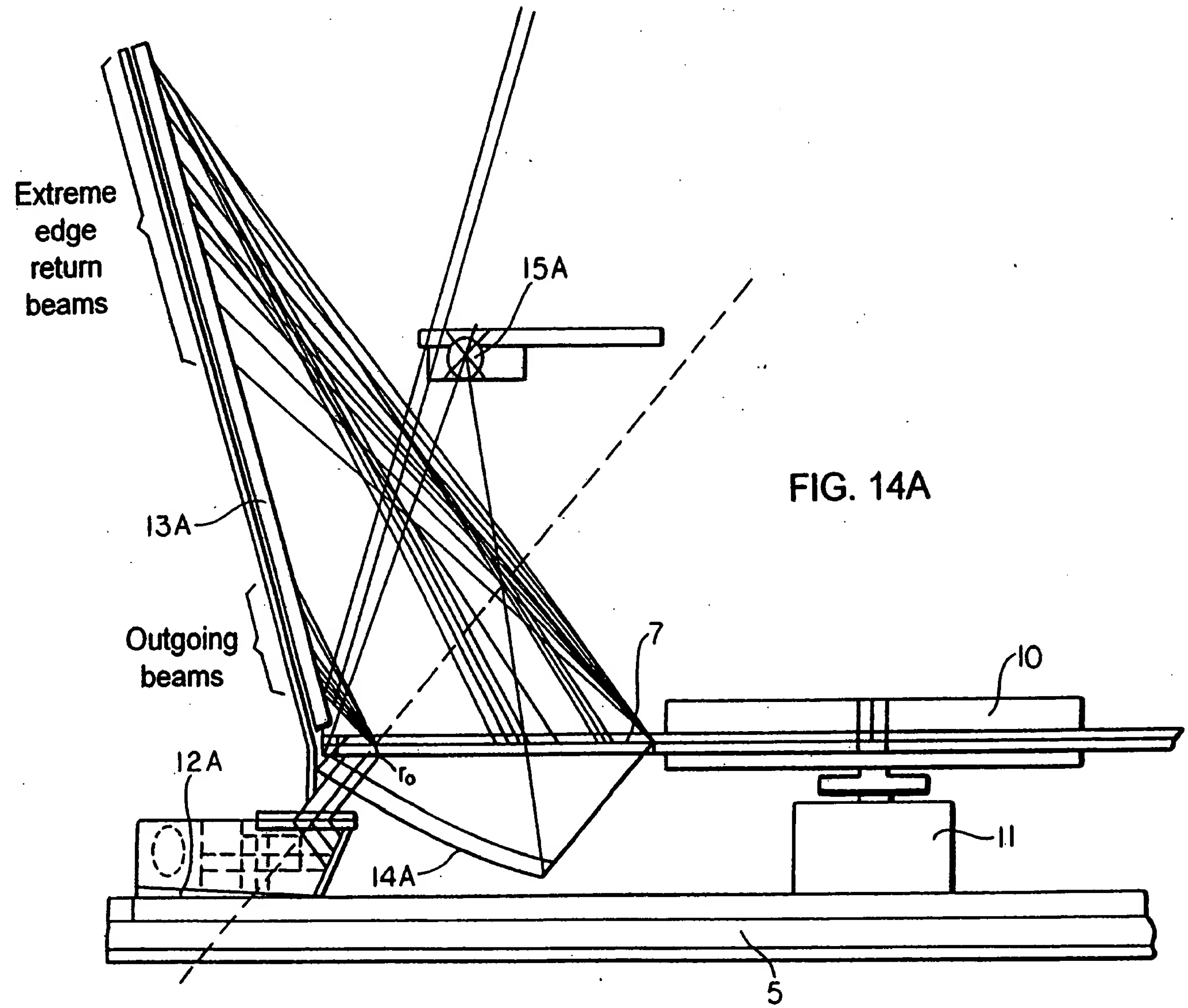
Extreme edge return beams
15A
13A
Outgoing beams
7
10
12A
r_0
11
14A
5

FIG. 14A

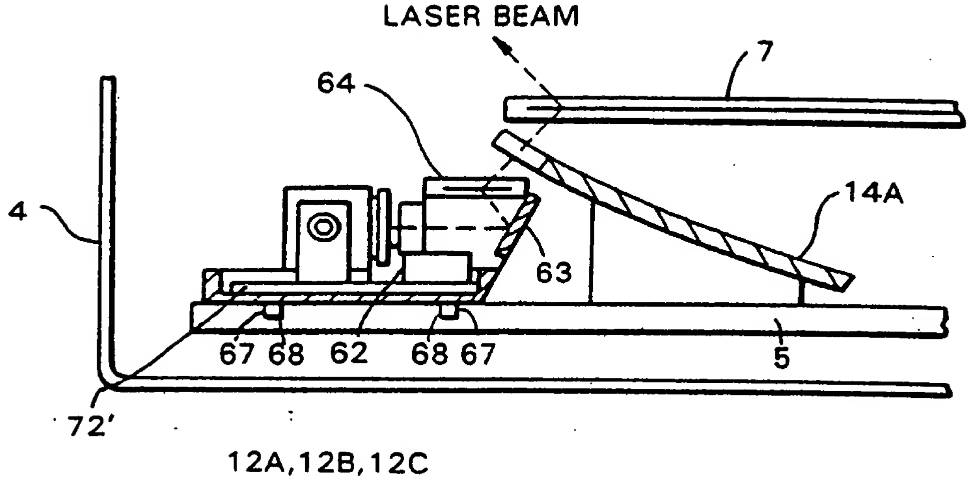

FIG. 15

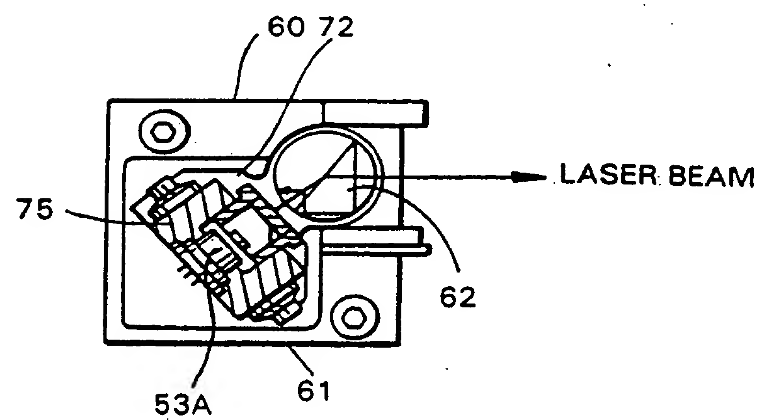

FIG. 15A

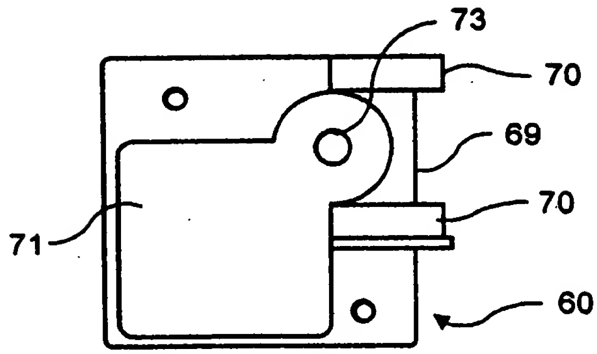

F I G. 15B

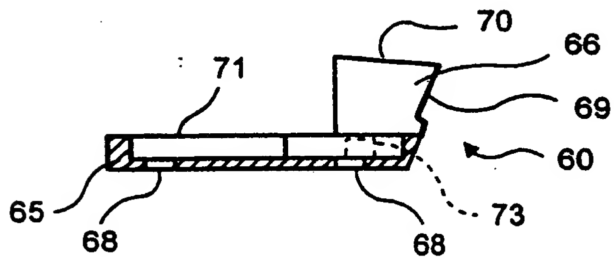

F I G. 15C

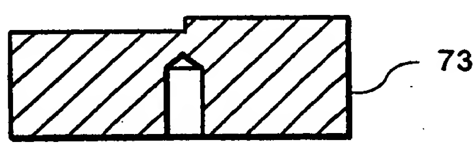

F I G. 15D1

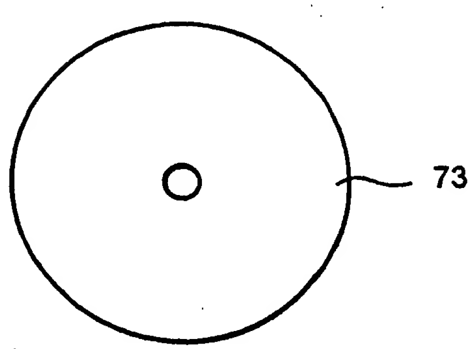

F I G. 15D2

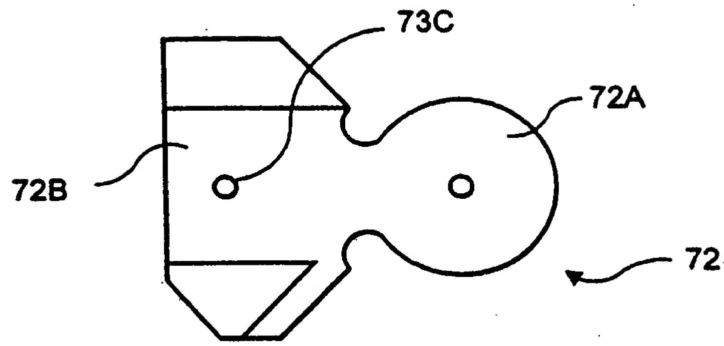

F I G. 15E1

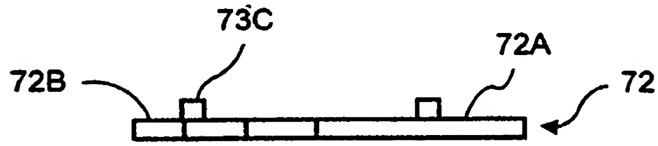

F I G. 15E2

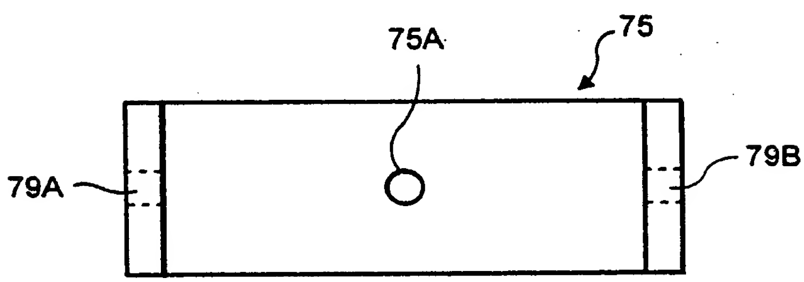

F I G. 15F1

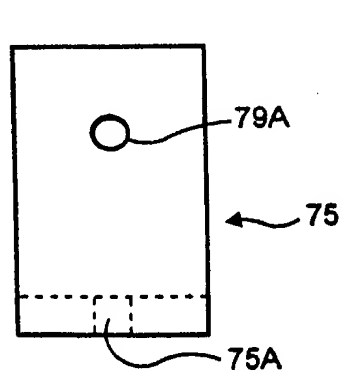

F I G. 15F2

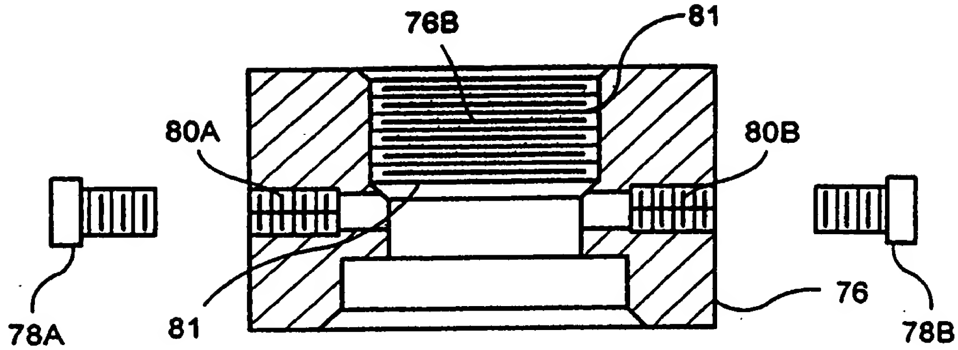

FIG. 15G1

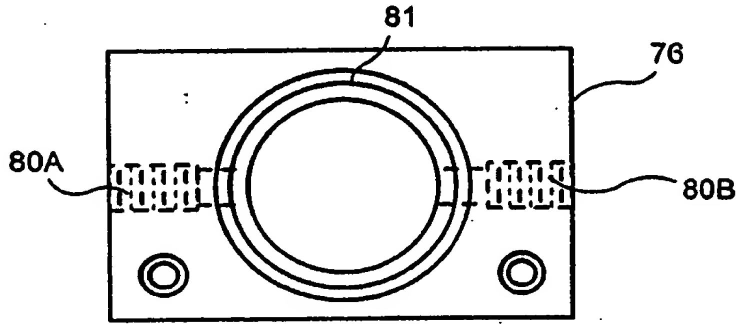

FIG. 15G2

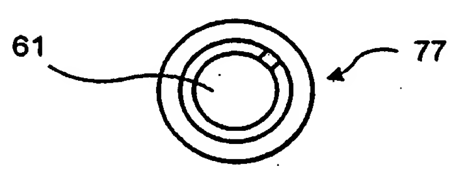

FIG. 15H1

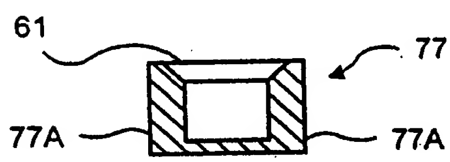

FIG. 15H2

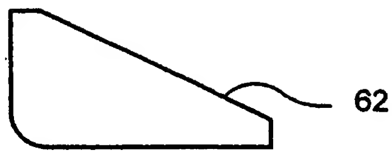

F I G. 15I1

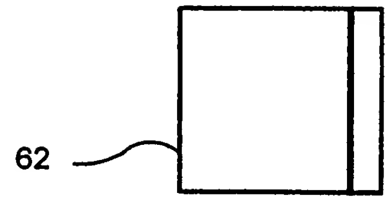

F I G. 15I2

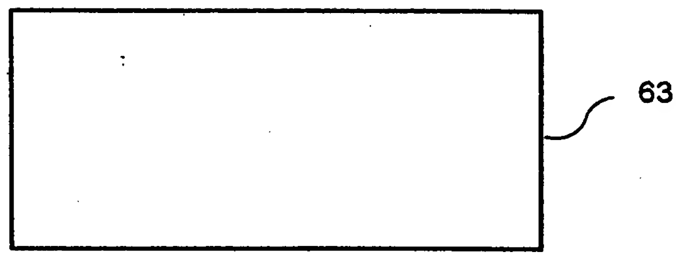

F I G. 15J

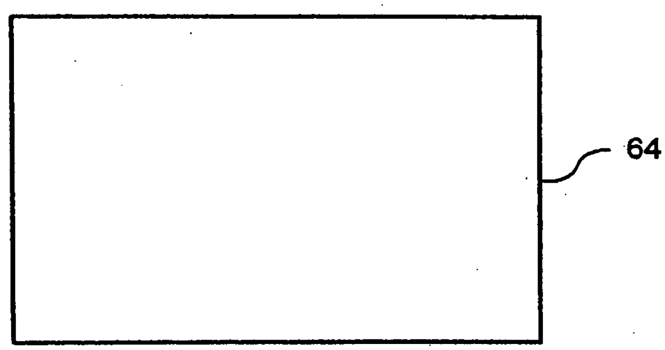

F I G. 15K

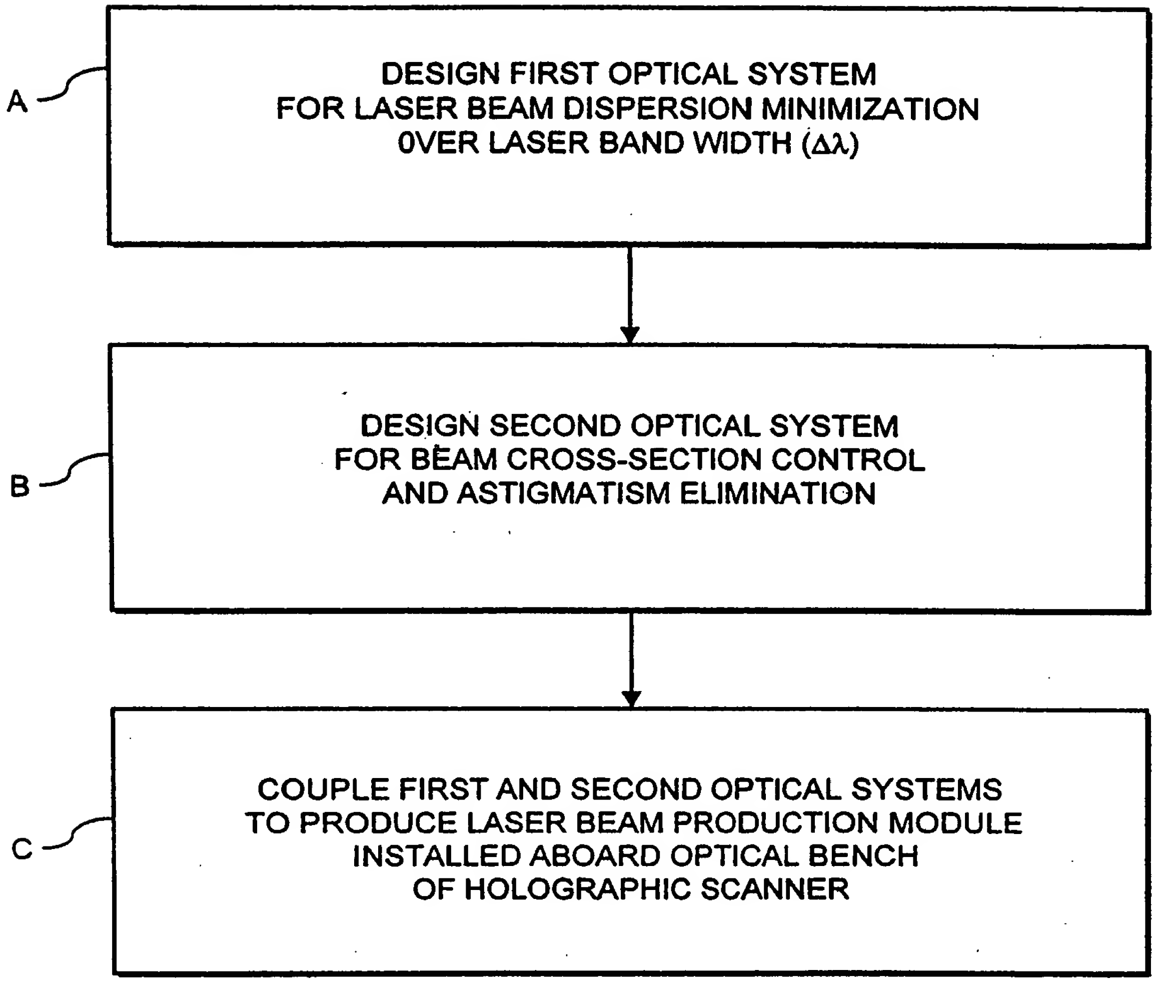
A
DESIGN FIRST OPTICAL SYSTEM
FOR LASER BEAM DISPERSION MINIMIZATION
OVER LASER BAND WIDTH (Δλ)
B
DESIGN SECOND OPTICAL SYSTEM
FOR BEAM CROSS-SECTION CONTROL
AND ASTIGMATISM ELIMINATION
C
COUPLE FIRST AND SECOND OPTICAL SYSTEMS
TO PRODUCE LASER BEAM PRODUCTION MODULE
INSTALLED ABOARD OPTICAL BENCH
OF HOLOGRAPHIC SCANNER

FIG. 16

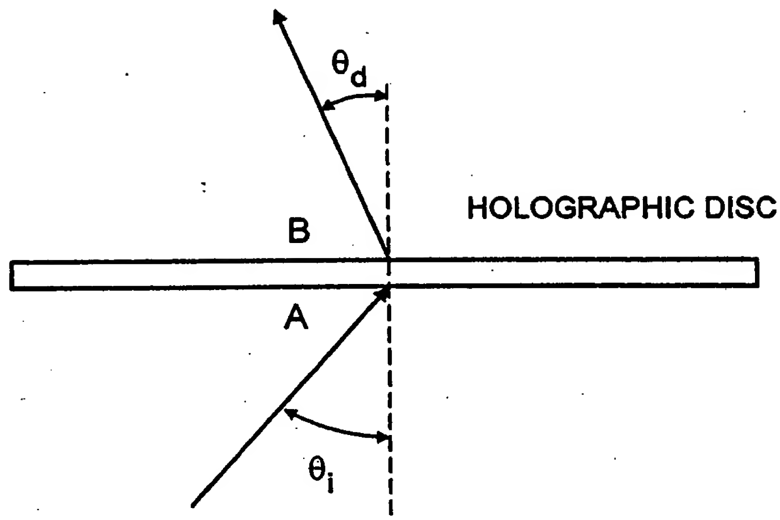

θ_i = ANGLE OF INCIDENCE

θ_d = ANGLE OF INCIDENCE

A = 90 DEGREES MINUS ANGLE θ_i

B = 90 DEGREES MINUS ANGLE θ_d

FIG. 17A

θ.i.2 = ANGLE OF INCIDENCE AT HOLOGRAPHIC FACET

θ.d.c.2 = CONSTRUCTION ANGLE OF DIFFRACTION FOR HOLOGRAPHIC FACET

θ.d.2 = ANGLE OF DIFFRACTION OF HOLOGRAPHIC FACET

λ = WAVELENGTH (IN AIR)

λ.c = CONSTRUCTION WAVELENGTH FOR HOLOGRAPHIC FACET

d.2 = GRATING SPACING IN HOLOGRAPHIC FACET

FIG. 17B

$$\mathrm{deg} := \frac{\pi}{180}$$

λ_c := .670 microns

λ := .650, .651, ..., .690 microns

$\theta_{i.2}$:= 43 deg

$\theta_{d.C.2}$:= 37 deg

FIG. 17B1

$$d_2 := \frac{\lambda_c}{\sin\left[\theta_{i.2}\right] + \sin\left[\theta_{d.c.2}\right]} \text{ microns} \qquad d_2 = 0.52188$$

$$\theta_{d.2}(\lambda) := \mathrm{asin}\left[\left[\frac{\lambda}{d_2}\right] - \sin\left[\theta_{i.2}\right]\right]$$

FIG. 17C

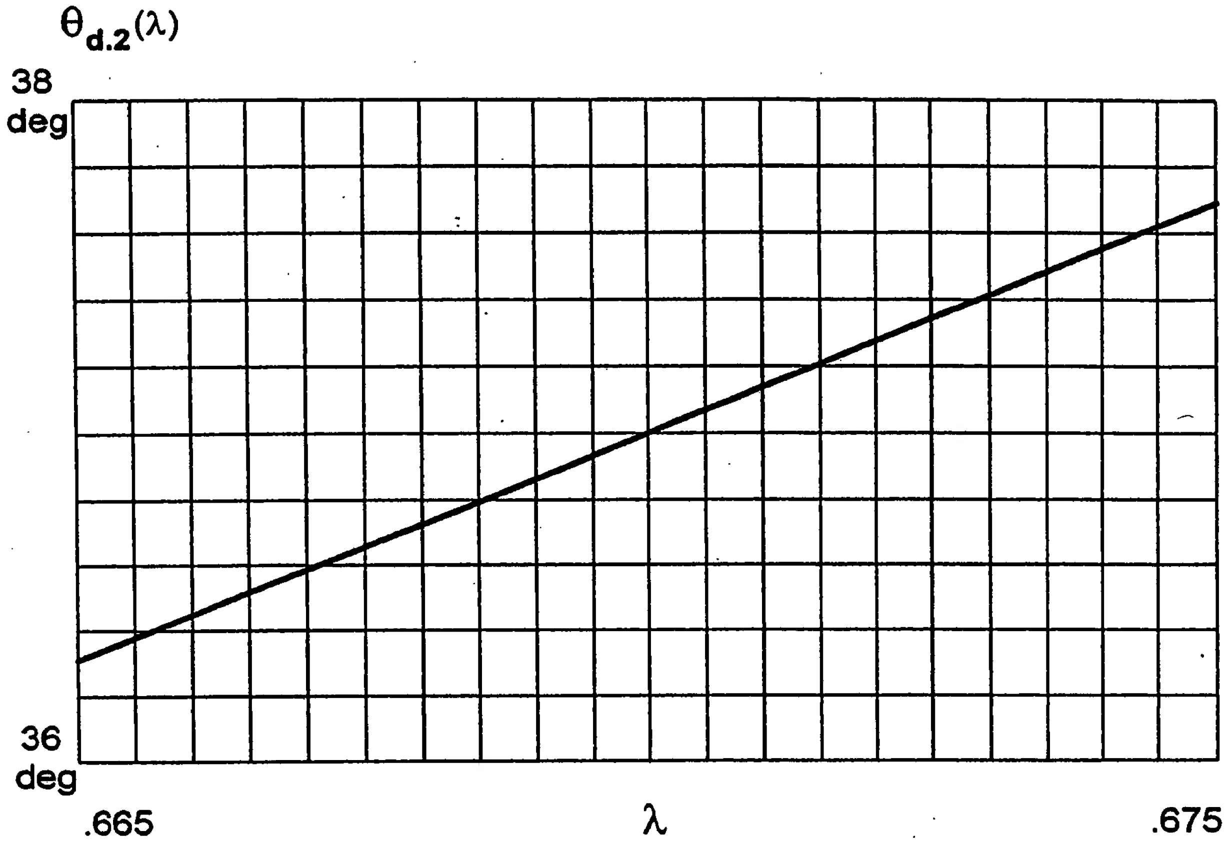

FIG. 17D

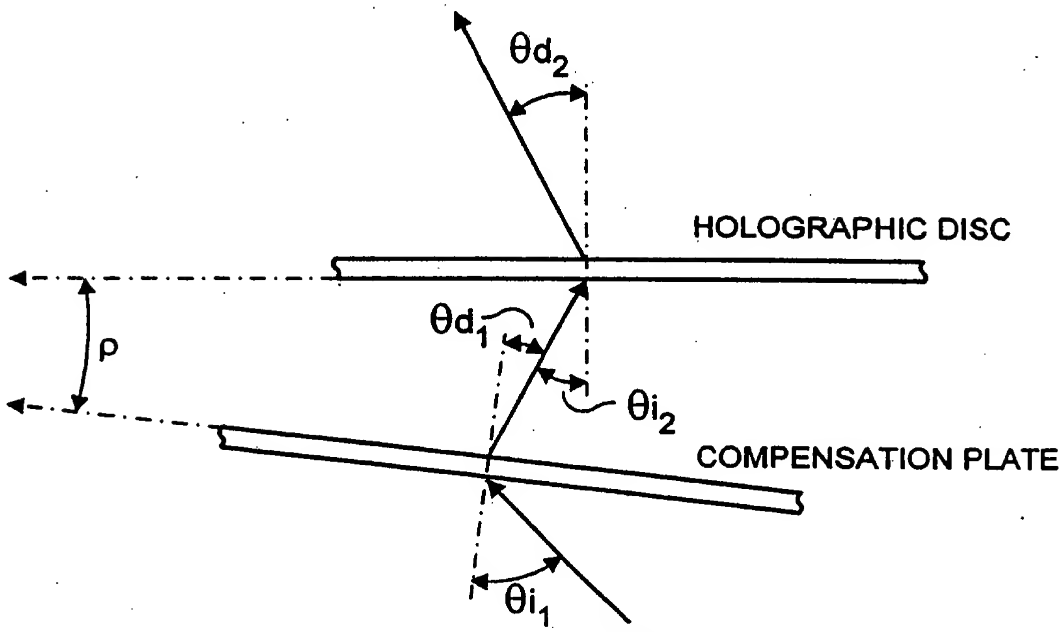
COMPENSATED OUTPUT BEAM
θd2
HOLOGRAPHIC DISC
ρ
θd1
θi2
COMPENSATION PLATE
θi1
CIRCULARIZED INPUT BEAM

F I G. 18A

COMPENSATION PLATE ADDED - WITH TILT ANGLE.
TILT ANGLE RELATIVE TO HOLOGRAPHIC FACET - ρ

θ.i.1 = ANGLE OF INCIDENCE FOR COMPENSATION PLATE (FIXED)

θ.d.c.1 = CONSTRUCTION ANGLE OF DIFFRACTION OF COMPENSATION PLATE

θ.d.1 = ANGLE OF DIFFRACTION OF COMPENSATION PLATE

λ = WAVELENGTH (IN AIR)

λ.c = CONSTRUCTION WAVELENGTH

d.1 = GRATING SPACING IN COMPENSATION PLATE

ρ = TILT ANGLE OF COMPENSATION PLATE RELATIVE TO HOLOGRAPHIC FACET

F I G. 18B

$\theta_{i.1} := 41.5 \text{ deg}$

$\rho := -1.5 \text{ deg}$

$d_1 = 0.50557 \text{ deg}$

$\theta_{d.C.1} = 41.5 \text{ deg}$

$\theta_{d.C.2} := 37 \text{ deg}$

F I G. 18B1

$$\theta_{d.C.1} = \theta_{i.2} + \rho$$

$$(1) \quad d_1 := \frac{\lambda_c}{\sin[\theta_{i.1}] + \sin[\theta_{d.c.1}]} \text{ microns}$$

$$(2) \quad \theta_{d.1}(\lambda) := \operatorname{asin}\left[\left[\frac{\lambda}{d_1}\right] - \sin[\theta_{i.1}]\right]$$

$$(3) \quad \theta_{d.2}(\lambda) :=$$

$$= \operatorname{asin}\left[\frac{\lambda}{d_2} - \sin\left[\operatorname{asin}\left[\frac{\lambda}{d_1} - \sin[\theta_{i.1}]\right] - \rho\right]\right]$$

FIG. 18C

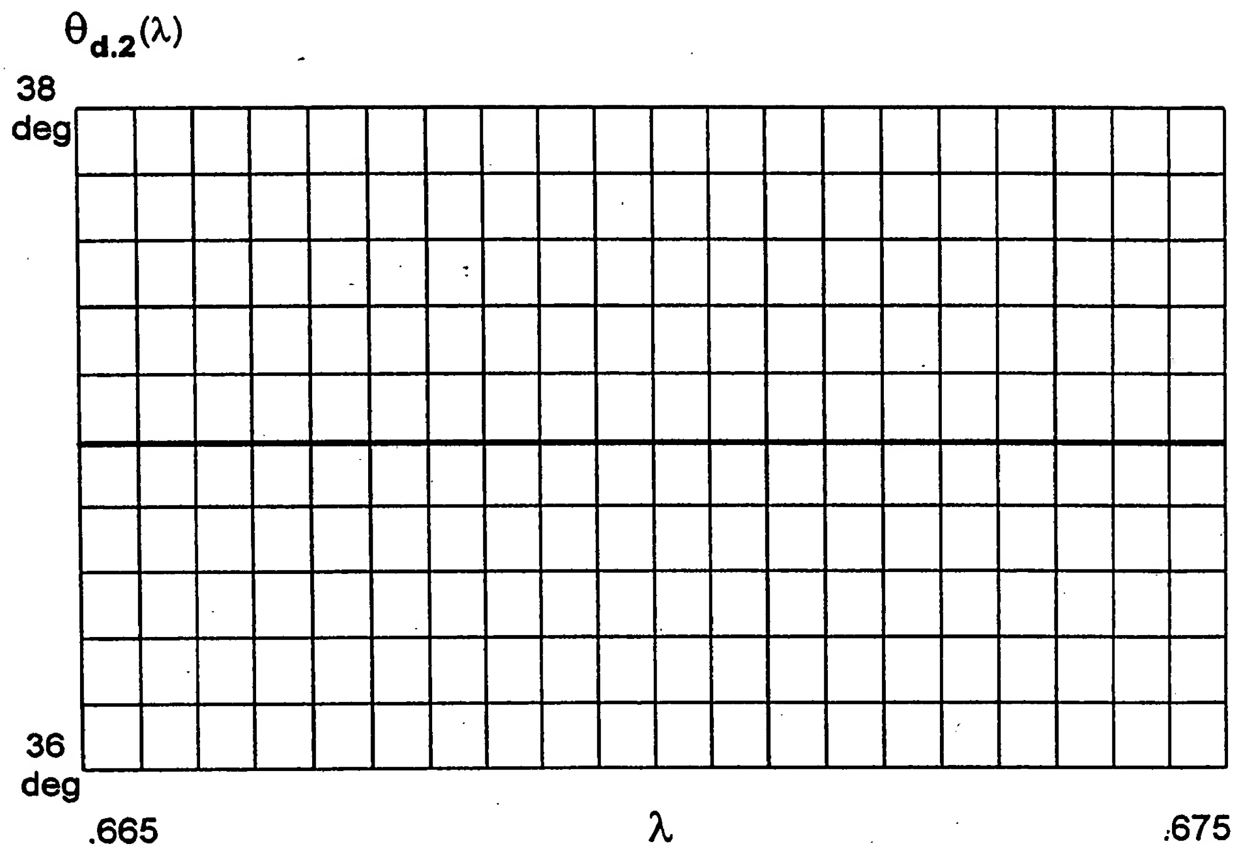

F I G. 18D

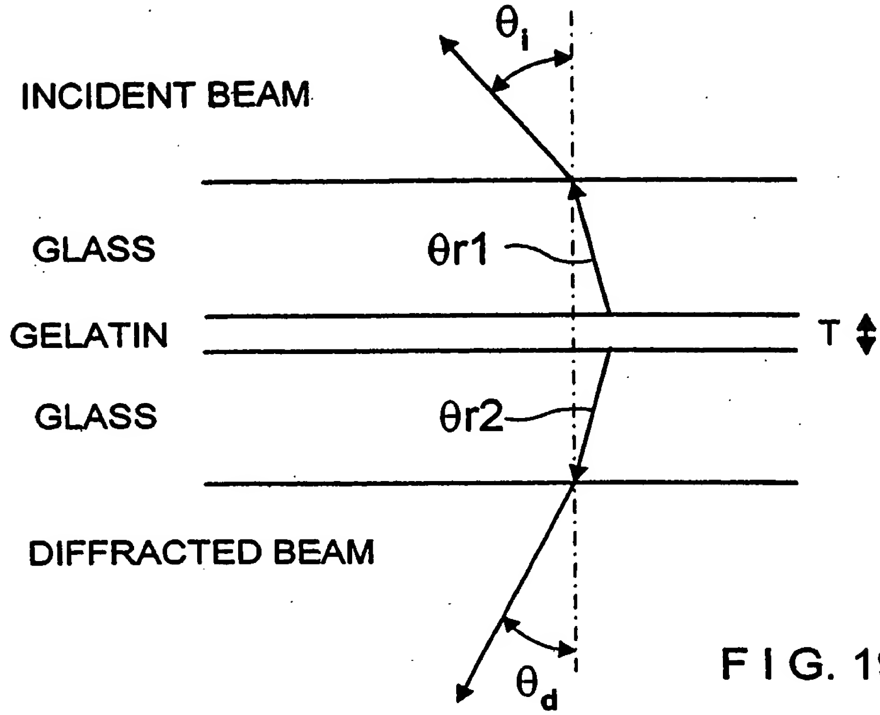

FIG. 19A

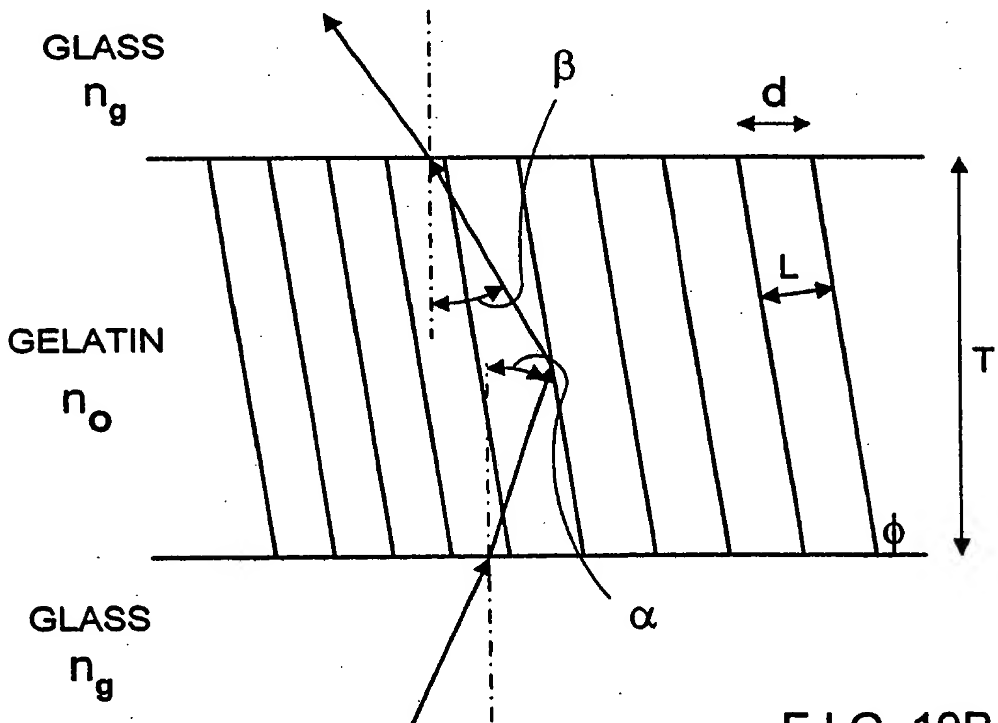

FIG. 19B

CHANGE IN CONSTRUCTION BEAM ANGLES FOR A CHANGE IN WAVELENGTH BETWEEN CONSTRUCTION AND RECONSTRUCTION. THIS PROGRAM CALCULATES THE EXTERNAL ANGLE OF INCIDENCE AND EXTERNAL ANGLE OF DIFFRACTION FOR THE CONSTRUCTION WAVELENGTH WHEN THE EXTERNAL ANGLE OF INCIDENCE AND EXTERNAL ANGLE OF DIFFRACTION ARE GIVEN FOR THE RECONSTRUCTION WAVELENGTH. BRAGG CONDITION IS MAINTAINED IN BOTH CASES SO THAT THE BRAGG PLANE TILT IS UNCHANGED.

$$deg = \frac{\pi}{180}$$

$n_0 := 1.53$	AVERAGE REFRACTIVE INDEX OF THE MEDIUM BEFORE PROCESSING
$n_2 := 1.4$	AVERAGE REFRACTIVE INDEX OF THE MEDIUM AFTER PROCESSING
$\lambda_1 := 0.670$	RECONSTRUCTION WAVELENGTH (VISIBLE LASER DIODE)
$\lambda_2 := 0.488$	CONSTRUCTION WAVELENGTH (ARGON LASER)
$\theta_{i.1} := 41.5\ deg$	ANGLE OF INCIDENCE AT RECONSTRUCTION
$\theta_{d.1} := 41.5\ deg$	ANGLE OF DIFFRACTION AT RECONSTRUCTION

F I G. 19C

HOE CONSTRUCTION ANGLES AT SECOND WAVELENGTH

REFERENCE BEAM	OBJECT BEAM
$\theta_e = \theta_{i.2} = 28.857\ deg$	$\theta_o = \theta_{d.2} = 28.857\ deg$

F I G. 19E

(1) $$\alpha_1 := \operatorname{asin}\left[\frac{\sin[\theta_{i.1}]}{n_2}\right]$$

ANGLE OF INCIDENCE INSIDE THE MEDIUM AFTER PROCESSING

$\alpha_1 = 28.249$ deg

(2) $$\beta_1 := \operatorname{asin}\left[\frac{\sin[\theta_{d.1}]}{n_2}\right]$$

ANGLE OF DIFFRACTION INSIDE THE MEDIUM AFTER PROCESSING

$\beta_1 = 28.249$ deg

$$d := \frac{\lambda_1}{\sin[\theta_{i.1}] + \sin[\theta_{d.1}]}$$

$d = 0.506$ microns

$\frac{1000}{d} = 1.978 \; 10^3$ lines per mm.

(3) $$\phi := \frac{\pi}{2} - \frac{\beta_1 - \alpha_1}{2}$$

TILT ANGLE OF THE BRAGG PLANES

$\phi = 90$ deg

(4) $$\theta_{0.1} := \alpha_1 + \frac{\pi}{2} - \phi$$

ANGLE RELATIVE TO THE BRAGG PLANES

$\theta_{0.1} = 28.249$ deg

(6) $$L := \frac{\lambda_1}{2\, n_2 \sin[\theta_{0.1}]}$$

SEPARATION OF THE BRAGG PLANES.

BRAGG CONDITION EQUATION.

$\frac{1}{L} = 1.978 \qquad \frac{1}{L}\sin(\phi) = 1.978$

(7) $$\theta_{0.2} := \operatorname{asin}\left[\frac{\lambda_2}{2\, n_0\, L}\right]$$

ANGLE RELATIVE TO THE BRAGG PLANES FOR THE SECOND WAVELENGTH SATISFYING THE BRAGG CONDITION - BEFORE PROCESSING

$\theta_{0.2} = 18.387$ deg

FIG. 19D1

(8) $\alpha_2 := \theta_{0.2} + \phi - \frac{\pi}{2}$

ANGLE OF INCIDENCE INSIDE THE MEDIUM FOR THE SECOND WAVELENGTH - BEFORE PROCESSING

$\alpha_2 = 18.387$ deg

(9) $\beta_2 := \alpha_2 + \pi - 2\phi$

ANGLE OF DIFFRACTION INSIDE THE MEDIUM FOR THE SECOND WAVELENGTH - BEFORE PROCESSING

$\beta_2 = 18.387$ deg

(10) $\theta_{i.2} := \operatorname{asin}\left[n_0 \sin\left[\alpha_2\right]\right]$

ANGLE OF INCIDENCE (REFERENCE BEAM) FOR THE SECOND WAVELENGTH - EXTERNAL

$\theta_{i.2} = 28.857$ deg

(11) $\theta_{d.2} := \operatorname{asin}\left[n_0 \sin\left[\beta_2\right]\right]$

ANGLE OF DIFFRACTION (OBJECT BEAM) FOR THE SECOND WAVELENGTH - EXTERNAL

$\theta_{d.2} = 28.857$ deg

FIG. 19D2

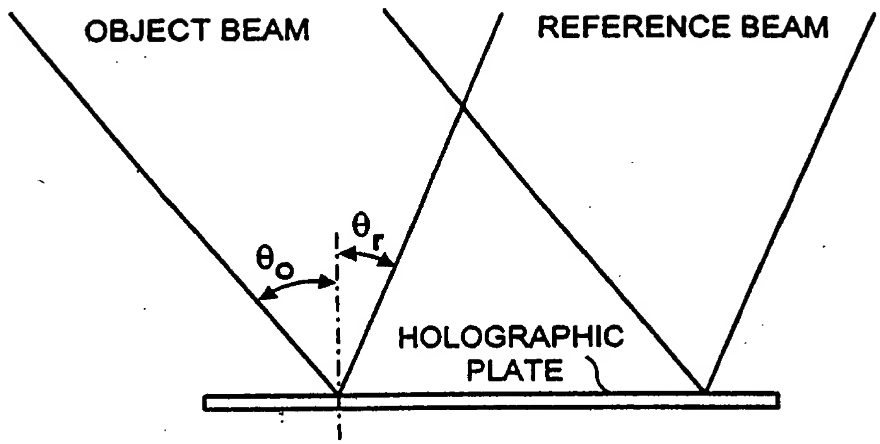

θ_o = OBJECT BEAM ANGLE OF INCIDENCE
θ_r = REFERENCE BEAM ANGLE OF INCIDENCE

FIG. 19F

ASTIGMATIC DIFFERENCE IN A LASER DIODE

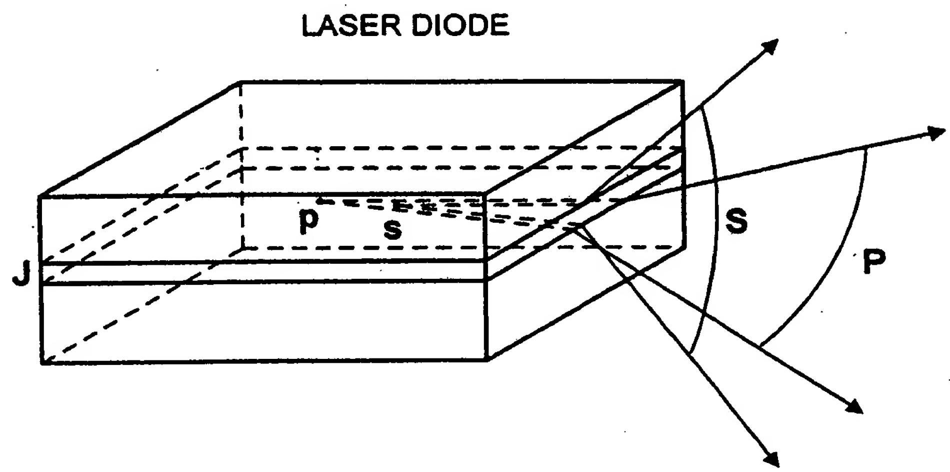

s = EFFECTIVE SOURCE OF WAVEFRONT PERPENDICULAR TO JUNCTION

p = EFFECTIVE SOURCE OF WAVEFRONT PARALLEL TO JUNCTION

S = EXTERNAL WAVEFRONT PERPENDICULAR TO JUNCTION

P = EXTERNAL WAVEFRONT PARALLEL TO JUNCTION

J = DIOD JUNCTION LAYERS

F I G. 20

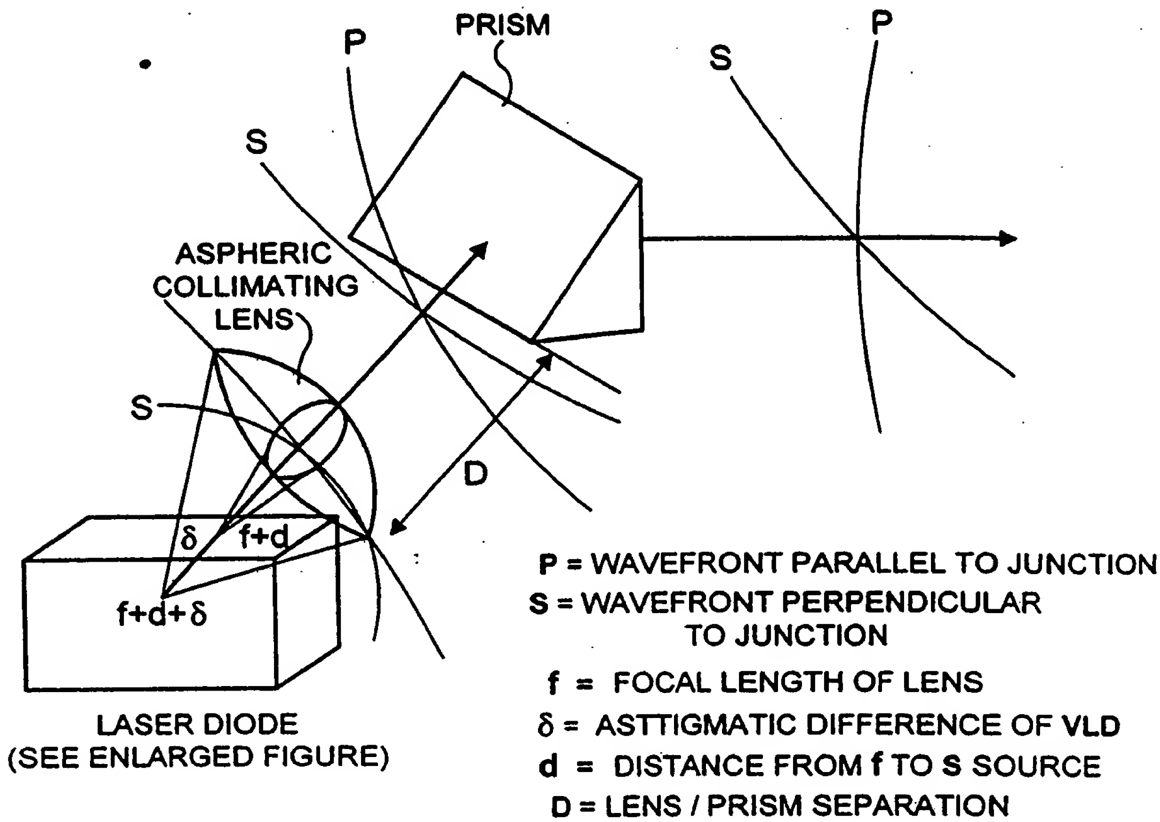

FIG. 20A

CIRCULARIZATION AND ASTIGMATISM ELIMINATION

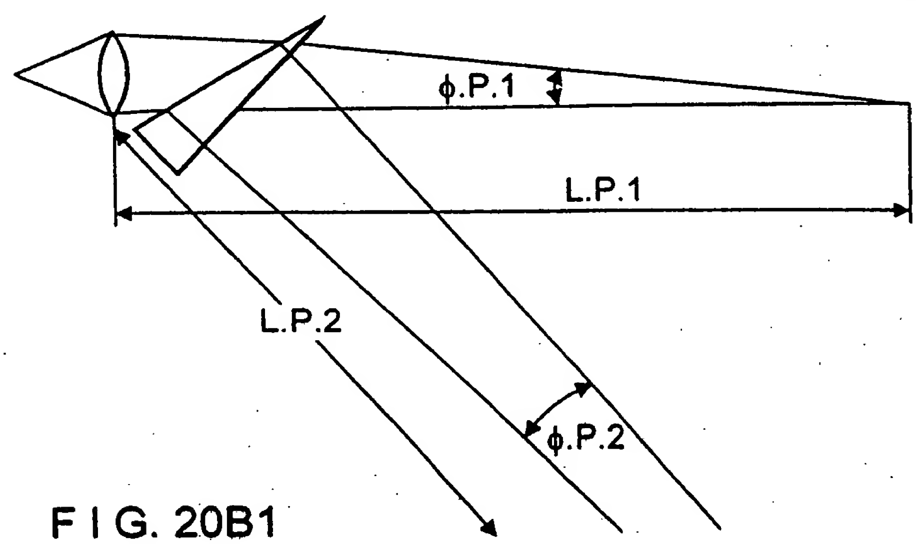

FIG. 20B1

ENLARGED SECTION

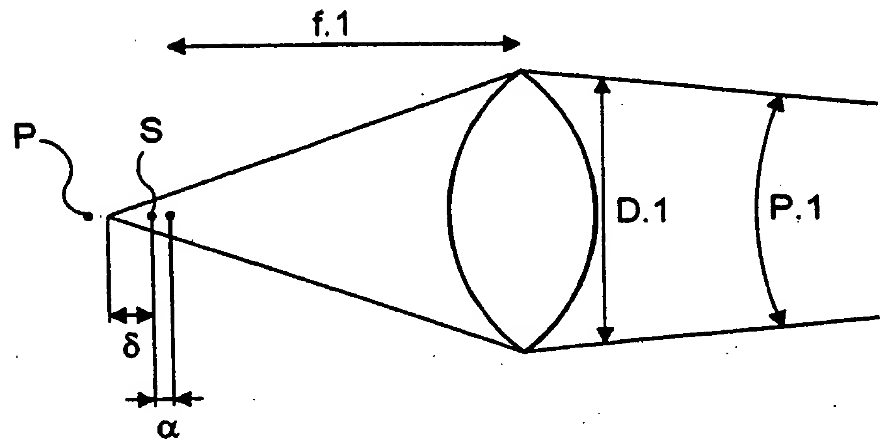

F I G. 20B2

ENLARGED SECTION

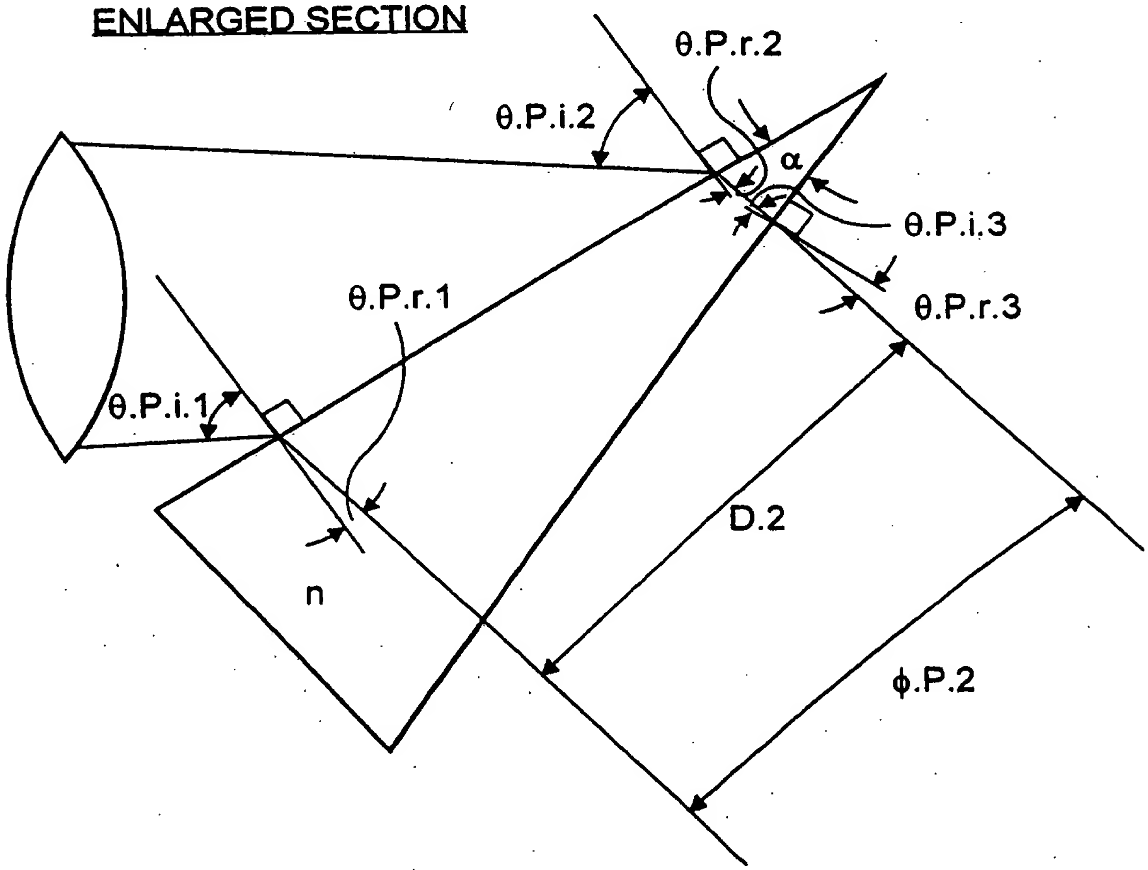

F I G. 20B3

ANALYSIS OF ASTIGMATIC DIFFERENCE REDUCTION WITH A CIRCULARIZING PRISM FOR THE GENERAL CASE WHERE BOTH S AND P BEAMS ARE CONVERGING.

f.1 = FOCAL LENGTH OF COLLIMATING LENS
d = DISTANCE FROM FOCAL POINT OF COLLAMATING LENS TO S-BEAM SOURCE
δ = ASTIGMATIC DIFFERENCE OF LASER DIODE
D.1 = P- BEAM DIAMETER LEAVING COLLIMATING LENS
D.2 = EXPANDED P- BEAM DIAMETER LEAVING PRISM
M = BEAM EXPANSION FACTOR = D.2 / D.1
n = REFRACTIVE INDEX OF PRISM MATERIAL
θ.P.i.1 = ANGLE OF INCIDENCE OF LOWER PORTION OF CONVERGING P-BEAM AT PRISM
θ.P.i.2 = ANGLE OF INCIDENCE OF UPPER PORTION OF CONVERGING P-BEAM AT PRISM
ϕ.P.1 = CONVERGENCE OF P- BEAM LEAVING COLLIMATING LENS
ϕ.S.1 = CONVERGENCE OF S- BEAM LEAVING COLLIMATING LENS
ϕ.P.2 = CONVERGENCE OF P- BEAM LEAVING PRISM
ϕ.S.1 = ϕ.S.1 = CONVERGENCE OF S- BEAM LEAVING PRISM
L.P.1 = IMAGE DISTANCE FOR P SOURCE IMAGED BY COLLIMATING LENS
L.P.2 = IMAGE DISTANCE FOR P SOURCE AFTER INSERTING PRISM
L.S.1 = IMAGE DISTANCE FOR S SOURCE IMAGED BY COLLIMATING LENS
L.S.2 = L.S.1 = IMAGE DISTANCE FOR S SOURCE AFTER INSERTING PRISM
θ.P.r.1 = ANGLE OF REFRACTION OF LOWER PORTION OF CONVERGING P-BEAM IN PRISM
θ.P.r.2 = ANGLE OF REFRACTION OF UPPER PORTION OF CONVERGING P-BEAM IN PRISM
α = PRISM APEX ANGLE = θ.P.r.1 (BY DESIGN FOR CONVENIENCE)
θ.P.i.3 = ANGLE OF INCIDENCE OF UPPER PORTION OF CONVERGING P-BEAM AT SECOND SURFACE OF PRISM = θ.P.r.1 - θ.P.r.2 = = α - θ.P.r.2
θ.P.r.3 = ANGLE OF REFRACTION OF UPPER PORTION OF CONVERGING P-BEAM LEAVING SECOND SURFACE OF PRISM = ϕ.P.2

FIG. 20C

ASSUMED VALUE OF FIXED PARAMETERS: $\deg = \frac{\pi}{180}$

$n := 1.72$ (REFRACTIVE INDEX OF SF10 GLASS AT 675 mm.)

$f_1 := 4.5$ mm $\delta := .01$ mm

$D_1 := 1$ mm $\theta_{P.i.1} := 78$ deg

VARIABLE PARAMETER:

$d := .0000000001, .00001, \ldots .001$ mm

FIG. 20C1

$$(1)\quad L_{P.1}(d) := \frac{f_1^{\,2}}{d+\delta} \qquad (2)\quad L_{S.1}(d) := \frac{f_1^{\,2}}{d}$$

$$(3)\quad \phi_{P.1}(d) := \operatorname{atan}\left[\frac{D_1}{L_{P.1}(d)}\right]$$

$$(4)\quad \phi_{S.1}(d) := \operatorname{atan}\left[\frac{D_1}{L_{S.1}(d)}\right]$$

$$(5)\quad M := \frac{\cos\left[\operatorname{asin}\left[\frac{\sin[\theta_{P.i.1}]}{n}\right]\right]}{\cos[\theta_{P.i.1}]} \qquad M = 3.9563$$

$$(6)\quad D_2 := M\,D_1 \qquad D_2 = 3.9563$$

$$(7)\quad \theta_{P.i.2}(d) := \theta_{P.i.1} - \phi_{P.1}(d)$$

$$(8)\quad \theta_{P.r.1} := \operatorname{asin}\left[\frac{\sin[\theta_{P.i.1}]}{n}\right] \qquad \theta_{P.r.1} = 34.659\ \mathrm{deg}$$

$$(9)\quad \alpha := \theta_{P.r.1} \qquad \alpha = 34.659\ \mathrm{deg}$$

$$(10)\quad \theta_{P.r.2}(d) := \operatorname{asin}\left[\frac{\sin[\theta_{P.i.2}(d)]}{n}\right]$$

FIG. 20D

(11) $\theta_{P.i.3}(d) := \theta_{P.r.1} - \theta_{P.r.2}(d)$

(12) $\theta_{P.r.3}(d) := \mathrm{asin}\left[n \ \sin\left[\theta_{P.i.3}(d)\right]\right]$

(13) $\phi_{P.2}(d) := \theta_{P.r.3}(d)$

(14) $L_{P.2}(d) := \dfrac{D_2}{\tan\left[\phi_{P.2}(d)\right]}$

(15) $L_{S.2}(d) := L_{S.1}(d)$

FIG. 20D1

S AND P IMAGE DISTANCES IN THE IMAGE PLANE OF THE COLLIMATING LENS AS A FUNCTION OF THE DISTANCE FROM THE FOCAL POINT OF THE COLLIMATING LENS TO THE S SOURCE. PRISM PLACED AFTER THE COLLIMATING LENS. θ.P.i.1 IS THE ANGLE OF INCIDENCE OF THE LOWER PORTION OF THE P-BEAM ON THE HYPOTENUSE OF THE PRISM. δ IS THE VLD ASTIGMATIC DIFFERENCE.

S AND P IMAGE LOCATIONS - COLLIMATING LENS AND PRISM ONLY

$n = 1.72$ $f_1 = 4.5$ mm $\theta_{P.I.1} = 78$ deg $\delta = 0.01$ mm

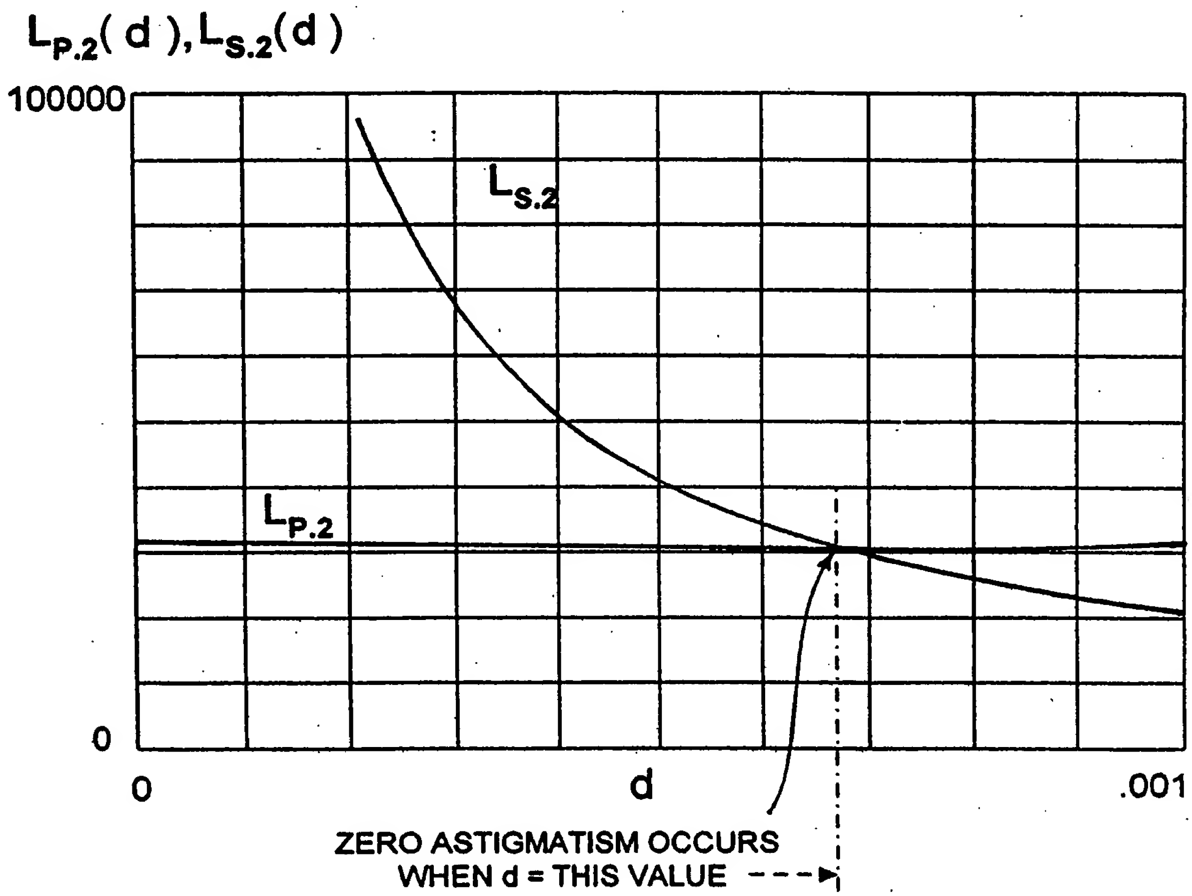

$d := .00068338$ mm

$L_{P.2}(d) = 2.9632 \cdot 10^4$mm $L_{S.2}(d) = 2.9632 \cdot 10^4$mm

F I G. 20E

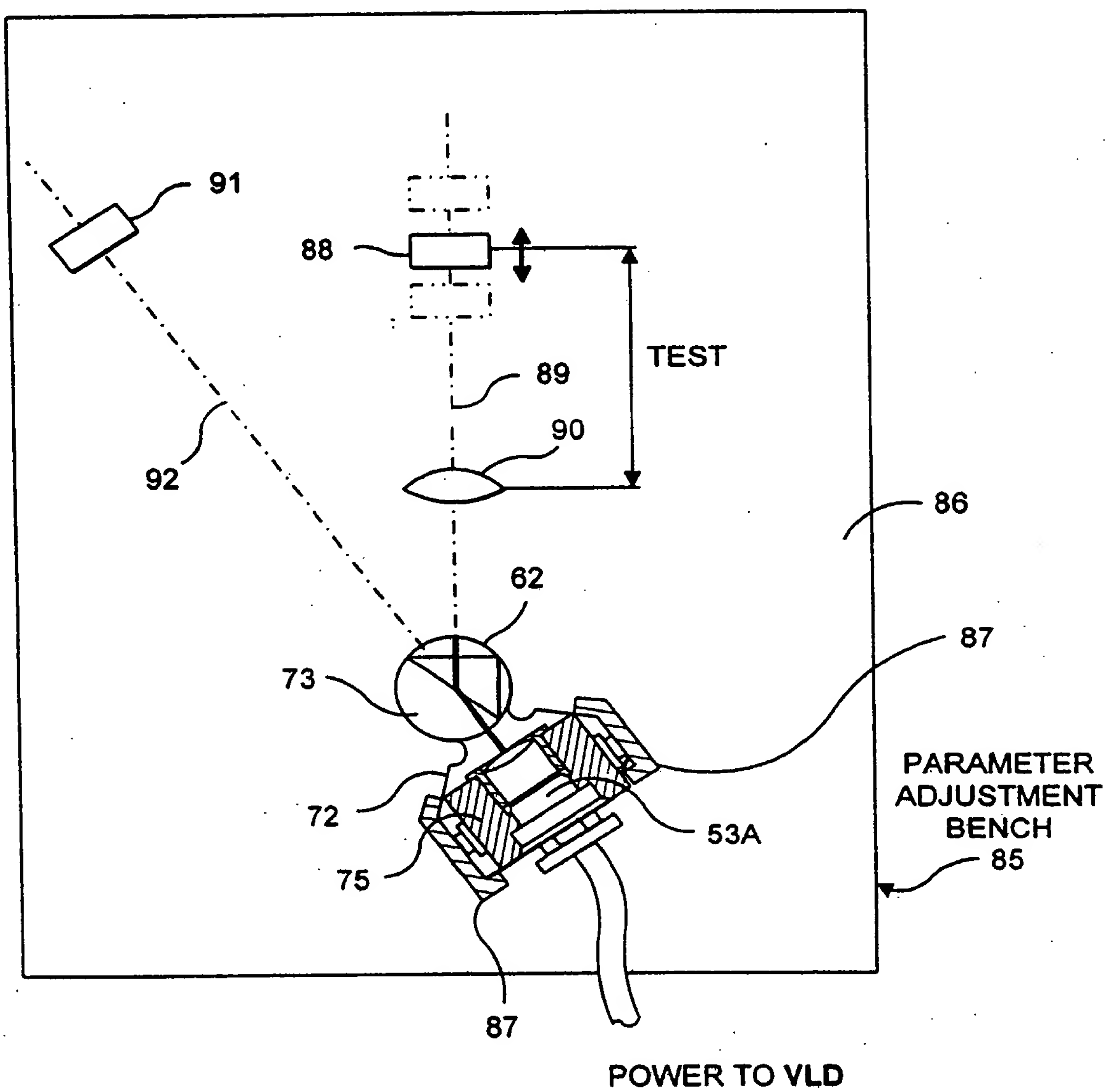
91
88
TEST
89
90
92
86
62
87
73
PARAMETER
ADJUSTMENT
BENCH
85
72
53A
75
87
POWER TO VLD

F I G. 21A

A — REALIZE PARAMETERS IN GEOMETRICAL OPTICS MODEL FOR SECOND OPTICAL SYSTEM, EXCEPT VLD-TO-LENS DISTANCE **d** AND Θ_{PI1} AND Θ_{PI2} (I.E. $\Theta_{PRISM\text{-}TILT}$)

↓

B — SET INITIAL VALUES FOR **d** AND $\Theta_{PRISM\text{-}TILT}$ USING ACCEPTABLE CRITERIA (ROUGH-IN STEP)

↓

C — SET $\Theta_{PRISM\text{-}TILT}$ SO THAT DESIRED ELLIPSICITY (ASPECT-RATIO) OF LASER BEAM IS ACHIEVED ON SECOND SURFACE OF THE PRISM

↓

D — ADJUST **d** SO THAT RADIUS OF CURVATURE OF THE **S** AND **P** CYLINDRICAL WAVEFRONTS ARE SUBSTANTIALLY EQUAL AT SECOND SURFACE OF PRISM, PRODUCING A SPHERICAL WAVEFRONT WITH CONVERGING RADIUS

↓

E — VARY **d** TO ADJUST RADIUS OF CURVATURE OF **S** CYLINDRICAL WAVEFRONT TO CAUSE BOTH **S** AND **P** WAVEFRONTS TO FOCUS TO A POINT SUCH THAT THE DIFFRACTED LASER BEAM FOCUSES TO ITS DESIGNED FOCAL PLANE IN SCANNING VOLUME

↓

F — ADJUST PRISM TILT ANGLE $\Theta_{PRISM\text{-}TILT}$ UNTIL RADIUS OF CURVATURE OF **P** CYLINDRICAL WAVEFRONT IS ONCE AGAIN EQUAL TO RADIUS OF CURVATURE OF THE **S** CYLINDRICAL WAVEFRONT, PRODUCING A SPHERICAL WAVEFRONT AT THE SECOND SURFACE PRISM

FIG. 21B

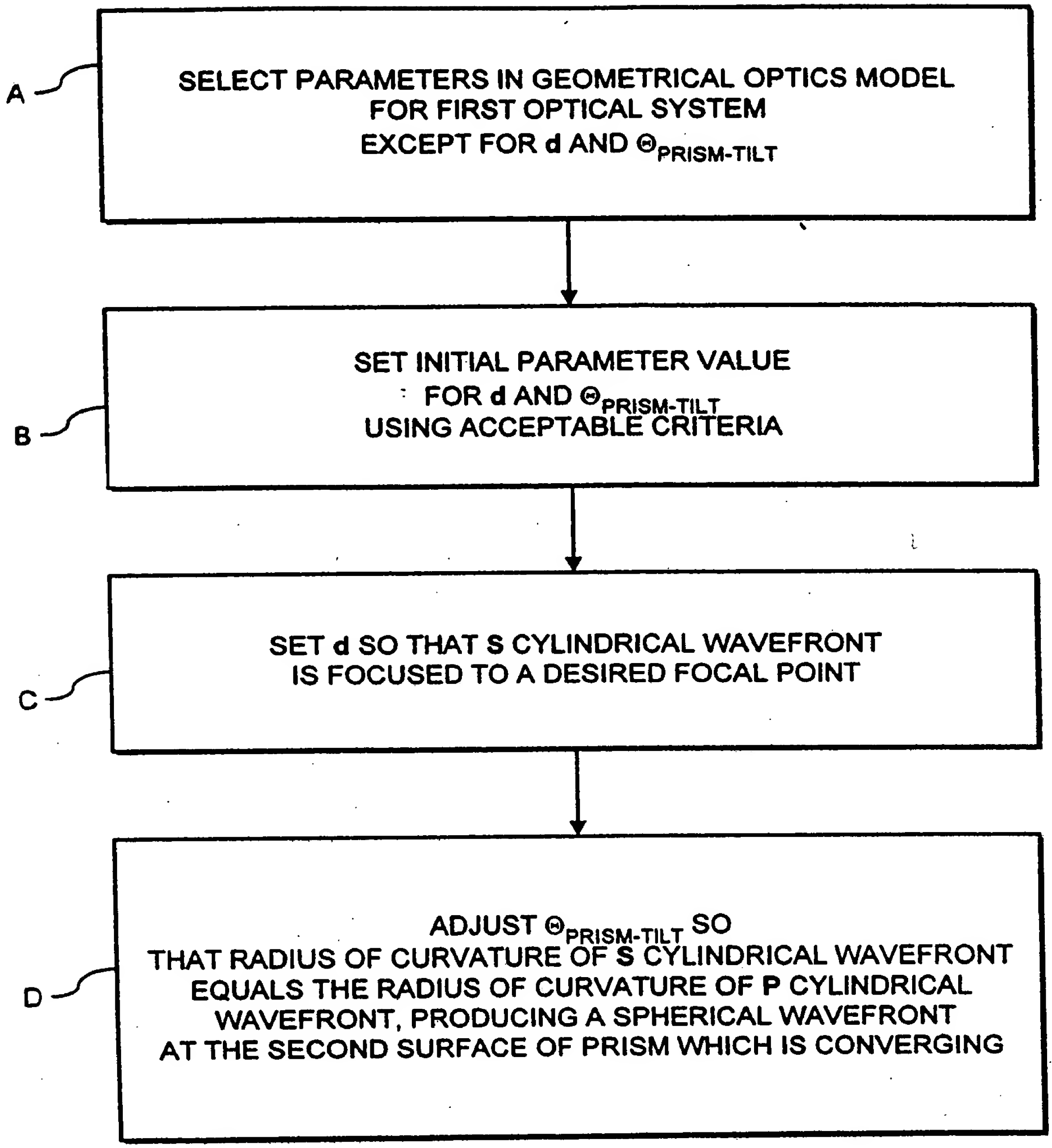
A
SELECT PARAMETERS IN GEOMETRICAL OPTICS MODEL FOR FIRST OPTICAL SYSTEM EXCEPT FOR d AND $\Theta_{PRISM-TILT}$
B
SET INITIAL PARAMETER VALUE FOR d AND $\Theta_{PRISM-TILT}$ USING ACCEPTABLE CRITERIA
C
SET d SO THAT S CYLINDRICAL WAVEFRONT IS FOCUSED TO A DESIRED FOCAL POINT
D
ADJUST $\Theta_{PRISM-TILT}$ SO THAT RADIUS OF CURVATURE OF S CYLINDRICAL WAVEFRONT EQUALS THE RADIUS OF CURVATURE OF P CYLINDRICAL WAVEFRONT, PRODUCING A SPHERICAL WAVEFRONT AT THE SECOND SURFACE OF PRISM WHICH IS CONVERGING

FIG. 21C

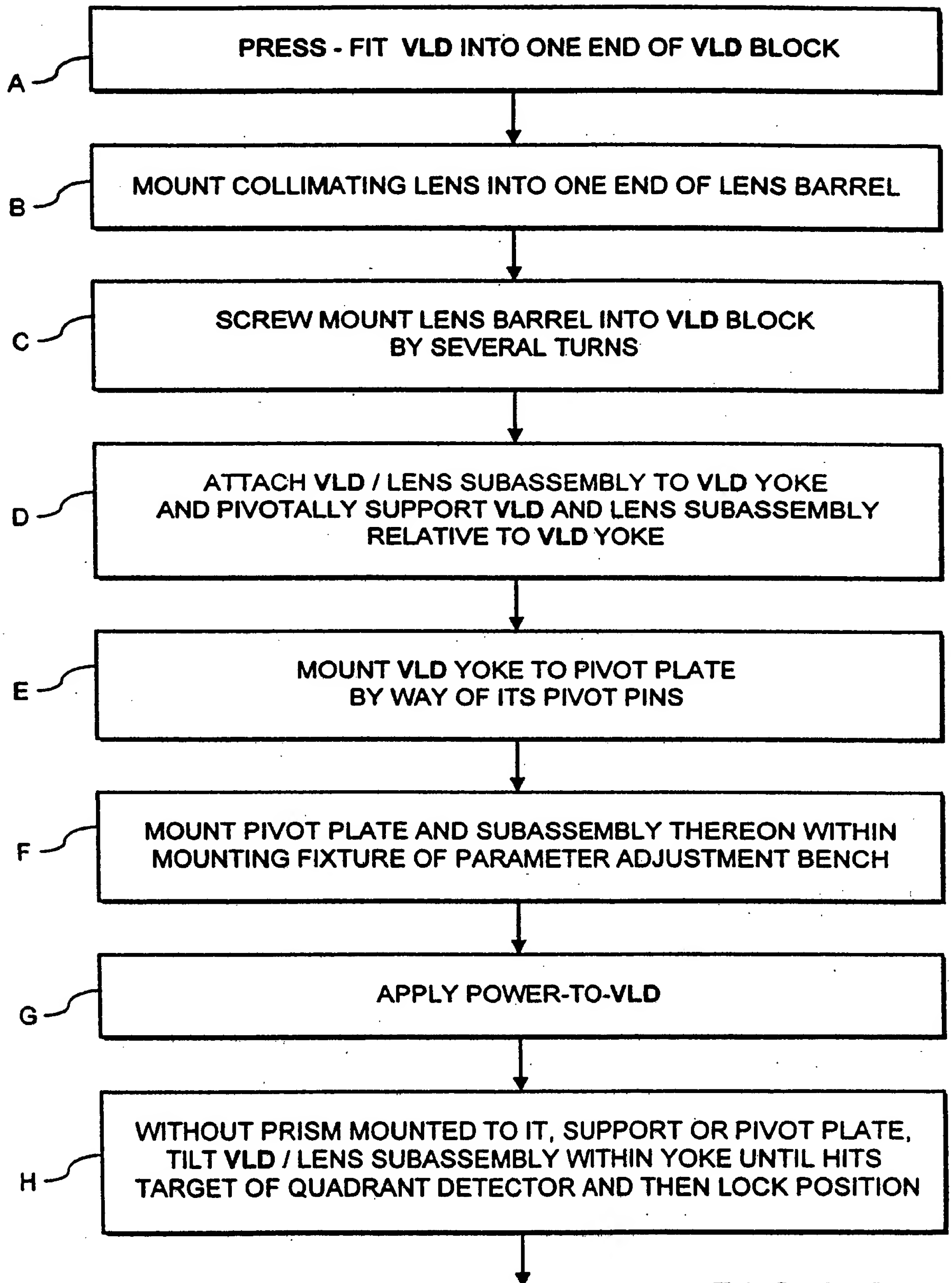
A
PRESS - FIT VLD INTO ONE END OF VLD BLOCK
B
MOUNT COLLIMATING LENS INTO ONE END OF LENS BARREL
C
SCREW MOUNT LENS BARREL INTO VLD BLOCK BY SEVERAL TURNS
D
ATTACH VLD / LENS SUBASSEMBLY TO VLD YOKE AND PIVOTALLY SUPPORT VLD AND LENS SUBASSEMBLY RELATIVE TO VLD YOKE
E
MOUNT VLD YOKE TO PIVOT PLATE BY WAY OF ITS PIVOT PINS
F
MOUNT PIVOT PLATE AND SUBASSEMBLY THEREON WITHIN MOUNTING FIXTURE OF PARAMETER ADJUSTMENT BENCH
G
APPLY POWER-TO-VLD
H
WITHOUT PRISM MOUNTED TO IT, SUPPORT OR PIVOT PLATE, TILT VLD / LENS SUBASSEMBLY WITHIN YOKE UNTIL HITS TARGET OF QUADRANT DETECTOR AND THEN LOCK POSITION

FIG. 21C1

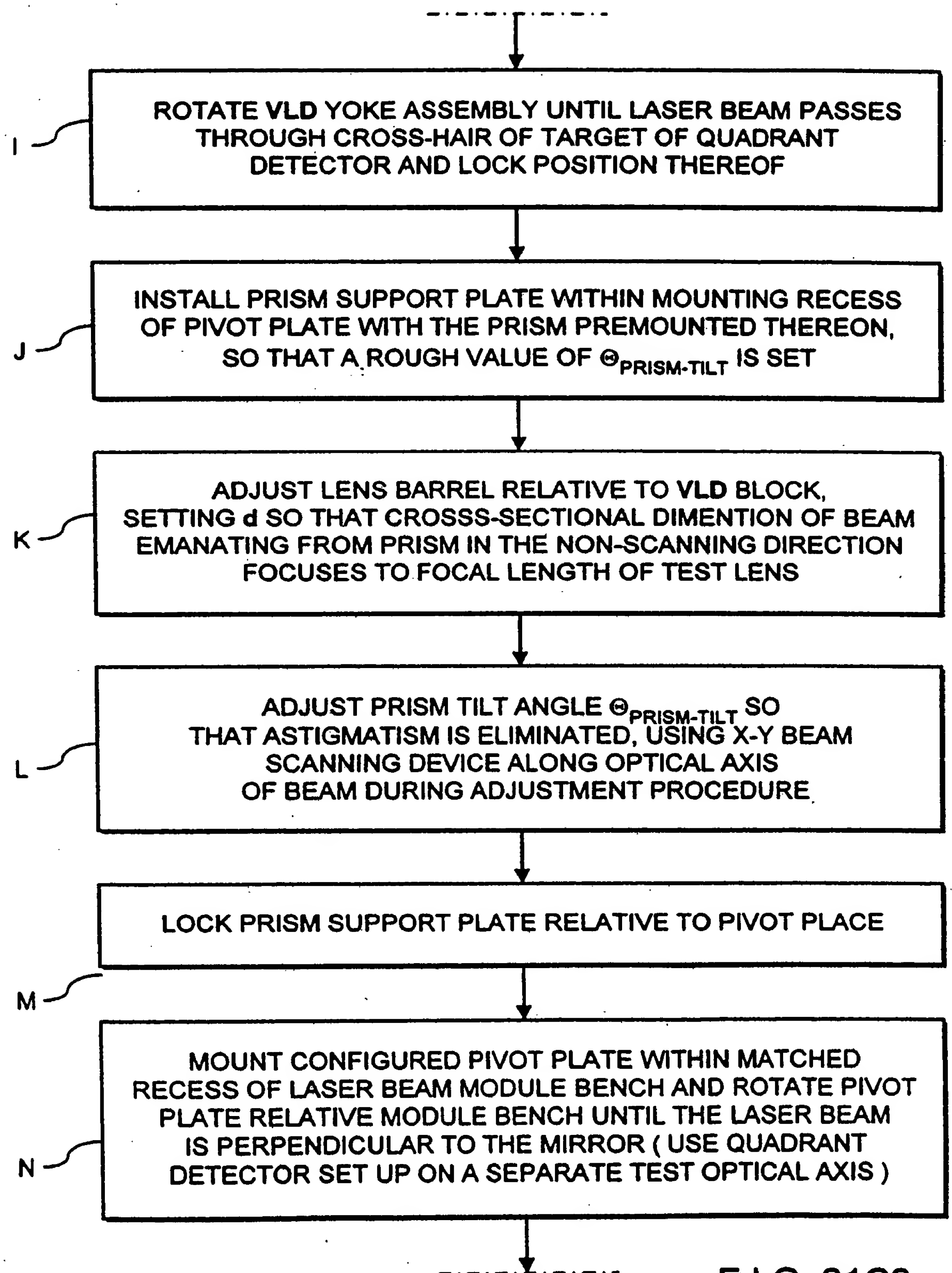
ROTATE VLD YOKE ASSEMBLY UNTIL LASER BEAM PASSES THROUGH CROSS-HAIR OF TARGET OF QUADRANT DETECTOR AND LOCK POSITION THEREOF
I
INSTALL PRISM SUPPORT PLATE WITHIN MOUNTING RECESS OF PIVOT PLATE WITH THE PRISM PREMOUNTED THEREON, SO THAT A ROUGH VALUE OF $\Theta_{PRISM-TILT}$ IS SET
J
ADJUST LENS BARREL RELATIVE TO VLD BLOCK, SETTING d SO THAT CROSSS-SECTIONAL DIMENTION OF BEAM EMANATING FROM PRISM IN THE NON-SCANNING DIRECTION FOCUSES TO FOCAL LENGTH OF TEST LENS
K
ADJUST PRISM TILT ANGLE $\Theta_{PRISM-TILT}$ SO THAT ASTIGMATISM IS ELIMINATED, USING X-Y BEAM SCANNING DEVICE ALONG OPTICAL AXIS OF BEAM DURING ADJUSTMENT PROCEDURE
L
LOCK PRISM SUPPORT PLATE RELATIVE TO PIVOT PLACE
M
MOUNT CONFIGURED PIVOT PLATE WITHIN MATCHED RECESS OF LASER BEAM MODULE BENCH AND ROTATE PIVOT PLATE RELATIVE MODULE BENCH UNTIL THE LASER BEAM IS PERPENDICULAR TO THE MIRROR (USE QUADRANT DETECTOR SET UP ON A SEPARATE TEST OPTICAL AXIS)
N

FIG. 21C2

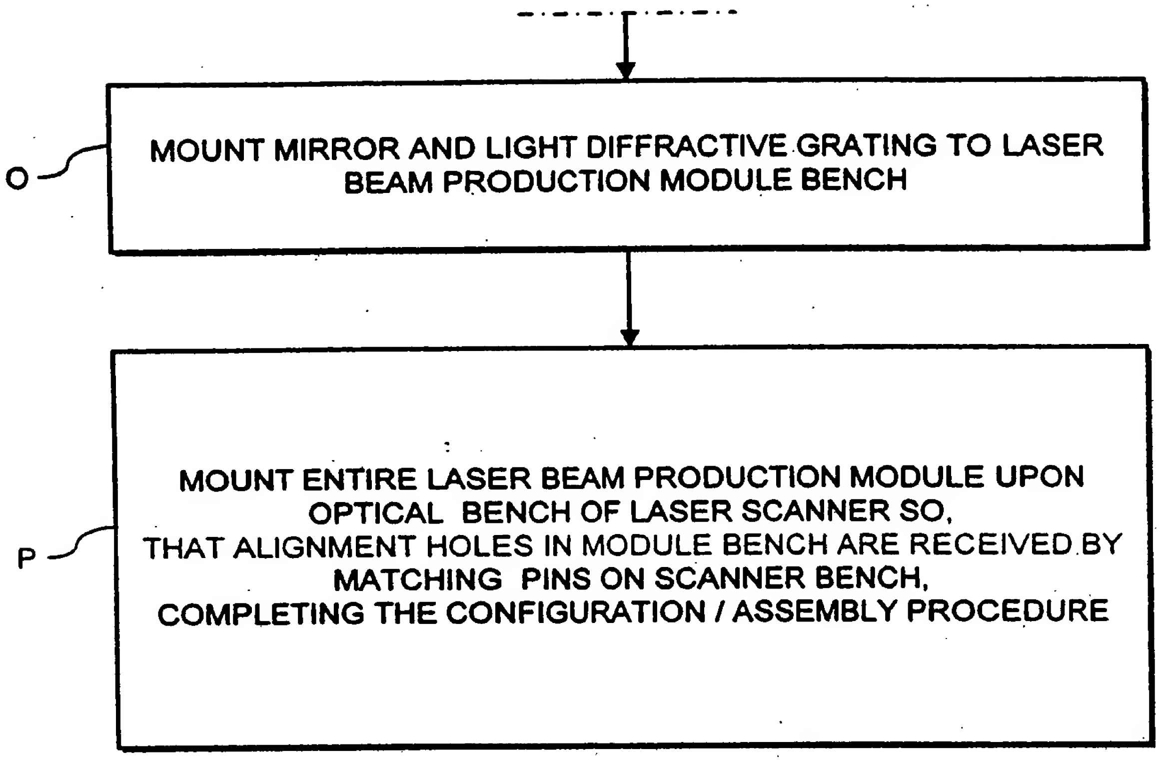
MOUNT MIRROR AND LIGHT DIFFRACTIVE GRATING TO LASER BEAM PRODUCTION MODULE BENCH
O
MOUNT ENTIRE LASER BEAM PRODUCTION MODULE UPON OPTICAL BENCH OF LASER SCANNER SO, THAT ALIGNMENT HOLES IN MODULE BENCH ARE RECEIVED BY MATCHING PINS ON SCANNER BENCH, COMPLETING THE CONFIGURATION / ASSEMBLY PROCEDURE
P

FIG. 21C3

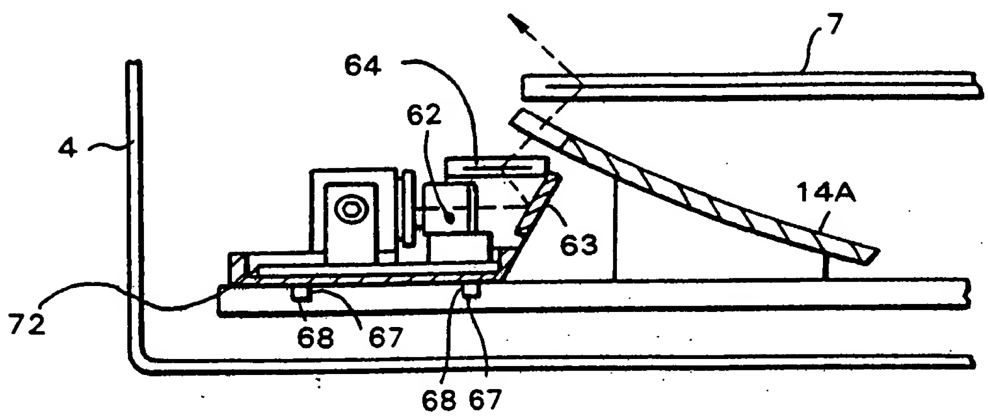

FIG. 21D

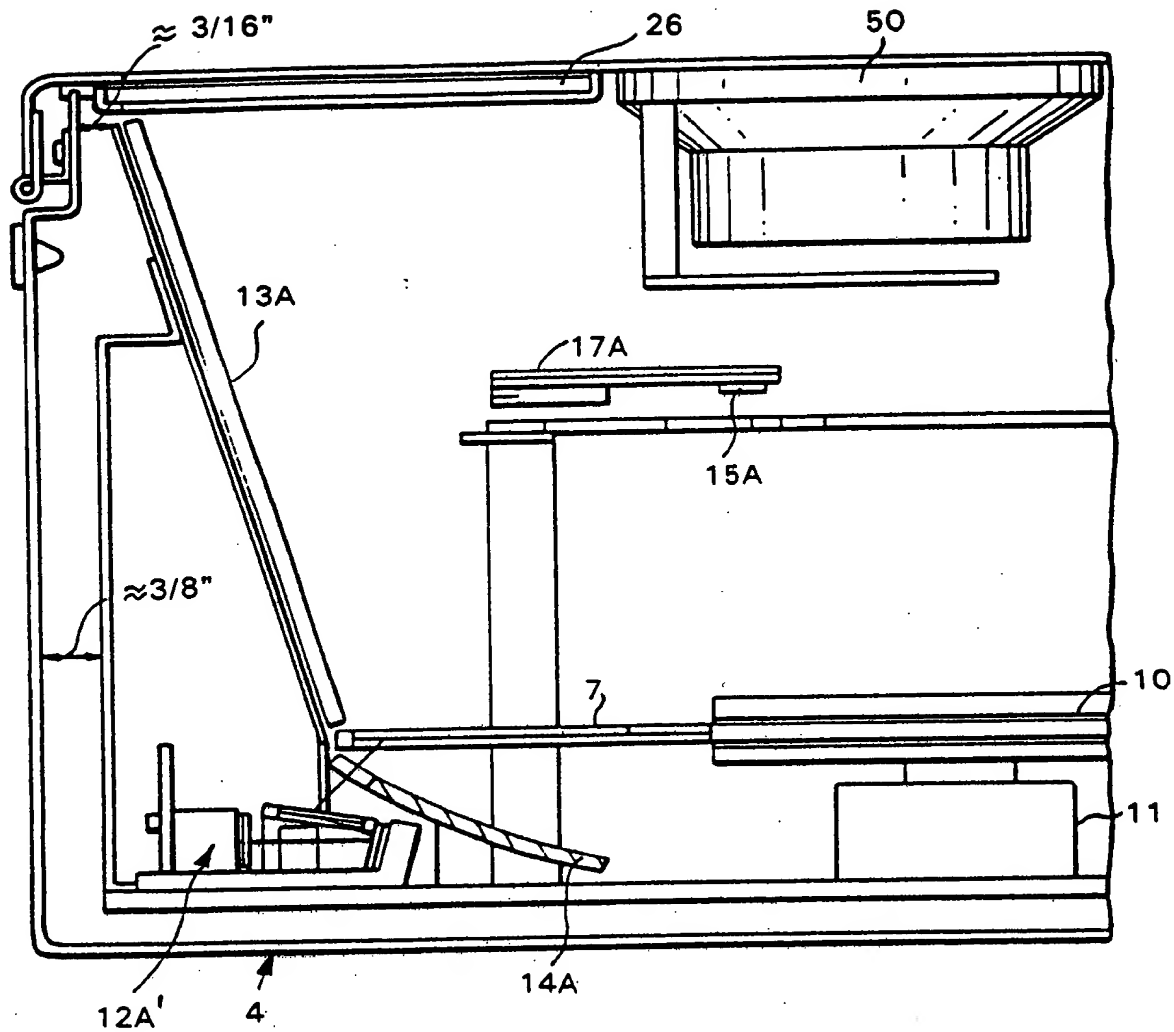

FIG. 22

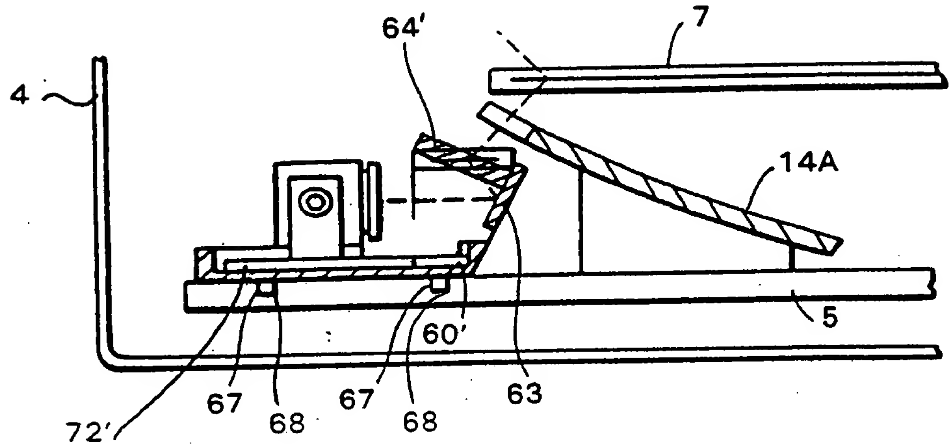

FIG. 23

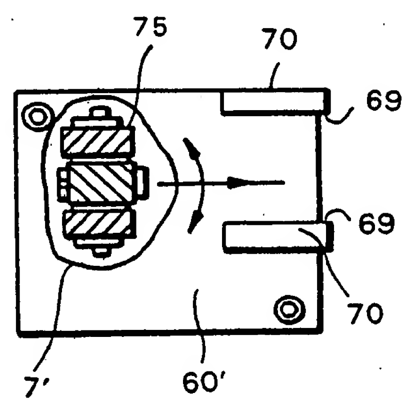

FIG. 23A

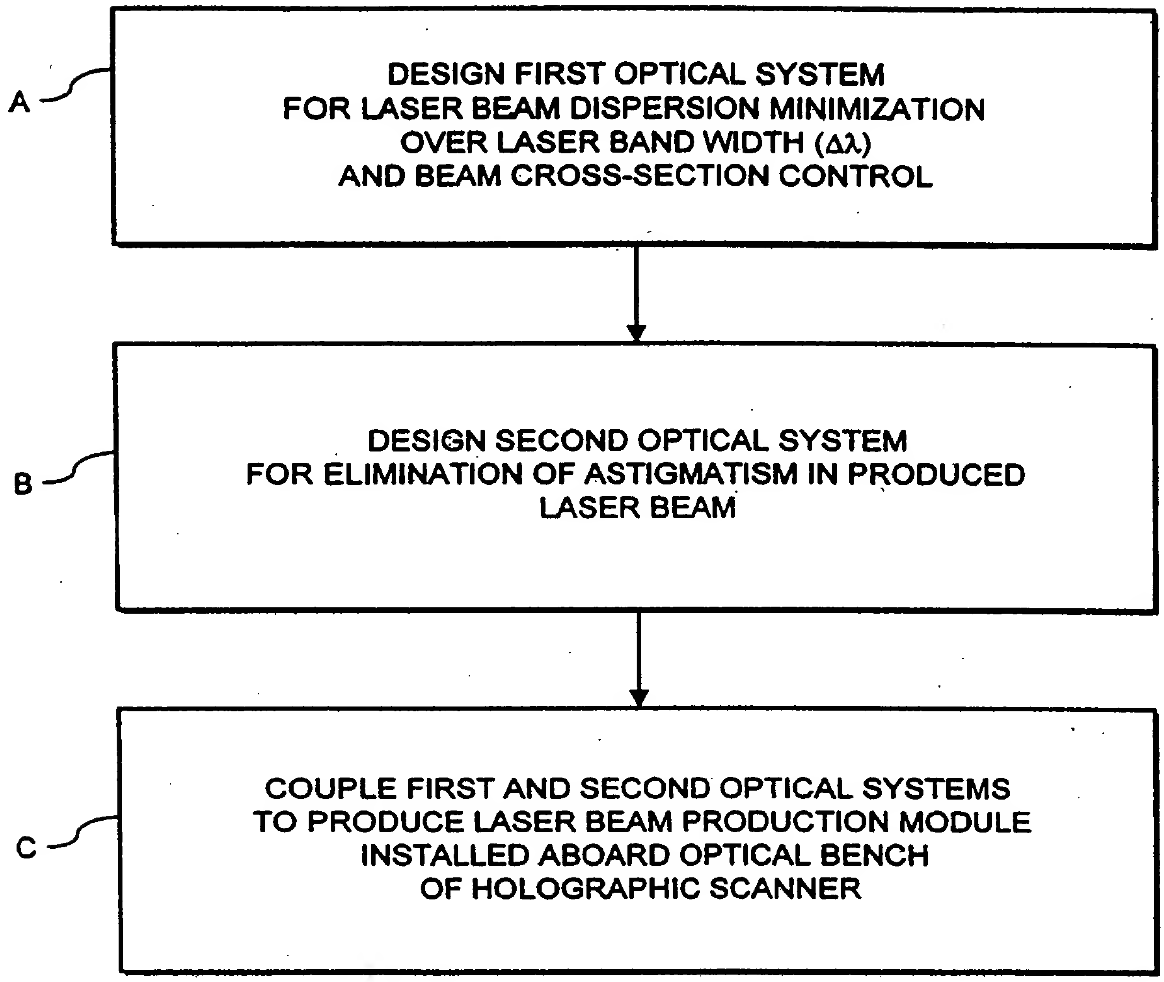
A
DESIGN FIRST OPTICAL SYSTEM FOR LASER BEAM DISPERSION MINIMIZATION OVER LASER BAND WIDTH (Δλ) AND BEAM CROSS-SECTION CONTROL
B
DESIGN SECOND OPTICAL SYSTEM FOR ELIMINATION OF ASTIGMATISM IN PRODUCED LASER BEAM
C
COUPLE FIRST AND SECOND OPTICAL SYSTEMS TO PRODUCE LASER BEAM PRODUCTION MODULE INSTALLED ABOARD OPTICAL BENCH OF HOLOGRAPHIC SCANNER

FIG. 24

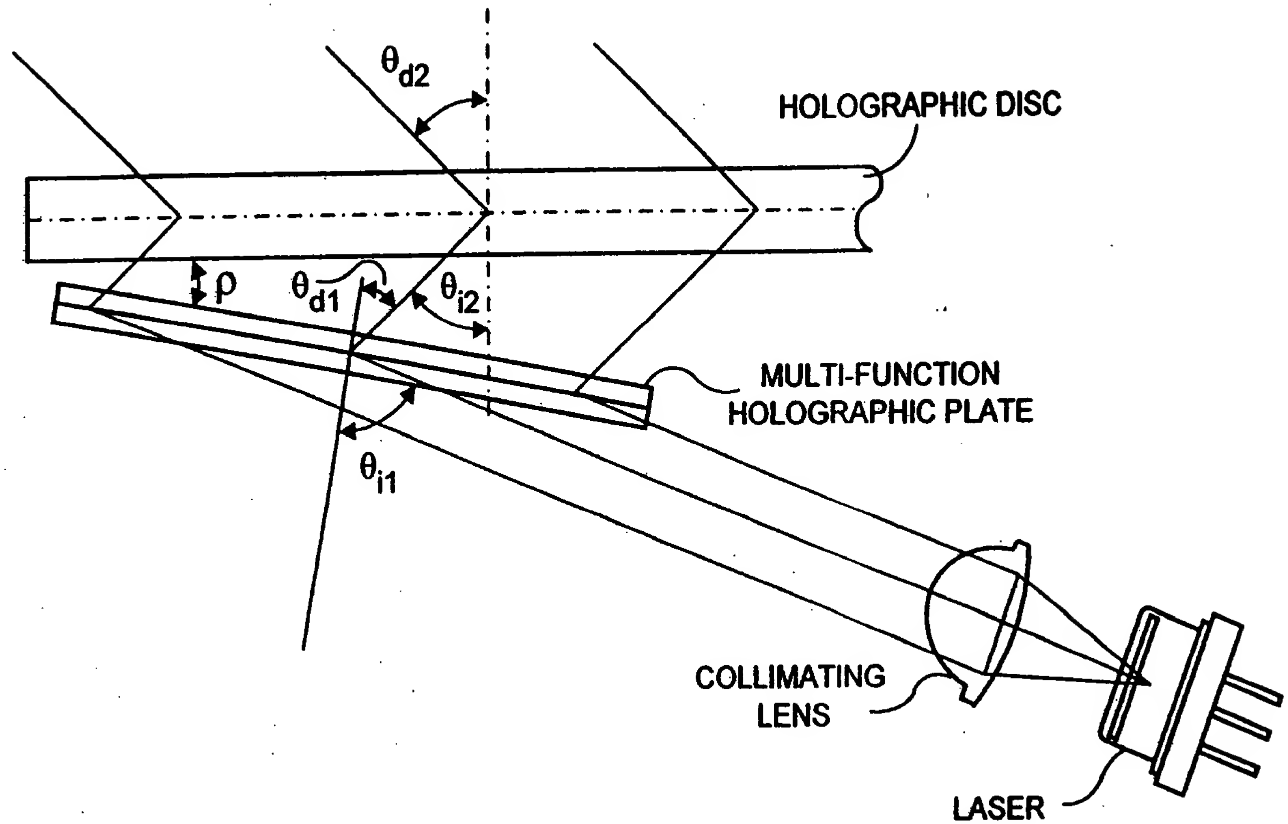
θ_{d2}
HOLOGRAPHIC DISC
ρ
θ_{d1}
θ_{i2}
MULTI-FUNCTION
HOLOGRAPHIC PLATE
θ_{i1}
COLLIMATING
LENS
LASER

F I G. 25A

ANALYSIS OFTHE MULTI-FUNCTION HOLOGRAPHIC PLATE. THIS ANALYSIS WILL DETRMINE THE ANGLE OF INCIDENCE AND ANGLE OF DIFFFRACTION AND ORIENTATION ANGLE, RELATIVE TO THE HOLOGRAPHIC DISC, FOR A PRE- DISC HOLOGRAPHIC PLATE THAT SIMULTANEOUSLY ACCOMPLISHES ALL OF THE FUNCTIONS OF BEAM CIRCULARIZATION, ELIMINATION OF DISPERSION AND ELIMINATION OF ASTIGMATISM. (THE ELIMINATION OF ASTIGMATISM IS ACTUALLY ACCOMPLISHED BY ADJUSTING THE LASER / COLLIMATION LENS SEPARATION AFTER THE BEAM EXPANSION RATIO IS ESTABLISHED FOR THE CIRCULARIZING FUNCTION.) THE MULTI-FUNCTION HOLOGRAPHIC PLATE IS PLACED BETWEEN THE COLLIMATING LENS AND HOLOGRAPHIC DISC.

A DESIRED BEAM EXPANSION RATIO IS SELECTED AND THE ANGLES OF INCIDENCE AND DIFFRACTION FOR THE HOLOGRAPHIC DISC ARE GIVEN. WAVELENGTH IS ALSO GIVEN. THE FINAL RESULT IS A SINGLE GRAPH CONTAINING TWO PLOTS OF THE ANGLE OF INCIDENCE VS. MULTI-FUNCTION PLATE ORIENTATION ANGLE FOR TWO SITUATIONS - OBTAINING THE DESIRED BEAM EXPANSION RATIO AND OBTAINING ZERO DISPERSION. WHERE THESE TWO CURVES INTERSECT, BOTH REQUIREMENTS WILL BE MET SIMULTANEOUSLY.

D.1 = BEAM DIAMETER LEAVING COLLIMATING LENS
D.2 = EXPANDED BEAM DIAMETER LEAVING MULTI-FUNCTION HOLOGRAPHIC PLATE
M = BEAM EXPANSION FACTOR = D.2 / D.1
d.2 = GRATING SPACING OF THE HOLOGRAPHIC DISC (microns)
d.1 = GRATING SPACING OF THE MULTI-FUNCTION HOLOGRAPHIC PLATE (microns)
θ.i.2 = ANGLE OF INCIDENCE OF BEAM AT HOLOGRAPHIC DISC
θ.d.2 = ANGLE OF INCIDENCE OF BEAM LEAVING HOLOGRAPHIC DISC
θ.i.1.M = ANGLE OF INCIDENCE OF BEAM AT HOLOGRAPHIC MULTI-FUNCTION PLATE THAT WILL PROVIDE THE DESIRED BEAM EXPANSION RATIO, M
θ.i.1.D = ANGLE OF INCIDENCE OF BEAM AT HOLOGRAPHIC MULTI-FUNCTION PLATE THAT WILL PROVIDE ZERO DISRERSION FOR THE BEAM LEAVING THE HOLOGRAPHIC DISC
θ.d.1.M = ANGLE OF DIFFRACTION OF BEAM LEAVING MULTI-FUNCTION PLATE THAT WILL PROVIDE THE DESIRED BEAM EXPANSION RATIO, M
θ.d.1.D = ANGLE OF DIFFRACTION OF BEAM LEAVING MULTI-FUNCTION PLATE THAT WILL PROVIDE ZERO DISRERSION FOR THE BEAM LEAVING THE HOLOGRAPHIC DISC
ρ = ORIENTATION ANGLE OF MULTI-FUNCTION PLATE RELATIVE TO THE HOLOGRAPHIC DISC
λ = WAVELENGTH OF LASER BEAM (microns)

FIG. 25B

ASSUMED PARAMETERS:

$M := 3$ BEAM EXPANSION RATIO $\qquad deg = \frac{\pi}{180}$

$\lambda := .670$ microns WAVELENGTH OF LASER

$\theta_{i.2} := 43\ deg$ ANGLE OF INCIDENCE AT HOLOGRAPHIC DISC

$\theta_{d.2} := 37\ deg$ ANGLE OF DIFFRACTION AT HOLOGRAPHIC DISC

$\rho := -5\ deg, -5.1\ deg, \ldots, -12\ deg$

F I G. 25B1

(1) $$d_2 := \frac{\lambda}{\sin[\theta_{i.2}] + \sin[\theta_{d.2}]}$$ GRATING SPACING FOR HOLOGRAPHIC DISC

(2) $$\theta_{i.1.M}(\rho) := \operatorname{acos}\left[\frac{\cos[\theta_{i.2}+\rho]}{M}\right]$$ ANGLE OF INCIDENCE AT PLATE TO GIVE THE DESIRED BEAM EXPANSION RATIO

(3) $$\theta_{d.1.M}(\rho) := \theta_{i.2}+\rho$$ CORRESPONDING ANGLE OF DIFFRACTION

(4) $$d_{1.M}(\rho) := \left[\frac{\lambda}{\sin[\theta_{i.1.M}(\rho)] + \sin[\theta_{d.1.M}(\rho)]}\right]$$ RESULTANT GRATING SPACING

(5) $$\theta_{i.1.D}(\rho) := = \operatorname{asin}\left[\lambda\frac{\cos[\theta_{i.2}+\rho]}{d_2\cos[\theta_{i.2}]} - \sin[\theta_{i.2}+\rho]\right]$$ ANGLE OF INCIDENCE AT PLATE TO GIVE ZERO DISPERSION

(6) $$\theta_{d.1.D}(\rho) := \theta_{i.2}+\rho$$ CORRESPONDING ANGLE OF DIFFRACTION

(7) $$d_{1.D}(\rho) := \left[\frac{\lambda}{\sin[\theta_{i.1.D}(\rho)] + \sin[\theta_{d.1.D}(\rho)]}\right]$$ RESULTANT GRATING SPACING

FIG. 25C

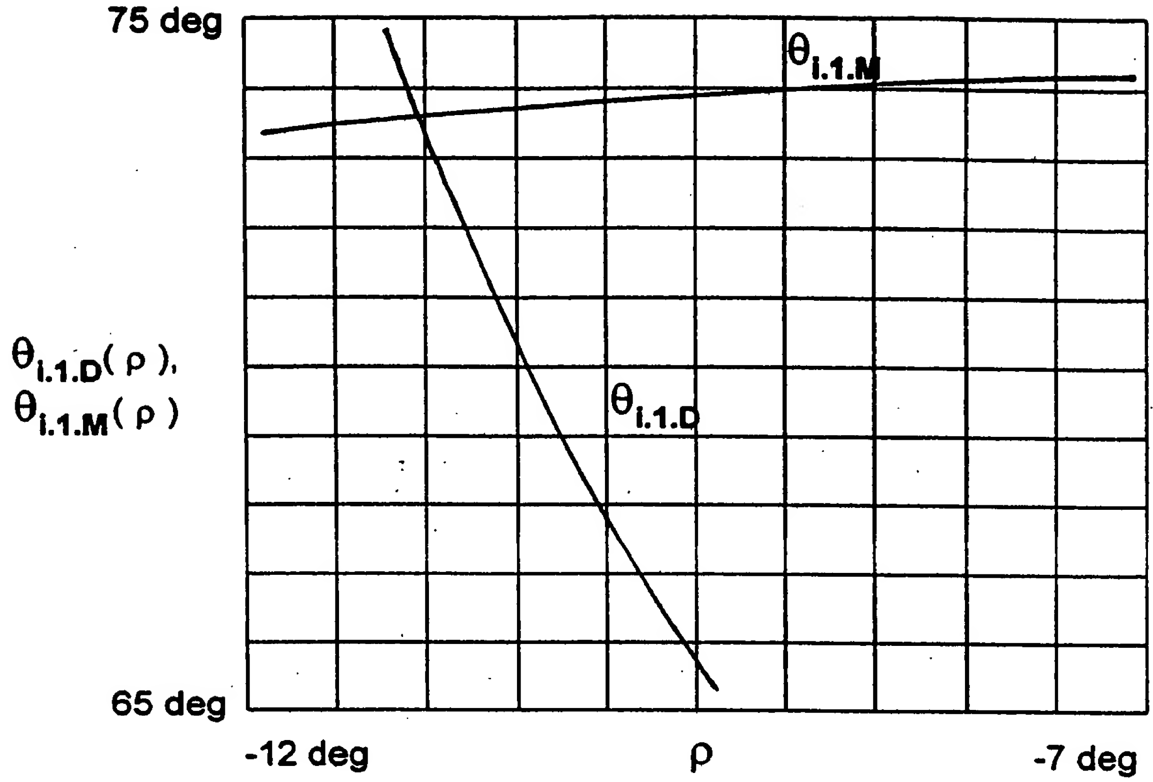

$\rho := -11.01\text{deg}$

ORIENTATION ANGLE, RELATIVE TO THE HOLOGRAPHIC DISC, OF THE MULTI-FUNCTION HOLOGRAPHIC PLATE FOR ZERO DISPERSION AND A BEAM EXPANSION RATIO OF 3.0

F I G. 25D

CONSTRUCTION PARAMETERS FOR THE MULTI- FUNCTION HOLOGRAPHIC PLATE AT 670 nm WAVELENGTH

$\theta_{i.1.M}(\rho) = 73.57777674$ deg $\theta_{i.1.D}(\rho) = 73.54631956$ deg

$\theta_{d.1.M}(\rho) = 31.99$ deg $\theta_{d.1.D}(\rho) = 31.99$ deg

$d_{1.M}(\rho) = 0.44997378$ microns $d_{1.D}(\rho) = 0.45002074$ microns

F I G. 25E

GEOMETRICAL OPTICS MODEL FOR BRAGG SENSITIVITY ANALYZER

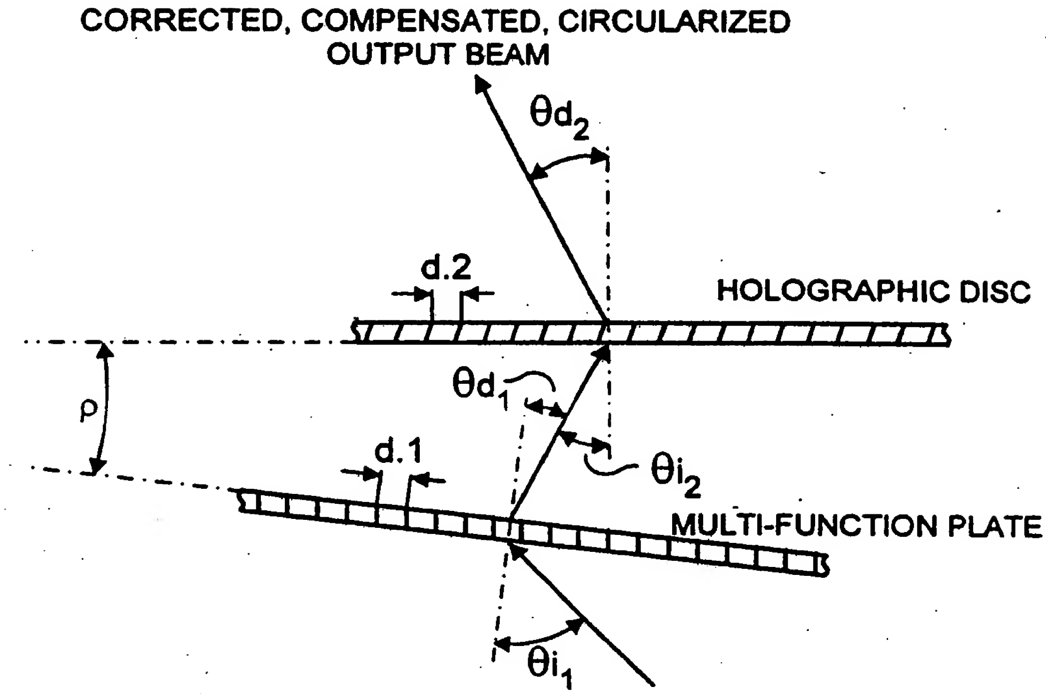

F I G. 26

ANALYSIS OF THE DISPERSION OF THE MULTI-FUNCTION HOLOGRAPHIC PLATE

THIS ANALYSIS WILL SHOW THE VARIATION OF DIFFRACTION ANGLE FOR THE BEAM LEAVING THE HOLOGRAPHIC DISC WHEN THE MULTI-FUNCTION HOLOGRAPHIC PLATE IS USED WITH THE CONSTRUCTION PARAMETERS AS CALCULATED ABOVE AND WITH THE ORIENTATION ANGLE, RELATIVE TO THE HOLOGRAPHIC DISC, AS ALSO CALCULATED ABOVE.

θ.i.1 = ANGLE OF INCIDENCE FOR MULTI-FUNCTION PLATE (FIXED - SEE ABOVE)

θ.d.c.1 = CONSTRUCTION ANGLE OF DIFFRACTION OF MULTI-FUNCTION PLATE (FIXED - SEE ABOVE)

θ.d.1 = ANGLE OF DIFFRACTION OF MULTI-FUNCTION PLATE (VARIES WITH WAVELENGTH)

θ.d.c.1 = CONSTRUCTION ANGLE OF DIFFRACTION OF HOLOGRAPHIC DISC (FIXED - SEE θ.d.2 IN ABOVE ANALYSIS)

θ.d.2 = ANGLE OF DIFFRACTION OF BEAM LEAVING HOLOGRAPHIC DISC (VARIES WITH WAVELENGTH)

λ = WAVELENGTH (IN AIR)

λ.c = CONSTRUCTION WAVELENGTH (= .670 microns)

d.1 = GRATING SPACING IN MULTI-FUNCTION PLATE (FIXED - SEE ABOVE)

ρ = TILT ANGLE OF MULTI-FUNCTION PLATE RELATIVE TO HOLOGRAPHIC DISC (FIXED - SEE ABOVE)

FIG. 27A

$\lambda_c := .670$ microns $\qquad \theta_{d.C.2} := 37$ deg $\qquad \theta_{i.2} := 43$ deg

$\theta_{i.1} := \theta_{i.1.M}(\rho) \qquad \theta_{d.C.1} := \theta_{i.2} + \rho$

$\lambda := .650, .6501, \ldots, .690 \qquad \theta_{d.C.1} = 31.99$ deg

FIG. 27B

(1) $$d_1 := \frac{\lambda_c}{\sin\left[\theta_{i.1}\right] + \sin\left[\theta_{d.c.1}\right]} \text{ microns}$$

$$d_1 = 0.44997378$$

(2) $$\theta_{d.1}(\lambda) := \operatorname{asin}\left[\left[\frac{\lambda}{d_1}\right] - \sin\left[\theta_{i.1}\right]\right]$$

(3) $$M := \left[\frac{\cos\left[\theta_{d.c.1}\right]}{\cos\left[\theta_{i.1}\right]}\right] \qquad M = 3$$

(4) $$\theta_{d.2}(\lambda) :=$$

$$= \operatorname{asin}\left[\frac{\lambda}{d_2} - \sin\left[\operatorname{asin}\left[\frac{\lambda}{d_1} - \sin\left[\theta_{i.1}\right]\right] - \rho\right]\right]$$

F I G. 27C

DISPERSION CHARACTERISTIC GRAPH AND SAMPLE VALUES

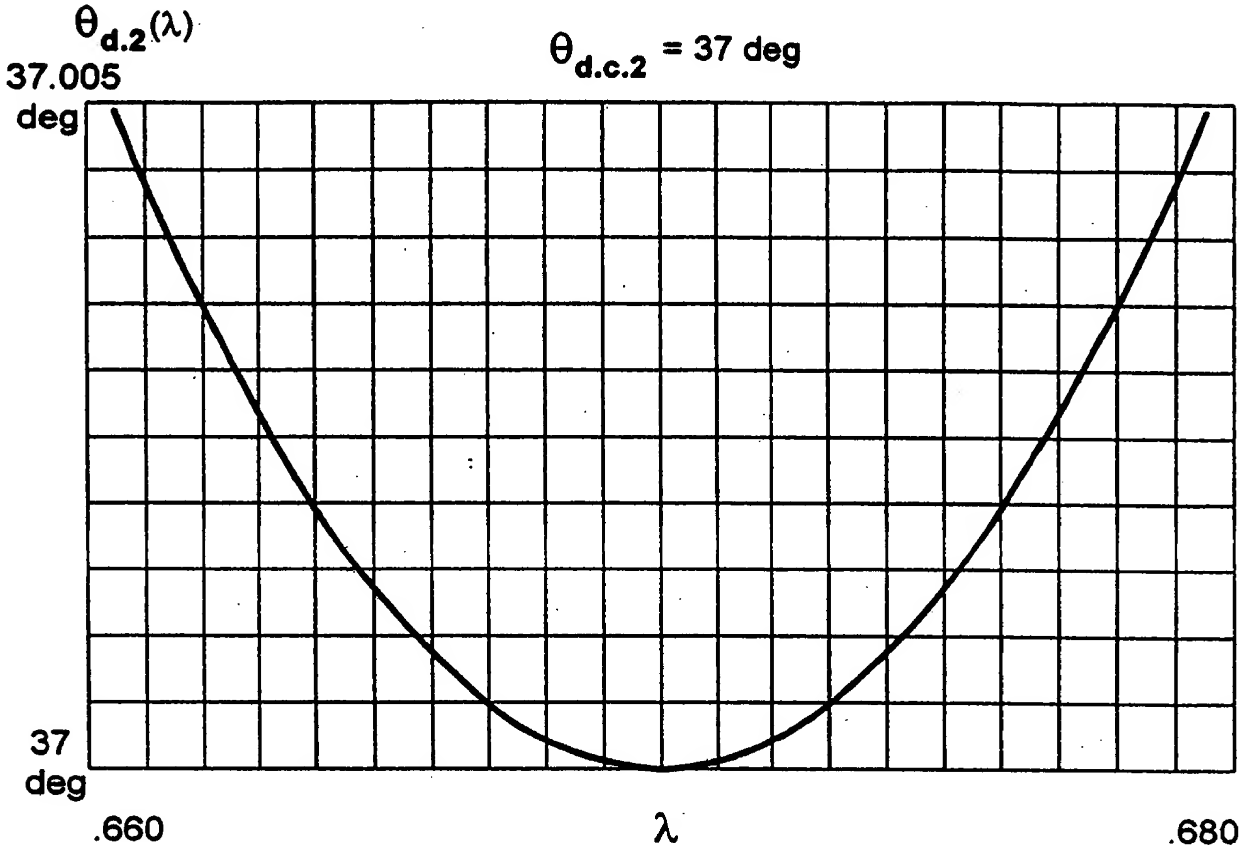

F I G. 27D

λ := .660 microns — $\theta_{d.2}(\lambda)$ = 37.00560129 deg

λ := .665 microns — $\theta_{d.2}(\lambda)$ = 37.00144699 deg

λ := .670 microns — $\theta_{d.2}(\lambda)$ = 37 deg

λ := .675 microns — $\theta_{d.2}(\lambda)$ = 37.00132623 deg

λ := .680 microns — $\theta_{d.2}(\lambda)$ = 37.00549609 deg

$\delta\theta_{d.2} := \theta_{d.2}(.675) - \theta_{d.2}(.670)$ — $\delta\theta_{d.2}$ = 0.00132623 deg

F I G. 27D1

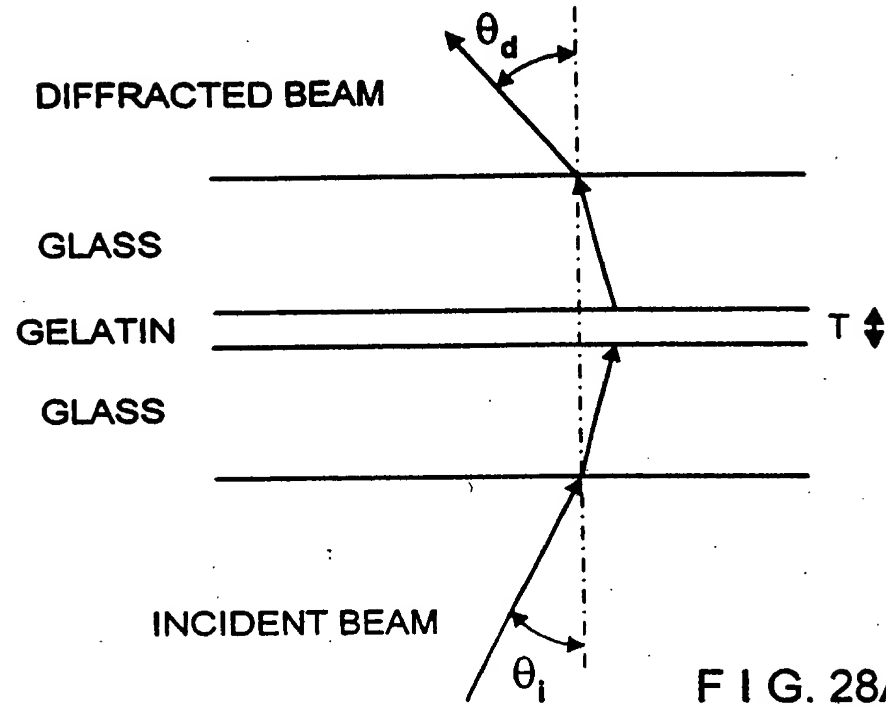

FIG. 28A1

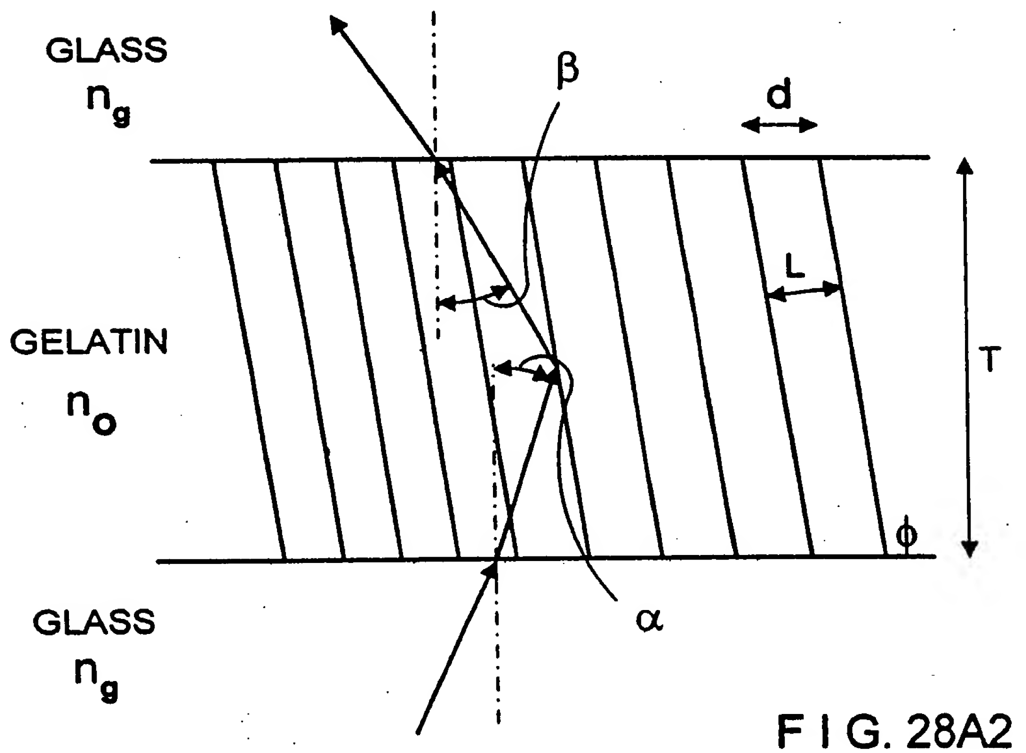

FIG. 28A2

CHANGE IN CONSTRUCTION BEAM ANGLES FOR A CHANGE IN WAVELENGTH BETWEEN CONSTRUCTION AND RECONSTRUCTION. THIS PROGRAM CALCULATES THE EXTERNAL ANGLE OF INCIDENCE AND EXTERNAL ANGLE OF DIFFRACTION FOR THE CONSTRUCTION WAVELENGTH WHEN THE EXTERNAL ANGLE OF INCIDENCE AND EXTERNAL ANGLE OF DIFFRACTION ARE GIVEN FOR THE RECONSTRUCTION WAVELENGTH. BRAGG CONDITION IS MAINTAINED IN BOTH CASES SO THAT THE BRAGG PLANE TILT IS UNCHANGED.

$$deg = \frac{\pi}{180}$$

$n_0 := 1.53$	AVERAGE REFRACTIVE INDEX OF THE MEDIUM BEFORE PROCESSING
$n_2 := 1.4$	AVERAGE REFRACTIVE INDEX OF THE MEDIUM AFTER PROCESSING
$\lambda_1 := .670$	RECONSTRUCTION WAVELENGTH (VISIBLE LASER DIODE)
$\lambda_2 := .488$	CONSTRUCTION WAVELENGTH (ARGON LASER)
$\theta_{i.1} := 77\ deg$	ANGLE OF INCIDENCE AT RECONSTRUCTION
$\theta_{d.1} := 31.5\ deg$	ANGLE OF DIFFRACTION AT RECONSTRUCTION

FIG. 28B

HOE CONSTRUCTION ANGLES AT SECOND WAVELENGTH

REFERENCE BEAM	OBJECT BEAM
$\theta_{i.2} = \theta_R = 54.143\ deg$	$\theta_{d.2} = \theta_O = 15.915\ deg$

FIG. 28D

(1) $\alpha_1 := \operatorname{asin}\left[\dfrac{\sin[\theta_{i.1}]}{n_2}\right]$

ANGLE OF INCIDENCE INSIDE THE MEDIUM AFTER PROCESSING

$\alpha_1 = 44.105$ deg

(2) $\beta_1 := \operatorname{asin}\left[\dfrac{\sin[\theta_{d.1}]}{n_2}\right]$

ANGLE OF DIFFRACTION INSIDE THE MEDIUM AFTER PROCESSING

$\beta_1 = 21.914$ deg

$d := \dfrac{\lambda_1}{\sin[\theta_{i.1}] + \sin[\theta_{d.1}]}$

$d = 0.448$ microns

$\dfrac{1000}{d} = 2.234\ 10^3$ lines per mm.

(3) $\phi := \dfrac{\pi}{2} - \dfrac{\beta_1 - \alpha_1}{2}$

TILT ANGLE OF THE BRAGG PLANES

$\phi = 101.086$ deg

(4) $\theta_{0.1} := \alpha_1 + \dfrac{\pi}{2} - \phi$

ANGLE RELATIVE TO THE BRAGG PLANES

$\theta_{0.1} = 34.198$ deg

(6) $L := \dfrac{\lambda_1}{2\ n_2 \sin[\theta_{0.1}]}$

SEPARATION OF THE BRAGG PLANES.
BRAGG CONDITION EQUATION.

$L = 0.442$ microns

(7) $\theta_{0.2} := \operatorname{asin}\left[\dfrac{\lambda_2}{2\ n_0\ L}\right]$

ANGLE RELATIVE TO THE BRAGG PLANES FOR THE SECOND WAVELENGTH SATISFYING THE BRAGG CONDITION - BEFORE PROCESSING

$\theta_{0.2} = 21.619$ deg

FIG. 28C1

(8) $\alpha_2 := \theta_{0.2} + \phi - \frac{\pi}{2}$

ANGLE OF INCIDENCE INSIDE THE MEDIUM FOR THE SECOND WAVELENGTH - BEFORE PROCESSING

$\alpha_2 = 32.705$ deg

(9) $\beta_2 := \alpha_2 + \pi - 2\phi$

ANGLE OF DIFFRACTION INSIDE THE MEDIUM FOR THE SECOND WAVELENGTH - BEFORE PROCESSING

$\beta_2 = 10.534$ deg

(10) $\theta_R := \operatorname{asin}\left[n_0 \sin\left[\alpha_2\right]\right]$

ANGLE OF INCIDENCE (REFERENCE BEAM) FOR THE SECOND WAVELENGTH - EXTERNAL

$\theta_R = 54.143$ deg

(11) $\theta_O := \operatorname{asin}\left[n_0 \sin\left[\beta_2\right]\right]$

ANGLE OF DIFFRACTION (OBJECT BEAM) FOR THE SECOND WAVELENGTH - EXTERNAL

$\theta_O = 15.915$ deg

F I G. 28C2

CONSTRUCTION OF A MULTI-FUNCTION HOLOGRAPHIC PLATE

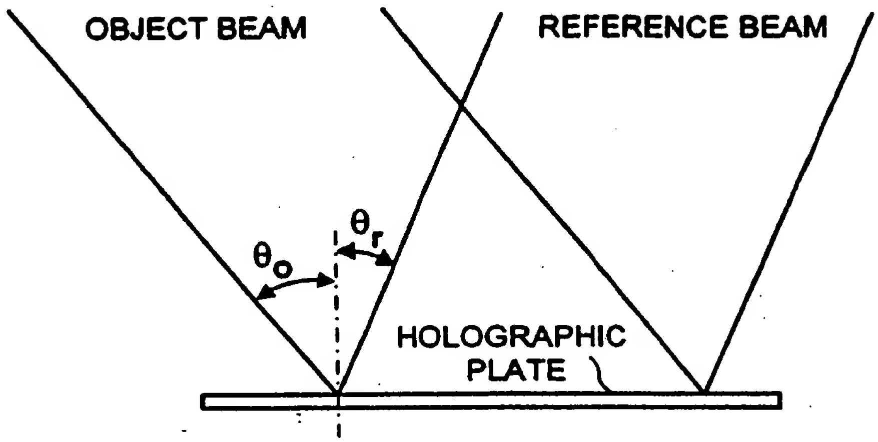

θ_o = OBJECT BEAM ANGLE OF INCIDENCE

θ_r = REFERENCE BEAM ANGLE OF INCIDENCE

FIG. 29

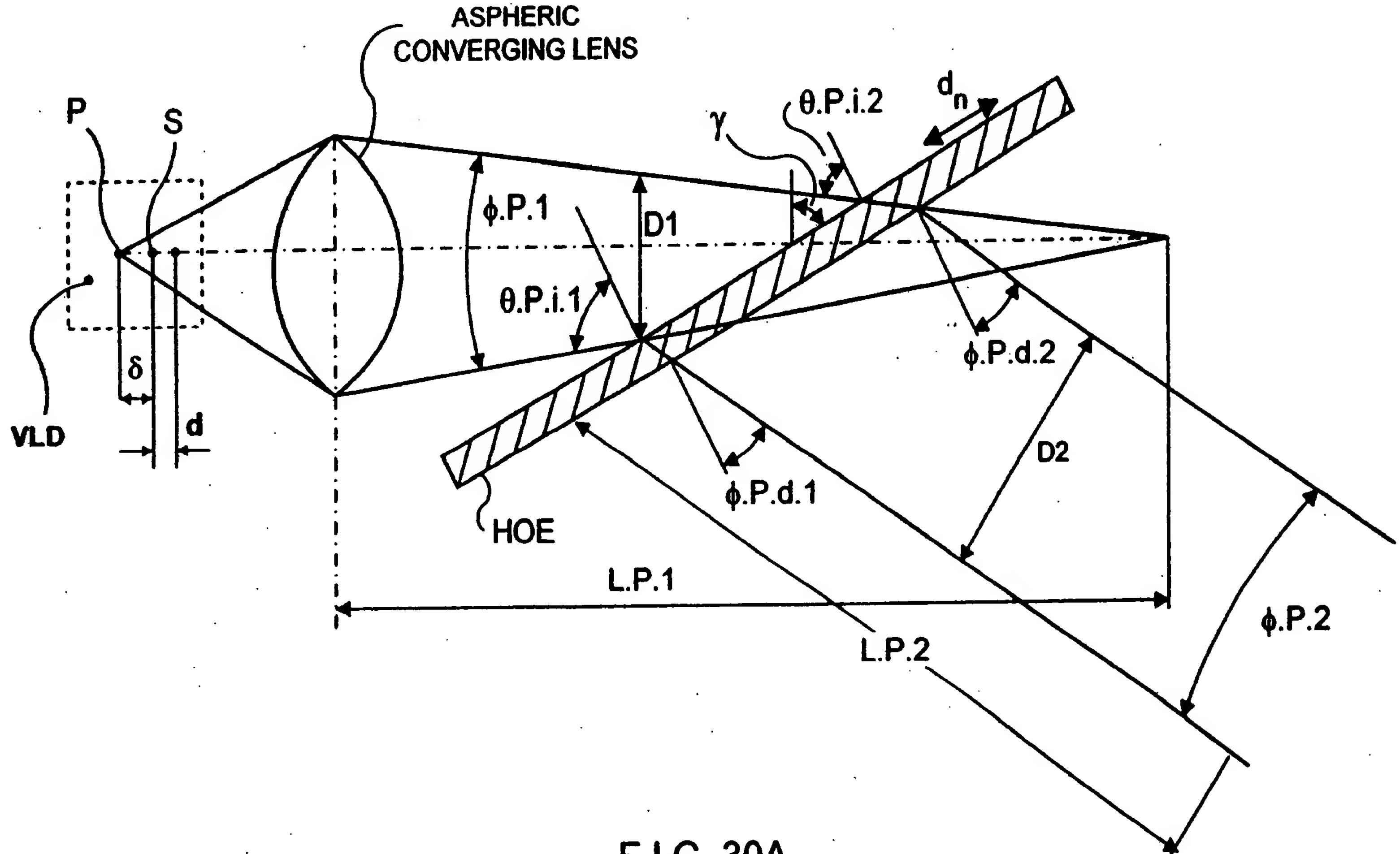
ASPHERIC
CONVERGING LENS
P
S
VLD
δ
d
ϕ.P.1
D1
θ.P.i.1
γ
θ.P.i.2
d_n
ϕ.P.d.2
ϕ.P.d.1
HOE
D2
L.P.1
L.P.2
ϕ.P.2

F I G. 30A

CIRCULARIZATION AND ASTIGMATISM ELIMINATION WITH A HOE

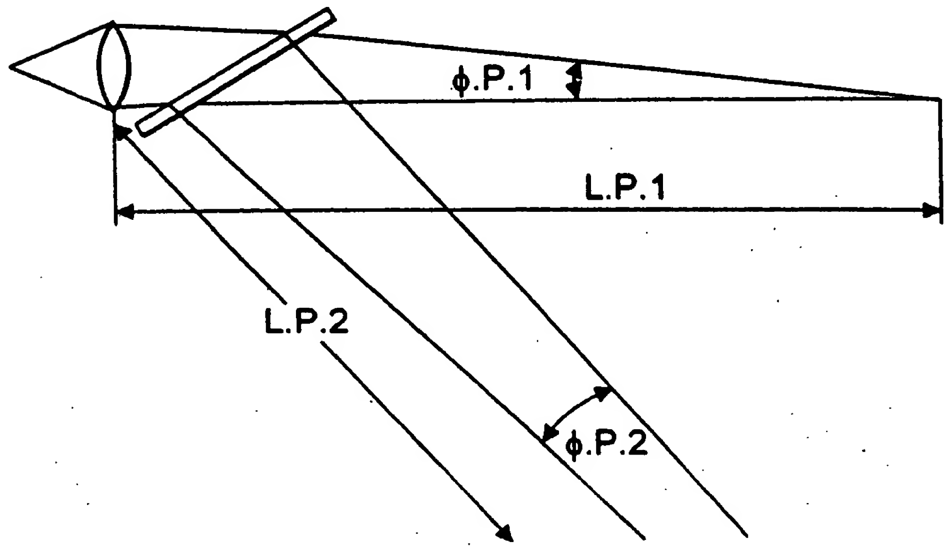

F I G. 30A1

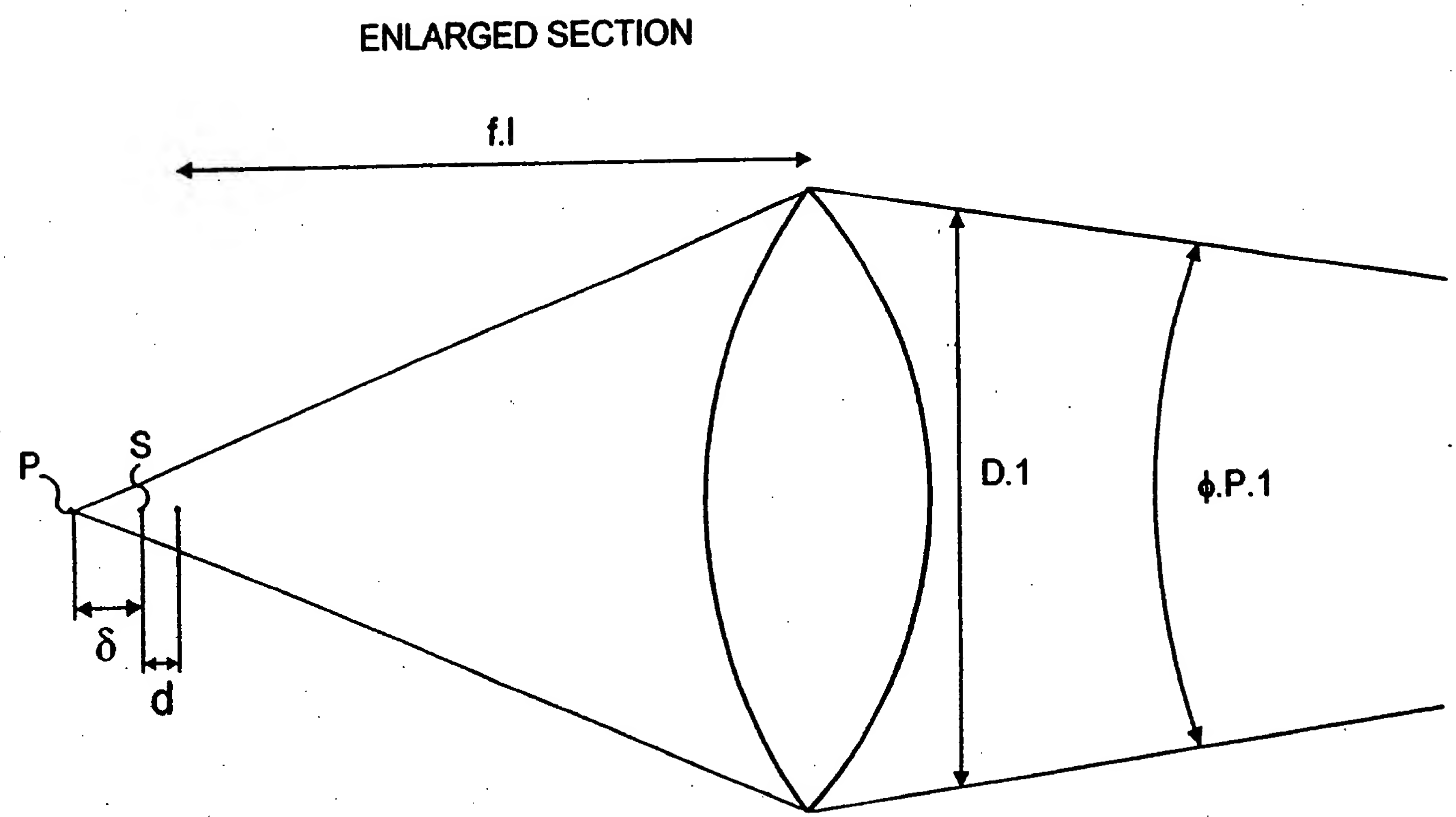

F I G. 30A2

ENLARGED SECTION

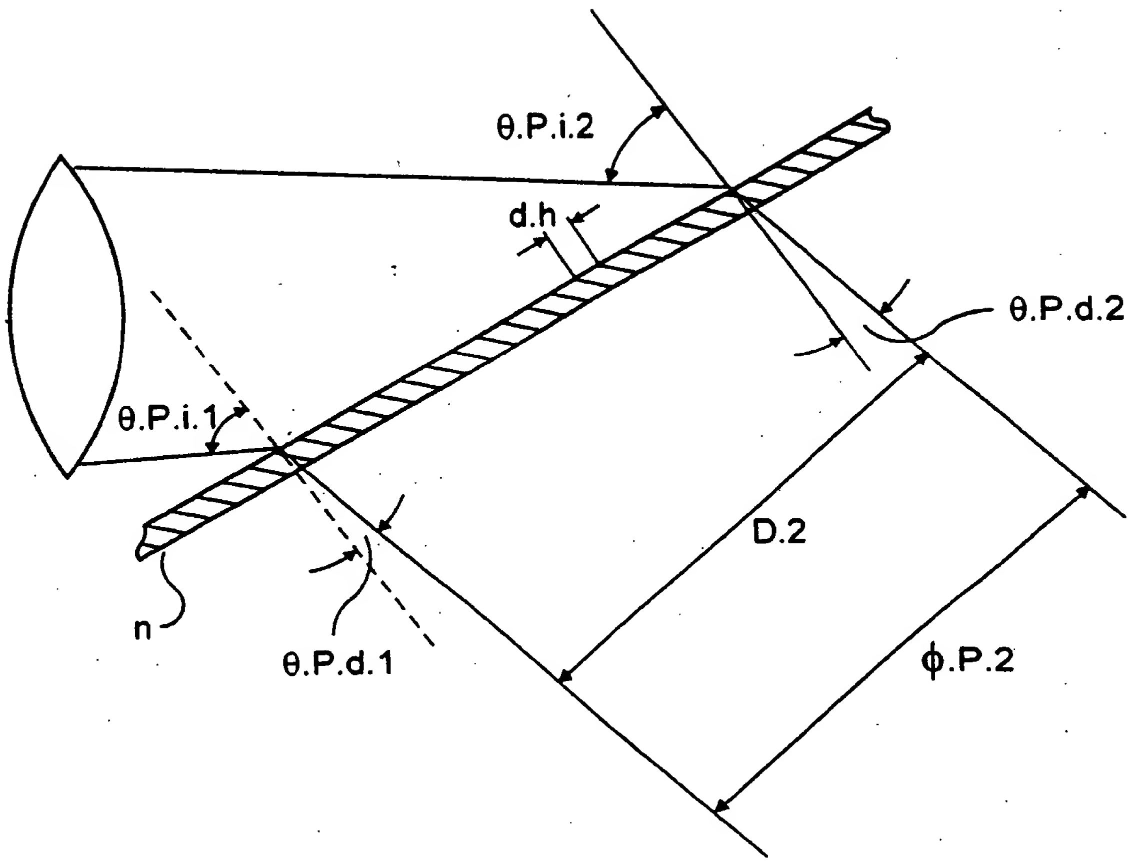

FIG. 30A3

ANALYSIS OF ASTIGMATIC DIFFERENCE REDUCTION WITH A CIRCULARIZING HOLOGRAPHIC OPTICAL ELEMENTS (HOE) FOR GENERAL CASE WHERE BOTH S AND P BEAMS ARE CONVERGING. THE HOE IN THIS CASE IS A SIMPLE,FIXED-SPATIAL-FREQUENCY HOLOGRAPHIC DIFFRACTION GRATING.

f.1 = FOCAL LENGTH OF COLLIMATING LENS
d = DISTANCE FROM FOCAL POINT OF COLLAMATING LENS TO S-BEAM SOURCE
δ = ASTIGMATIC DIFFERENCE OF LASER DIODE
D.1 = P- BEAM DIAMETER LEAVING COLLIMATING LENS
D.2 = EXPANDED P- BEAM DIAMETER LEAVING HOE
M = BEAM EXPANTION FACTOR = D.2 / D.1
d.h = GRATING SPACING OF HOE GRATING (mm)
θ.P.i.1 = ANGLE OF INCIDENCE OF LOWER PORTION OF CONVERGING P-BEAM AT HOE
θ.P.i.2 = ANGLE OF INCIDENCE OF UPPER PORTION OF CONVERGING P-BEAM AT HOE
ϕ.P.1 = CONVERGENCE OF P- BEAM LEAVING COLLIMATING LENS
ϕ.S.1 = CONVERGENCE OF S- BEAM LEAVING COLLIMATING LENS
ϕ.P.2 = CONVERGENCE OF P- BEAM LEAVING HOE
ϕ.S.1 = ϕ.S.1 = CONVERGENCE OF S- BEAM LEAVING HOE
L.P.1 = IMAGE DISTANCE FOR P SOURCE IMAGED BY COLLIMATING LENS
L.P.2 = IMAGE DISTANCE FOR P SOURCE AFTER INSERTING HOE
L.S.1 = IMAGE DISTANCE FOR S SOURCE IMAGED BY COLLIMATING LENS
L.S.2 = L.S.1 = IMAGE DISTANCE FOR S SOURCE AFTER INSERTIG HOE
θ.P.d.1 = ANGLE OF DIFFRACTION OF LOWER PORTION OF CONVERGING P-BEAM AT HOE
θ.P.d.2 = ANGLE OF DIFFRACTION OF UPPER PORTION OF CONVERGING P-BEAM AT HOE
λ = WAVELENGTH OF LASER BEAM

FIG. 30B

ASSUMED VALUE OF FIXED PARAMETERS: $\deg = \frac{\pi}{180}$

$\lambda := .000670\ \mathrm{mm}$ $\theta_{P.i.1} := 73.6\ \deg$ $\theta_{P.d.1} := 32\ \deg$

$f_1 := 4.5\ \mathrm{mm}$ $D_1 := 1\ \mathrm{mm}$ $\delta := .01\ \mathrm{mm}$

VARIABLE PARAMETER:

$d := .00000000001, .00004, \ldots .004\ \mathrm{mm}$

FIG. 30B1

$$d_h := \frac{\lambda}{\sin[\theta_{P.i.1}] + \sin[\theta_{P.i.1}]}$$

(1) $$L_{P.1}(d) := \frac{f_1^2}{d+\delta}$$ (2) $$L_{S.1}(d) := \frac{f_1^2}{d}$$

(3) $$\phi_{P.1}(d) := \operatorname{atan}\left[\frac{D_1}{L_{P.1}(d)}\right]$$

(4) $$\phi_{S.1}(d) := \operatorname{atan}\left[\frac{D_1}{L_{S.1}(d)}\right]$$

(5) $$M := \frac{\cos\left[\operatorname{asin}\left[\frac{\lambda}{d_h} - \sin[\theta_{P.i.1}]\right]\right]}{\cos[\theta_{P.i.1}]}$$ $M = 3.003626$

(6) $$D_2 := M D_1$$ $D_2 = 3.003626$

(7) $$\theta_{P.i.2}(d) := \theta_{P.i.1} - \phi_{P.1}(d)$$

FIG. 30C1

(8) $\theta_{P.d.1} := \operatorname{asin}\left[\frac{\lambda}{d_h} - \sin\left[\theta_{P.i.1}\right]\right]$ $\theta_{P.d.1} = 32\ \mathrm{deg}$

(9) $\theta_{P.d.2}(d) := \operatorname{asin}\left[\frac{\lambda}{d_h} - \sin\left[\theta_{P.i.2}(d)\right]\right]$

(10) $\phi_{P.2}(d) := \theta_{P.d.2}(d) - \theta_{P.d.1}$

(11) $L_{P.2}(d) := \frac{D_2}{\tan\left[\phi_{P.2}(d)\right]}$

(12) $L_{S.2}(d) := L_{S.1}(d)$

F I G. 30C2

S AND P IMAGE DISTANCES IN THE IMAGE PLANE OF THE FOCUSING LENS AS A FUNCTION OF THE DISTANCE FROM THE FOCAL POINT OF THE COLLIMATING LENS TO THE S SOURCE. HOE PLACED AFTER THE COLLIMATING LENS. θ.P.i.1 IS THE ANGLE OF INCIDENCE OF THE LOWER PORTION OF THE P-BEAM ON THE SURFACE OF THE HOE. δ IS THE VLD ASTIGMATIC DIFFERENCE.

S AND P IMAGE LOCATIONS - COLLIMATING LENS AND HOE ONLY

$\lambda =$ 0.00067 mm $\quad f_1 = 4.5$ mm $\quad \theta_{P.i.1} =$ 73.6 deg $\quad \delta =$ 0.01 mm

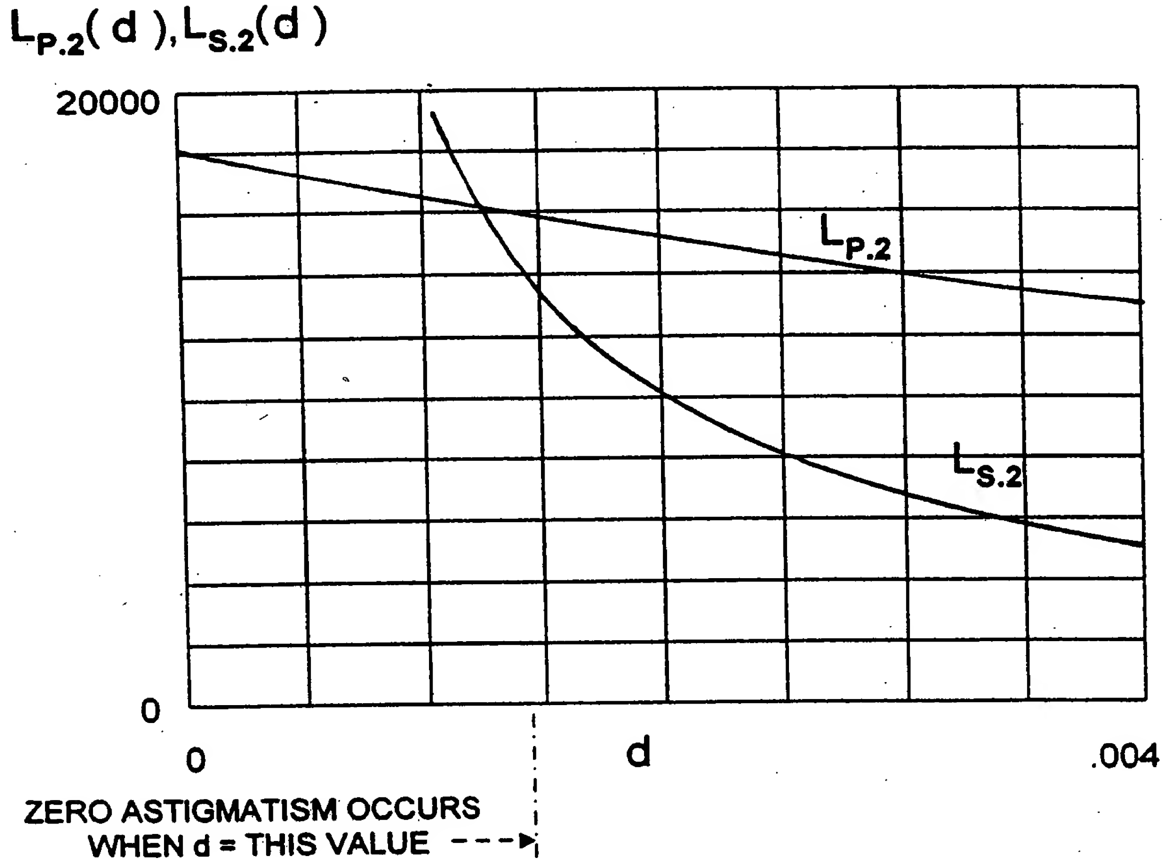

d := .001248 mm

$L_{P.2}(d) = 1.622582 \cdot 10^4$ mm $\qquad L_{S.2}(d) = 1.622596 \; 10^4$ mm

FIG. 30D

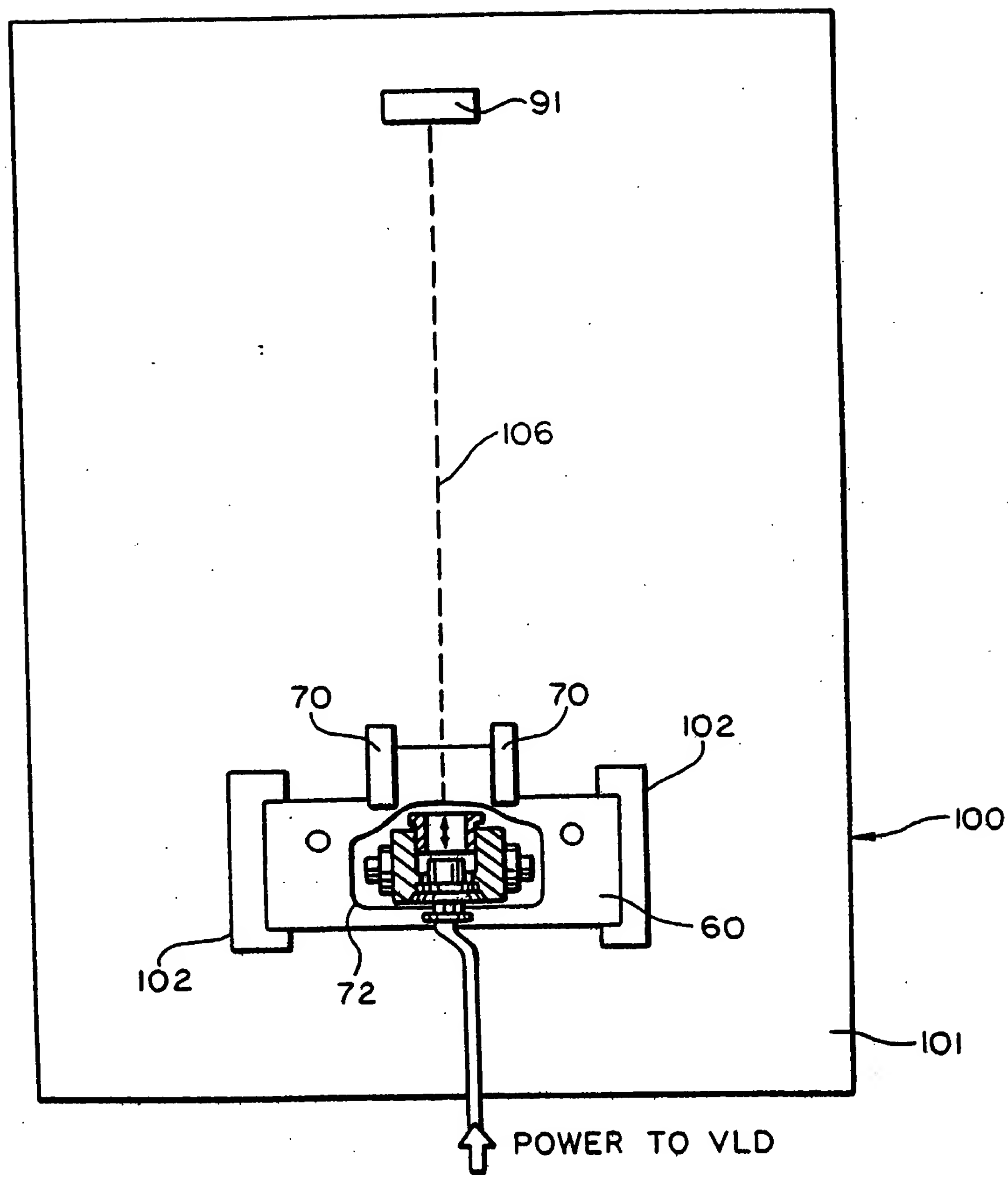

FIG. 31A1

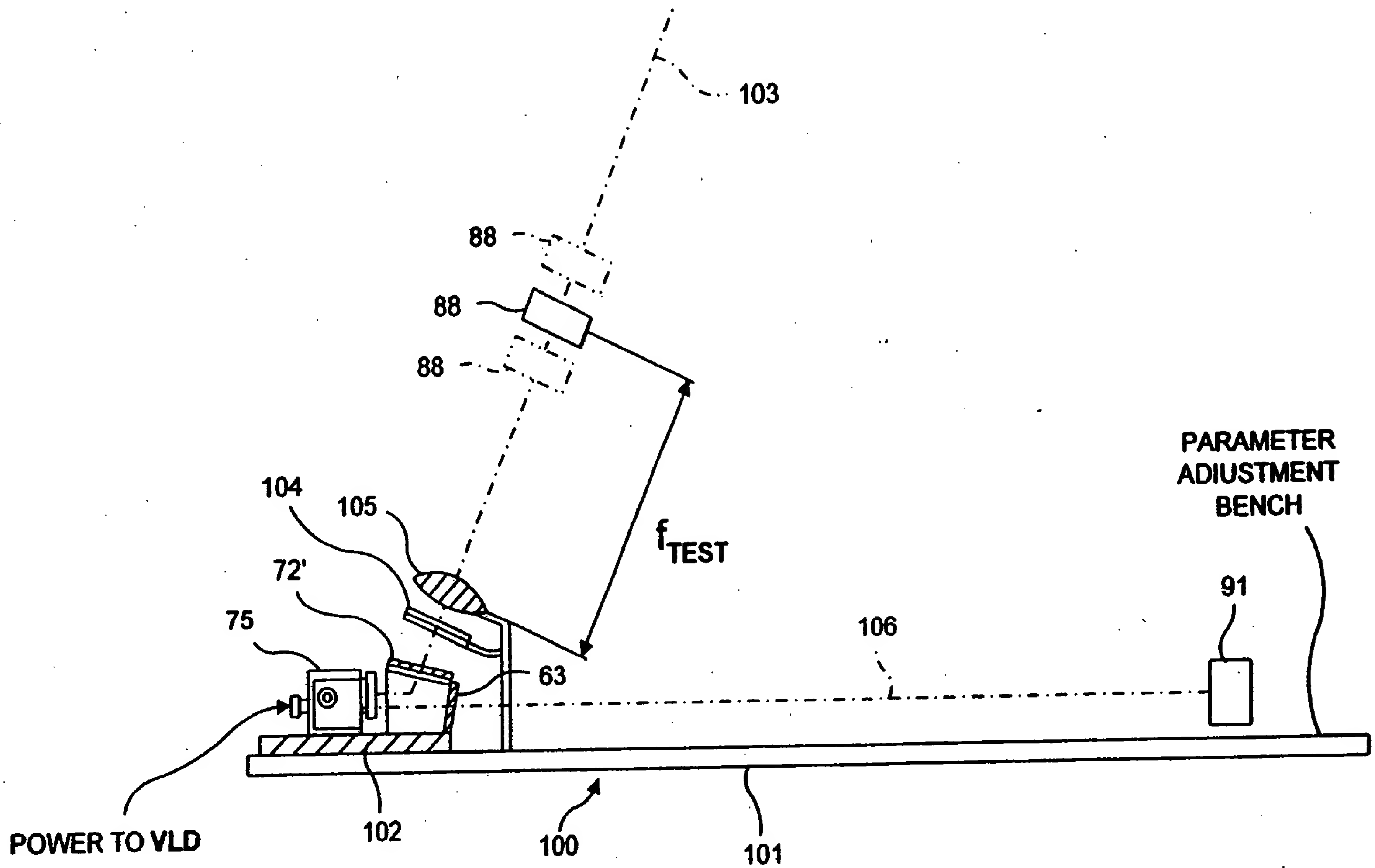
103
88
88
88
104
105
72'
75
f_{TEST}
63
106
91
PARAMETER
ADIUSTMENT
BENCH
POWER TO VLD
102
100
101

F I G. 31A2

A — REALIZE IN THE SECOND OPTICAL SYSTEM, VALUES FOR ALL PARAMETERS IN ITS GEOMETRICAL OPTICS MODEL, EXCEPT FOR THE VLD-TO-LENS DISTANCE **d**

B — SET (I.E. FIX) $\Theta_{GRATING\text{-}TILT}$ AS A CONSTRAINT IN CONFIGURATION PROCESS

C — ADJUST **d** SO THAT RADIUS OF CURVATURE OF BOTH **S** AND **P** CYLINDRICAL WAVEFRONTS ARE MADE EQUAL AT SECOND SURFACE OF GRATING, PRODUCING SPHERICAL COVERGING WAVEFRONT THEREFROM, FREE OF ASTIGMATISM WITH DESIRED BEAM ASPECT-RATIO

D — COUPLE FIRST AND SECOND OPTICAL SYSTEMS TO PROVIDE A LASER BEAM PRODUCTION MODULE MOUNTED ON THE SCANNER BENCH, WITH Θ_{Pi1} (I.E. $\Theta_{GRATING\text{-}TILT}$) AND ρ_0 SET TO ENSURE ASTIGMATISM ELIMINATION AND BEAM DISPERSION MINIMIZATION

F I G. 31B

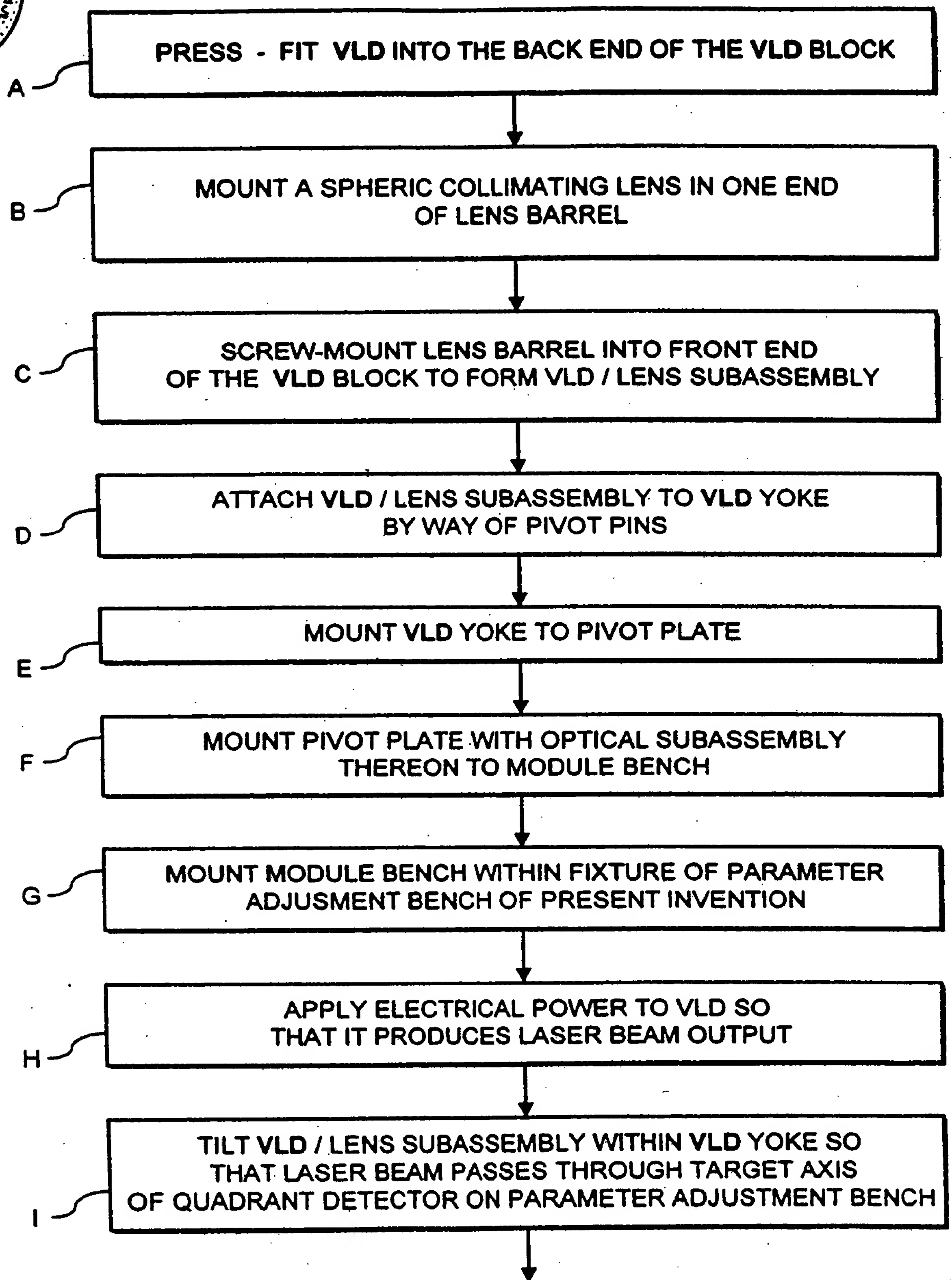
PRESS - FIT VLD INTO THE BACK END OF THE VLD BLOCK
A
MOUNT A SPHERIC COLLIMATING LENS IN ONE END OF LENS BARREL
B
SCREW-MOUNT LENS BARREL INTO FRONT END OF THE VLD BLOCK TO FORM VLD / LENS SUBASSEMBLY
C
ATTACH VLD / LENS SUBASSEMBLY TO VLD YOKE BY WAY OF PIVOT PINS
D
MOUNT VLD YOKE TO PIVOT PLATE
E
MOUNT PIVOT PLATE WITH OPTICAL SUBASSEMBLY THEREON TO MODULE BENCH
F
MOUNT MODULE BENCH WITHIN FIXTURE OF PARAMETER ADJUSMENT BENCH OF PRESENT INVENTION
G
APPLY ELECTRICAL POWER TO VLD SO THAT IT PRODUCES LASER BEAM OUTPUT
H
TILT VLD / LENS SUBASSEMBLY WITHIN VLD YOKE SO THAT LASER BEAM PASSES THROUGH TARGET AXIS OF QUADRANT DETECTOR ON PARAMETER ADJUSTMENT BENCH
I

FIG. 31C1

J — ROTATE VLD YOKE SUBASSEMBLY UNTIL LASER BEAM PASSES THROUGH TARGET CROSS-HAIR OF QUADRANT DETECTOR AND THEN LOCK VLD / LENS SUBASSEMBLY AND YOKE IN THE ALIGNED POSITION

K — INSTALL MIRROR AND LIGHT DIFFRACTIVE GRATING UPON MODULE BENCH

L — ADJUST VLD-TO-LENS DISTANCE d BY ROTATING LENS BARREL RELATIVE TO VLD BLOCK SO THAT ASTIGMATISM IS ELIMINATED; USE BEAM SCANNING DEVICE TO MEASURE BEAM CROSS-SECTIONS TO DETERMINE THAT ASTIGMATISM IS ELIMINATED; LOCK LENS BARREL WHEN CONDITION IS ATTAINED

M — MOUNT PRECONFIGURED LASER BEAM PRODUCTION MODULE TO OPTICAL BENCH OF HOLOGRAPHIC LASER SCANNER USING ALIGNMENT PINS AND HOLES TO ENSURE GRATING TILT ANGLE ρ_0 IS REALIZED FOR BEAM DISPERSION MINIMIZATION

FIG. 31C2

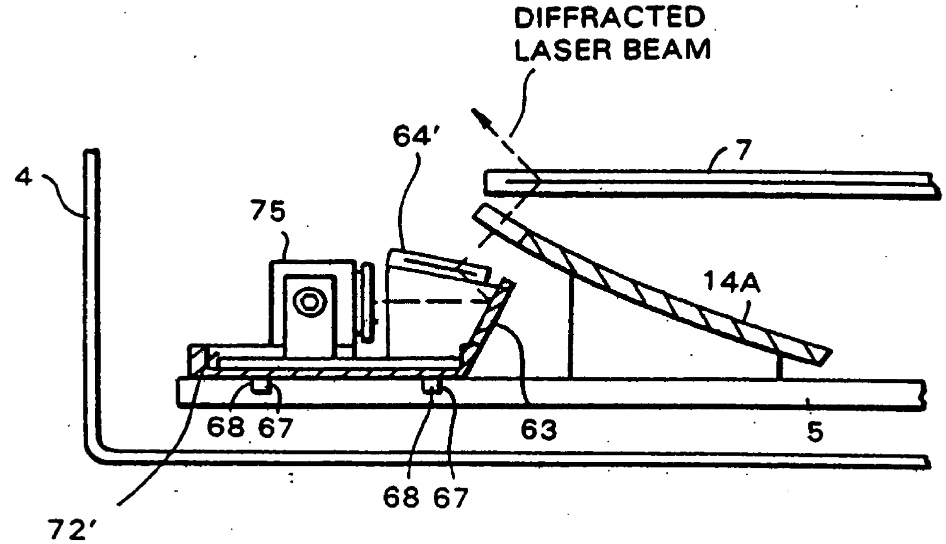

FIG. 31D

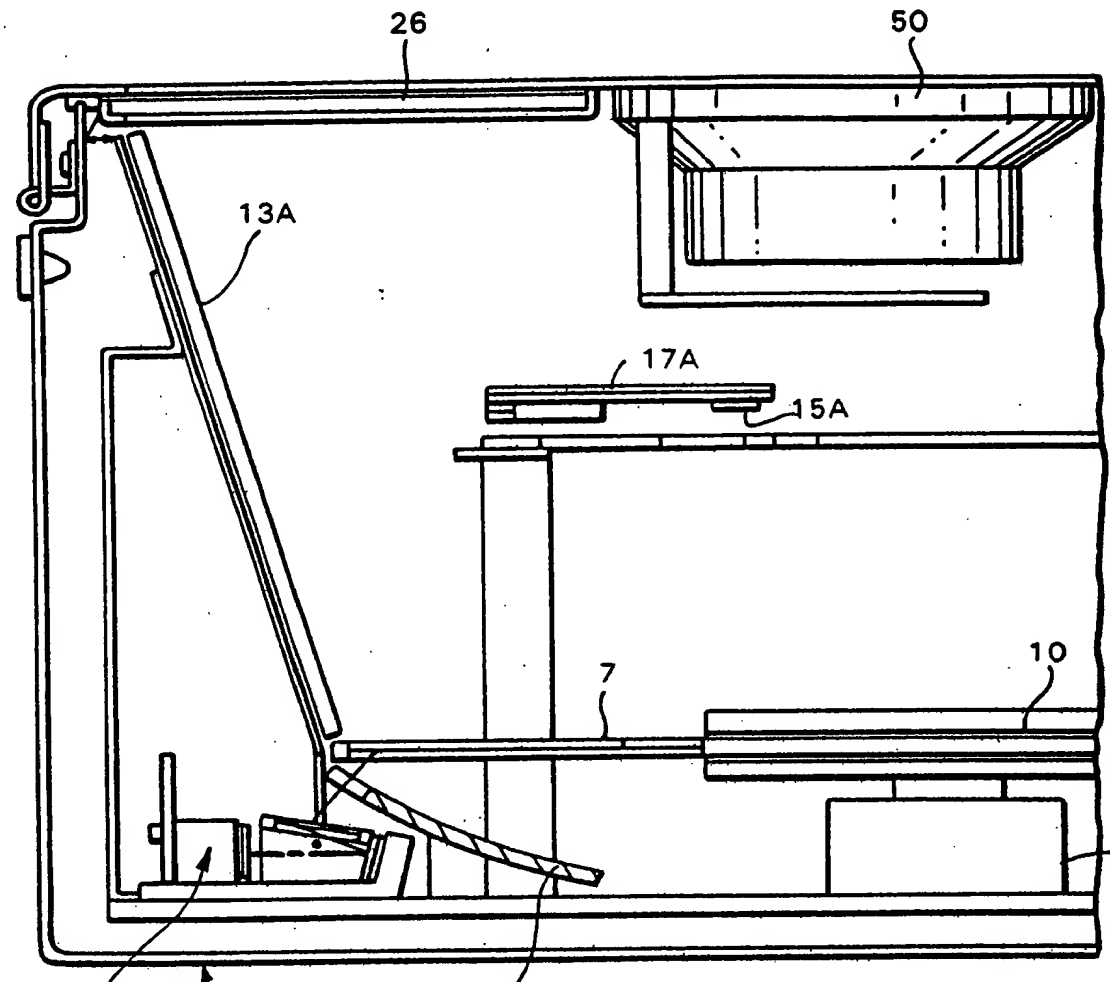

CASE: NO-CROSS-POLARIZER BEFORE PHOTODETECTOR

FIG. 32

A — CREATE 3-D GEOMETRICAL MODEL OF HOLOGRAPHIC LASER SCANNER BASED ON PARAMETERS OBTAINED FROM PRIOR STAGES OF SCANNER DESIGN METHOD, EXCLUDING PARABOLIC LIGHT COLLECTION MIRRORS AND PHOTODETECTORS

↓

B — PERFORM BRAGG SENSITIVITY ANALYSIS ON EACH HOLOGRAPHIC FACET USING THE HSD WORKSTATION TO DETERMINE THE RANGE OF INCIDENCE ANGLES OFF BRAGG, AT WHICH LIGHT RAYS REFLECTED OFF THE PARABOLIC MIRROR CAN?WILL BE TRANSMITTED THROUGH THE FACETS WITH MINIMUM DIFFRACTION (I.E. MAXIMUM TRANSMISSION) TOWARDS THE PHOTODETECTOR DURING LIGHT COLLECTION OPERATIONS

↓

C — USE THE HSD WORKSTATION TO TRACE ALL INCOMING LIGHT RAYS REFLECTED OFF A BAR CODE SYMBOL ANYWHERE IN THE SPECIFIED SCANNING VOLUME ONTO THE FACETS OF THE PREDESIGNED SCANNING DISC, AND BASED ON THIS ANALYSIS, IDENTIFY A POINT(S) ABOVE THE SCANNING DISC AND BELOW TOP EDGE OF ASSOCIATED BEAM FOLDING MIRROR, WHICH IS FREE OF INCOMING LIGHT RAYS

↓

D — LOCATE THE POSITION (I.E. CENTER AND OPTICAL AXIS ORIENTATION) OF THE PHOTODETECTORS USING THE "RAY FREE POINT" INFORMATION ACQUIRED DURING BLOCK C ABOVE

↓

F I G. 33A

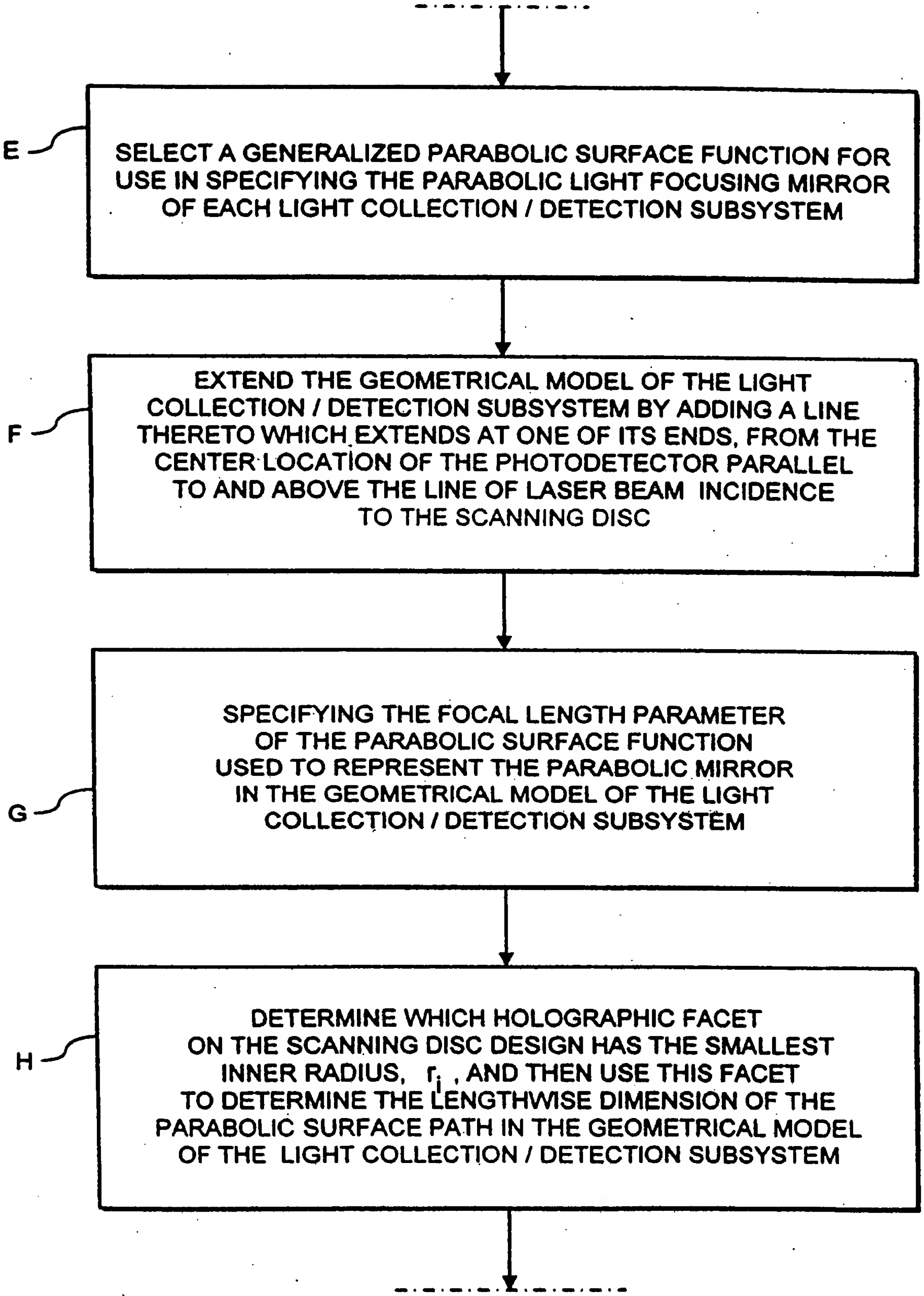
E
SELECT A GENERALIZED PARABOLIC SURFACE FUNCTION FOR USE IN SPECIFYING THE PARABOLIC LIGHT FOCUSING MIRROR OF EACH LIGHT COLLECTION / DETECTION SUBSYSTEM
F
EXTEND THE GEOMETRICAL MODEL OF THE LIGHT COLLECTION / DETECTION SUBSYSTEM BY ADDING A LINE THERETO WHICH EXTENDS AT ONE OF ITS ENDS, FROM THE CENTER LOCATION OF THE PHOTODETECTOR PARALLEL TO AND ABOVE THE LINE OF LASER BEAM INCIDENCE TO THE SCANNING DISC
G
SPECIFYING THE FOCAL LENGTH PARAMETER OF THE PARABOLIC SURFACE FUNCTION USED TO REPRESENT THE PARABOLIC MIRROR IN THE GEOMETRICAL MODEL OF THE LIGHT COLLECTION / DETECTION SUBSYSTEM
H
DETERMINE WHICH HOLOGRAPHIC FACET ON THE SCANNING DISC DESIGN HAS THE SMALLEST INNER RADIUS, r_i, AND THEN USE THIS FACET TO DETERMINE THE LENGTHWISE DIMENSION OF THE PARABOLIC SURFACE PATH IN THE GEOMETRICAL MODEL OF THE LIGHT COLLECTION / DETECTION SUBSYSTEM

FIG. 33B

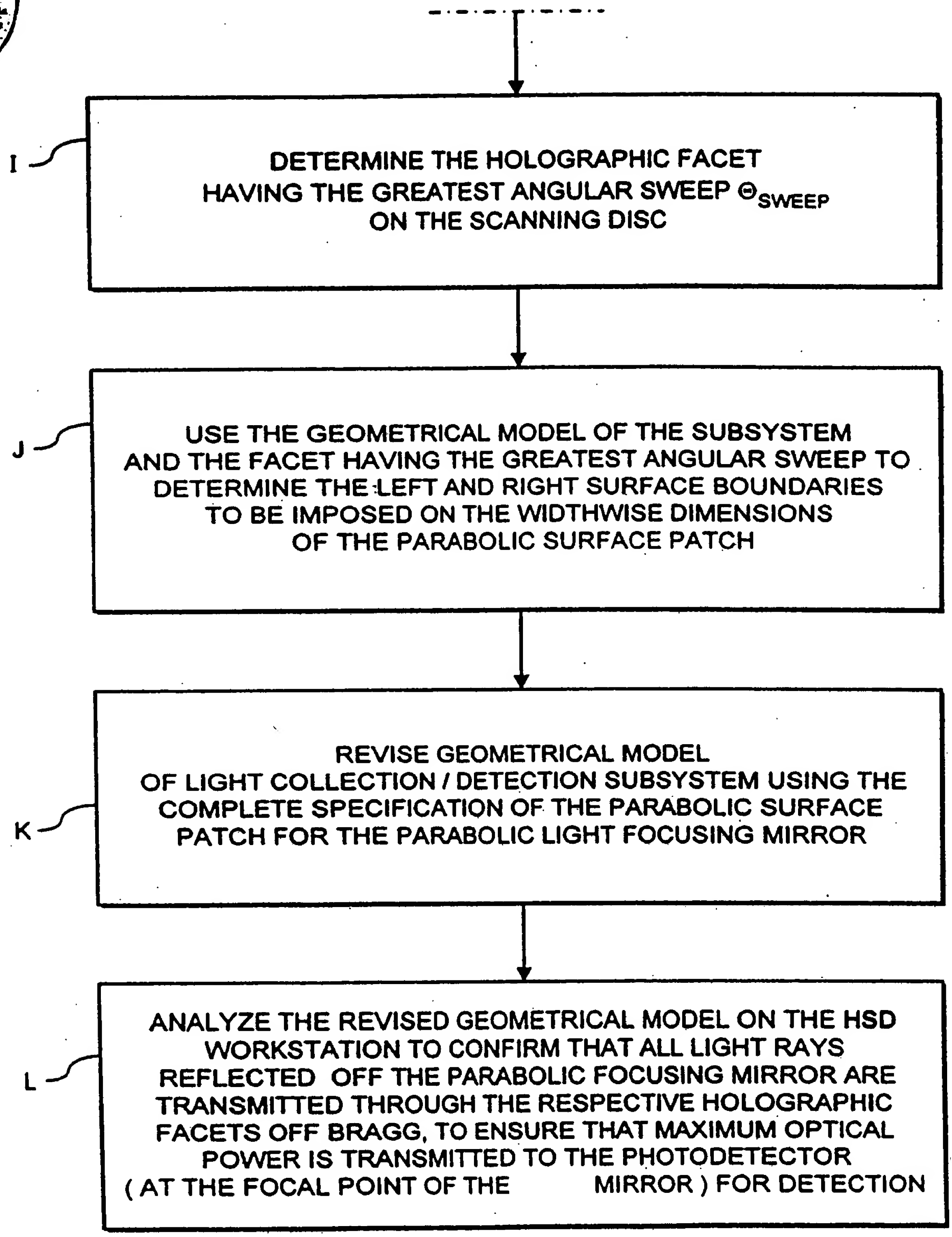
I
DETERMINE THE HOLOGRAPHIC FACET HAVING THE GREATEST ANGULAR SWEEP Θ_{SWEEP} ON THE SCANNING DISC
J
USE THE GEOMETRICAL MODEL OF THE SUBSYSTEM AND THE FACET HAVING THE GREATEST ANGULAR SWEEP TO DETERMINE THE LEFT AND RIGHT SURFACE BOUNDARIES TO BE IMPOSED ON THE WIDTHWISE DIMENSIONS OF THE PARABOLIC SURFACE PATCH
K
REVISE GEOMETRICAL MODEL OF LIGHT COLLECTION / DETECTION SUBSYSTEM USING THE COMPLETE SPECIFICATION OF THE PARABOLIC SURFACE PATCH FOR THE PARABOLIC LIGHT FOCUSING MIRROR
L
ANALYZE THE REVISED GEOMETRICAL MODEL ON THE HSD WORKSTATION TO CONFIRM THAT ALL LIGHT RAYS REFLECTED OFF THE PARABOLIC FOCUSING MIRROR ARE TRANSMITTED THROUGH THE RESPECTIVE HOLOGRAPHIC FACETS OFF BRAGG, TO ENSURE THAT MAXIMUM OPTICAL POWER IS TRANSMITTED TO THE PHOTODETECTOR (AT THE FOCAL POINT OF THE MIRROR) FOR DETECTION

FIG. 33C

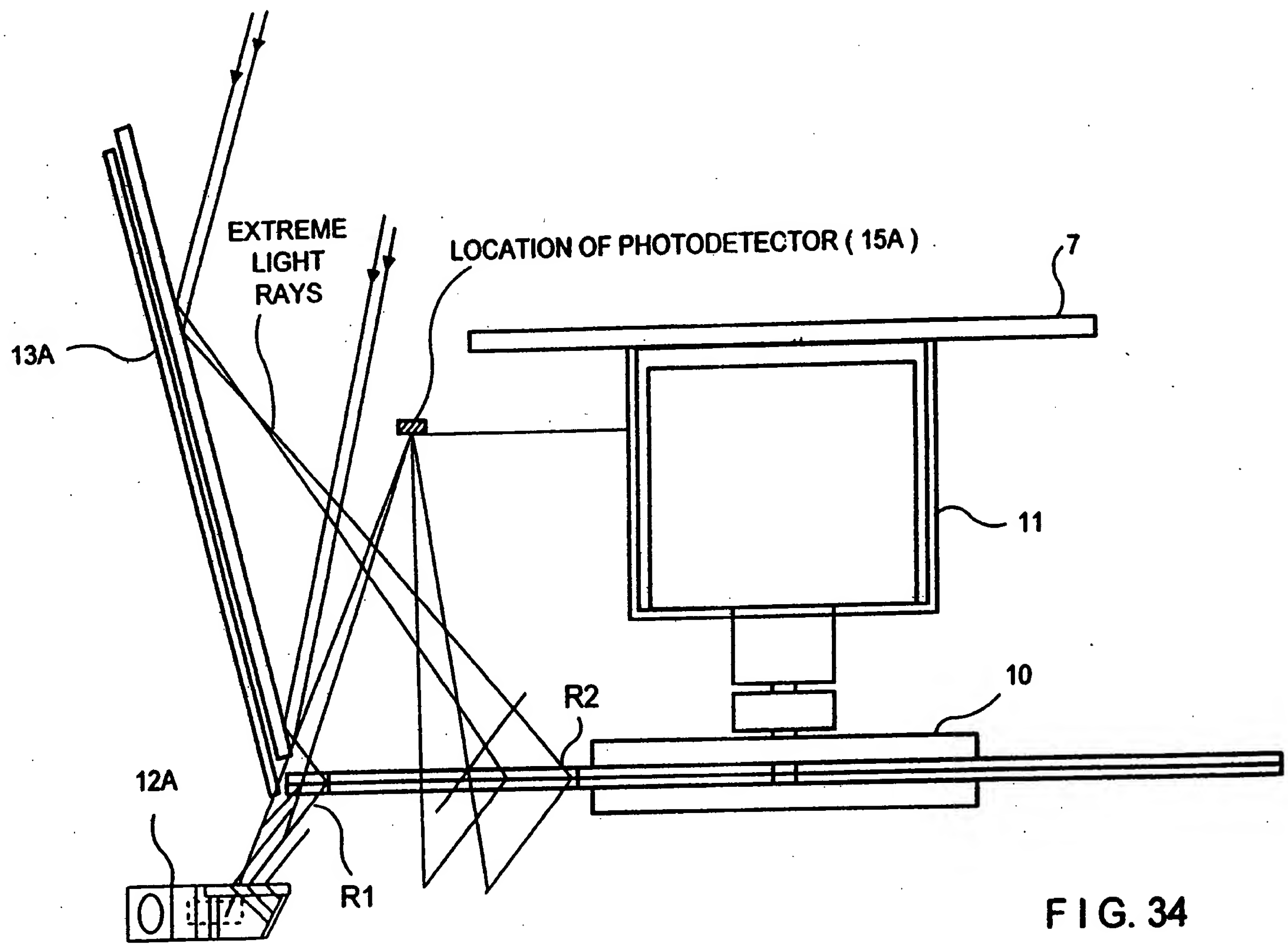
EXTREME
LIGHT
RAYS
LOCATION OF PHOTODETECTOR (15A)
7
13A
11
10
R2
12A
R1

F I G. 34

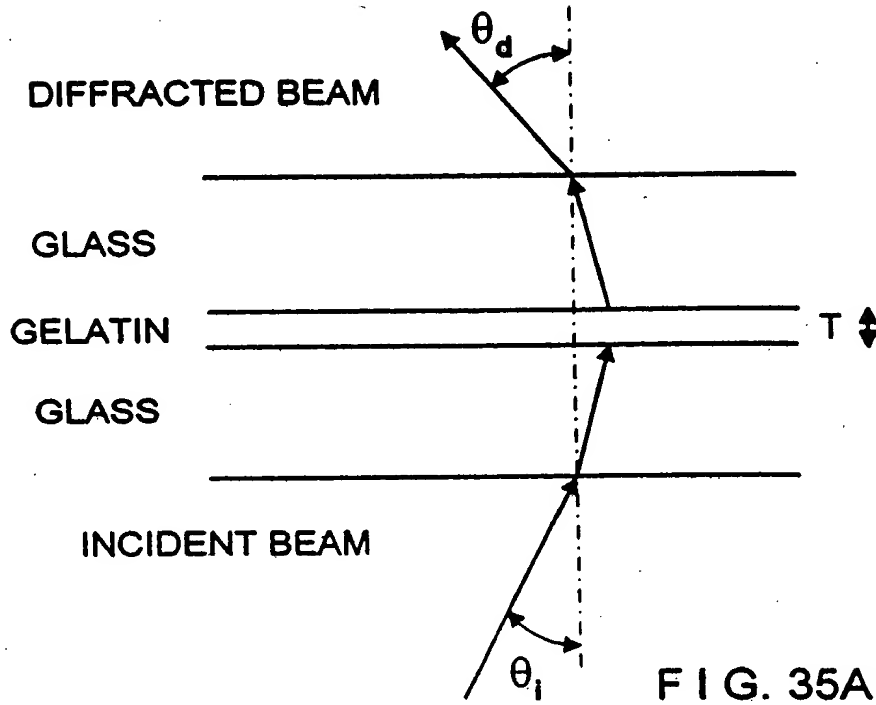

F I G. 35A1

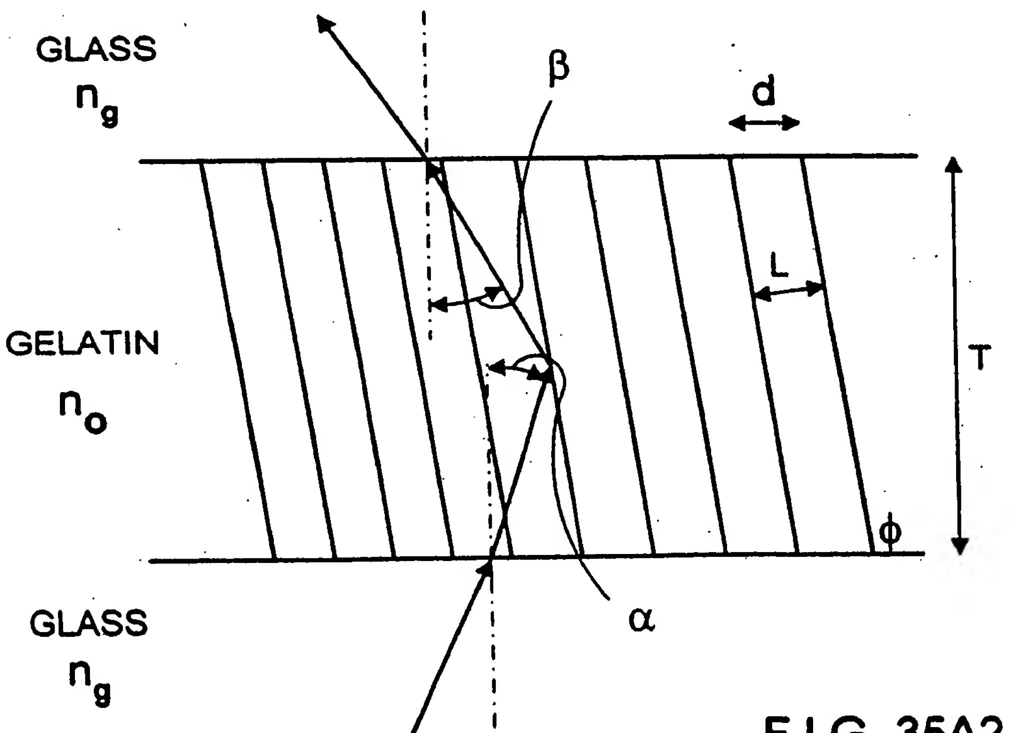

F I G. 35A2

S AND P POLARIZATION DIFFRACTION EFFICIENCY FOR THE TECH20 HOLOGRAPHIC SCANNING DISC AS FUNCTIONS OF THE EXTERNAL ANGLE OF INCIDENCE.

S AND P DIFFRACTION EFFICIENCY AS A FUNCTION OF THE DEVIATION FROM THE BRAGG ANGLE. SLANTED FRINGES ARE INCLUDED. IN THIS FILE, WE ARE CONSIDERING THE EXTERNAL ANGLES. THE EXTERNAL ANGLES ARE RELATED TO THE INTERNAL ANGLES VIA SNELL'S LAW. THE INTERNAL ANGLES ARE θ.0, α, AND β, WHERE 2θ.0 = (α + β). .
α = THE ANGLE OF REFRACTION, β - THE INTERNAL ANGLE OF DIFFRACTION, AND θ.0 IS THE ANGLE BETWEEN THE REFRACTED BEAM AND THE BRAGG PLANES. THE EXTERNAL ANGLES ARE θ.i (THE ANGLE OF INCIDENCE) AND θ.d (THE ANGLE OF DIFFRACTION).

DEFINITIONS:

θ_i = ANGLE OF INCIDENCE (EXTERNAL)
α = ANGLE OF INCIDENCE (INTERNAL)
β = ANGLE OF DIFFRACTION (INTERNAL)
δ = DEVIATION FROM THE BRAGG ANGLE (INTERNAL)
δ.0 = DEVIATION FROM THE BRAGG ANGLE (EXTERNAL)
ϕ = TILT OF BRAGG PLANES
= $\pi/2$ FOR NO TILT
L = SEPARATION OF THE BRAGG PLANES
T = THICKNESS OF HOE MEDIUM
d = EXTERNAL FRINGE SPACING
n0 = AVERAGE REFRACTIVE INDEX OF THE HOE MEDIUM
n1 = delta-n OF HOE FRINGE STRUCTURE
λ_a = WAVELENGTH IN AIR
$\delta\lambda$ = DEVIATION FROM λ_a(BRAGG λ)

FIG. 35B

FIXED, OR ESTABLISHED PARAMETERS:

n0, n1, θ_i, θ_d, δ, $\delta\lambda$, λ_a, T.

$$deg = \frac{\pi}{180}$$

$n_0 := 1.4$

$n_1 := 0.146$

$\theta_i := 43\ deg$

$\theta_d := 27.2\ deg$

$\delta_e := 0\ deg, .2\ deg, \ldots, .70\ deg$

$\delta_\lambda := 0$

$T := 2.2$

$\lambda_a := .670$

F I G. 35B1

(1) $\alpha := \operatorname{asin}\left[\frac{\sin[\theta_i]}{n_0}\right]$

(2) $\beta := \operatorname{asin}\left[\frac{\sin[\theta_d]}{n_0}\right]$

(3) $\phi := \frac{\pi}{2} - \frac{\beta - \alpha}{2}$

(4) $d := \frac{\lambda_a}{[n_0(\sin(\alpha) + \sin(\beta))]}$ GRATING EQUATION

(5) $L := d \sin(\phi)$

(6) $C_R := \cos(\alpha)$

(7) $C_S := \cos(\alpha) - \frac{\lambda_a}{n_0 L}\cos(\phi)$

(8) $N := \pi n_1 \frac{T}{\lambda_a \sqrt{C_R C_S}}$

(9) $\delta[\delta_e] := \left[\operatorname{asin}\left[\frac{\sin[\theta_i + \delta_e]}{n_0}\right] - \alpha\right]$

(10) $\Gamma[\delta_e] := 2\pi\,\delta[\delta_e]\frac{\sin(\phi - \alpha)}{L} - \delta_\lambda \frac{\pi}{n_0 L^2}$

(11) $S[\delta_e] := \Gamma[\delta_e]\frac{T}{2 C_S}$

F I G. 35C1

DIFFRACTION EFFICIENCIES: E_s AND E_p AS A FUNCTION OF δ.e

$$(12)\quad E_s[\delta_e] := \frac{\left[\sin\left[\sqrt{N^2 + S[\delta_e]^2}\right]\right]^2}{1 + \frac{S[\delta_e]^2}{N^2}}$$

$$(13)\quad E_p[\delta_e] :=$$

$$= \frac{\left[\sin\left[\sqrt{(N\cos(2(\alpha - \phi)))^2 + S[\delta_e]^2}\right]\right]^2}{1 + \frac{S[\delta_e]^2}{(N\cos(2(\alpha - \phi)))^2}}$$

$$(14)\quad E_{av}[\delta_e] := \frac{E_s[\delta_e] + E_p[\delta_e]}{2}$$

FIG. 35C2

RELATIVE DIFFRACTION EFFICIENCY FOR UNPOLARIZED LIGHT AS A FUNCTION OF DEVIATION FROM THE BRAGG ANGLE - FACET 1

$\lambda_a = .67 \quad n_0 = 1.4 \quad n_1 = 0.146 \quad \theta_i = 43$ deg

$\theta_d = 27.2$ deg $\quad T = 2.2$

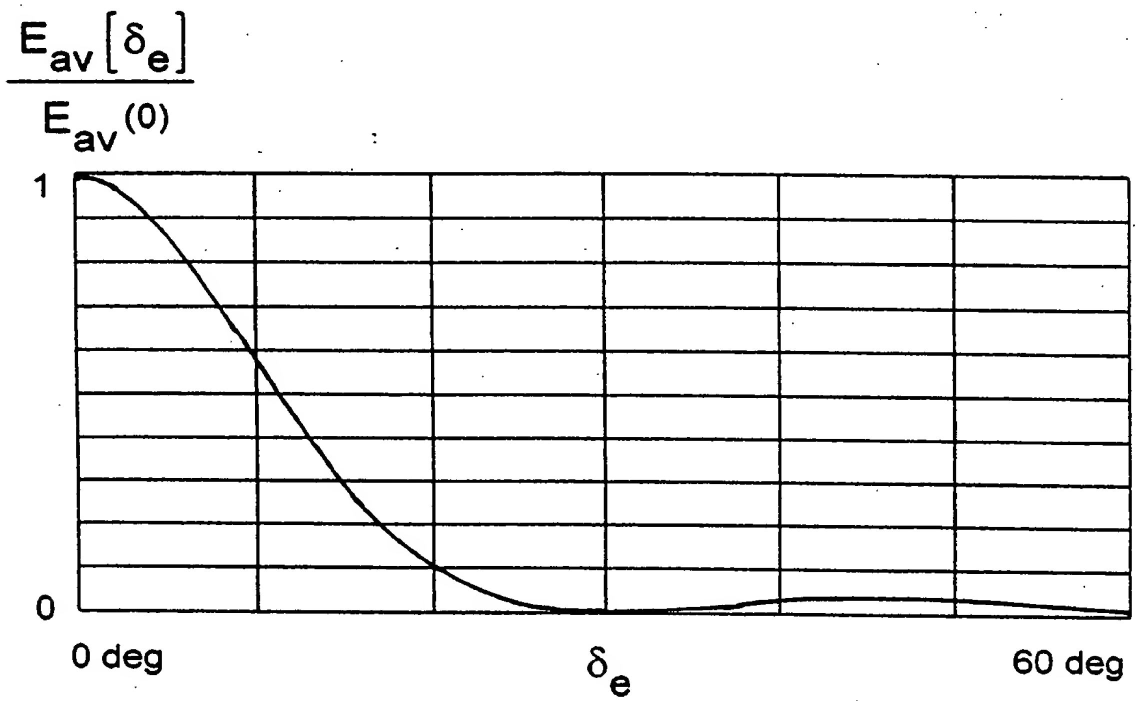

FIG. 35D1

RELATIVE DIFFRACTION EFFICIENCY FOR UNPOLARIZED LIGHT AS A FUNCTION OF DEVIATION FROM THE BRAGG ANGLE - FACET 16

$\lambda_a = .670 \quad n_0 = 1.4 \quad n_1 = 0.145 \quad \theta_i = 43$ deg

$\theta_d = 41.8$ deg $\quad T = 2.2$

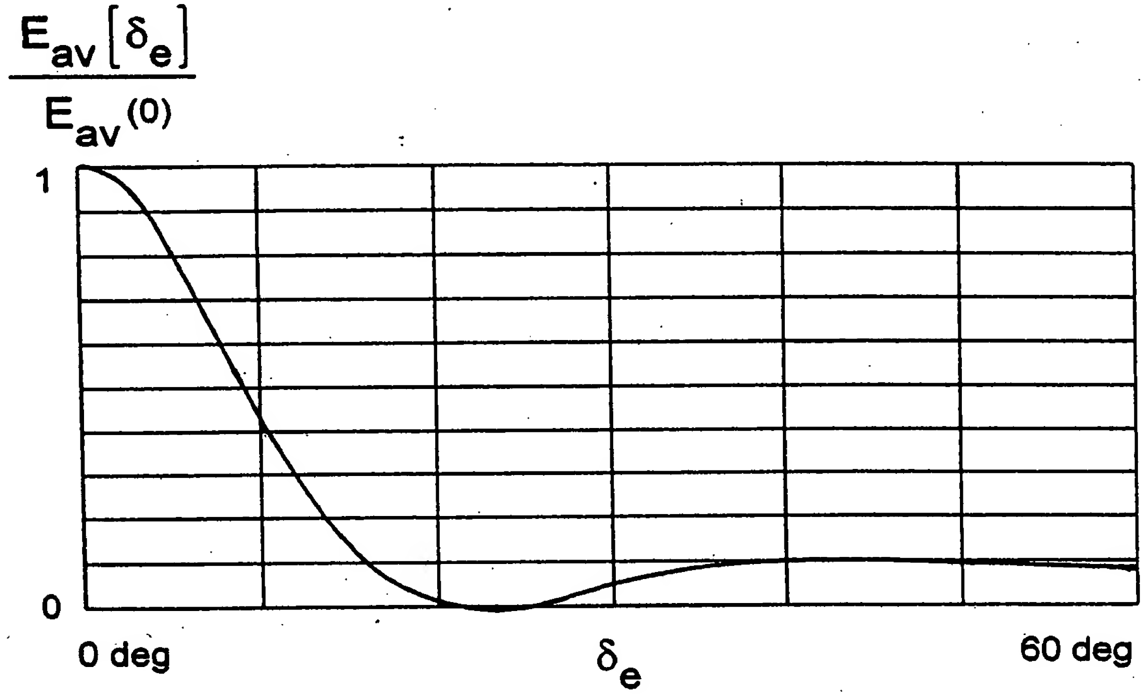

F I G. 35D2

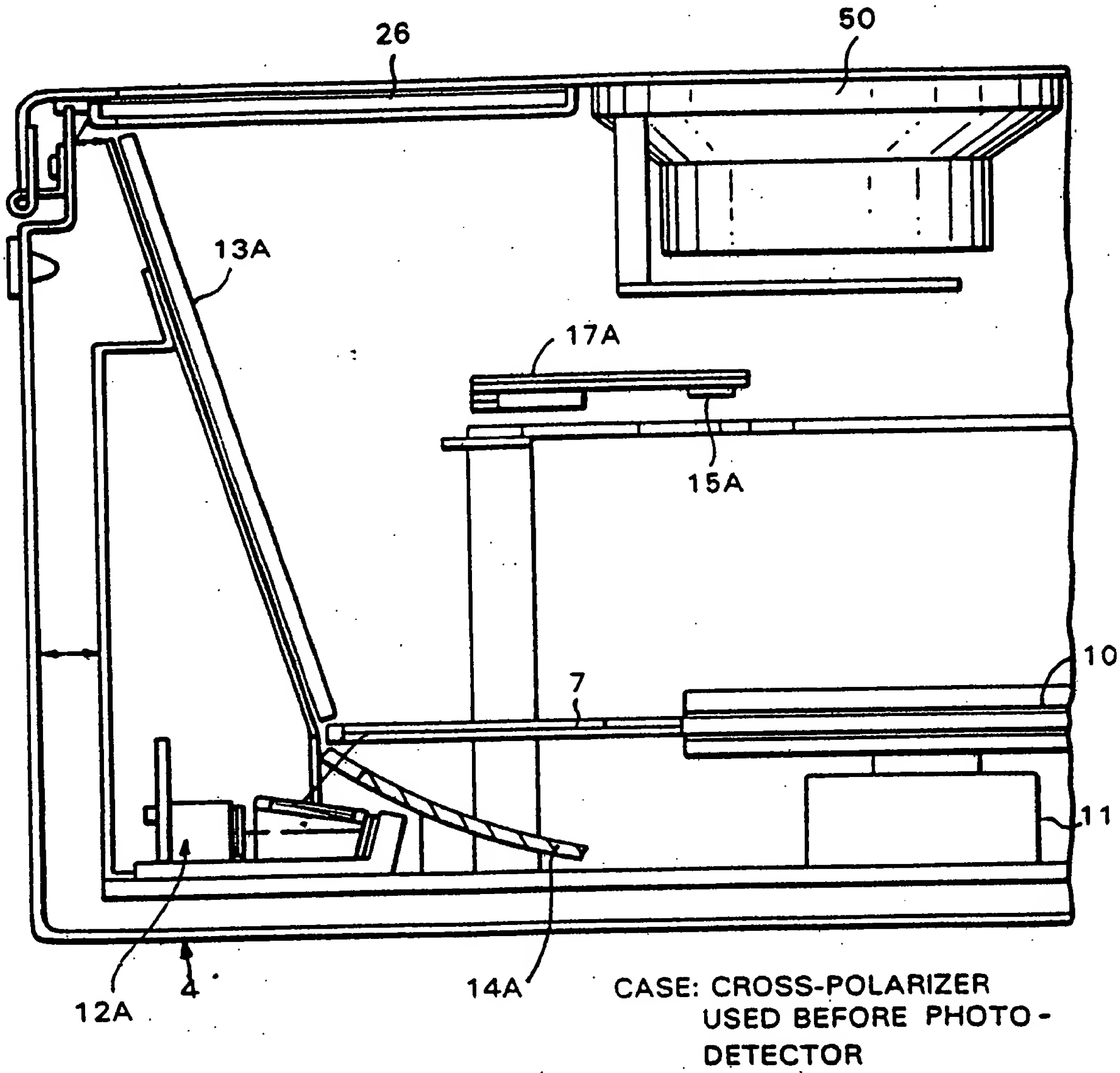
26
50
13A
17A
15A
10
7
11
12A
4
14A
CASE: CROSS-POLARIZER
USED BEFORE PHOTO-
DETECTOR

FIG. 36

S POLARIZATION DIFFRACTION EFFICIENCY FOR THE TECH20 HOLOGRAPHIC SCANNING DISC AS A FUNCTION OF THE EXTERNAL ANGLE OF INCIDENCE. THIS IS THE SECOND CASE OF INTEREST WHEN A CROSSED POLARIZER IS USED ON THE DETECTOR.

S DIFFRACTION EFFICIENCY AS A FUNCTION OF THE DEVIATION FROM THE BRAGG ANGLE . SLANTED FRINGES ARE INCLUDED. IN THIS FILE, WE ARE CONSIDERING THE EXTERNAL ANGLES. THE EXTERNAL ANGLES ARE RELATED TO THE INTERNAL ANGLES VIA SNELL'S LAW. THE INTERNAL ANGLES ARE θ.0, α, AND β , WHERE 2θ.0 = (α + β). .
α = THE ANGLE OF REFRACTION, β - THE INTERNAL ANGLE OF DIFFRACTION, AND θ.0 IS THE ANGLE BETWEEN THE REFRACTED BEAM AND THE BRAGG PLANES. THE EXTERNAL ANGLES ARE θ.i (THE ANGLE OF INCIDENCE) AND θ.d (THE ANGLE OF DIFFRACTION).

DEFINITIONS:

θ_i = ANGLE OF INCIDENCE (EXTERNAL)
α = ANGLE OF INCIDENCE (INTERNAL)
β = ANGLE OF DIFFRACTION (INTERNAL)
δ = DEVIATION FROM THE BRAGG ANGLE (INTERNAL)
$\delta.0$ = DEVIATION FROM THE BRAGG ANGLE (EXTERNAL)
ϕ = TILT OF BRAGG PLANES
= $\pi/2$ FOR NO TILT
L = SEPARATION OF THE BRAGG PLANES
T = THICKNESS OF HOE MEDIUM
d = EXTERNAL FRINGE SPACING
n0 = AVERAGE REFRACTIVE INDEX OF THE HOE MEDIUM
n1 = delta-n OF HOE FRINGE STRUCTURE
λ_a = WAVELENGTH IN AIR
$\delta\lambda$ = DEVIATION FROM λ_a (BRAGG λ)

F I G. 37A

FIXED, OR ESTABLISHED PARAMETERS:

n0, n1, θ_i, θ_d, δ, $\delta\lambda$, λ_a, T.

$$deg = \frac{\pi}{180}$$

$n_0 := 1.4$

$n_1 := 0.146$

$\theta_i := 43\ deg$

$\theta_d := 27.2\ deg$

$\delta_e := 0\ deg, .2\ deg, ..., .70\ deg$

$\delta_\lambda := 0$

$T := 2.2$

$\lambda_a := .670$

F I G. 37A1

(1) $$\alpha := \operatorname{asin}\left[\frac{\sin[\theta_i]}{n_0}\right]$$

(2) $$\beta := \operatorname{asin}\left[\frac{\sin[\theta_d]}{n_0}\right]$$

(3) $$\phi := \frac{\pi}{2} - \frac{\beta - \alpha}{2}$$

(4) $$d := \frac{\lambda_a}{[n_0(\sin(\alpha) + \sin(\beta))]}$$ GRATING EQUATION

(5) $$L := d \sin(\phi)$$ (6) $$C_R := \cos(\alpha)$$

(7) $$C_S := \cos(\alpha) - \frac{\lambda_a}{n_0 L}\cos(\phi)$$

(8) $$N := \pi n_1 \frac{T}{\lambda_a \sqrt{C_R C_S}}$$

(9) $$\delta[\delta_e] := \left[\operatorname{asin}\left[\frac{\sin[\theta_i + \delta_e]}{n_0}\right] - \alpha\right]$$

(10) $$\Gamma[\delta_e] := 2\pi\,\delta[\delta_e]\frac{\sin(\phi - \alpha)}{L} - \delta_\lambda \frac{\pi}{n_0 L^2}$$

(11) $$S[\delta_e] := \Gamma[\delta_e]\frac{T}{2 C_S}$$

S-POLARIZATION DIFFRACTION EFFICIENCY: E_S AS A FUNCTION OF δ.e

(12) $$E_S[\delta_e] := \frac{\left[\sin\left[\sqrt{N^2 + S[\delta_e]^2}\right]\right]^2}{1 + \frac{S[\delta_e]^2}{N^2}}$$

F I G. 37B

RELATIVE DIFFRACTION EFFICIENCY FOR S-POLARIZED LIGHT AS A FUNCTION OF DEVIATION FROM THE BRAGG ANGLE - FACET 1

$\lambda_a = .67 \quad n_0 = 1.4 \quad n_1 = 0.146 \quad \theta_i = 43\ \mathrm{deg}$

$\theta_d = 27.2\ \mathrm{deg} \quad T = 2.2$

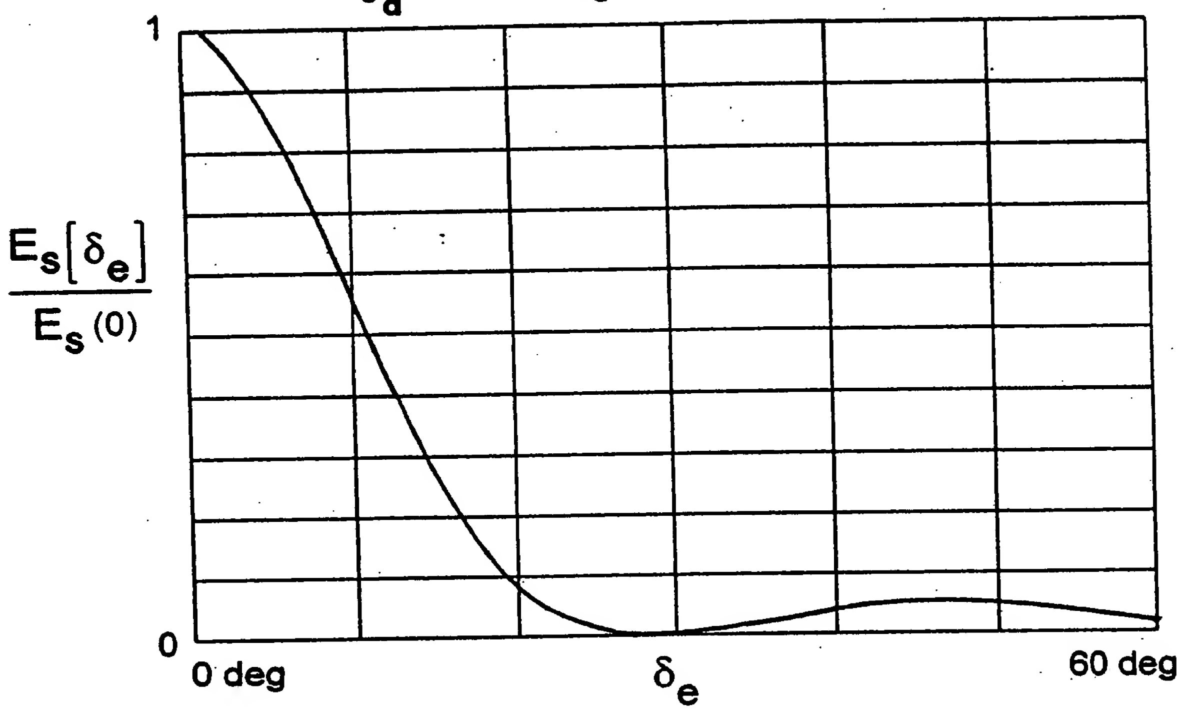

$$\mathrm{PerCentLoss} := 100 \left[\frac{1}{28\ \mathrm{deg}}\right] \left[\int_{25\ \mathrm{deg}}^{53\ \mathrm{deg}} \frac{E_s[\delta_e]}{E_s(0)}\, d\delta_e\right]$$

$$\mathrm{PerCentLoss} := 3$$

F I G. 37C1

$\lambda_a = .670 \quad n_0 = 1.4 \quad n_1 = 0.145 \quad \theta_i = 43\ \text{deg}$

$\theta_d = 41.8\ \text{deg} \quad T = 2.2$

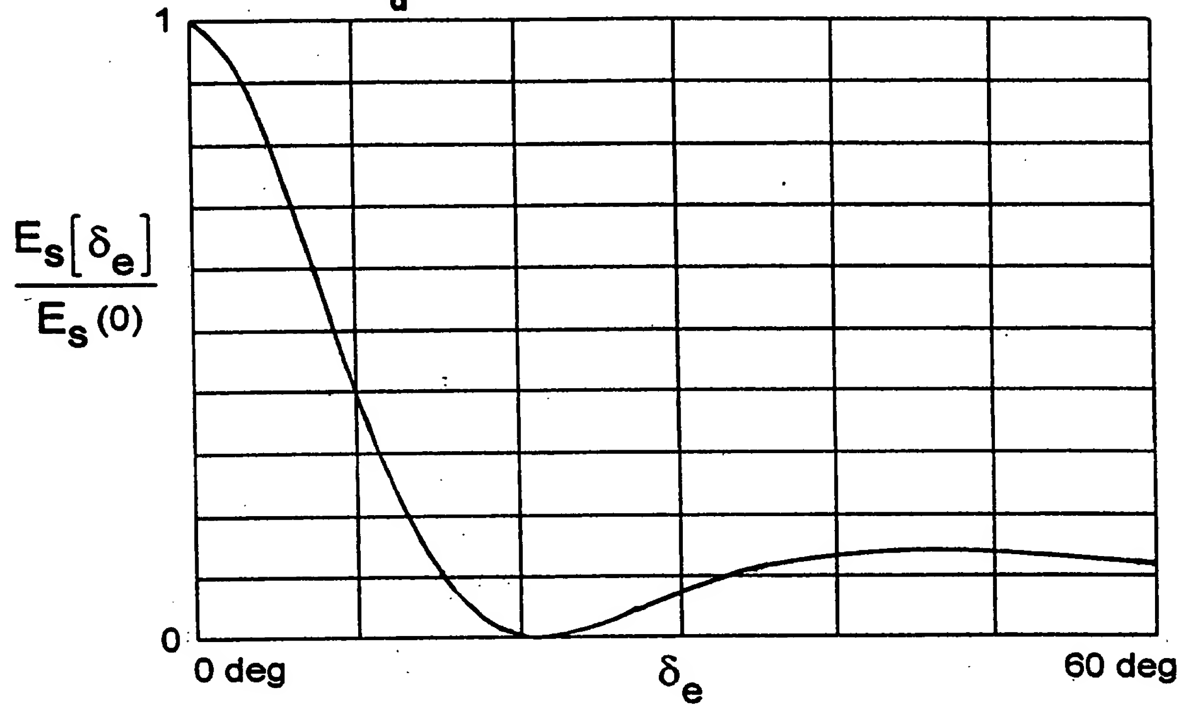

$$\text{PerCentLoss} := 100 \left[\frac{1}{28\ \text{deg}}\right] \left[\int_{25\ \text{deg}}^{53\ \text{deg}} \frac{E_s[\delta_e]}{E_s(0)}\, d\delta_e\right]$$

$$\text{PerCentLoss} := 10.972$$

F I G. 37C2

P POLARIZATION DIFFRACTION EFFICIENCY FOR THE TECH20 HOLOGRAPHIC SCANNING DISC AS A FUNCTION OF THE EXTERNAL ANGLE OF INCIDENCE. THIS IS THE CASE OF INTEREST WHEN A CROSSED POLARIZER IS USED ON THE DETECTOR.

P DIFFRACTION EFFICIENCY AS A FUNCTION OF THE DEVIATION FROM THE BRAGG ANGLE . SLANTED FRINGES ARE INCLUDED. IN THIS FILE, WE ARE CONCIDERING THE EXTERNAL ANGLES. THE EXTERNAL ANGLES ARE RELATED TO THE INTERNAL ANGLES VIA SNELL'S LAW. THE INTERNAL ANGLES ARE θ.0, a, AND β , WHERE 2θ.0 = (α + β). .
α = THE ANGLE OF REFRACTION, β - THE INTERNAL ANGLE OF DIFFRACTION, AND θ.0 IS THE ANGLE BETWEEN THE REFRACTED BEAM AND THE BRAGG PLANES. THE EXTERNAL ANGLES ARE θ.I (THE ANGLE OF INCIDENCE) AND θ.d (THE ANGLE OF DIFFRACTION).

DEFINITIONS:

θ_i = ANGLE OF INCIDENCE (EXTERNAL)
α = ANGLE OF INCIDENCE (INTERNAL)
β = ANGLE OF DIFFRACTION (INTERNAL)
δ = DEVIATION FROM THE BRAGG ANGLE (INTERNAL)
δ.0 = DEVIATION FROM THE BRAGG ANGLE (EXTERNAL)
ϕ = TILT OF BRAGG PLANES
= $\pi/2$ FOR NO TILT
L = SEPARATION OF THE BRAGG PLANES
T = THICKNESS OF HOE MEDIUM
d = EXTERNAL FRINGE SPACING
n0 = AVERAGE REFRACTIVE INDEX OF THE HOE MEDIUM
n1 = delta-n OF HOE FRINGE STRUCTURE
λ_a = WAVELENGTH IN AIR
$\delta\lambda$ = DEVIATION FROM λ_a(BRAGG λ)

FIG. 38A

FIXED, OR ESTABLISHED

PARAMETERS: n0, Δn1, θ_i, θ_d, δ, $\delta\lambda$, λ_a, T.

$\text{deg} = \frac{\pi}{180}$

$n_0 := 1.4$

$\Delta n_1 := 0.146$

$\theta_i := 43\ \text{deg}$

$\theta_d := 27.2\ \text{deg}$

$\delta := 0\ \text{deg}, .2\ \text{deg}, \ldots, .70\ \text{deg}$

$\delta_\lambda := 0$

$T := 2.2$

$\lambda_a := .670$

F I G. 38A1

(1) $\alpha := \text{asin}\left[\dfrac{\sin[\theta_i]}{n_0}\right]$

(2) $\beta := \text{asin}\left[\dfrac{\sin[\theta_d]}{n_0}\right]$

(3) $\phi := \dfrac{\pi}{2} - \dfrac{\beta - \alpha}{2}$

(4) $d := \dfrac{\lambda_a}{[n_0(\sin(\alpha) + \sin(\beta))]}$ GRATING EQUATION

(5) $L := d \sin(\phi)$

(6) $C_R := \cos(\alpha)$

(7) $C_s := \cos(\alpha) - \dfrac{\lambda_a}{n_0 L} \cos(\phi)$

(8) $N := \pi n_1 \dfrac{T}{\lambda_a \sqrt{C_R C_s}}$

(9) $\delta[\delta_e] := \left[\text{asin}\left[\dfrac{\sin[\theta_i + \delta_e]}{n_0}\right] - \alpha\right]$

(10) $\Gamma[\delta_e] := 2\pi\,\delta[\delta_e]\dfrac{\sin(\phi - \alpha)}{L} - \delta_\lambda \dfrac{\pi}{n_0 L^2}$

(11) $S[\delta_e] := \Gamma[\delta_e]\dfrac{T}{2 C_s}$

FIG. 38B1

P-POLARIZATION DIFFRACTION EFFICIENCY:
E_p AS A FUNCTION OF δ.e

$$(12)\quad E_P[\delta_e] := \frac{\left[\sin\left[\sqrt{(N\cos(2(\alpha-\phi)))^2 + S[\delta_e]^2}\right]\right]^2}{1+\dfrac{S[\delta_e]^2}{(N\cos(2(\alpha-\phi)))^2}}$$

F I G. 38B2

RELATIVE DIFFRACTION EFFICIENCY FOR P-POLARIZED LIGHT AS A FUNCTION OF DEVIATION FROM THE BRAGG ANGLE - FACET 1

$\lambda_a = .670 \quad n_0 = 1.4 \quad n_1 = 0.146 \quad \theta_i = 43$ deg

$\theta_d = 27.2$ deg $\quad T = 2.2$

$$\frac{E_P[\delta_e]}{E_P(0)}$$

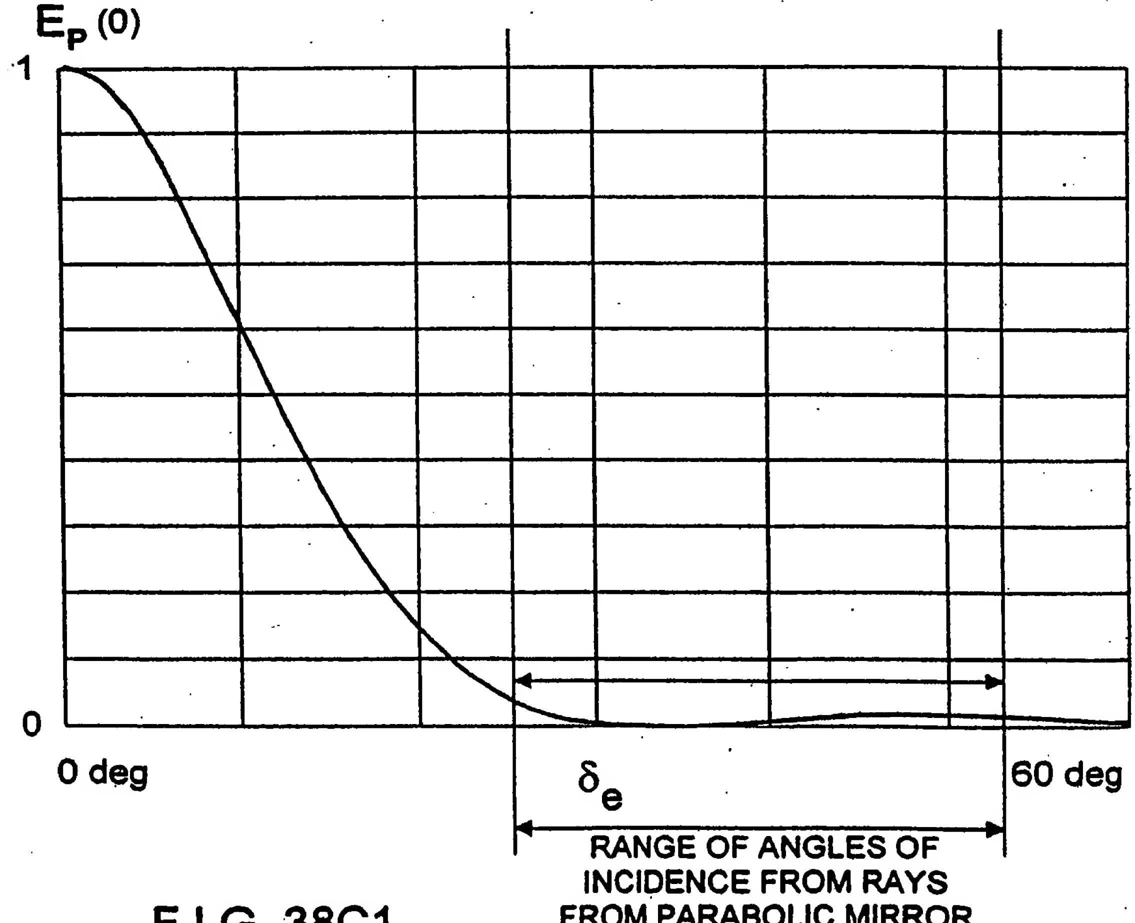

F I G. 38C1

RELATIVE DIFFRACTION EFFICIENCY FOR P-POLARIZED LIGHT AS A FUNCTION OF DEVIATION FROM THE BRAGG ANGLE - FACET 16

$\lambda_a = .670 \quad n_0 = 1.4 \quad n_1 = 0.145 \quad \theta_i = 43$ deg

$\theta_d = 41.8$ deg $\quad T = 2.2$

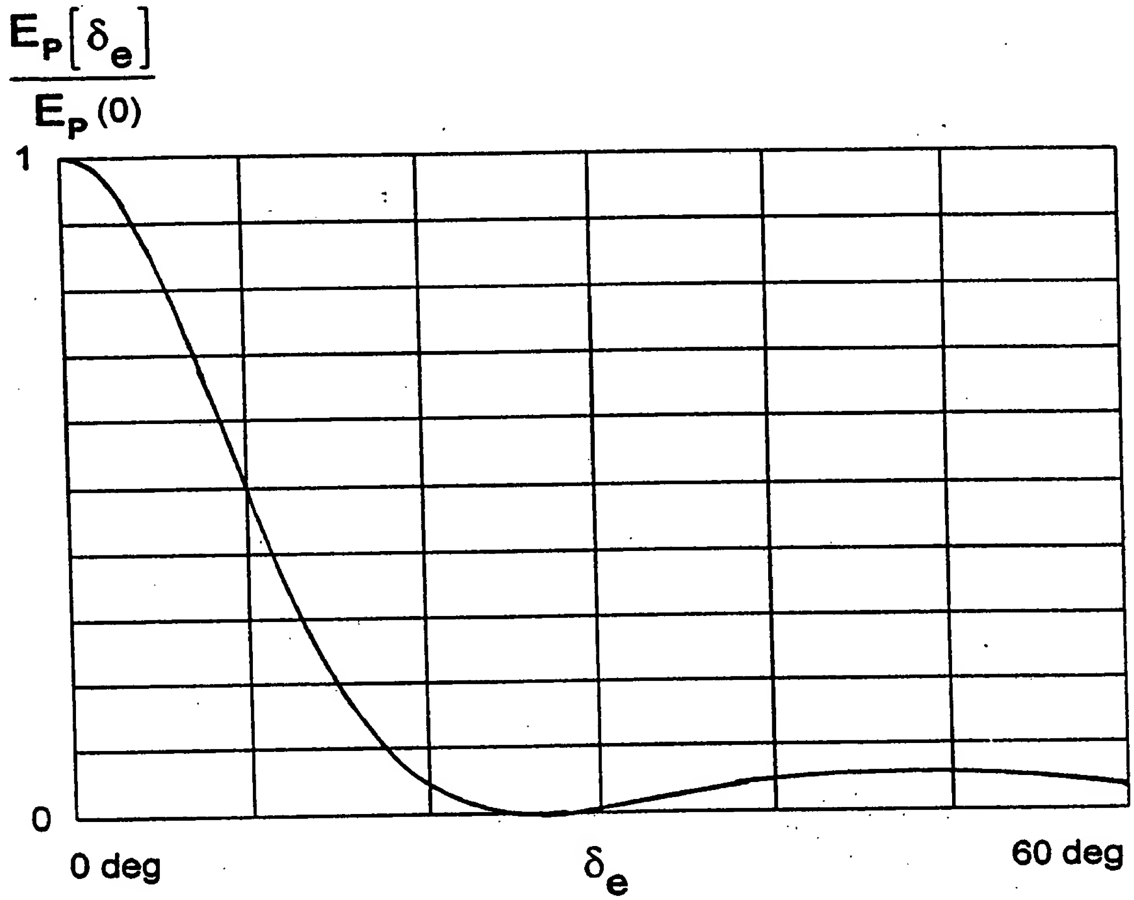

FIG. 38C2

GEOMETRICAL MODEL OF LIGHT COLLECTION SUBSYSTEM

$A = 52.9^{\circ}$
$B = 24^{\circ}$

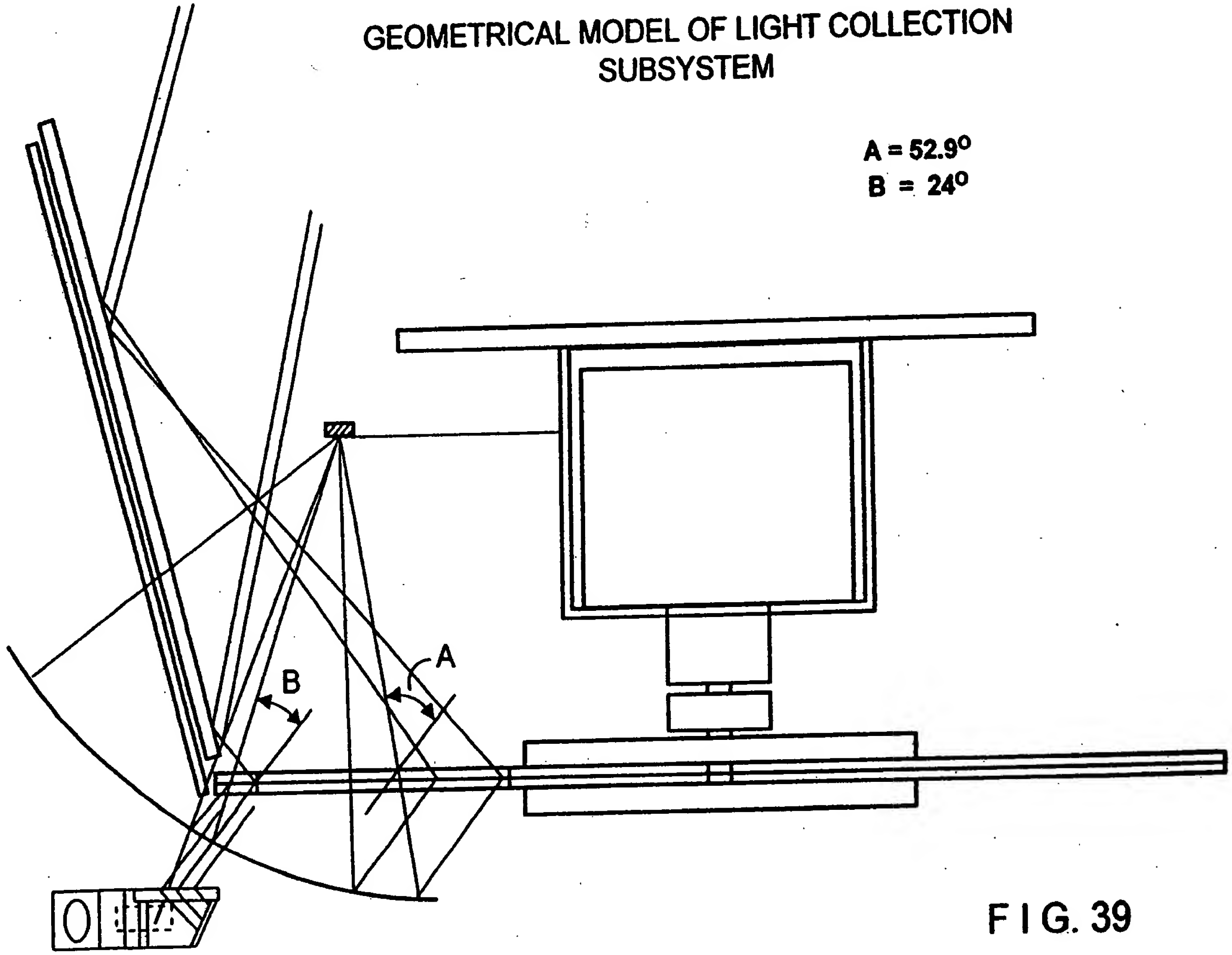

FIG. 39

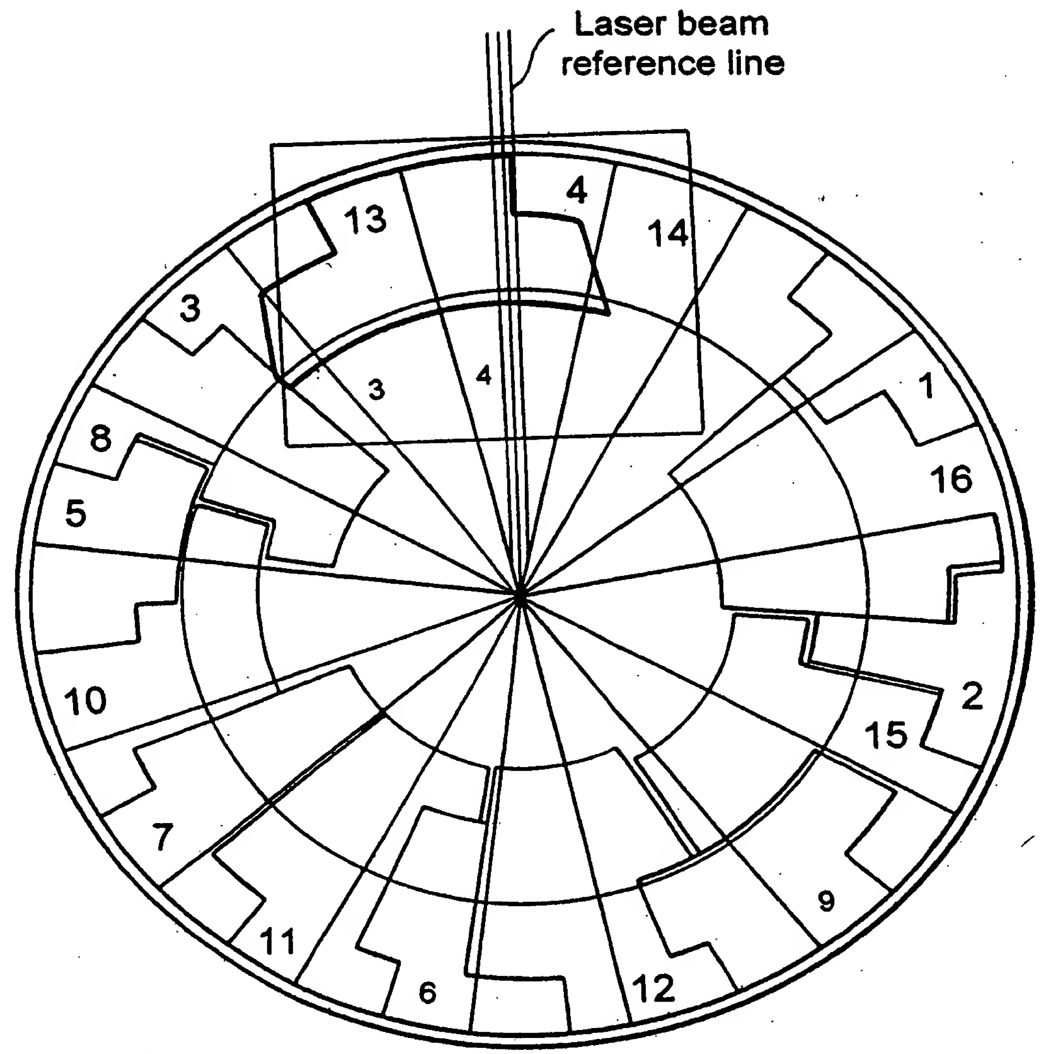

FIG. 40A

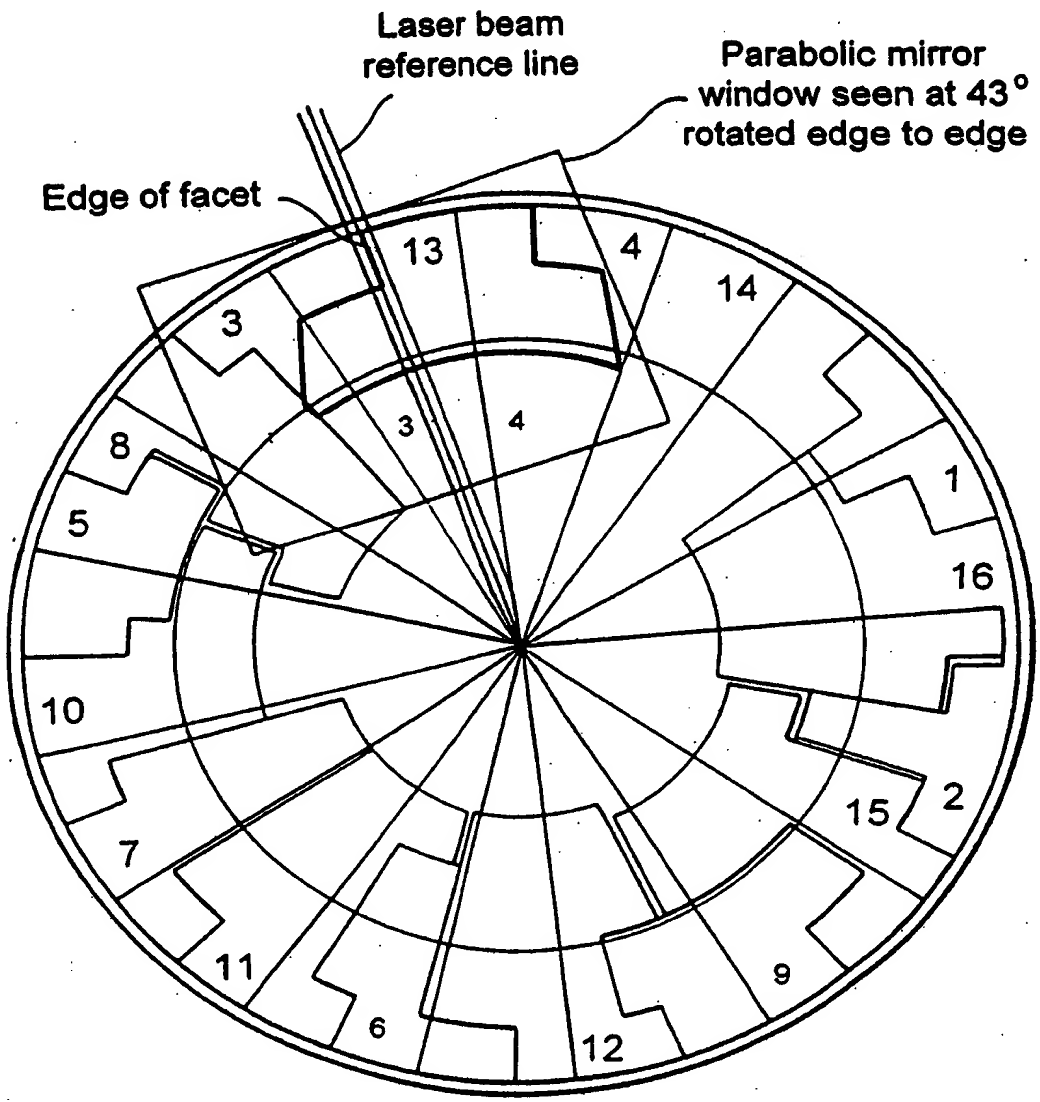
Laser beam
reference line
Parabolic mirror
window seen at 43°
rotated edge to edge
Edge of facet
13
4
14
3
3
4
8
1
5
16
10
2
15
7
11
9
6
12

FIG. 40B

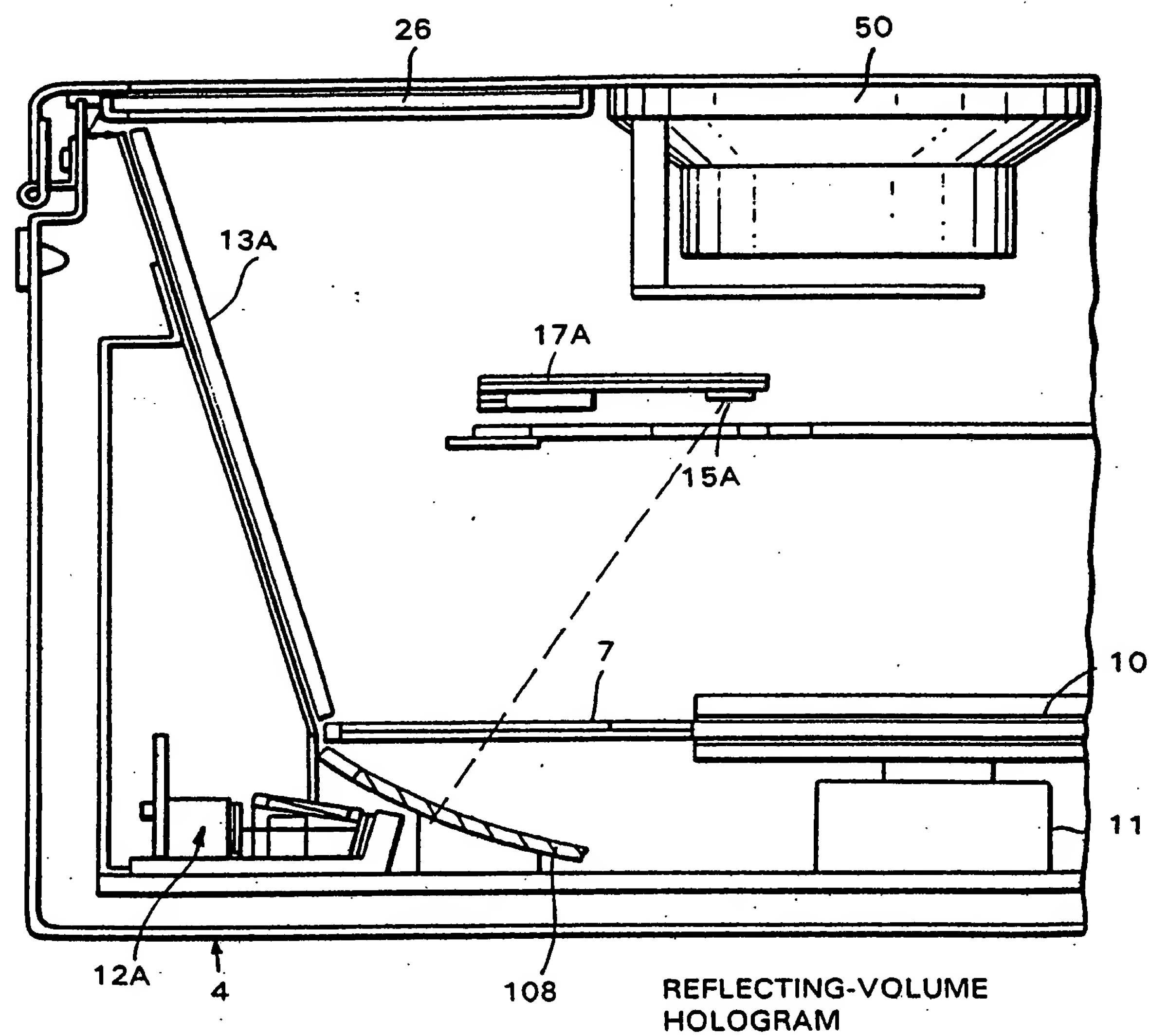

FIG. 41

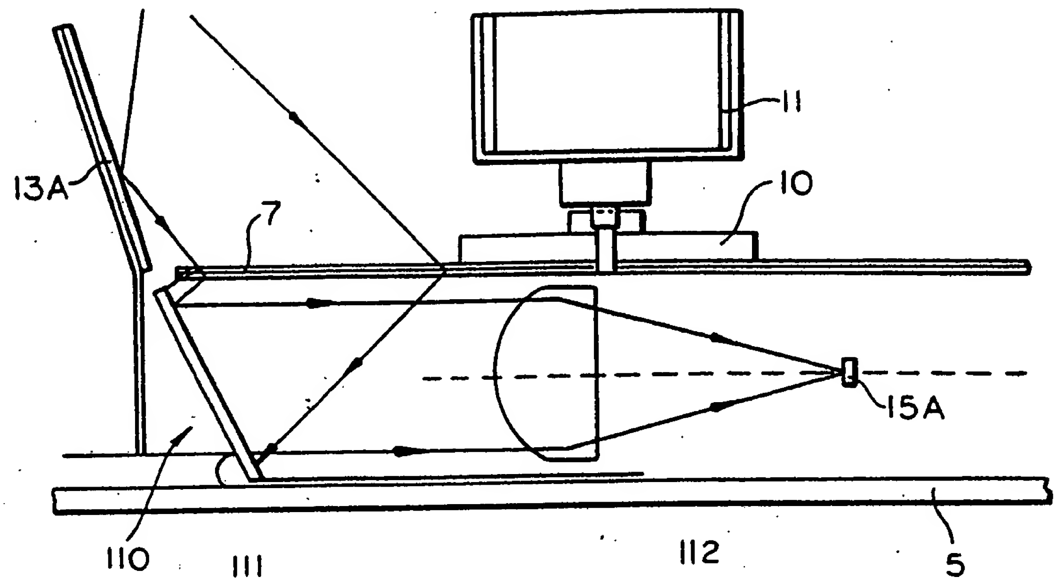

FIG. 42

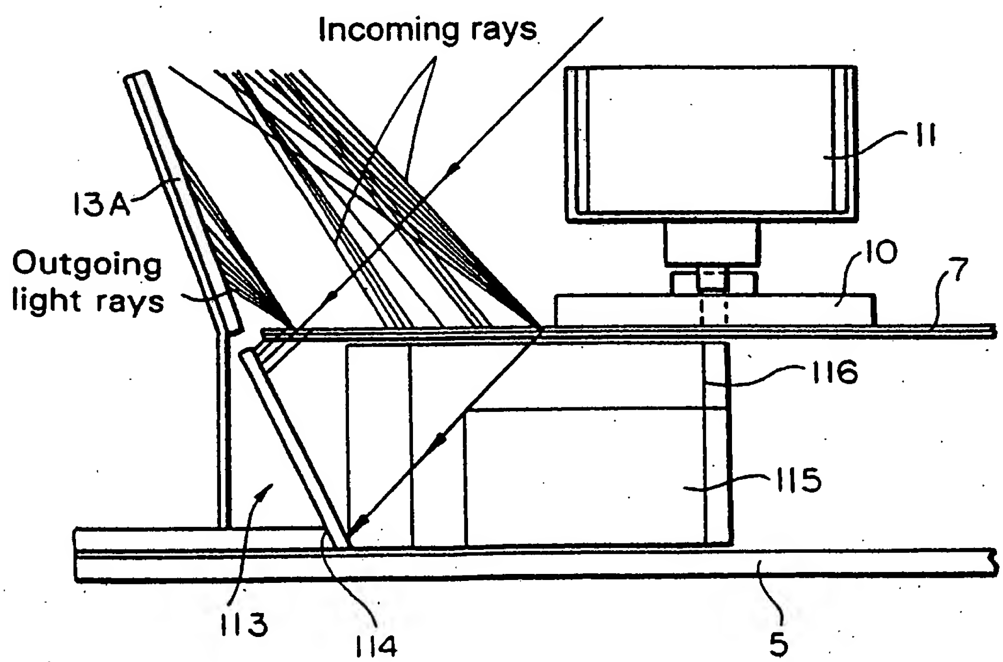

FIG. 43A

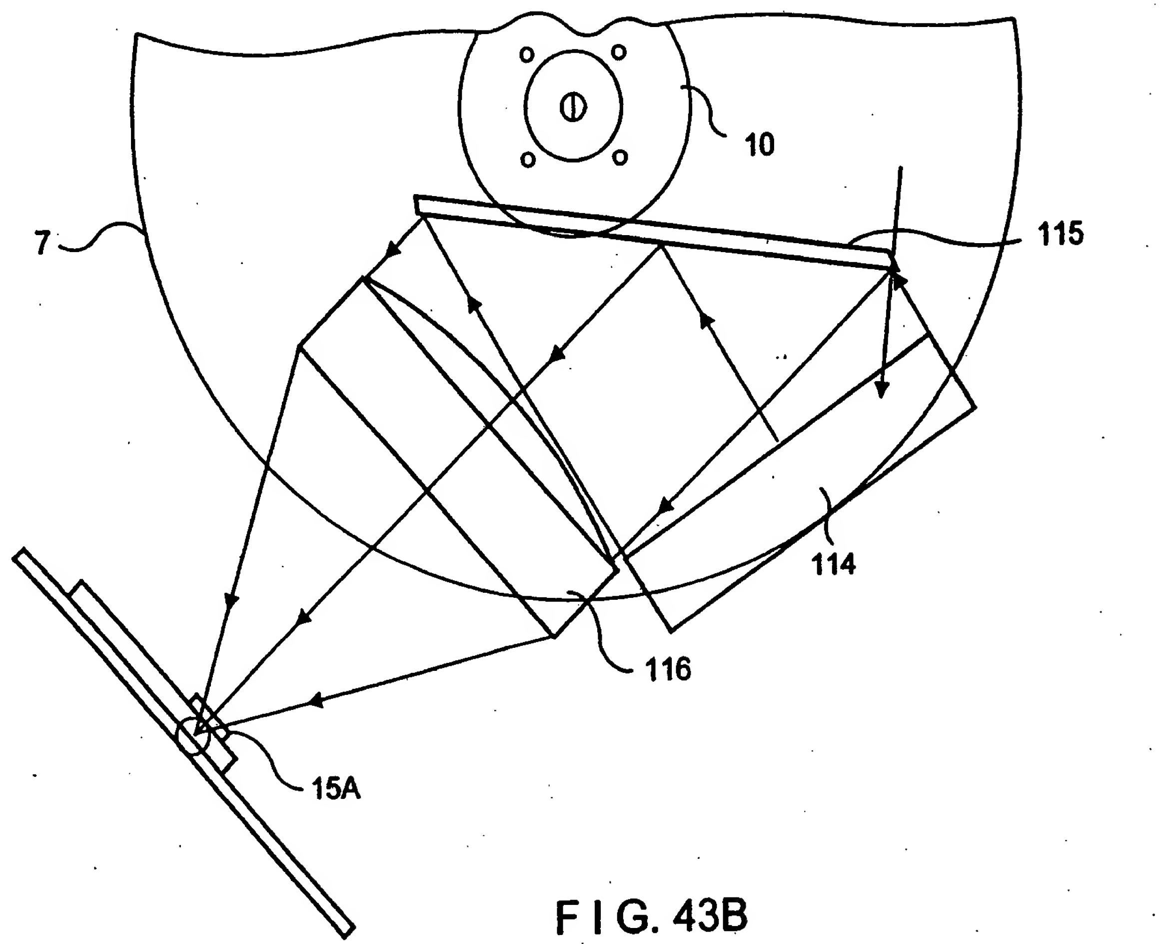

F I G. 43B

SCANNING DISC REALIZED USING REFLECTION-VOLUME HOLOGRAPHIC FACETS

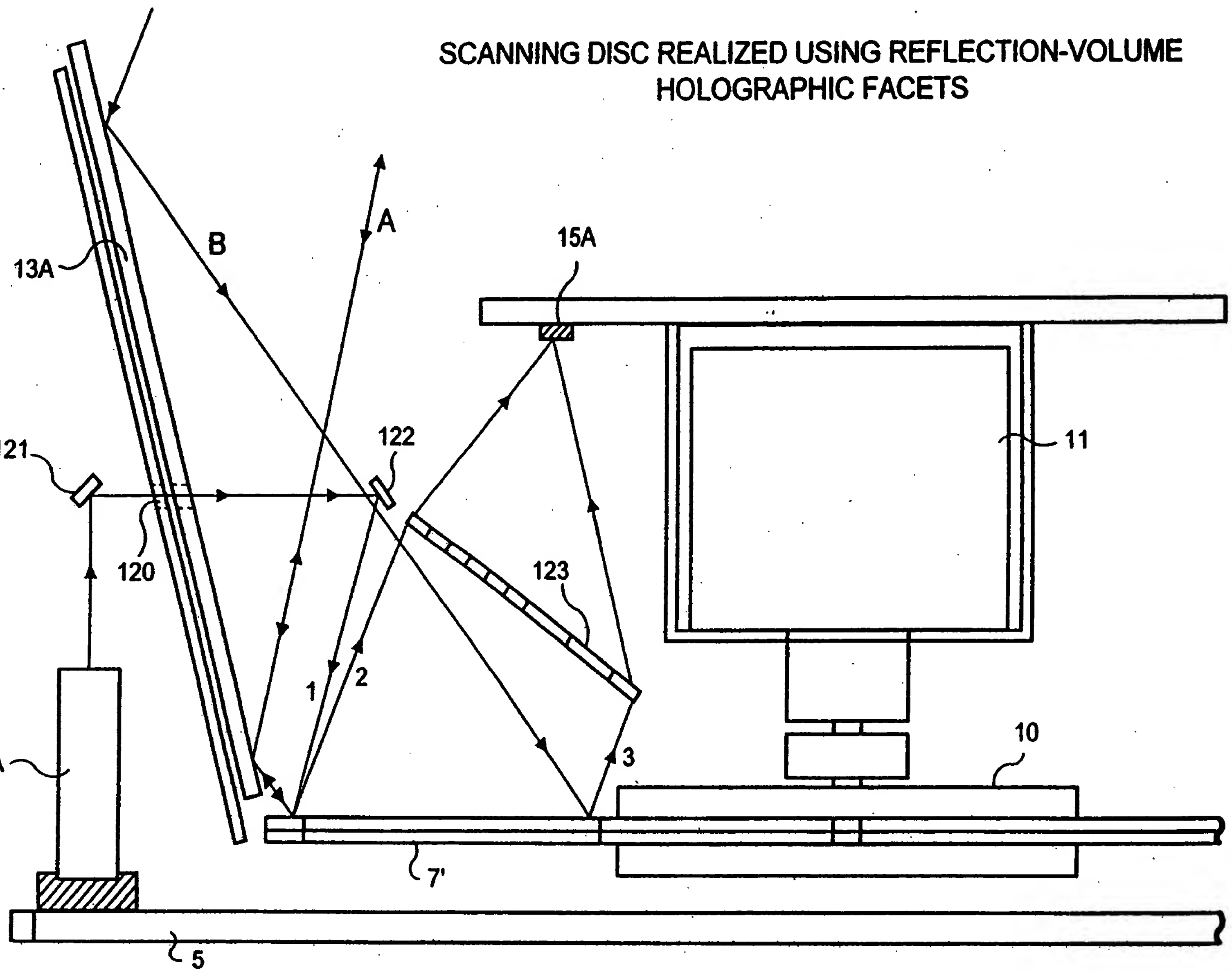

FIG. 44

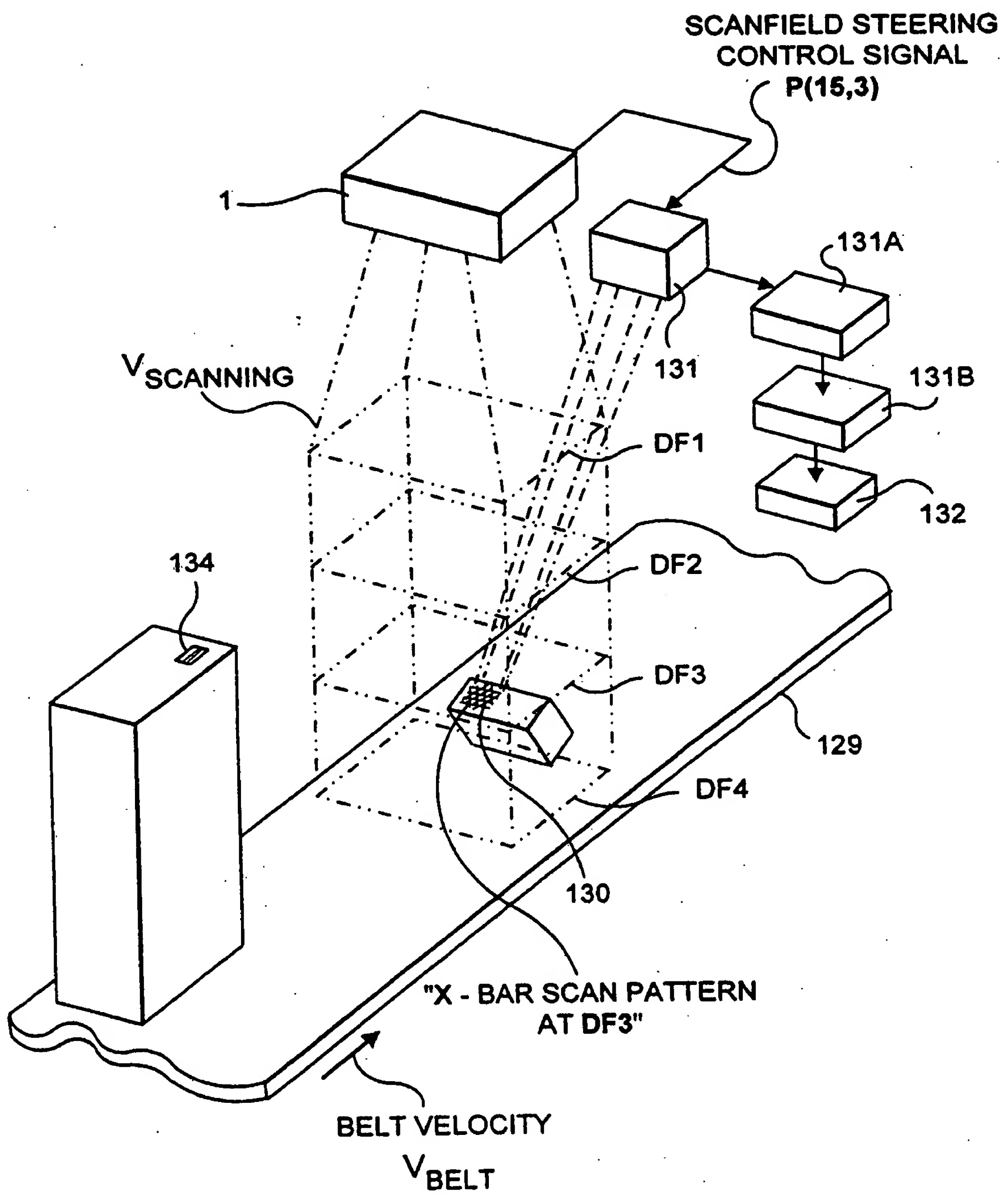
SCANFIELD STEERING
CONTROL SIGNAL
P(15,3)
1
131A
131
131B
$V_{SCANNING}$
DF1
132
134
DF2
DF3
129
DF4
130
"X - BAR SCAN PATTERN
AT DF3"
BELT VELOCITY
V_{BELT}

F I G. 45A

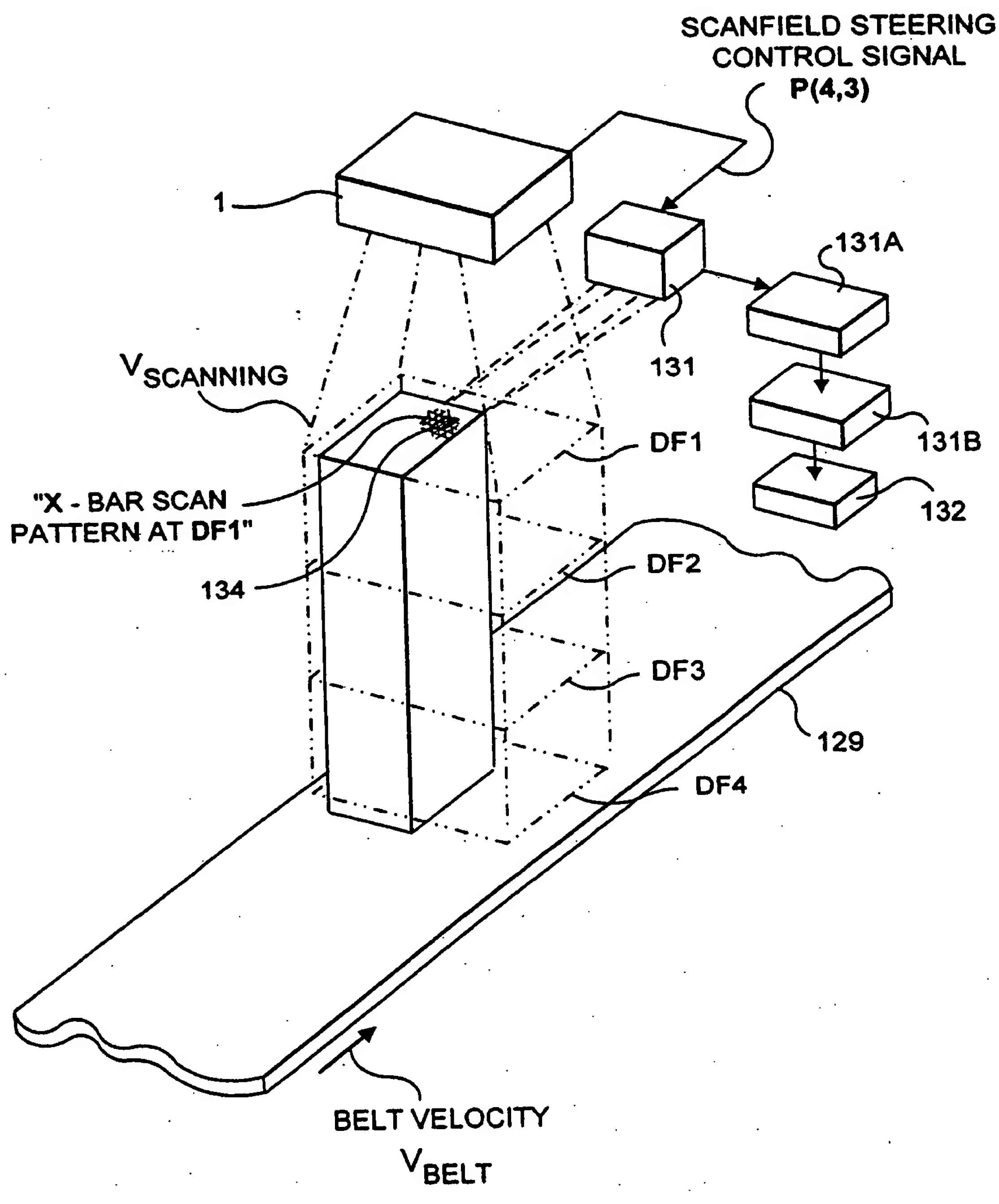
SCANFIELD STEERING
CONTROL SIGNAL
P(4,3)
1
131A
131
131B
132
$V_{SCANNING}$
DF1
"X - BAR SCAN
PATTERN AT DF1"
DF2
134
DF3
129
DF4
BELT VELOCITY
V_{BELT}

F I G. 45B

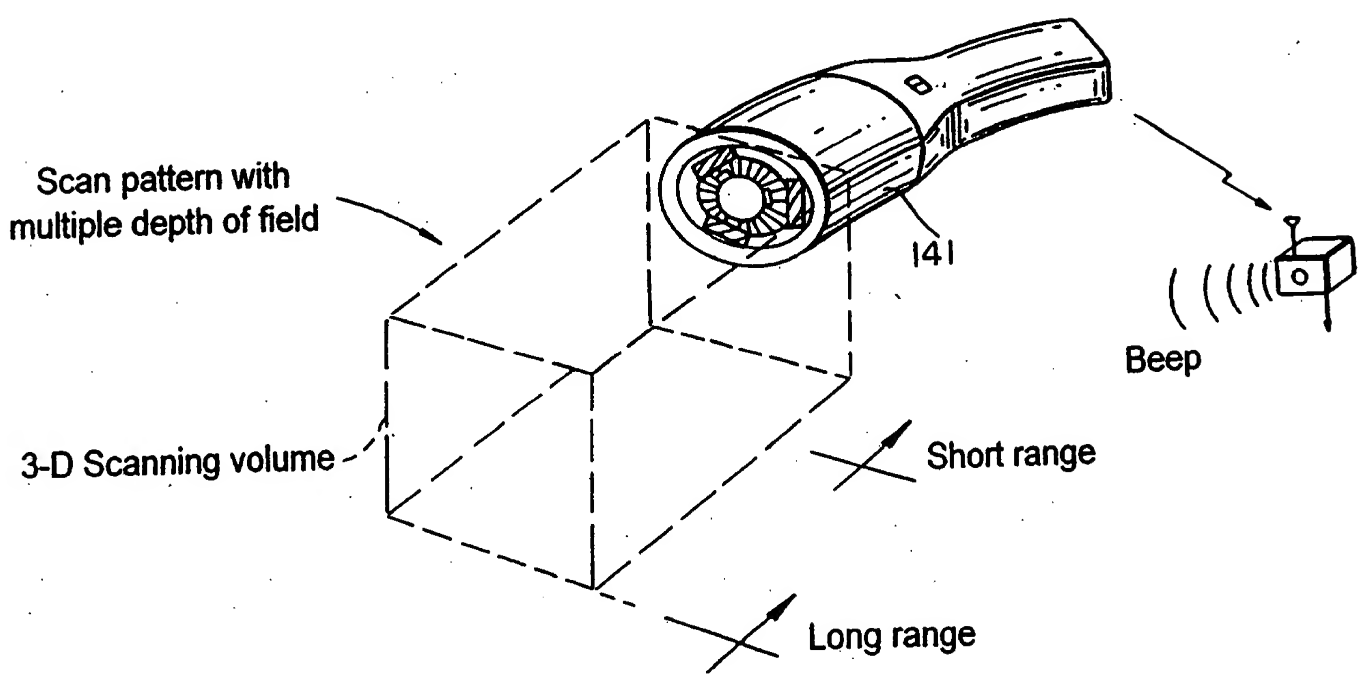
Scan pattern with
multiple depth of field
3-D Scanning volume
141
Beep
Short range
Long range

FIG. 46

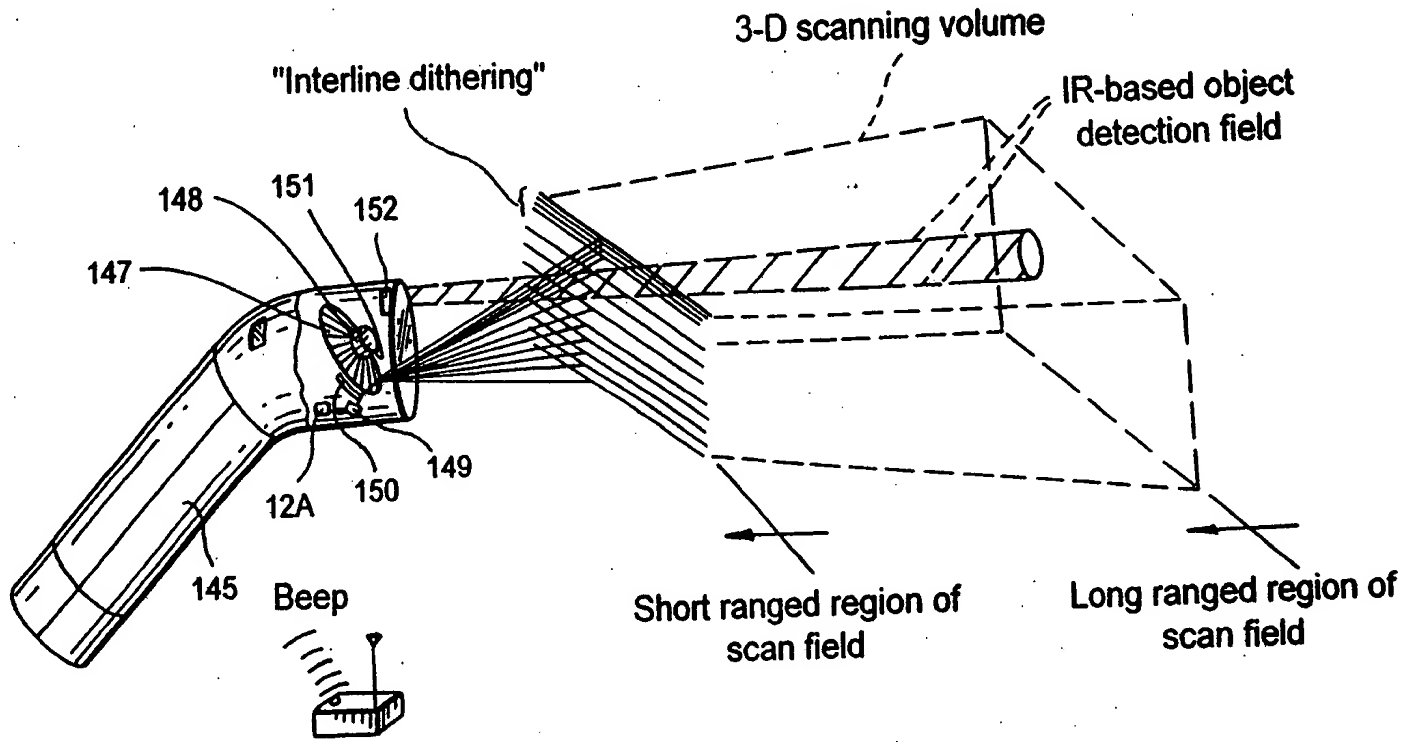
3-D scanning volume
"Interline dithering"
IR-based object detection field
148
151
152
147
149
150
12A
145
Beep
Short ranged region of scan field
Long ranged region of scan field

FIG. 47

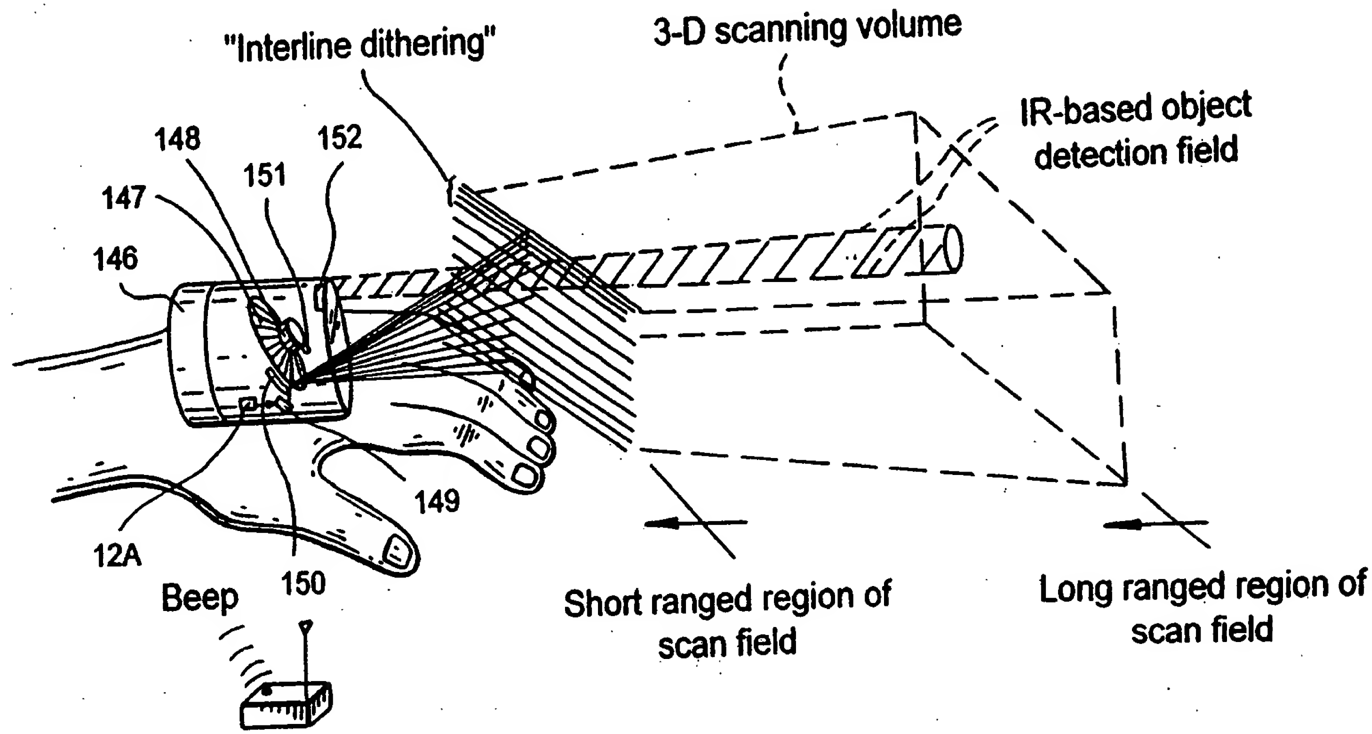
"Interline dithering"
3-D scanning volume
IR-based object detection field
148
152
151
147
146
149
12A
150
Beep
Short ranged region of scan field
Long ranged region of scan field

FIG. 48